

REFERENCE USE ONLY

REPORT NO. DOT-TSC-OST-75-43

MIDLATITUDE MEASUREMENTS
OF L-BAND IONOSPHERIC SCINTILLATION
WITH THE ATS-5 SPACECRAFT

W.E. Brown III
G.G. Haroules
W.I. Thompson III



SEPTEMBER 1975
FINAL REPORT

DOCUMENT IS AVAILABLE TO THE PUBLIC
THROUGH THE NATIONAL TECHNICAL
INFORMATION SERVICE, SPRINGFIELD,
VIRGINIA 22161

Prepared for
U.S. DEPARTMENT OF TRANSPORTATION
OFFICE OF THE SECRETARY
Office of the Assistant Secretary for Systems Development
and Technology, Office of Systems Engineering
Washington DC 20590

NOTICE

This document is disseminated under the sponsorship of the Department of Transportation in the interest of information exchange. The United States Government assumes no liability for its contents or use thereof.

NOTICE

The United States Government does not endorse products or manufacturers. Trade or manufacturers' names appear herein solely because they are considered essential to the object of this report.

1. Report No. OT-TSC-OST-75-43	2. Government Accession No.	3. Recipient's Catalog No.	
4. Title and Subtitle MIDLATITUDE MEASUREMENTS OF L-BAND IONOSPHERIC SCINTILLATION WITH THE ATS-5 SPACECRAFT		5. Report Date September 1975	6. Performing Organization Code
		8. Performing Organization Report No. DOT-TSC-OST-75-43	
7. Author(s) V.E. Brown III, G.G. Haroules, and W.I. Thompson III		10. Work Unit No. (TRAIS) OS334/R5154	11. Contract or Grant No.
9. Performing Organization Name and Address U.S. Department of Transportation Transportation Systems Center Pendall Square Cambridge MA 02142		13. Type of Report and Period Covered Final Report June - December 1974	
		14. Sponsoring Agency Code	
12. Sponsoring Agency Name and Address U.S. Department of Transportation Office of the Secretary Office of the Assistant Secretary for Systems Development and Technology, Off. of Sys. Engineering Washington DC 20590		15. Supplementary Notes	

16. Abstract

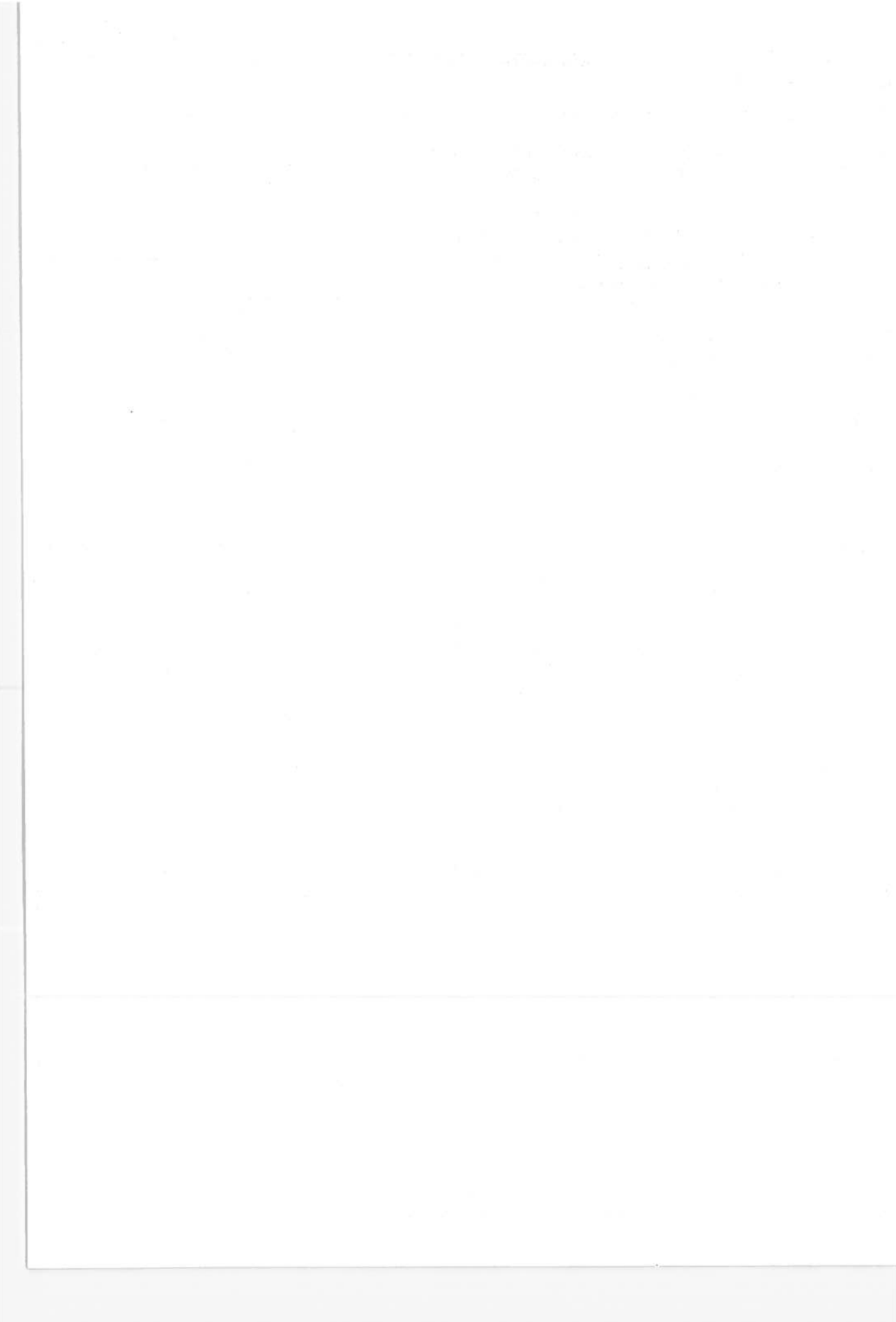
This report presents some results of L-band signal level measurements taken from the ATS-5 spacecraft operating in the narrow-band frequency translation mode. The uplink signal was sent from the DOT/TSC/Westford Propagation Facility in Westford, Massachusetts, which has geographic coordinates of latitude: 42.60 deg. N and longitude: 71.50 deg. W and is thus a midlatitude site. The uplink signal was transponded by the NASA ATS-5 spacecraft and re-radiated back to earth. The signal was received by several L-band receiving systems located at the Westford facility.

The data are presented weekly, monthly and seasonal plots of the root-mean-square of the probability density function and the 90th percentile level of the probability distribution function of the received signal amplitude. Sample analog recordings of the signal are also presented along with the corresponding computer calculated statistics.

Brief equipment descriptions are included along with a description of an automatic data collection platform which was used during some of the measurements.

17. Key Words Amplitude Scintillation Measurements L-Band (1550 MHz) ATS-5 Geostationary Satellite EROSAT	18. Distribution Statement DOCUMENT IS AVAILABLE TO THE PUBLIC THROUGH THE NATIONAL TECHNICAL INFORMATION SERVICE, SPRINGFIELD, VIRGINIA 22161
---	---

19. Security Classif. (of this report) Unclassified	20. Security Classif. (of this page) Unclassified	21. No. of Pages 192	22. Price
--	--	-------------------------	-----------



PREFACE

This report presents some results of L-band signal level measurements taken from the ATS-5 geostationary spacecraft during the period December 1973 - July 1974. The measurements were made at the DOT/TSC/Westford Propagation Facility in Westford, Massachusetts.

The authors would like to acknowledge the support of and the constructive criticism offered by Mr. Richard Beam of the Office of the Assistant Secretary for Systems Development and Technology, DOT and Mr. Joseph Gutwein of the Transportation Systems Center, Cambridge, Massachusetts. We would particularly like to thank Mr. Paul Podlesny for his "beyond the call of duty" service at the Westford Propagation Facility.

We would also like to acknowledge the assistance from several of the personnel of the ATS Operations and Control Center at the NASA Goddard Space Flight Center. In particular Mr. Howard Pedolsky for his scheduling support and Mr. Fredric Kissel, Mr. Joseph Gifford and Mr. Robert Youngblood for their numerous discussions and many helpful comments.

We would like to acknowledge the assistance of the staff of the General Electric Radio-Optical Observatory in Schenactady, New York. In particular Mr. James Lewis as well as Mr. Roy Anderson and Dr. George Millman of the General Electric Company.

Ionogram data in the form of F-plots used in connection with this study were obtained from World Data Center A for Solar-Terrestrial Physics in Boulder, Colorado. We would especially like to thank H. I. Brophy and R. A. Conkright of the Ionospheric Data Branch and W. Paulishak, Chief of the Geomagnetic Data Branch of WDC-A for their cooperation.

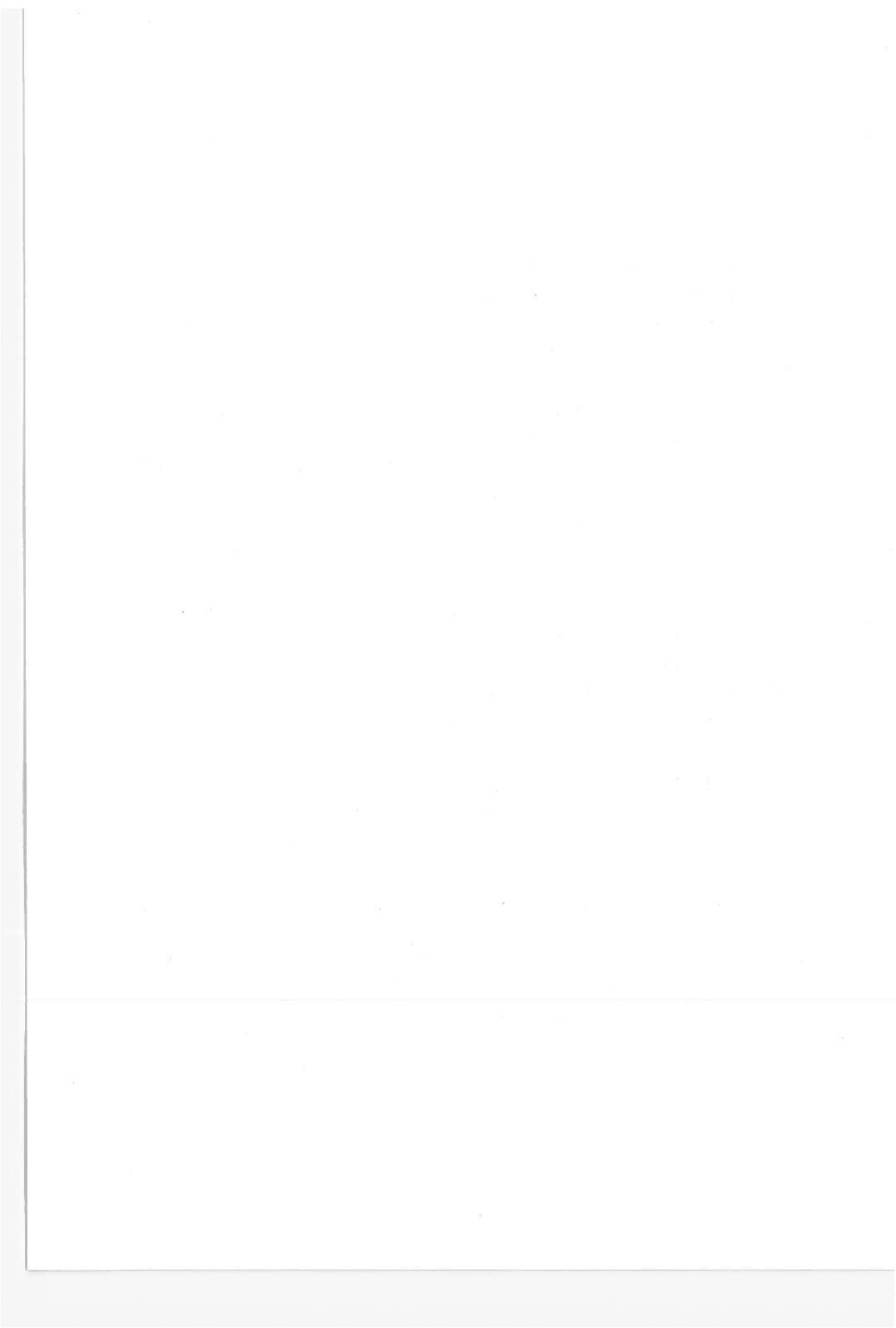


TABLE OF CONTENTS

<u>Section</u>	<u>Page</u>
1. INTRODUCTION.....	1-1
2. WESTFORD PROPAGATION FACILITY.....	2-1
2.1 L-Band Receiving Equipment.....	2-1
2.2 L-Band Transmitting Equipment.....	2-12
2.3 L-Band Link Calculations.....	2-15
2.4 Data Acquisition.....	2-22
3. REMOTE MEASUREMENT SYSTEM.....	3-1
3.1 Introduction.....	3-1
3.2 Platform L-Band Receiving System.....	3-7
3.3 ADCP L-Band Calibration.....	3-11
3.4 Automatic Receiver Tuning.....	3-14
3.5 L-Band Radio Link Calculations.....	3-14
3.6 ADCP VHF System.....	3-16
3.7 ADCP Computer Programs.....	3-16
3.8 Westford Computer Programs for Operation of the Remote Platform.....	3-25
4. ATS-5 L-BAND DATA.....	4-1
4.1 Discussion.....	4-1
4.2 Temporal Analysis.....	4-14
4.3 Seasonal Analysis.....	4-23
4.3.1 Winter.....	4-23
4.3.2 Spring.....	4-23
4.3.3 Summer.....	4-27
4.3.4 Seasonal Summary.....	4-27
4.4 Distribution of the Maximum Values.....	4-27
4.5 Geomagnetic Variations.....	4-34
4.6 Observed Semi-Diurnal Variations.....	4-34
5. CONCLUSIONS & RECOMMENDATIONS.....	5-1
5.1 Conclusions.....	5-1
5.2 Recommendations.....	5-3
6. REFERENCES.....	6-1
APPENDIX A - SITING REQUIREMENTS FOR THE AUTOMATIC DATA COLLECTION PLATFORM.....	A-1

TABLE OF CONTENTS (CONTINUED)

<u>Section</u>	<u>Page</u>
APPENDIX B - TABLE OF OBSERVATION TIMES.....	B-1
APPENDIX C - WEEKLY TEMPORAL DIAGRAMS.....	C-1
APPENDIX D - ANALYSIS OF MAXIMUM VALUES.....	D-1
APPENDIX E - ADAPTATION OF PHASE MEASUREMENT CAPABILITY TO THE WESTFORD SITE AND THE AUTOMATIC DATA COLLECTION PLATFORM.....	E-1

LIST OF ILLUSTRATIONS

<u>Figure</u>	<u>Page</u>
2-1. Map of ATS-5 - Westford Propagation Facility (Boston) Geometry.....	2-3
2-2. Aerial Photograph of the DOT/TSC/Westford Propagation Facility.....	2-4
2-3. Photograph of the DOT/TSC/Westford Propagation Facility Looking Northeast.....	2-5
2-4. Photograph of 10-Foot Diameter Antennas Used in the L-Band Receivers.....	2-6
2-5. Schematic Diagram of the L-Band Receiving System at the Westford Propagation Facility.....	2-7
2-6. Photograph of Two 10-Foot Diameter Antennas Mounted in Nike-Ajax Mounts.....	2-8
2-7. Photograph of 10-Foot Diameter Antenna Mounted Atop a 30-Foot High Tower.....	2-9
2-8. Photograph of the L-Band 15-Foot Diameter Transmitting Antenna.....	2-13
2-9. Block Diagram of the L-Band Exciter/Power Amplifier..	2-14
2-10. ATS-5 L-Band Narrowband Frequency Translation Mode Transponder Compression (December 12, 1973).....	2-16
3-1. Diagram of the Remote Scintillation Data Collection Experiment.....	3-2
3-2. Photograph of the Automatic Data Collection Platform's Electronic Equipment.....	3-3
3-3. Photograph of the VHF and L-Band Antennas Used with the Automatic Data Collection Platform.....	3-4
3-4. Simplified Block Diagram of the ADCP.....	3-6
3-5. L-Band Section of ADCP's Receiver.....	3-8
3-6. Intermediate Frequency Portion of the ADCP Receiver..	3-9

LIST OF ILLUSTRATIONS (CONTINUED)

<u>Figure</u>	<u>Page</u>
3-7. ADCP's L-Band Receiver Detector Voltage Versus the 70 MHZ Input Signal Strength.....	3-12
3-8. ADCP's L-Band Receiver Response for the 10.7 MHZ Amplifier, Filter and Square-Law Detector.....	3-13
3-9. Detailed Functional Block Diagram of the VHF Portion of the Remote Facility.....	3-17
4-1. Example of Analog Data and Computer Calculated Statistics (23 April 1974).....	4-3
4-2. Example of Analog Data and Computer Calculated Statistics (29 April 1974).....	4-4
4-3. Example of Analog Data and Computer Calculated Statistics (29 May 1974, 2230 EDST).....	4-5
4-4. Example of Analog Data and Computer Calculated Statistics (29 May 1974, 2045 EDST).....	4-6
4-5. Example of Analog Data and Computer Calculated Statistics (1 April 1974).....	4-7
4-6. Analog Strip-Chart Recordings for the ATS-5 L-Band Signal on 3 Channels (11 July 1974).....	4-8
4-7a. Example of a Computer Generated Strip-Chart Record from Automatic Data Collection Platform Data (22 July 1974).....	4-9
4-7b. Example of a Computer Generated Strip-Chart Record from Automatic Data Collection Platform Data (22 July 1974).....	4-10
4-7c. Example of a Computer Generated Strip-Chart Record from Automatic Data Collection Platform Data (22 July 1974).....	4-11
4-8. Probability Density Plots for Automatic Data Collection Platform Data (22 July 1974).....	4-12
4-9. Probability Distribution Plots for Automatic Data Collection Platform Data (22 July 1974).....	4-13
4-10. Temporal Diagram for December 1973.....	4-15
4-11. Temporal Diagram for January 1974.....	4-16

LIST OF ILLUSTRATIONS (CONTINUED)

<u>Figure</u>	<u>Page</u>
4-12. Temporal Diagram for February 1974.....	4-17
4-13. Temporal Diagram for March 1974.....	4-18
4-14. Temporal Diagram for April 1974.....	4-19
4-15. Temporal Diagram for May 1974.....	4-20
4-16. Temporal Diagram for June 1974.....	4-21
4-17. Temporal Diagram for July 1974.....	4-22
4-18. Temporal Diagrams for December 1973, January 1974 and February 1974 and the Combination into a "Winter" Curve.....	4-24
4-19. Temporal Diagram for "Winter".....	4-25
4-20. Temporal Diagrams for March 1974, April 1974 and May 1974 Along with the Combination into a "Spring" Curve.	4-26
4-21. Temporal Diagram for "Spring".....	4-28
4-22. Temporal Diagram for June 1974 and July 1974 Along with the Combination into a "Summer" Curve.....	4-29
4-23. Temporal Diagrams for "Summer".....	4-30
4-24. Temporal Diagrams for "Winter", "Spring" and "Summer".	4-31
4-25. Cumulative Frequency Distribution Plotted from Data of Table 4-2.....	4-32
4-26. Comparison of "3-HR Scintillation Index" with Planetary Magnetic Index Kp (Dec. 1973 - July 1974)...	4-35
4-27. Histogram of Scintillation Measurements by Planetary Magnetic Index and "3-HR Scintillation Index".....	4-36
4-28. Diurnal Variation of 1-Hour Scintillation Index for the 625 Hours of Observations.....	4-38
A-1. Physical Layout of Automatic Data Collection Platform.	A-2
A-2. Platform Antenna System Layout.....	A-3
C-1. Temporal Diagram for 3-7 December 1973.....	C-2
C-2. Temporal Diagram for 10-13 December 1973.....	C-3

LIST OF ILLUSTRATIONS (CONTINUED)

<u>Figure</u>	<u>Page</u>
C-3. Temporal Diagram for 18-20 December 1973.....	C-4
C-4. Temporal Diagram for 26-29 December 1973.....	C-5
C-5. Temporal Diagram for 2-5 January 1974.....	C-6
C-6. Temporal Diagram for 7-10 January 1974.....	C-7
C-7. Temporal Diagram for 14-17 January 1974.....	C-8
C-8. Temporal Diagram for 21-24 January 1974.....	C-9
C-9. Temporal Diagram for 28-30 January 1974.....	C-10
C-10. Temporal Diagram for 4-7 February 1974.....	C-11
C-11. Temporal Diagram for 11-15 February 1974.....	C-12
C-12. Temporal Diagram for 18-21 February 1974.....	C-13
C-13. Temporal Diagram for 25-28 February 1974.....	C-14
C-14. Temporal Diagram for 5-8 March 1974.....	C-15
C-15. Temporal Diagram for 11-16 March 1974.....	C-16
C-16. Temporal Diagram for 18-22 March 1974.....	C-17
C-17. Temporal Diagram for 25-30 March 1974.....	C-18
C-18. Temporal Diagram for 1-4 April 1974.....	C-19
C-19. Temporal Diagram for 8-10 April 1974.....	C-20
C-20. Temporal Diagram for 15-18 April 1974.....	C-21
C-21. Temporal Diagram for 22-25 April 1974.....	C-22
C-22. Temporal Diagram for 29 April - 2 May 1974.....	C-23
C-23. Temporal Diagram for 7-9 May 1974.....	C-24
C-24. Temporal Diagram for 13-16 May 1974.....	C-25
C-25. Temporal Diagram for 20-23 May 1974.....	C-26
C-26. Temporal Diagram for 28 May 1974.....	C-27

LIST OF ILLUSTRATIONS (CONTINUED)

Figure

C-27. Temporal Diagram for 3-6 June 1974..... C-28

C-28. Temporal Diagram for 10-13 June 1974..... C-29

C-29. Temporal Diagram for 17-20 June 1974..... C-30

C-30. Temporal Diagram for 24-27 June 1974..... C-31

C-31. Temporal Diagram for 1-2 July 1974..... C-32

C-32. Temporal Diagram for 8-9 July 1974..... C-33

C-33. Temporal Diagram for 15-18 July 1974..... C-34

C-34. Temporal Diagram for 22 July 1974..... C-35

D-1. Plot of Maximum R.M.S. File Values versus Time of
Year for the ATS-5 L-Band Amplitude Measurements
(From Table D-10)..... D-15

E-1. Block Diagram of a Phase Measurement System for
L-Band..... E-2

LIST OF TABLES

<u>Table</u>	<u>Page</u>
1-1. SUMMARY OF IONOSPHERIC SCINTILLATION MEASUREMENTS IN THE SHF BAND.....	1-2
2-1. COORDINATES AND RANGE OF WESTFORD PROPAGATION FACILITY AND THE ATS-5 SPACECRAFT FOR A SUBIONOSPHERIC HEIGHT OF 350 km.....	2-2
2-2. POWER BUDGET FOR ATS-5 - WESTFORD PROPAGATION FACILITY L-BAND LINK.....	2-19
3-1. L-BAND LINK POWER BUDGET.....	3-15
3-2A. POWER BUDGETS FOR THE VHF UPLINKS BETWEEN THE ADCP AND THE ATS-1 OR ATS-3 SPACECRAFT AT 149.22 MHz.....	3-18
3-2B. POWER BUDGETS FOR THE VHF DOWNLINKS BETWEEN THE ADCP AND THE ATS-1 OR ATS-3 SPACECRAFT AT 135.60 MHz.....	3-18
3-3. ADCP COMPUTER COMMANDS.....	3-19
4-1. SYMBOLS USED IN THE TEMPORAL DIAGRAMS OF ATS-5 SIGNAL STRENGTH.....	4-14
4-2. FREQUENCY DISTRIBUTION FOR DATA OF TABLE D-9.....	4-33
A-1. TABLE OF SHIPPING WEIGHTS AND SIZES OF EQUIPMENT IN THE AUTOMATIC DATA COLLECTION PLATFORM.....	A-4
A-2. POWER REQUIREMENTS OF THE AUTOMATIC DATA COLLECTION PLATFORM.....	A-5
A-3. ELEVATION ANGLES FROM VARIOUS SITES TO THE ATS-5, AND 6 SPACECRAFTS.....	A-5
A-4. SPECIFICATION SUMMARY OF THE AUTOMATIC DATA COLLECTION PLATFORM.....	A-6
B-1. SUMMARY OF ATS-5 L-BAND SCINTILLATION OBSERVATIONS...	B-2
D-1. DISTRIBUTION OF THE ROOT-MEAN-SQUARE AND 90TH-PERCENTILE MAXIMUM 15-MINUTE VALUES FOR DECEMBER 1973	D-2
D-2. DISTRIBUTION OF THE ROOT-MEAN-SQUARE AND 90TH-PERCENTILE MAXIMUM 15-MINUTE VALUES FOR JANUARY 1974.	D-3
D-3. DISTRIBUTION OF THE ROOT-MEAN-SQUARE AND 90TH-PERCENTILE MAXIMUM 15-MINUTE VALUES FOR FEBRUARY 1974	D-4

LIST OF TABLES (CONTINUED)

<u>Table</u>	<u>Page</u>
D-4. DISTRIBUTION OF THE ROOT-MEAN-SQUARE AND 90TH- PERCENTILE MAXIMUM 15-MINUTE VALUES FOR MARCH 1974....	D-5
D-5. DISTRIBUTION OF THE ROOT-MEAN-SQUARE AND 90TH- PERCENTILE MAXIMUM 15-MINUTE VALUES FOR APRIL 1974....	D-6
D-6. DISTRIBUTION OF THE ROOT-MEAN-SQUARE AND 90TH- PERCENTILE MAXIMUM 15-MINUTE VALUES FOR MAY 1974.....	D-7
D-7. DISTRIBUTION OF THE ROOT-MEAN-SQUARE AND 90TH- PERCENTILE MAXIMUM 15-MINUTE VALUES FOR JUNE 1974.....	D-8
D-8. DISTRIBUTION OF THE ROOT-MEAN-SQUARE AND 90TH- PERCENTILE MAXIMUM 15-MINUTE VALUES FOR JULY 1974.....	D-10
D-9. TALLY SHEET AND FREQUENCY DISTRIBUTION FOR DATA OF TABLES D-1 THROUGH D-8.....	D-11
D-10. TALLY SHEET AND FREQUENCY DISTRIBUTION OF DATA IN TABLE D-9 BY MONTHS.....	D-14
D-11. APPROXIMATE VALUES OF SCINTILLATION RELATIVE TO R.M.S. FILE VALUES.....	D-16

LIST OF ABBREVIATIONS

amps.	amperes
ADCP	automatic data collection platform
AEROSAT	aeronautical satellite
AF	after
AIAA	American Institute of Astronautics & Aeronautics
ALSEP	Apollo Lunar Surface Experiment Package
Att.	attenuator
ATS	Applications Technology Satellite (NASA)
A/D	analog-to-digital
$A_c(t)$	amplitude
$A_p(t)$	amplitude
$A(t)$	amplitude
BF	before
BIE	bits in error
BW	bandwidth
cks.	clocks
combo	combination
C	combo
Cal.	calibrated
COMSAT	Communications Satellite Corporation
CW	continuous wave
deg.	degree(s)
dB	decibel
dBm	power relative to a milliwatt expressed in dB
dBw	power relative to a watt expressed in dB
Det.	detector
D	a distance
DC	direct current
DEC	Digital Equipment Corporation
DEI	Defense Electronics Industries
DOT	U.S. Department of Transportation
D/A	digital-to-analog
E	east
EDST	eastern daylight savings time

LIST OF ABBREVIATIONS (CONT.)

EIRP	equivalent isotropic radiated power
ERP	effective radiated power
EST	eastern standard time
f_o	received frequency
foF2	critical frequency of the F2 layer
F2	a layer of the earth's ionosphere
Gen.	generator
GE	General Electric Company
GHz	gigahertz
G_R	effective gain of a receiving antenna
G_T	effective gain of a transmitting antenna
H	height
HP	Hewlett Packard Company
HR	hour
HRS	hours
IF	intermediate frequency
INTELSAT	International Telecommunication Satellite Consortium
JGR	Journal of Geophysical Research
k	Boltzmann's constant, kilo
kbit	kilobit
km	kilometer
kHz	kilohertz
kw	kilowatt
K	degrees Kelvin
K_p	planetary magnetic index
lb	pound
L	transmission line loss; length; invariant latitude
LMT	local mean time
LO	local oscillator
LT	local time
L-band	The portion of the radio frequency spectrum between 1,000 MHz and 2,000 MHz (Wavelengths between 15 and 30 cm).

LIST OF ABBREVIATIONS (CONT.)

m	meter
ms	millisecond
MHz	megahertz
MIN.	minute
MT	magnetic tape
MT's	magnetic tapes
$n(t)$	additive noise
N	north
NASA	National Aeronautics & Space Administration
NBFT	narrow-band frequency translation
NF	noise figure
NPD	noise power density
N_o	noise power density
Off.	office
PLACE	position location and aircraft communications experiment
PREAMP	preamplifier
PSK	phase shift keying
P_c	free space path loss
P_R	received power
P_T	transmitted power
Rec.	receiver
Ref.	reference
$R(t)$	received signal
RF	radio frequency
RFI	radio frequency interference
RHCP	right-hand circular polarization
R.M.S.	root-mean-square
s	second
S	south
Sig.	signal
Sq. Law	square law
Sys.	systems
S-band	Super-high frequencies. The portion of the radio frequency spectrum between 3 GHz and 30 GHz (Wave- lengths between 1 and 10 cm).

LIST OF ABBREVIATIONS (CONT.)

S.I.	scintillation index
SSB	single sideband
SS	sunset
SW	switch, southwest
S/C	spacecraft
S/N	signal-to-noise ratio
Temp.	temperature.
T.P.	test point
TSC	Transportation Systems Center
TWT	traveling wave tube
T_A	antenna temperature
T_o	ambient temperature
T_R	receiver effective noise temperature
T_S	system temperature
T/R	transmit-receive
UN	United Nations
URSI	International Union of Radio Science (UN)
UT	universal time
U.S.	United States of America
U.S.A.	United States of America
V	volt(s)
VAC	volts alternating current
VHF	very high frequencies
VSWR	voltage standing-wave ratio
$V_{\text{Det. Sig.}}$	detector voltage with signal present
$V_{\text{Det. Noise}}$	detector voltage due to system noise
w	watt
W	west; width
WK	week
WPF	Westford Propagation Facility
X	a cartesian coordinate
Xmit	transmit

LIST OF ABBREVIATIONS (CONT.)

Y	a cartesian coordinate
z	a height
Z	a cartesian coordinate
#	number
λ	wavelength
π	a constant
$\theta(t)$	a constant phase angular frequency
ω_0	a constant angular frequency
®	registered trademark

1. INTRODUCTION

This report contains the results of a series of amplitude measurements of an L-band (1550 MHz) signal between the National Aeronautics & Space Administration's Applications Technology Satellite - 5 (ATS-5) and the DOT/TSC/Westford Propagation Facility in Westford, Massachusetts, U.S.A. The ATS-5 spacecraft is in an equatorial geostationary orbit and is used to repeat an L-band uplink signal from the Westford site. The resulting downlink signal is then measured and analyzed at the Westford Propagation Facility.

The experiment was initiated because the proposed aeronautical satellite (AEROSAT) system will use radio frequency links at L-band. Several propagation anomalies have been found on ground-to-spacecraft links at L-band and nearby frequencies. Table 1-1 summarizes several of the measurements. The experiment reported here was designed to quantify the propagation anomalies at a mid-latitude station.

Ionospheric scintillations are produced by irregularities in the electron density of the ionosphere which change the local index of refraction and thus modify the path and phase of radio waves passing through the ionosphere. Amplitude scintillations are produced when irregularities with dimensions of the order of the Fresnel dimension $(\pi \lambda z)^{1/2}$ move across the radio path. Here λ is the radio wavelength and z is the mean height of the irregular layer. The irregular density level is usually a few percent of the background density, the dimensions ranging from approximately 0.01 to 100 km and the drift velocities being about 0.1 km/s in the ionospheric F region. Three state-of-the-art papers on radio scintillation have been recently issued by Rufenach (1974) and Wernik et. al. (1973, 1974).

A brief description of the transmitting and receiving equipment used at the Westford site will be given in Section 2. A different receiving system which is part of the automatic data collection platform is described in Section 3. Section 3 also

TABLE 1-1. SUMMARY OF IONOSPHERIC SCINTILLATION MEASUREMENTS IN THE SHF BAND

Frequency (MHz)	Location	Maximum Fades (dB)	Date of Measurement	Reference(s)	Comments
1550	Ancon, Peru	6	1971 Spring Equinox	Golden & Sessions (1972)	Also presented at the 1972 Spring Meeting of the International Union of Radio Science (URSI). (Equatorial)
1550	Tangua, Brazil	7*	1972	Taur (1974)	ATS-5 (Equatorial)
1550	Ottawa, Ontario, Canada	2-3	1972	Ponnappa (1973)	(Midlatitude)
1550	Churchill, Manitoba, Canada	3-4	1972	Ponnappa (1973)	(Auroral latitude)
2200	Ascension Island Canary Islands	20-25	Nov. 1969- Jul. 1970	Christiansen (1971) Golden (1971)	(Equatorial From the lunar base ALSEP)
4000 & 6000	Equatorial Sites	4	1969+	Craft & Westerlund (1972)	(Equatorial) Also presented by Taur (1973). Data taken from geostationary communications satellites of the COMSAT and INTELSAT series.
6295	Longonot, Kenya	4	Mar. Apr. May 1971	Skinner et. al. (1971)	(Equatorial) INTELSAT III-F4 geostationary satellite.

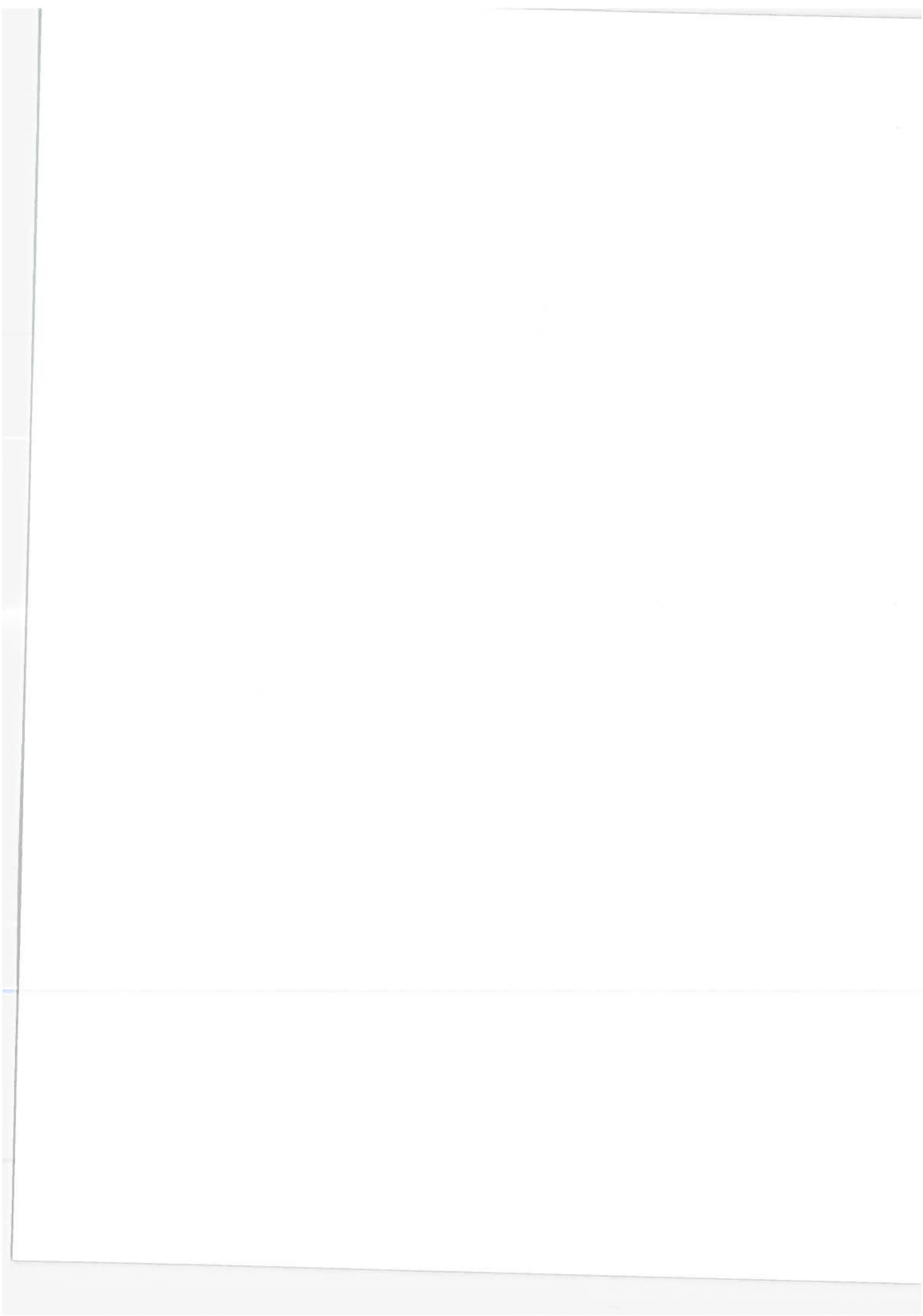
*peak-to-peak

discusses the details of the automatic data collection platform which is capable of being deployed to remote sites and being operated unmanned from the Westford Propagation Facility via a VHF link.

Section 4 presents weekly, monthly and seasonal plots of the root-mean-square of the probability density function and the 90th percentile level of the probability distribution function of the L-band amplitude scintillation data. Sample analog recordings of the signal level are also presented along with the corresponding computer calculated statistics so that both may be compared simultaneously.

Section 5 is devoted to conclusions and recommendations where specific experimental considerations on measuring phase scintillation is included.

There are several appendixes included which discuss such items as: siting requirements for the automatic data collection platform; observation times; weekly temporal diagrams; distribution of the maximum values and the phase measurement capabilities of the Westford site and the automatic data collection platform.



2. WESTFORD PROPAGATION FACILITY

The DOT/TSC/Westford Propagation Facility is located in Westford, Massachusetts, U.S.A. The geographic and geomagnetic coordinates are given in Table 2-1 and the ATS-5-to-Westford path is shown in Figure 2-1. An aerial photograph of the Westford Propagation Facility is shown in Figure 2-2 and a ground view looking northeast is presented in Figure 2-3. The various receiving systems used in this study will be discussed in the following sections.

2.1 L-BAND RECEIVING EQUIPMENT

The receiving systems used in this series of measurements have been described and discussed in great detail in a previous report by Brown, Haroules and Thompson (1974A). In the interest of continuity a brief description will be given here.

Three separate and independent receiving systems are used at L-band. Two of the systems are identical, the third, though similar, operates at different intermediate frequencies. All three systems used 10-foot diameter antennas with spiral feeds so that right circular polarization is received. Each has a radio frequency preamplifier mounted at the feed. Figure 2-4 shows the 10-foot reflectors involved. Figure 2-5 shows a block diagram of the three L-band receiving systems.

The two antennas mounted in the Nike-Ajax mounts shown in Figure 2-6 have their radio frequency preamplifiers and calibration circuits mounted in the waterproof and electromagnetically shielded enclosure directly behind the feed. The 10-foot diameter antenna in Figure 2-7 is mounted atop a 30-foot tower. This receiving station has preamplifiers mounted in the box on the side of the tower.

The feed line in the case of the two Nike-Ajax mounted reflectors is 3-inches long. In the case of the fixed reflector atop the tower the feed line is 7-feet long (The fixed

TABLE 2-1. COORDINATES AND RANGE OF WESTFORD PROPAGATION FACILITY AND THE ATS-5 SPACECRAFT FOR A SUBIONOSPHERIC HEIGHT OF 350 km

Quantity	Value	Notes
<u>ATS-5 Spacecraft</u>		
Subsatellite Longitude (deg.)	105.0 W	1
Subsatellite Latitude (deg.)	~0	1
<u>Penetration Point</u>		
Subionospheric Latitude of the Penetration Point (deg.)	39.1 N	2
Subionospheric Longitude of the Penetration Point	75.8 W	2,3
350 km Invariant Latitude (deg.)	54	-
<u>Westford Propagation Facility</u>		
Geographic Latitude (deg.)	42.6 N	-
Geographic Longitude (deg.)	71.5 W	4
Invariant Latitude (deg.)	55.0	5,6,7
Geomagnetic Latitude (deg.)	53.0 N	-
Geomagnetic Longitude (deg.)	2.0 W	-
Azimuth Propagation Angle from WPF (deg.)	224.0(SW)	1
Elevation Propagation Angle from WPF (deg.)	30.5	1
Approximate Range to ATS-5 (km)	38,585	1

- Notes: 1 NASA ATS-5 Orbital Predictions, NASA (1974)
 2 H.E. Whitney, private communication
 3 5 hours; 3 minutes; 12 seconds
 4 4 hours; 45 minutes; 58 seconds
 5 J.V. Evans and Holt (1973)
 6 Campbell and Matsushita (1967)
 7 At 300 km penetration point; J. E. Evans et al. (1969)

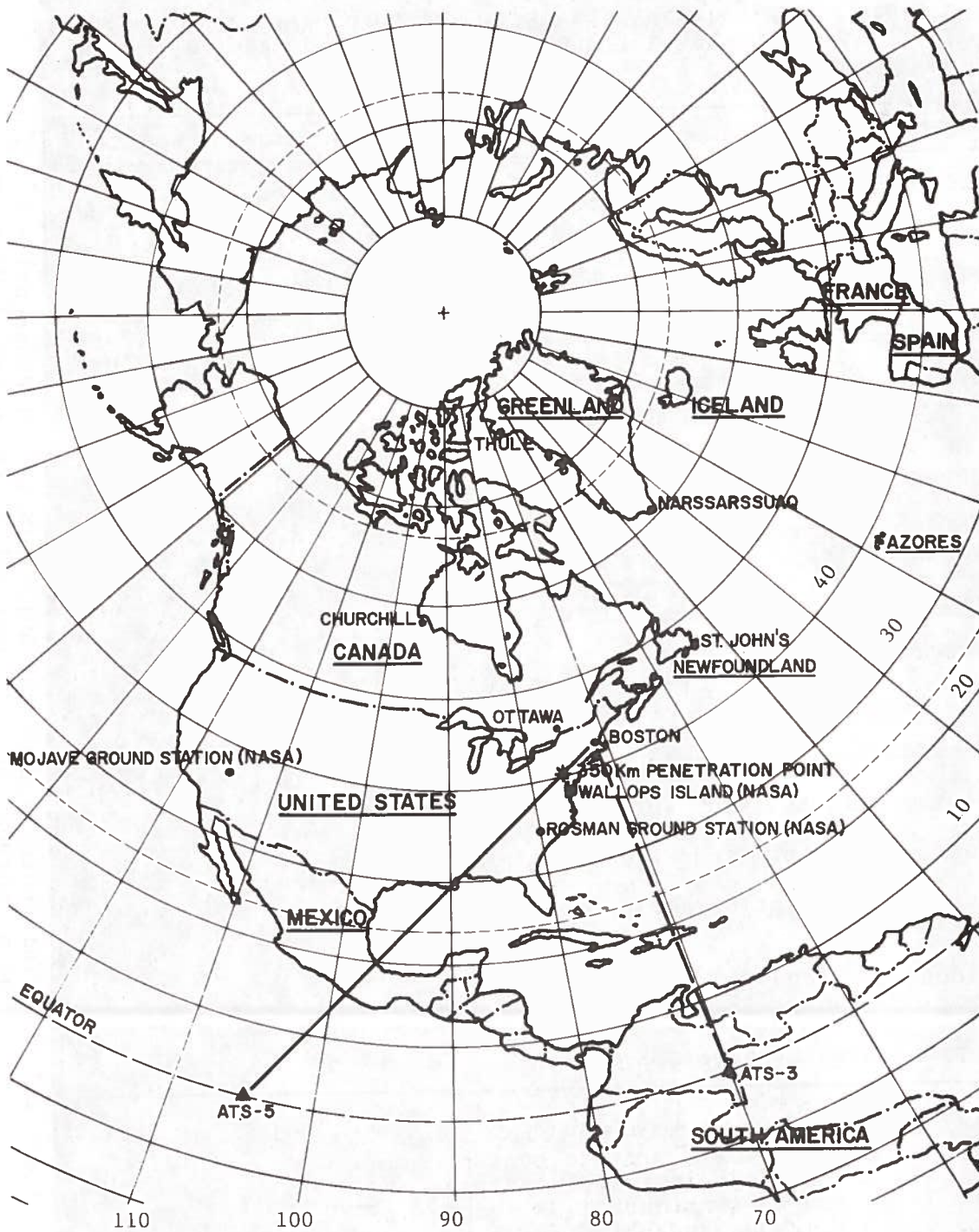


Figure 2-1. Map of ATS-5 - Westford Propagation Facility (Boston) Geometry

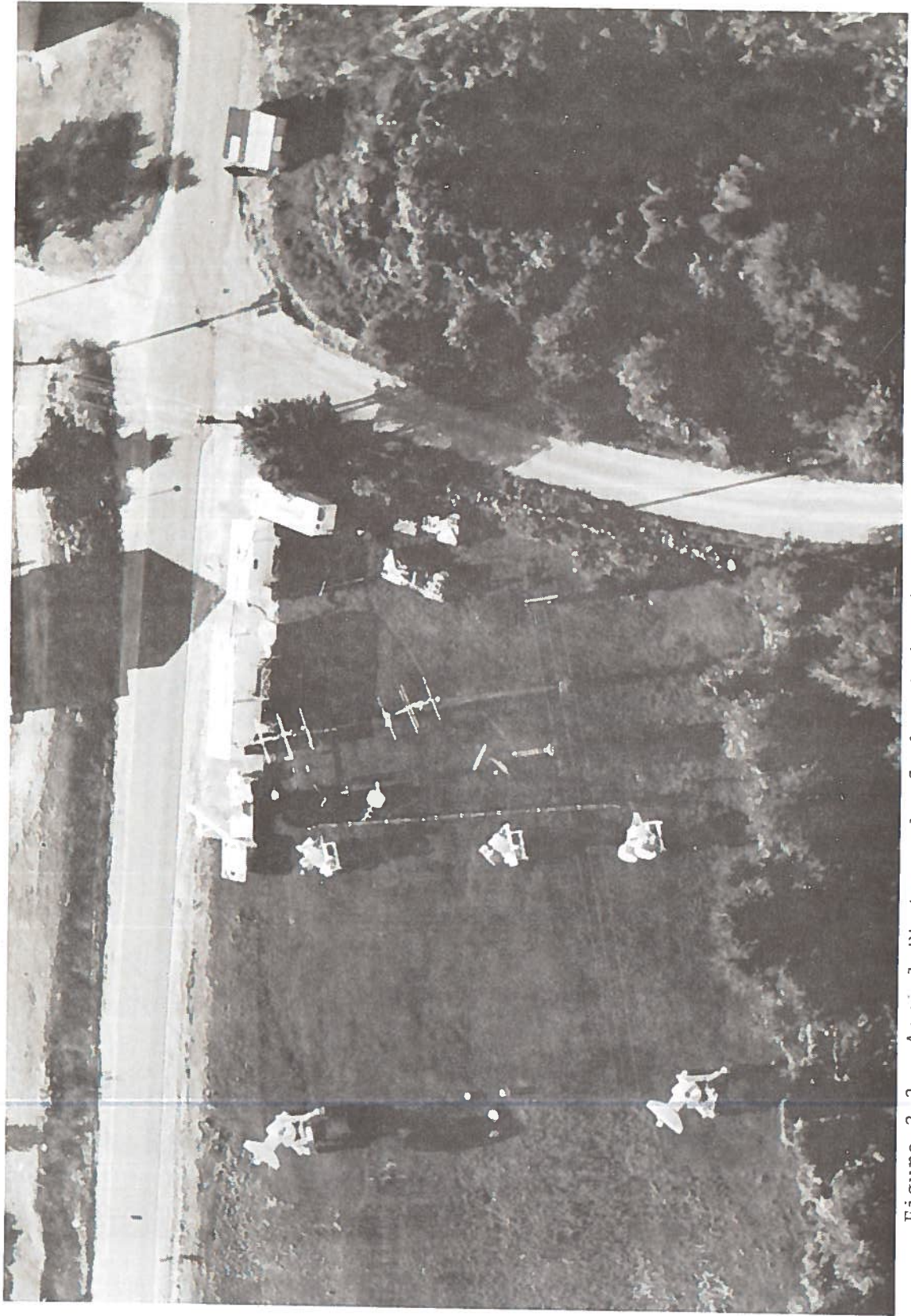


Figure 2-2. Aerial Photograph of the DOT/TSC/Westford Propagation Facility.
(Photo Courtesy of H.H. Danforth of the Haystack Microwave Research Facility)

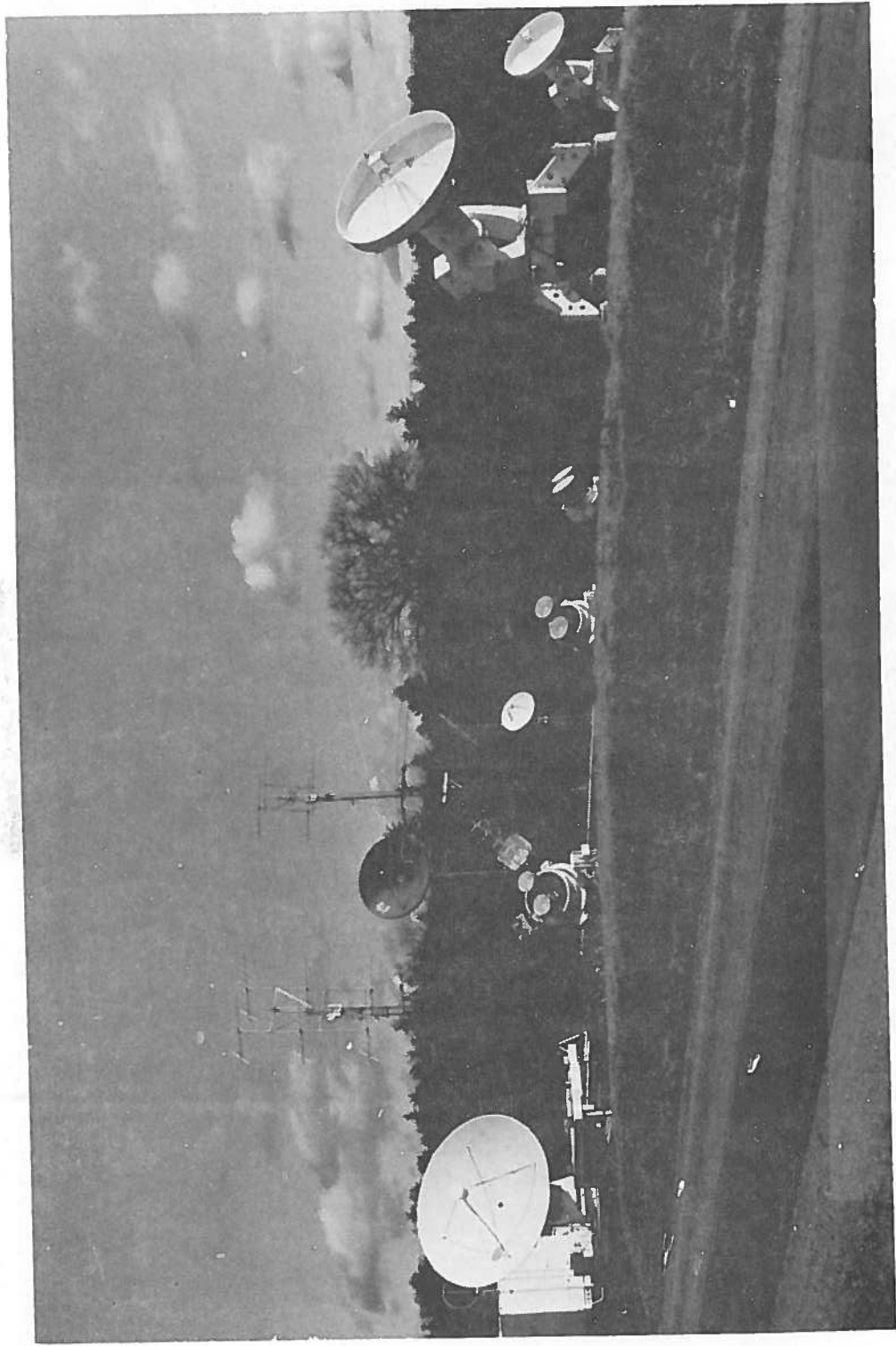


Figure 2-3. Photograph of the DOT/TSC/Westford Propagation Facility Looking Northeast

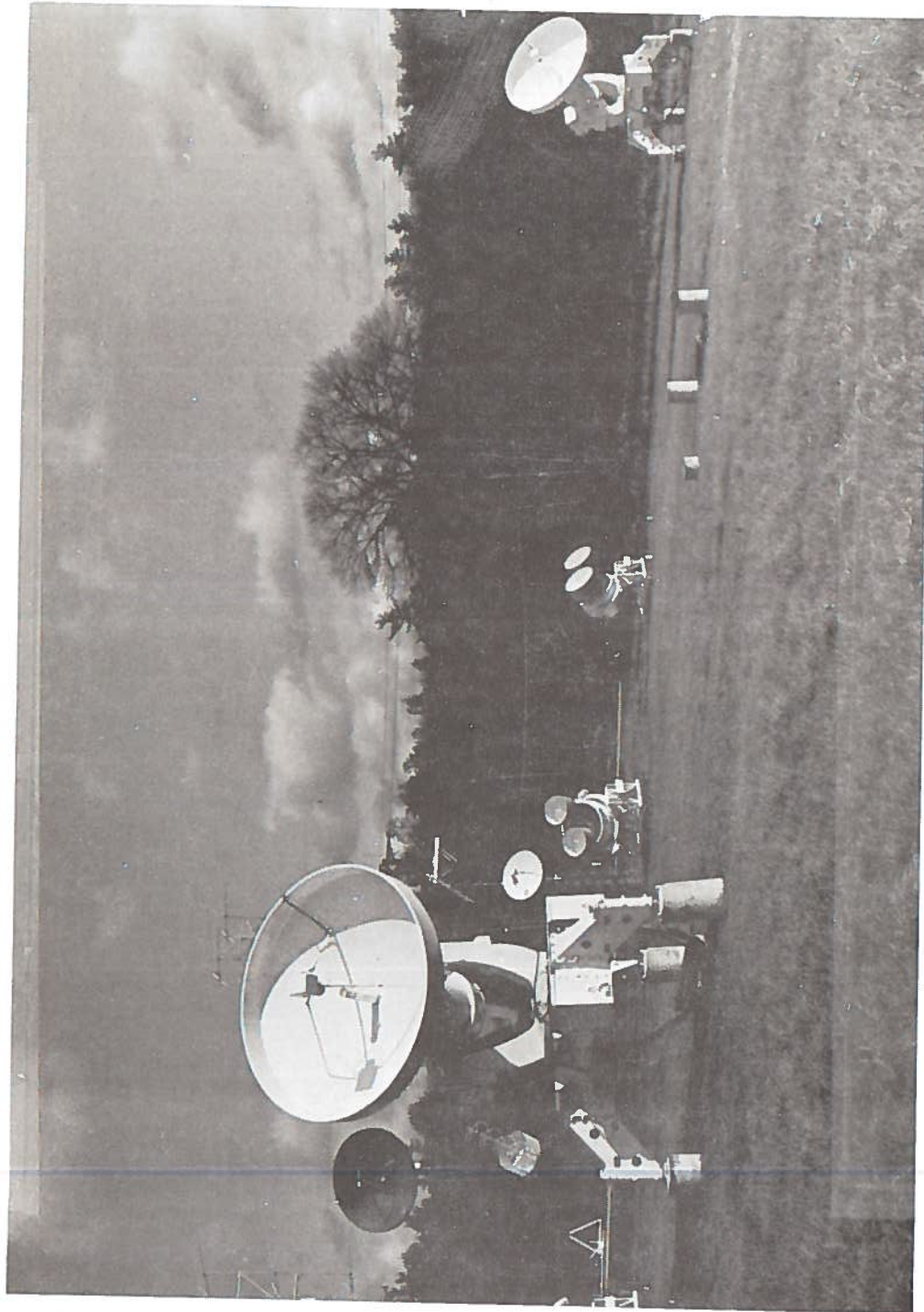


Figure 2-4. Photograph of 10-Foot Diameter Antennas Used in the L-Band Receivers

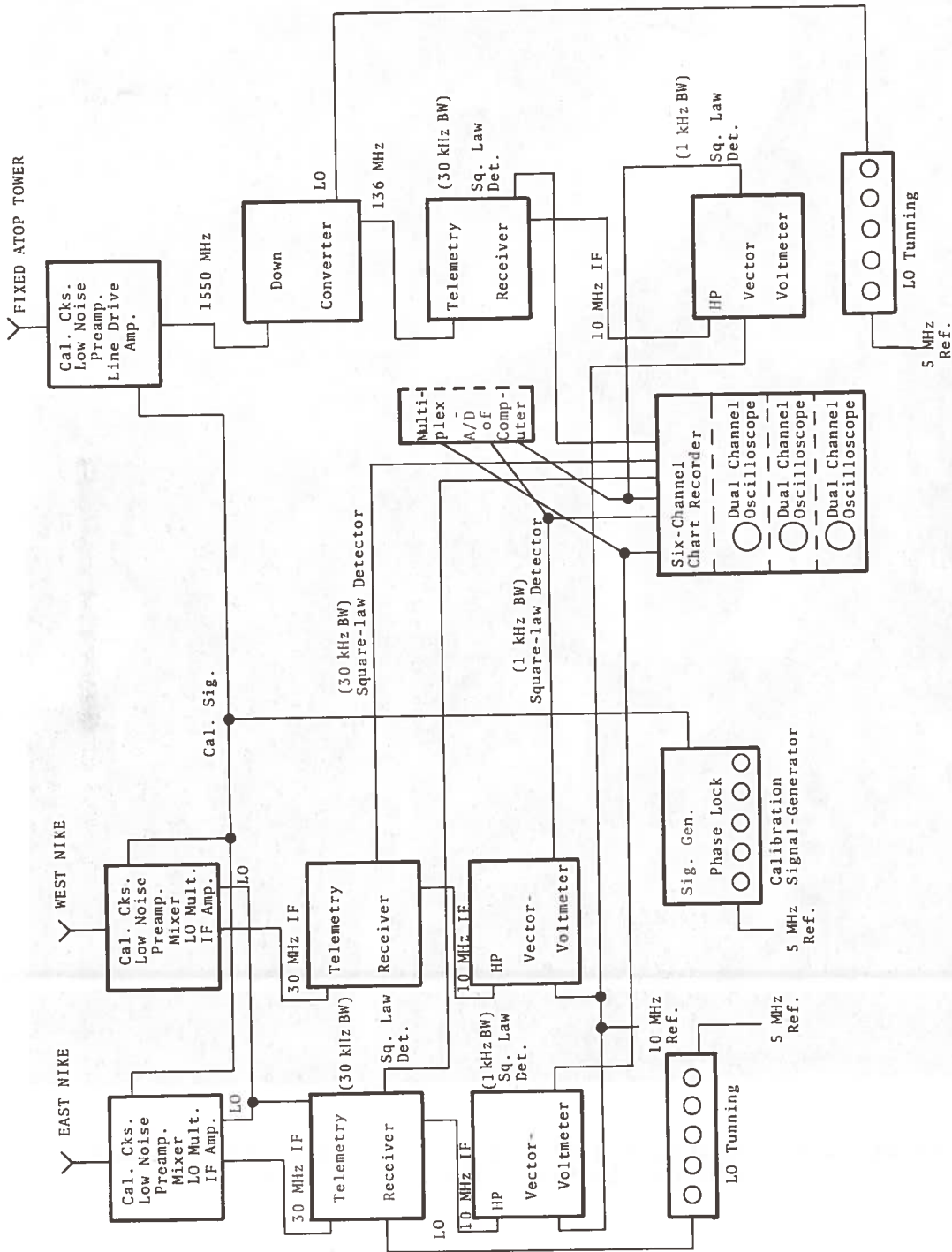


Figure 2-5. Schematic Diagram of the L-Band Receiving System at the Westford Propagation Facility



Figure 2-6. Photograph of Two 10-Foot Diameter Antennas Mounted in Nike-Ajax Mounts

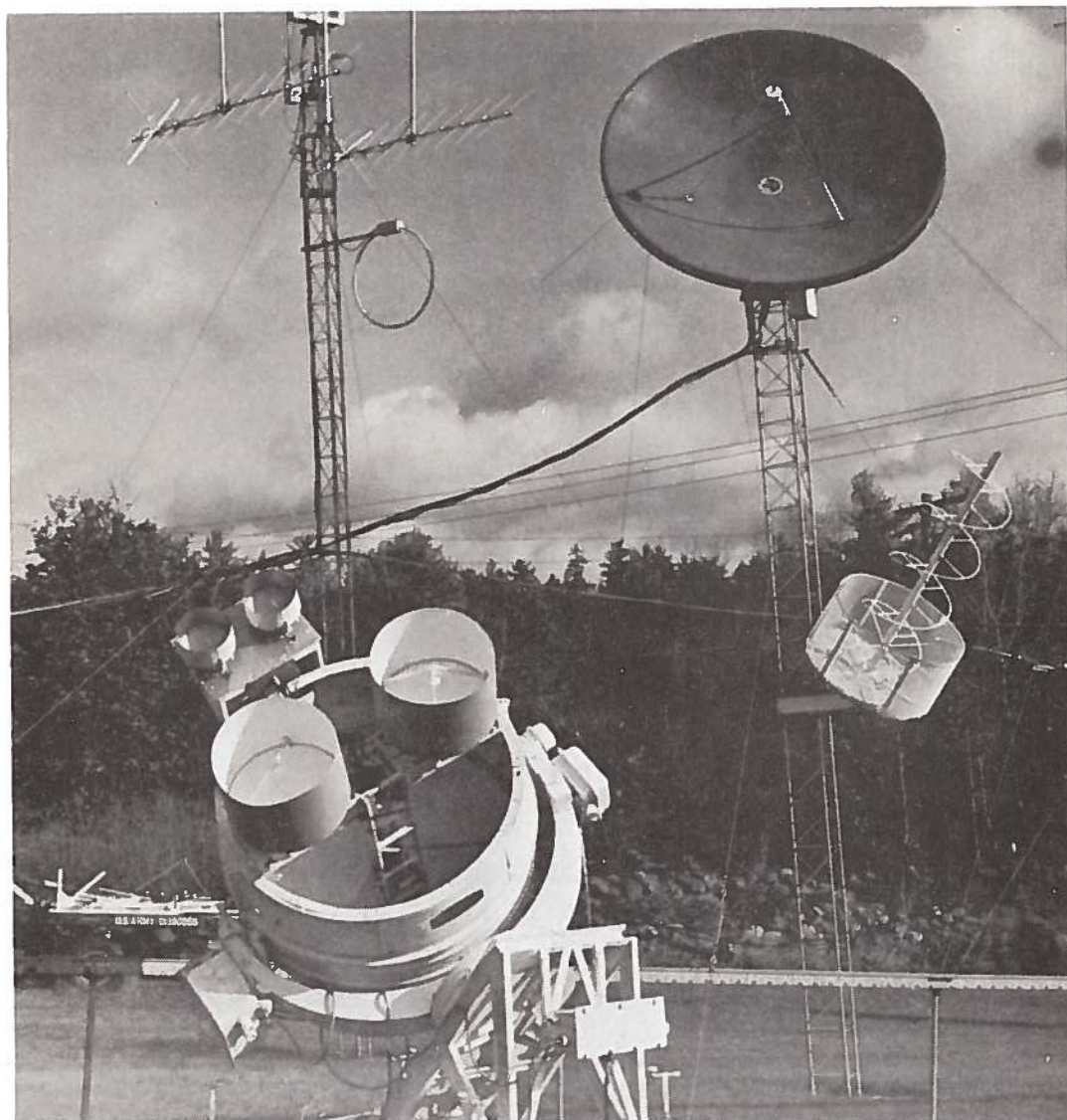


Figure 2-7. Photograph of 10-Foot Diameter Antenna Mounted Atop a 30-Foot High Tower

antenna was mounted as previously described so that the transmit diplexer could be mounted in the equipment box and the antenna system could be used for both transmitting and receiving if necessary.)

Those receiving systems mounted on the Nike-Ajax down-convert the amplified L-band signal to 30 MHz by the local oscillator-multiplier-mixer combination mounted in the large equipment boxes which are attached to the counter weights of the antenna pedestal. A 250 MHz reference local oscillator signal is sent to each Nike mount. This in turn is multiplied up to 1520 MHz and mixed with the L-band signal. The resultant 30 MHz intermediate frequency signal is amplified and routed back to a telemetry receiver located in the equipment van.

The radio frequency signal processing is different in the case of the fixed reflector installation. The received L-band signal is first amplified by a low-noise preamplifier (identical with those used in the Nike mounted reflectors.) The L-band signal is then fed to another L-band amplifier/line driver. The high level L-band signal is now routed into the equipment van. Internally, within the equipment van the L-band signal is down converted to 136 MHz and presented to a telemetry receiver.

The 30 MHz intermediate frequency signal from both Nike mounted antennas is processed by individual telemetry receivers. The receiver converts the 30 MHz to 10 MHz. It is then amplified, filtered, re-amplified and square-law detected. A portion of the 10 MHz signal after the filter is fed to a vector voltmeter. The reference for the vector voltmeter is 10 MHz from the station frequency standard. The second intermediate frequency (10 MHz) filter is a crystal filter with a 30 kHz bandwidth. The vector voltmeter has a bandwidth of 1 kHz.

The L-band signal from the fixed antenna is converted to 136 MHz by a local oscillator multiplier-mixer combination. The 136 MHz signal is fed to a telemetry receiver where it is first converted to 55 MHz then to 10 MHz. A portion of this 10 MHz signal is fed to a vector voltmeter. In the telemetry receiver the 10

MHz signal is amplified, filtered, re-amplified and square-law detected. The telemetry receiver with the 136 MHz input uses a crystal filter at 10 MHz with a bandwidth of 30 kHz.

The local oscillator reference signal at 250 MHz which is used by the receivers mounted on the Nike pedestals is controlled by a synthesizer operating at 60 MHz. Thus, tuning the synthesizer provides the L-band tuning in order that the received L-band signal from the ATS-5 will fall within the 1 kHz bandwidth of the vector voltmeter at 10 MHz. The local oscillator reference signal used with the receiving system employing the fixed reflector is also controlled by a frequency synthesizer. Likewise, this synthesizer is tuned to the proper frequency such that the received L-band signal falls within the 1 kHz bandwidth of the vector voltmeter.

The vector voltmeters are basically used as receivers. They employ a square-law detector following the 1 kHz filter. The voltage from the detector is amplified and is proportional to the power of the 10 MHz input signal. The square-law detectors in the telemetry receivers following the 30 kHz intermediate frequency filters also produce a DC voltage proportional to the power of the 10 MHz intermediate frequency signal.

The 30 kHz detector voltage from each of the three telemetry receivers is chart recorded simultaneously with the detected voltage from each of the three vector voltmeters. The instrument used to record the voltages has six channels. The calibration of the chart recorder is simplified because of the identical calibration of the three vector voltmeters. Also the calibration of the three 30 kHz detected voltages are the same.

It is only the three detected voltages from the narrow-band vector voltmeters that are digitized and recorded on magnetic tape for computer processing.

These points are covered in greater detail in the earlier referenced report along with all the detector calibrations and bandpass characteristics.

2.2 L-BAND TRANSMITTING EQUIPMENT

The L-band uplink signal to the ATS-5 spacecraft is radiated from Westford. The final amplifier is a 200 watt traveling wave tube operating in saturated condition. The 200 watt signal is carried through 50 feet of rigid feedline to the antenna feed of a 15-foot solid reflector (Figure 2-8). The antenna feed is such that right circulator polarization is transmitted. The antenna is mounted on an elevation-over-azimuth antenna mount shown in Figure 2-8. A 2 watt signal from the L-band exciter is used to drive the final traveling wave tube amplifier. A high power narrow-band filter installed after the output of the final amplifier insures that there are no out-of-band spurious responses transmitted.

The L-band exciter-driver, a double conversion type, is shown in Figure 2-9. The input to the exciter is at 70 MHz from the modulator unit. In this case the modulator signal is a pure continuous wave signal (actually the 70 MHz is derived from the station's 5 MHz by standard multiplying and filtering).

The 70 MHz signal is mixed with 500 MHz to provide an intermediate frequency of 570 MHz. The 500 MHz oscillator signal is derived and controlled precisely from a frequency synthesizer operating near 20 MHz. Thus by tuning the synthesizer the 570 MHz signal is tuned.

The 570 MHz signal is amplified, filtered and mixed with a 1080 MHz signal. The 1080 MHz signal is also produced by multiplying and filtering a 5 MHz signal from the station standard. The 570 MHz signal and the 1080 MHz are mixed and the resultant 1650 MHz signal is amplified, filtered and re-amplified up to the 2 watt level.

The output signal at 1650 MHz is thus derived from the station standard and is tunable by use of a frequency synthesizer (this synthesizer as with those used in the receiver are all phase locked to the station standard). The actual output frequency is 1651.270 MHz which when repeated by the ATS-5 spacecraft gives a downlink frequency of 1550.250 MHz.

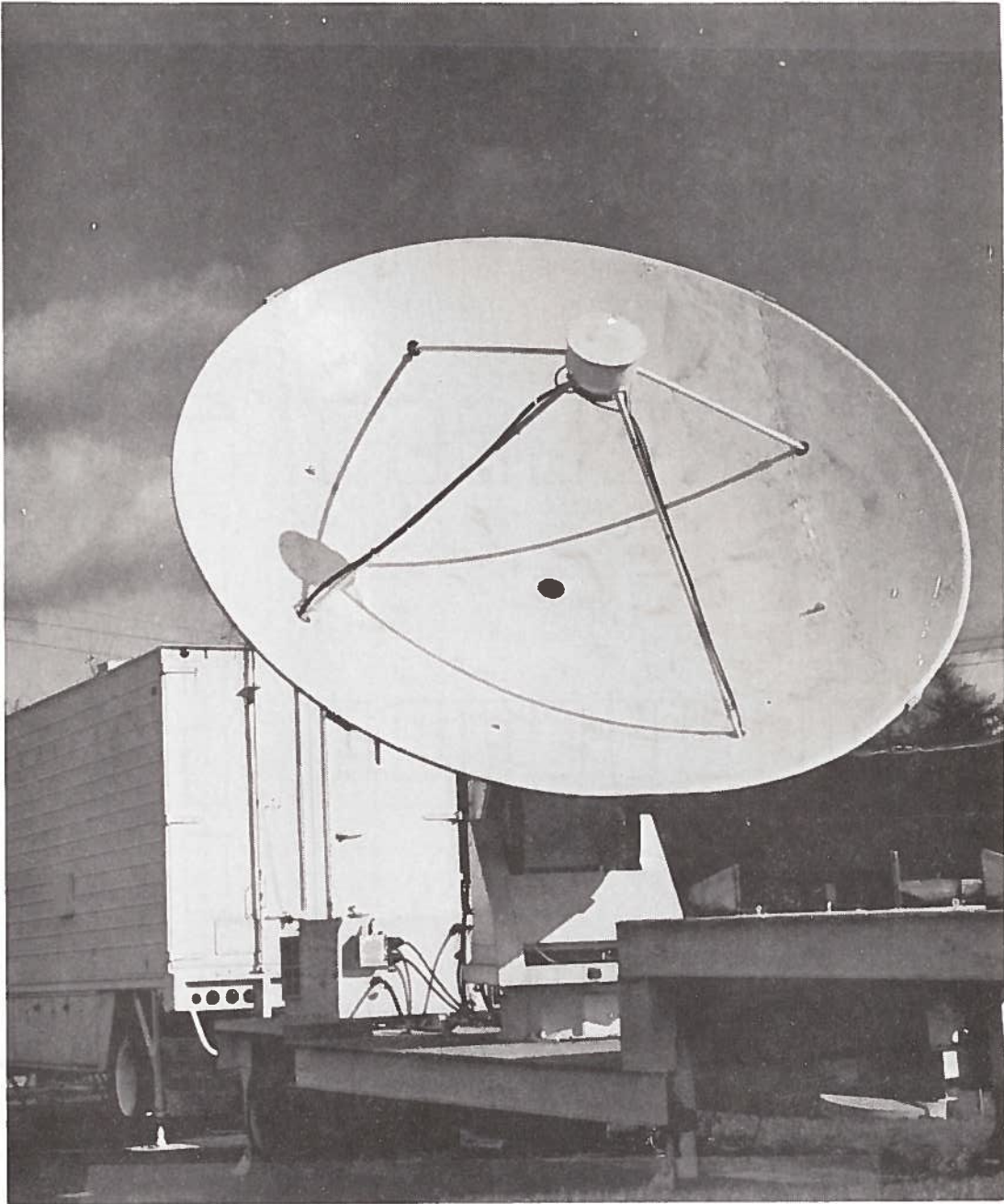


Figure 2-8. Photograph of the L-Band 15-Foot Diameter Transmitting Antenna

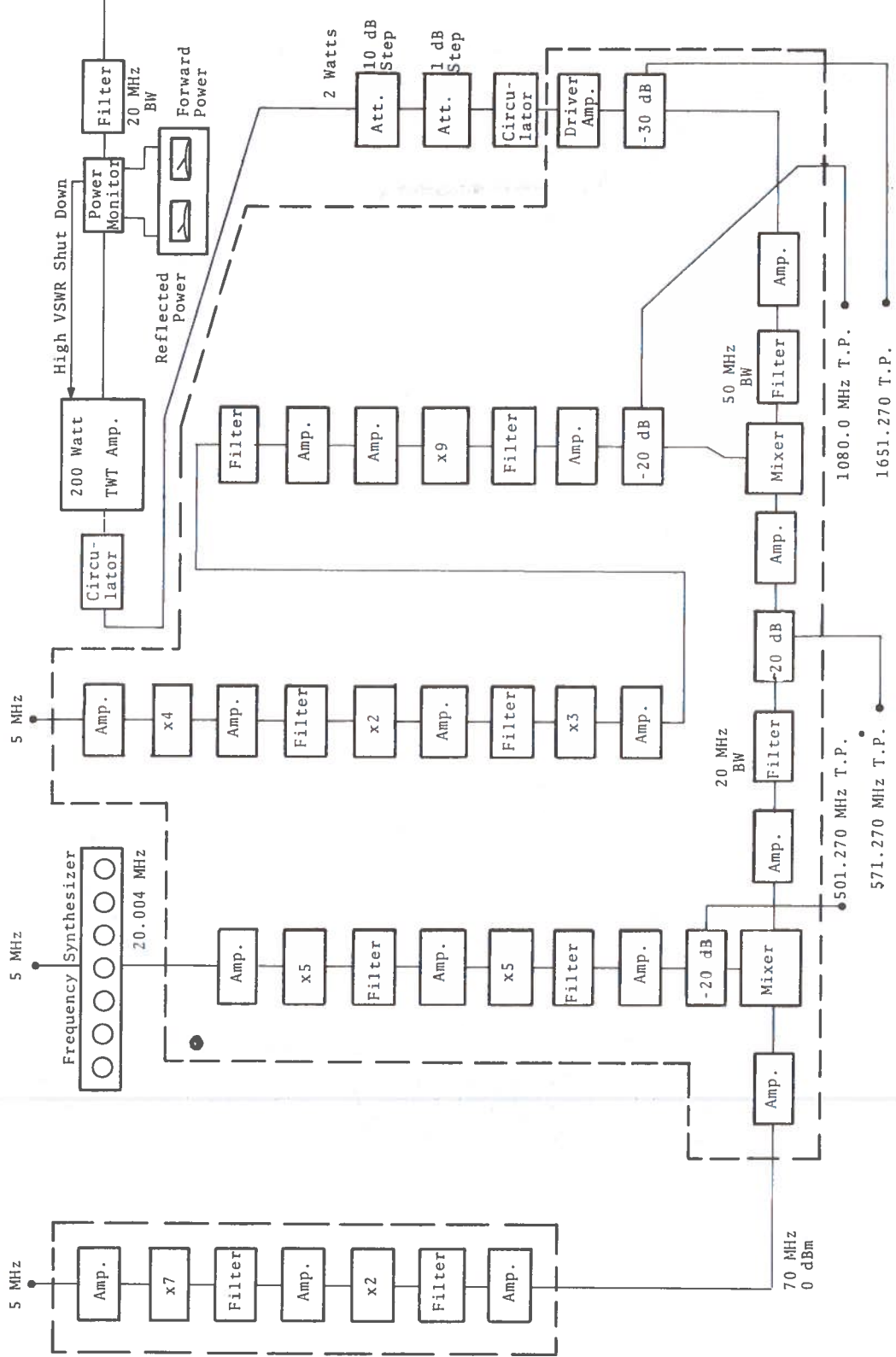


Figure 2-9. Block Diagram of the L-Band Exciter/Power Amplifier

One of the very important considerations in this series of measurements is to be sure that the uplink signal received at the ATS-5 does not fluctuate due to propagation variations. Thus adequate power must be transmitted to assure that the satellite remains saturated and does not re-transmit power fluctuations presented to its input under conditions of inadequate input. In order to determine the margin or amount by which the spacecraft transponder is saturated a test run was made. The results of the test are shown in Figure 2-10. Here the ground transmitter power is plotted against the received signal strength of the retransmitted signal. Note that with a reduction of about 7 dB in the transmitter power the downlink signal decreases only about 0.1 dB. Thus the 7 dB margin in the uplink is sufficient to keep the retransmitted downlink signal essentially unaffected by uplink propagation path fades.

2.3 L-BAND LINK CALCULATIONS

For transmitting and receiving antennas axially aligned in the far-field the power at the receiving terminal is expressed by the following relation:

$$P_R = (P_T G_T) G_R P_C \text{ watts} \quad (2-1)$$

where:

- $P_T G_T$: effective radiated power of the transmitted signal (w),
- P_T : transmitter power (w)
- G_T : effective power gain of transmit antenna on-axis (dB),
- G_R : effective power gain of receiving antenna on-axis (dB),
- $P_C = \left(\frac{\lambda}{4\pi D}\right)^2$: free space path loss,
- D : range between antennas (m),
- λ : wavelength of transmitted signal (m).

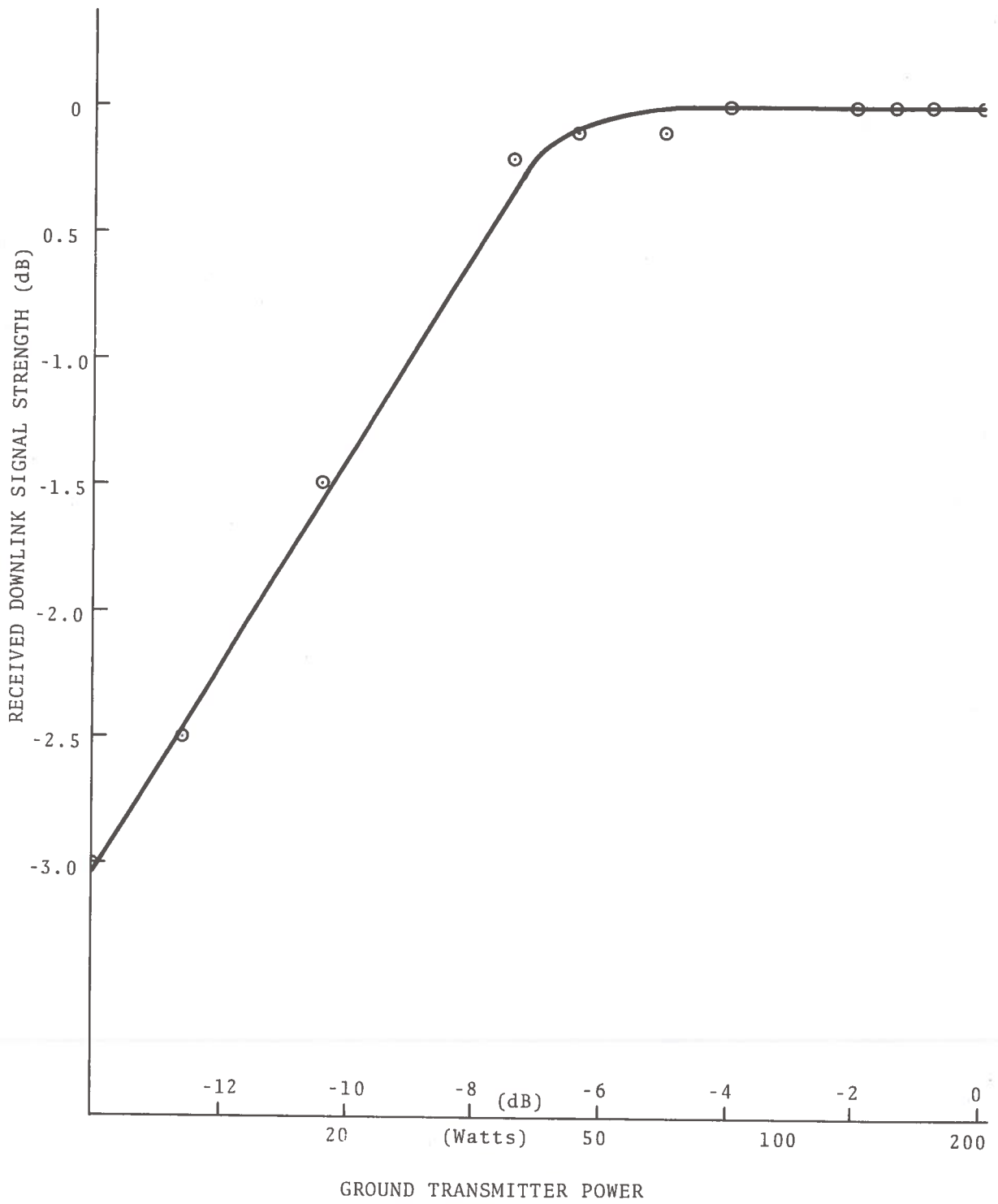


Figure 2-10. ATS-5 L-Band Narrowband Frequency Translation Mode Transponder Compression (December 12, 1973)

A_p : free space attenuation = $20 \log P_c$ (dB)

The receiver system temperature is from Kraus (1966);

$$T_S = T_A + T_O(1/L - 1) + 1/L T_R \quad (2-2)$$

where:

T_S : is the system temperature (K),

T_R : is the receiver's effective noise temperature (K),

L : is the receiver transmission line loss (dB), expressed as an efficiency factor,

T_A : is the sky temperature, estimated at 20K,

T_O : is the ambient temperature 290 K.

The received signal-to-receiver noise power density is

$$\frac{P_R}{N_O} = \frac{P_R}{kT_S} \text{ dB-Hz} \quad (2-3)$$

where:

N_O : is the receiver noise power density which is kT_S

k : is Boltzmann's constant 1.38×10^{-23} joules/K.

To calculate the ground effective radiated power, at the ground

P_{TG_T} , the following is applicable

$$P_{TG_T} = \begin{matrix} 23 \text{ dB} \\ \text{(transmitted)} \\ \text{power} \end{matrix} + \begin{matrix} 35 \text{ dB} \\ \text{(antenna)} \\ \text{gain} \end{matrix} - \begin{matrix} 1 \text{ dB} \\ \text{(feed)} \\ \text{loss} \end{matrix} = 57 \text{ dBw.} \quad (2-4)$$

To calculate the uplink path loss equation (2-1) with

$$\lambda = 0.181 \text{ m (1651.270 MHz)}$$

$$D = 38,500,000 \text{ m} = 3.85 \times 10^7 \text{ m}$$

the actual range varied between 3.877×10^7 m and 3.842×10^7 m

$$\left[\frac{1.81}{(4\pi)3.85} \times 10^{-8} \right]^2 = \left\{ 3.75 \times 10^{-10} \right\}^2 = 14.1 \times 10^{-20} = P_c \quad (2-5)$$

or expressed in dB: $A_p = + 11.5 \text{ dB} - 200 \text{ dB} = -188.5 \text{ dB}$

The received power into the spacecraft receiver is thus

$$P_R = + 57 \text{ dBw} + \begin{matrix} 15.0 \text{ dB} \\ \left(\begin{matrix} \text{Receiving} \\ \text{Antenna} \\ \text{Gain} \end{matrix} \right) \end{matrix} - \begin{matrix} 2.3 \text{ dB} \\ \left(\begin{matrix} \text{Receiver} \\ \text{Loss} \end{matrix} \right) \end{matrix} - \begin{matrix} 188.5 \text{ dB} \\ \left(\begin{matrix} \text{Free Space} \\ \text{Loss} \end{matrix} \right) \end{matrix} - \begin{matrix} 3.0 \text{ dB} \\ \left(\begin{matrix} \text{Other} \\ \text{Propagation} \\ \text{Losses} \end{matrix} \right) \end{matrix}$$

$$= - 121.8 \text{ dBw} \quad (2-6)$$

The receiver noise power density (N_o) of the ATS-5 is

$$N_o = 1.38 \times 10^{-23} \times 1760^\circ = 2.43 \times 10^{-20} \text{ w/Hz} \quad (2-7)$$

$$\left(\begin{matrix} \text{Boltzmann's} \\ \text{Constant} \end{matrix} \right) \left(\begin{matrix} \text{ATS-5} \\ \text{System} \\ \text{Temperature} \end{matrix} \right)$$

or expressed in dBw:

$$N_o = + 3.86 \text{ dBw} - 200 \text{ dBw} = - 196.14 \text{ dBw/Hz} \quad (2-8)$$

Thus

$$\frac{P_R}{N_o} = - 121.8 \text{ dBw} - (-196.14 \text{ dBw/Hz}) \quad (2-9)$$

$$= 74.3 \text{ dB-Hz}$$

The bandwidth of the ATS-5 in the narrow-band frequency translation mode is 2.5 MHz (64 dB). Thus the signal-to-noise ratio in the spacecraft intermediate frequency is

$$S/N = 10.3 \text{ dB} \quad (2-10)$$

The uplink and downlink calculations are summarized in Table 2-2.

To calculate the spacecraft effective radiated power, ($P_T G_T$) we have

$$10 \text{ dBw} + 14 \text{ dB} - 2 \text{ dB} = 22 \text{ dBw} \quad (2-11)$$

$$\left(\begin{matrix} \text{Spacecraft} \\ \text{Transmitter} \\ \text{TWT} \end{matrix} \right) \left(\begin{matrix} \text{Spacecraft} \\ \text{Transmit} \\ \text{Antenna Gain} \end{matrix} \right) \left(\begin{matrix} \text{Feed} \\ \text{Losses} \end{matrix} \right)$$

TABLE 2-2. POWER BUDGET FOR ATS-5 - WESTFORD PROPAGATION FACILITY L-BAND LINK

Factor	Value	Remarks
<u>Uplink (1651.270 MHz)</u>		
Ground Transmitter Power (dBw)	+ 23.0	200 watts
Feed Line Losses (dB)	- 1.0	
Antenna Gain (dB)	+ 35.0	15-foot diameter
GROUND ERP (dBw)	+ 57.0	
Path Loss (dB)	- 188.5	Note 1
Spacecraft Receiver Antenna Gain (dB)	+ 15.0	
Spacecraft Receiver Feed Line Loss (dB)	- 2.3	
Ground Antenna Pointing Error (dB)	- 1.0	
Polarization Loss (dB)	- 0.2	
Tropospheric Attenuation (dB)	- 0.2	
Spacecraft Pointing Error (dB)	- 1.6	Note 2
RECEIVED SIGNAL POWER INTO SPACECRAFT RECEIVER (dBw)	- 121.8	
Spacecraft Receiver Noise Temperature (K)	+1760.0	
Spacecraft Receiver NPD (dBw/Hz)	- 196.14	
RECEIVED CARRIER TO NPD RATIO (dB-Hz)	+ 74.3	
Spacecraft Receiver Noise BW (dB)	- 64.0	2.5 MHz
SIGNAL-TO-NOISE RATIO IN IF BANDPASS (dB)	+ 10.3	

continued

TABLE 2-2. POWER BUDGET FOR ATS-5 - WESTFORD PROPAGATION FACILITY L-BAND LINK (Continued)

Factor	Value	Remarks
<u>Downlink (1550.250 MHz)</u>		
Spacecraft Transmitter Power (dBw)	+ 10.0	1 TWT
Spacecraft Feed Line Losses (dB)	- 2.0	
Spacecraft Transmit Antenna Gain (dB)	+ 14.0	
NET SPACECRAFT ERP (dBw)	+ 22.0	
Path Loss (dB)	- 187.9	38,500 km, Note 1
Ground Receiver Antenna Gain (dB)	+ 30.0	10-ft. Diameter
Receiver Feed Line Loss (dB)	- 0.2	
Ground Antenna Pointing Error (dB)	- 1.0	
Polarization Loss (dB)	- 0.2	
Tropospheric Attenuation (dB)	- 0.2	
Spacecraft Pointing Error (dB)	- 1.6	Note 2
RECEIVED SIGNAL POWER INTO GROUND RECEIVER (dBw)	- 139.1	
Ground Receiver Noise Temperature (K)	+ 360.0	
Ground Receiver NPD (dBw/Hz)	- 203.0	
Received Signal to NPD Ratio (dB-Hz)	+ 63.9	
Spacecraft Received Power/NPD (dB-Hz)	+ 74.3	
Actual Carrier to NPD Ratio in Ground Receiver (dB-Hz)	+ 63.3	
Ground Receiver Bandwidth (dB)	- 30.0	1 kHz
Ground Receiver Bandwidth (dB)	- 44.8	30 kHz
Signal-to-Noise Ratio in Ground Receiver (dB)	+ 33.3	1 kHz BW
Signal-to-Noise ratio in Ground Receiver (dB)	+ 18.5	30 kHz BW

Note 1: Range goes from a minimum of 38,420 km to a maximum of 38,777 km. The value used above (38,500 km) is the nominal range.

Note 2: Corresponds to the maximum diurnal variation.

To calculate the path loss (see equation (2-1)):

$$\lambda = 0.194 \text{ m (1550.250 MHz)}$$

$$D = 3.85 \times 10^7 \text{ m}$$

$$P_c = \left\{ \frac{1.94 \times 10^{-8}}{4 \cdot \pi \cdot 3.85} \right\}^2 = [4.01 \times 10^{-10}]^2 = 16.08 \times 10^{-20} \quad (2-12)$$

expressed in dB: $A_p = + 12.1 \text{ dB} - 200 \text{ dB} = - 187.9 \text{ dB}$

The received power into the ground receiver is thus

$$P_R = +22 \text{ dBw} + \begin{matrix} \text{(Net} \\ \text{Spacecraft} \\ \text{ERP)} \end{matrix} + \begin{matrix} \text{(Ground} \\ \text{Receiver} \\ \text{Antenna} \\ \text{Gain)} \end{matrix} 30 \text{ dB} - \begin{matrix} \text{(Feed} \\ \text{Line} \\ \text{Loss)} \end{matrix} 0.2 \text{ dB} - \begin{matrix} \text{(Path} \\ \text{Loss)} \end{matrix} 187.9 \text{ dB} - \begin{matrix} \text{(Other} \\ \text{Propagation} \\ \text{Losses)} \end{matrix} 3.0 \text{ dB}$$

$$P_R = - 139.1 \text{ dBw} \quad (2-13)$$

The noise power density of a ground receiver is:

$$N_o = (1.38 \times 10^{-23})(360) = 4.97 \times 10^{-21} \text{ w/Hz} \quad (2-14)$$

or expressed in dBw: $+ 7.0 \text{ dBw} - 210.0 \text{ dBw} = - 203.0 \text{ dBw/Hz}$.

Therefore,

$$\frac{P_R}{N_o} = 139.1 \text{ dBw} - (-203.0 \text{ dBw/Hz}) = 63.9 \text{ dB-Hz}. \quad (2-15)$$

The received power-to-noise power density ratio in the spacecraft was 74.3 dB-Hz which, assuming no improvement due to the limiters in the spacecraft transponder, is the transmitted carrier-to-noise ratio. Thus, the actual carrier plus noise-to-noise ratio in the ground receiver is

$$63.9 \text{ dB/Hz} - 0.6 \text{ dB} = 63.3 \text{ dB-Hz} \quad (2-16)$$

Thus when using the 1 kHz bandwidth or the 30 kHz bandwidth of the ground receivers gives signal-to-noise ratios of 33.3 dB and 18.5 dB respectively. The calculation is summarized in Table 2-2.

2.4 DATA ACQUISITION

The automatic data acquisition is done using a Hewlett-Packard 2114B computer. The data measurements are preprocessed and stored on magnetic tape. The data taking is accomplished in 15-minute cycles. During the first 12 minutes of the cycle, measurements are conducted with the L-band signal from the spacecraft. The last three minutes of the cycle are used for calibrating the receivers and entering the calibration levels and other information into the computer through its teletype unit. The typed information resulting from the teletype printer is a permanent log of the data acquisition process. The data acquisition cycles start on the quarter-hour.

The actual voltages that are digitized, analyzed, and stored by the computer are the detector voltages from the vector voltmeters. This was discussed in Section 2.1 and is shown in Figure 2-5.

The procedure for the calibration and data acquisition is as follows. First the receiver tuning is verified to be certain that the signal falls within the passband of the vector voltmeter. The vector voltmeter's detector voltage is presented simultaneously to the computer's analog-to-digital converter, to a strip chart recorder, and to an oscilloscope. The visual response of the oscilloscope verifies the receiver tuning. Also, any indication of receiver overloading is simultaneously displayed by the oscilloscope. Since the ATS-5 signal is pulsed due to the spacecraft spinning the entire dynamic range of the signal is adequately displayed on the oscilloscope. This feature provides the opportunity to verify that there is no overloading of the receiver.

At this time it is appropriate to point out and illustrate a consideration that was discussed earlier in Section 2.2. Since the spacecraft transponder is operated well into saturation, the correct pointing of the ground transmit antenna cannot be accurately determined by monitoring the strength of the retransmitted signal on the ground. The procedure for adjusting the transmit antenna pointing is to monitor the apparent sidelobe level of the signal from the spacecraft.

As the spacecraft spins, its antenna pattern sweeps through the ground receiving antenna. Thus the response displayed on the oscilloscope of the ground receiving equipment is the spacecraft's apparent antenna pattern. When the main beam of the spacecraft antenna pattern is pointed toward the earth, the received signal in the spacecraft from the ground transmitter is large enough so that the transponder is saturated. However, when a side lobe of the spacecraft antenna pattern is pointed toward the earth, the received signal is considerably weaker, and in fact the transponder is operating in a linear manner. In this case, the retransmitted signal from the transponder is proportional to the strength of its received signal. The retransmitted signal that is beamed toward the Earth at this time is also through the spacecraft's antenna side lobe. Thus, the apparent spacecraft antenna side lobe displayed on the oscilloscope are with the transponder operating in its linear region. Therefore, the ground transmitter antenna is positioned to give the maximum signal possible in the sidelobe region by viewing the apparent side lobe level on the ground receiver oscilloscope. The peak of the received signal does not change during this adjustment. Only the limiters in the transponder are driven harder.

The antenna pointing is verified once each hour and the receiver tuning for the three receivers is verified every 15 minutes. At the same time the receiver's tuning frequency is verified, the oscilloscope display for each of the vector voltmeters is checked to insure that the receivers are linear. This calibration check cannot be verified from a chart recording.

The receiver calibration is performed by switching the receiver from the antenna feed to the cable from the calibrated signal generator. The phase-locked signal generator is adjusted in frequency to be sure it is centered in the receiver's 1 kHz pass-band. Then the signal generator level is adjusted until a full scale deflection is obtained on the vector voltmeter. The cable loss is accurately a priori known and has been adjusted to be the same for each receiver. Since the signal generator incorporates a precision level set and adjustable attenuator, the actual

absolute signal strength injected into the radio frequency input of the receiver is known. The attenuator setting which gives full scale on the vector voltmeter are typed into the computer by teletype input. All the cable losses and deflection constants of the vector voltmeter are stored in the computer program. Thus, during data acquisition the voltage developed by the vector voltmeter's detector is converted into absolute signal strength by the computer program.

A very important factor concerning calibration must be mentioned here. The calibration previously discussed was in fact a continuous wave calibration and the actual data received via the spacecraft is pulsed in nature. In order to use the type of continuous wave calibration mentioned earlier for pulsed measurements of the type generated by the ATS-5 the following precautions must be verified.

- a) The response of the receiving system to a pulsed signal must be very carefully analyzed to be sure that the receiver response is not changing as the pulse changes.
- b) The low-pass filtering of the detector's voltage should be such that the pulse shape is not distorted.
- c) Variations in signal strength during the pulse, especially during the peak, should not be smoothed. The above mentioned conditions and limitations were carefully checked in the instrumentation used in the ATS-5 measurements. The calibration and measurement of these effects is discussed in a previous report by Brown et. al. (1974A).

The procedure used by the data acquisition computer program is as follows: the digitized detector voltages reading are first converted to absolute signal strength using the calibration values. This continuous set of output voltage readings for the three receivers are converted for twenty-five seconds and stored in a buffer. At the end of that time the sequence of readings corresponding to one of the receivers is searched for pulses.

In order to determine the magnitude of the pulse, the program must check the strength of the signal to insure it is above a

certain minimum (this minimum is set for a signal-to-noise ratio of 10 dB). The program then checks the rising slope of the pulse. This condition must remain constant for five successive increasing readings. It then checks for the falling slope of the pulse. There must be three successively decreasing values of signal strength following the five rising values. If the test is met, the increasing values (i.e., the top) is kept as the pulse value. The measurements are made at about 8 millisecond intervals with a resolution of 0.1 dB. The rising and falling slopes of the signal are much greater than 0.1 dB in 8 milliseconds. Thus the program experiences no difficulty in sampling the pulse successively.

If a condition of pulse behavior should exist as large noise spikes which would generate a false peak on the pulse, then the criterion of the rising followed by the falling slope would not be satisfied and the pulse would be disregarded. The program, however, would continue to search for the next pulse. The amplitude of the pulses that do meet the criteria along with the time and receiver number are tape recorded for future analysis.

The computer program takes less than a second to search through the buffer of all the measurements of the three receivers, test the measurements, and record the results. After the testing and recording the program returns to taking data for 25 seconds. This procedure continues for 12 minutes after which time the receiver checking and calibration is done. This continues for the duration of the observing period which is nominally 6 hours.

As was pointed out in Section 2.1, the 30 kHz and 1 kHz bandwidths are strip-chart recorded as well as continuously displayed on oscilloscopes. A communication receiver is also connected to one of the receivers at its 10 MHz intermediate frequency output. This provides a continuous audio monitor of the signal so as to alert the observer if there are any changes that might be occurring in the received signal.

The processing of the data tapes is accomplished using a Hewlett-Packard 2114B computer. The operation of the computer processing program is initiated by reading the measurement values

into the computer from the magnetic tapes. The program then creates a probability density table from the data of each of the three receivers. The tables have two hundred entries corresponding to a twenty dB range in signal strength with a resolution of 0.1 dB. Since the signal strengths are recorded on the data tapes with a 0.1 dB resolution each measurement may be entered into a particular position in the two hundred entry table. If for some reason the measurement values is above or below the table range, the data point is disregarded.

The data from each of the three receivers is accumulated in individual probability density tables until all the 12 minutes of data for the period have been read in.

The data processing which amounts to processing the probability density tables is accomplished by the computer program. The program operates in a conversational mode. The conversation is accomplished via the operator typing commands into the keyboard of a data terminal and the computer in turn displaying its data on the cathode ray tube of the data terminal.

With the computer data displayed before him the operator can now compare the computer calculations with the analog strip-chart recordings of the data. If for instance there is receiver drift, it might not be all evident in the computer data since all time reference is lost in the probability density table, however, it would be quite obvious by referencing the strip-chart recordings. Three independent receivers are used, if a signal receiver should fail, the data is available from the other two receivers.

Investigation of the strip-chart recordings allows a quick-look capability when fluctuations are evident on all three receivers simultaneously. This provides assurances that one is observing a propagation effect not a receiver anomaly. If only one receiver were used and the signal varied the probability that an instability in the receiver is the cause is extremely high. Three independent receiver operating on the transmitted signal reduces the probability of receiver drift as well. Drift in all three data channels, simultaneously indicates frequency drift of the transmitter or the master oscillator in the spacecraft. When this is the case, the

drift will show up in the three narrow-band (1 kHz) channels but not in the three wide-band (30 kHz) channels. For this reason the three 30 kHz channels are strip-chart recorded along with the three 1 kHz channels. During the measurement program however, a frequency drift or change was never noted in any of the data taking (a counter was used simultaneously to measure the transmitter frequency as an additional check). Those drifts and changes that were noted in the data were always due to gain changes in a receiver since both the narrow 1 kHz and the wider 30 kHz channels of that receiver both exhibited the same changes and drifts. The actual amount of drift was measured during the calibration period between the data periods.

Thus, by having both the analog strip-chart recording and the computer calculations available, the operator may select the best of the three receivers. If for some reason it is desired to edit out extraneous values from the computer data, this may also be done. Once the probability density that is to be used has been selected from the three available, it is displayed again with respect to its mean. The root-mean-square and the 90th percentile values are calculated and displayed at this time also.

The data taking periods were nominally 6 hours in length and occurred during the first three days of the week. The first day the data is taken for the 6 hours preceding sunset. The next day data is taken for approximately 3 hours before sunset to 3 hours after sunset. The third day the data is taken for the 6 hours following sunset.

The time used for the sunset time is that time when the section of the signal path at an altitude of 350 km falls into darkness. In other words, sunset at the 350 km penetration point of the signal path. This time is approximately two hours later than local sunset.

Consequently, a density table which represents twelve minutes of data is stored in a computer file and is labeled as to the number of hours, to the nearest quarter hour, before or after sunset or as sunset. For example, the first day of the week might be from 6.00 hours before sunset to 0.25 hours before sunset.

The processed data is compiled and assembled by weeks. Thus the measurements of the three days are used to represent the week. The procedure for combining the data is to add together those density tables which represent the same time interval with respect to sunset.

3. REMOTE MEASUREMENT SYSTEM

3.1 INTRODUCTION

The schematic diagram of the automatic data collection platform (ADCP) hardware is presented in Figure 3-1. In the figure are simplified functional block diagrams of the instrumentation which comprise the automatic data collection platform and the central data collection facility which is located at the DOT/TSC/Westford Propagation Facility in Westford, Massachusetts. Figure 3-1 also presents a function description of the various radio frequency links between the Applications Technology Satellite spacecrafts, the remote facility and the central facility. Figure 3-2 is a photograph of the automatic data collection platform's electronic equipment and Figure 3-3 is a photograph of the VHF and L-band antennas used with the platform.

The measurement system works as follows. The remote facility is sent all of its command and control functions via a coded VHF signal sent from the central facility. When given the proper command the remote facility monitors the scheduled L-band transmissions. The remote facility then processes, formats, and stores the L-band data until given an additional command. Upon command the remote facility transmits the processed L-band data by modulating the VHF link back to the central facility. The L-band data is demodulated from the VHF link at the central facility and further processed. A sample of data taken with the remote facility is presented in Figure 4-7.

Coded VHF signals are transmitted from the VHF transmitting system at the central facility to the ATS-1 or ATS-3 spacecraft at 149.22 MHz and are retransmitted by the satellite at 135.6 MHz to the remote facility. The 135.6 MHz signals are received by the remote facilities' VHF antenna and decoded by the remote facilities' VHF receiver. The decoded instructions are sent to the central processing unit of the remote facilities' computer to initiate the L-band receiver to make the particular measurement desired. The L-band measurements are processed, reformatted and

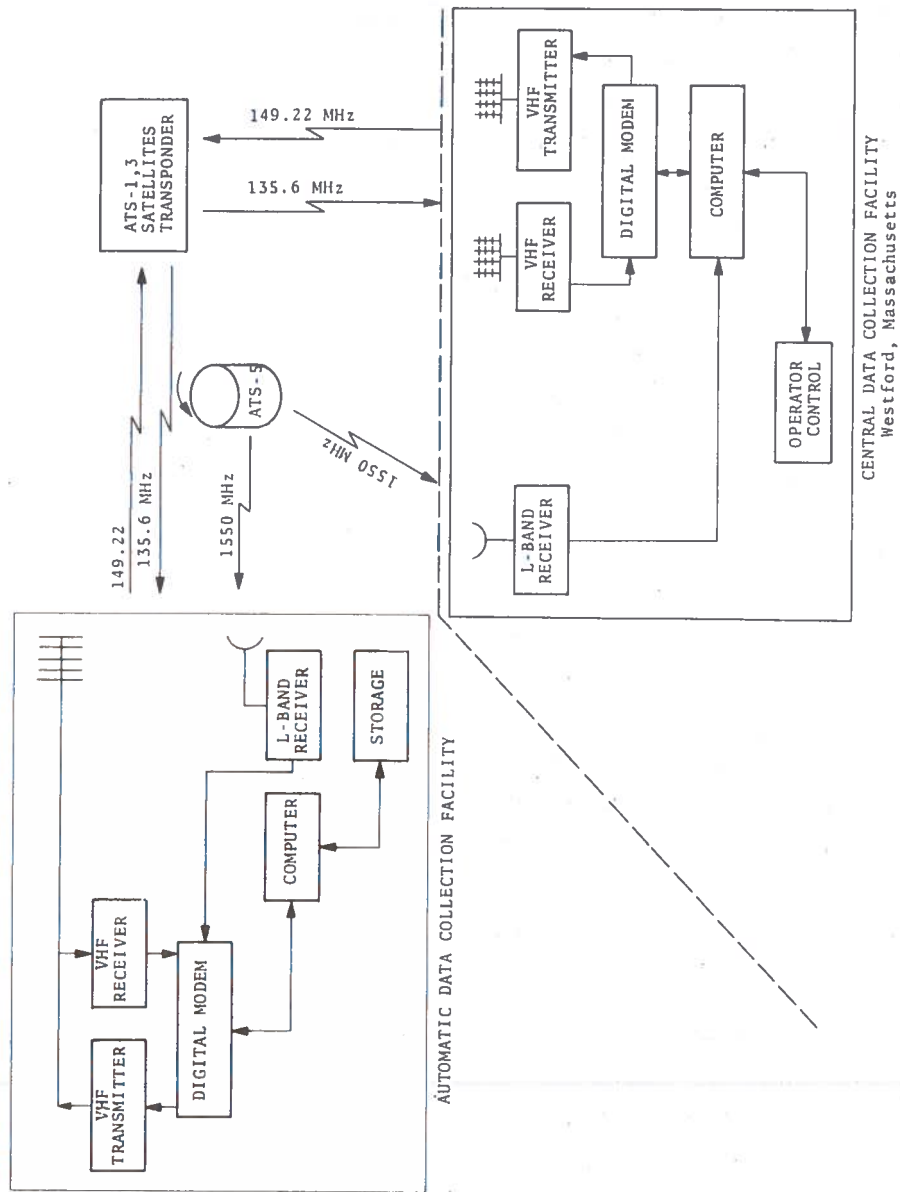


Figure 3-1. Diagram of the Remote Scintillation Data Collection Experiment

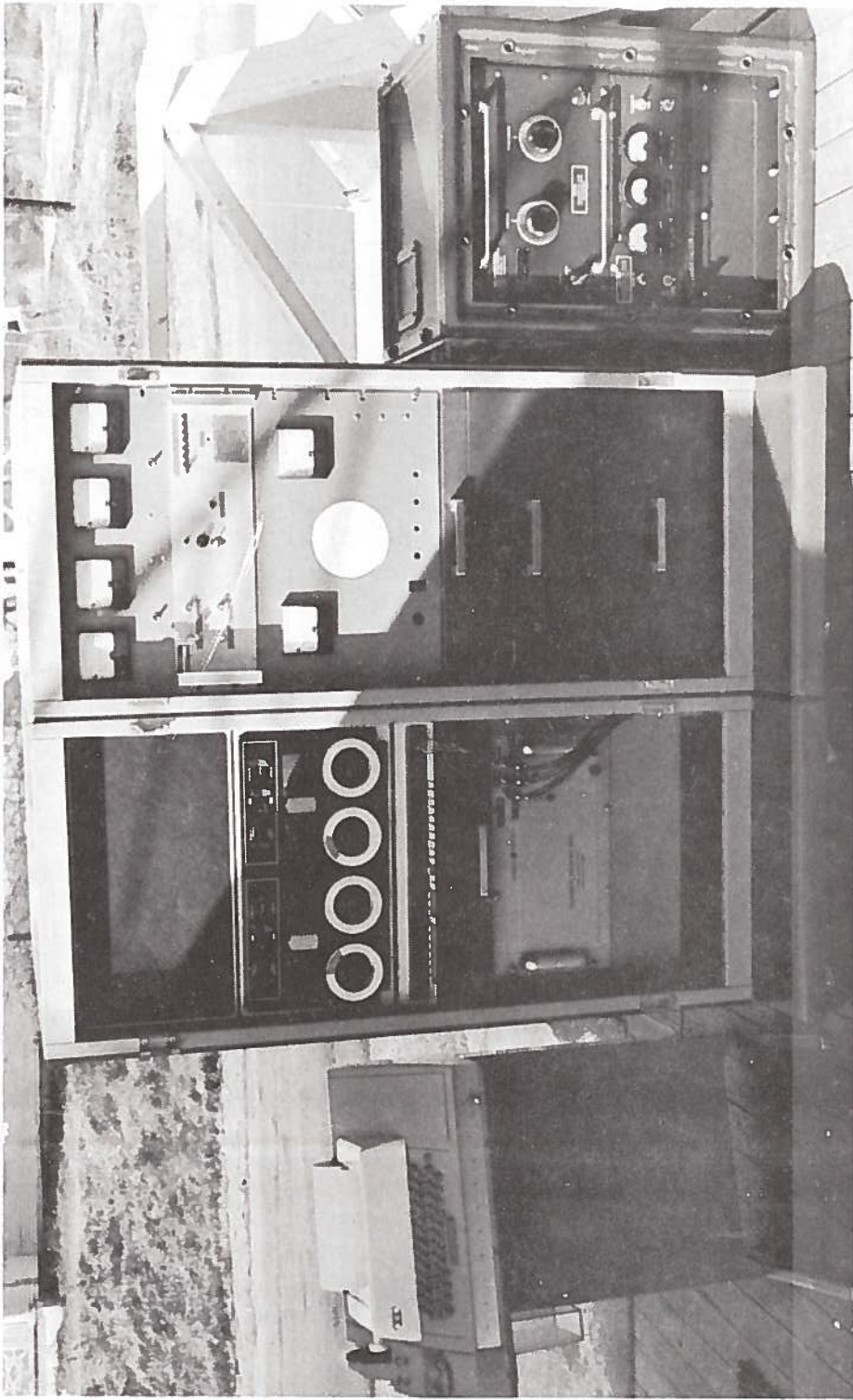


Figure 3-2. Photograph of the Automatic Data Collection Platform's Electronic Equipment

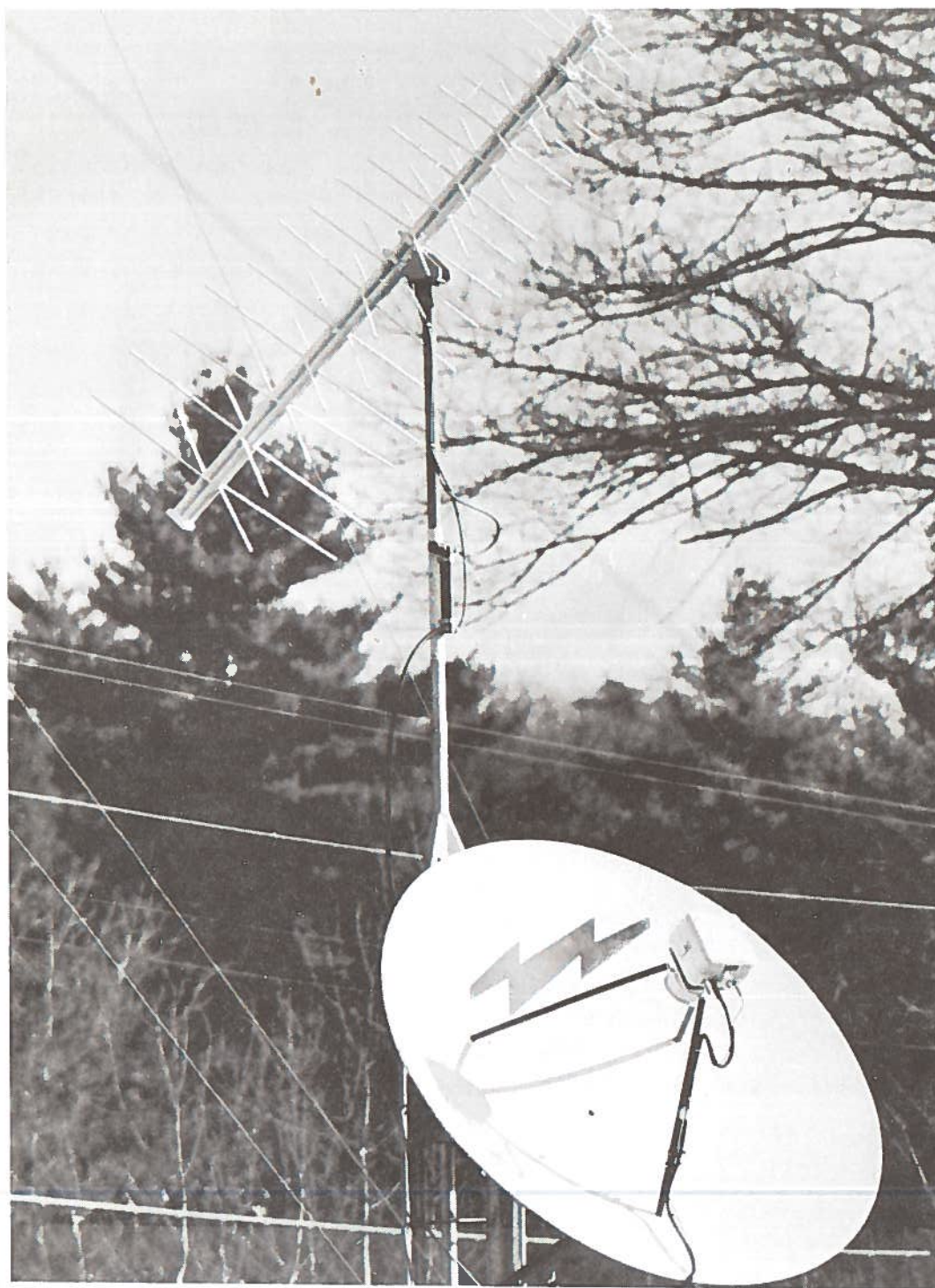


Figure 3-3. Photograph of the VHF and L-Band Antennas Used with the Automatic Data Collection Platform

stored on magnetic tape. When the proper command is received, the digital data from the magnetic tape is pulse code modulated on the 149.22 MHz VHF uplink to the appropriate geostationary satellite.* The data relayed back at 135.6 MHz will not be received by the VHF receiver at the remote facility because the receiver will be disconnected from the antenna during the transmit cycle. The VHF receiver at the central facility decodes the data and routes it to its computer's central processing unit. The data passes from the central processing unit to disc storage at the central facility for later processing after all the data from the current observing period has been received.

The remote facility will operate in a fully unmanned mode. It can receive L-band signals and measure the amplitude of the signals, digitize the signals via an 8-bit analog-to-digital converter, and record the samples together with timing information on magnetic tape and be capable of preprocessing the recorded data. Using the data scheme described herein, it is possible to store 60 hours of data at the remote facility before transmission. The L-band signal-to-noise ratio will be about 23 dB,** with the overall accuracy of the measurement being about 0.5 dB. This number includes equipment instabilities, receiver noise and processing errors. Figure 3-4 is a simplified block diagram of the ADCP.

The remote facility can be interrogated at any time through a VHF transponder via the ATS-1 or ATS-3 spacecraft based upon the availability of satellite time. The selected data can be relayed back to the central facility through the satellite upon command.

Additional details are given by Brown et. al. (1974B).

*The transmission of the data back via the pulse code modulation over the VHF links avoids scintillation contamination by the VHF links.

**This is with a spacecraft effective radiated power of 23 dBw, which is typical of most present and proposed L-band transponders.

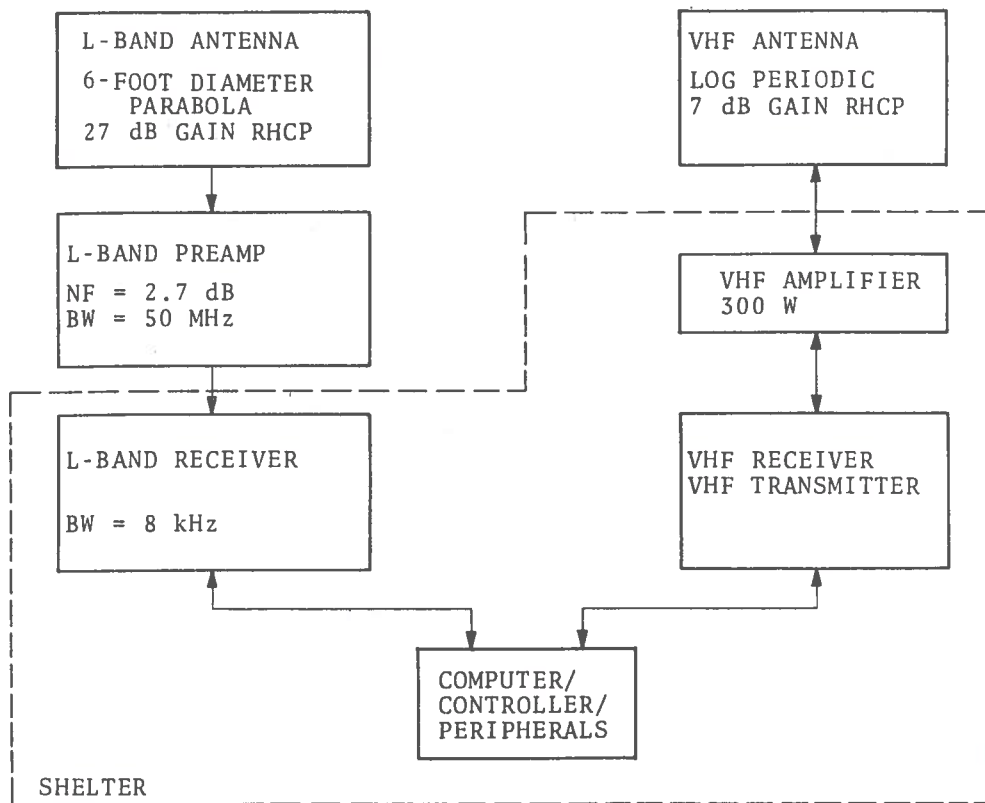


Figure 3-4. Simplified Block Diagram of the ADCP

3.2 PLATFORM L-BAND RECEIVING SYSTEM

The L-band portion of the ADCP's receiving system is shown in Figure 3-5. The 70 MHz portion of the system is shown in Figure 3-6.

The L-band section of the receiver uses a six-foot diameter reflector with a spiral feed for the reception of right-hand circular polarization. The radio frequency preamplifiers and filters are mounted directly behind the feed thus making the feedline simply the connectors and adapters on the spiral feed. The input preamplifier has a noise figure of 2.7 dB and a bandwidth of 50 MHz. Following the input preamplifier is a four-section bandpass filter with a 20 MHz bandwidth. Following the filter is a line driver amplifier with a 100 MHz bandwidth. The overall gain of the two and the filter is 45 dB. The preamplifiers and filter are housed in a weather-proof electromagnetically-shielded case with provisions for a heater.

The high level signal from the antenna assembly is cabled to the L-band receiving equipment mounted in the equipment rack. The L-band signal is then converted down to the first intermediate frequency in a broadband mixer. The radio frequency input bandpass of the mixer is 1 to 2 GHz and the intermediate frequency output bandpass is 10-200 MHz. The conversion gain at 70 MHz (radio frequency in to intermediate frequency out) is 25 dB.

The first local oscillator is a crystal-controlled oscillator with a stability of one part per million. The crystal of the first local oscillator may be replaced, at present the local oscillator crystal provides for reception at 1550.250 MHz.

The L-band receiver's sensitivity may be calculated as was done in Section 2 using equation (2-2):

$$T_S = T_A + T_o(1/L - 1) + 1/L T_R \quad (3-1)$$

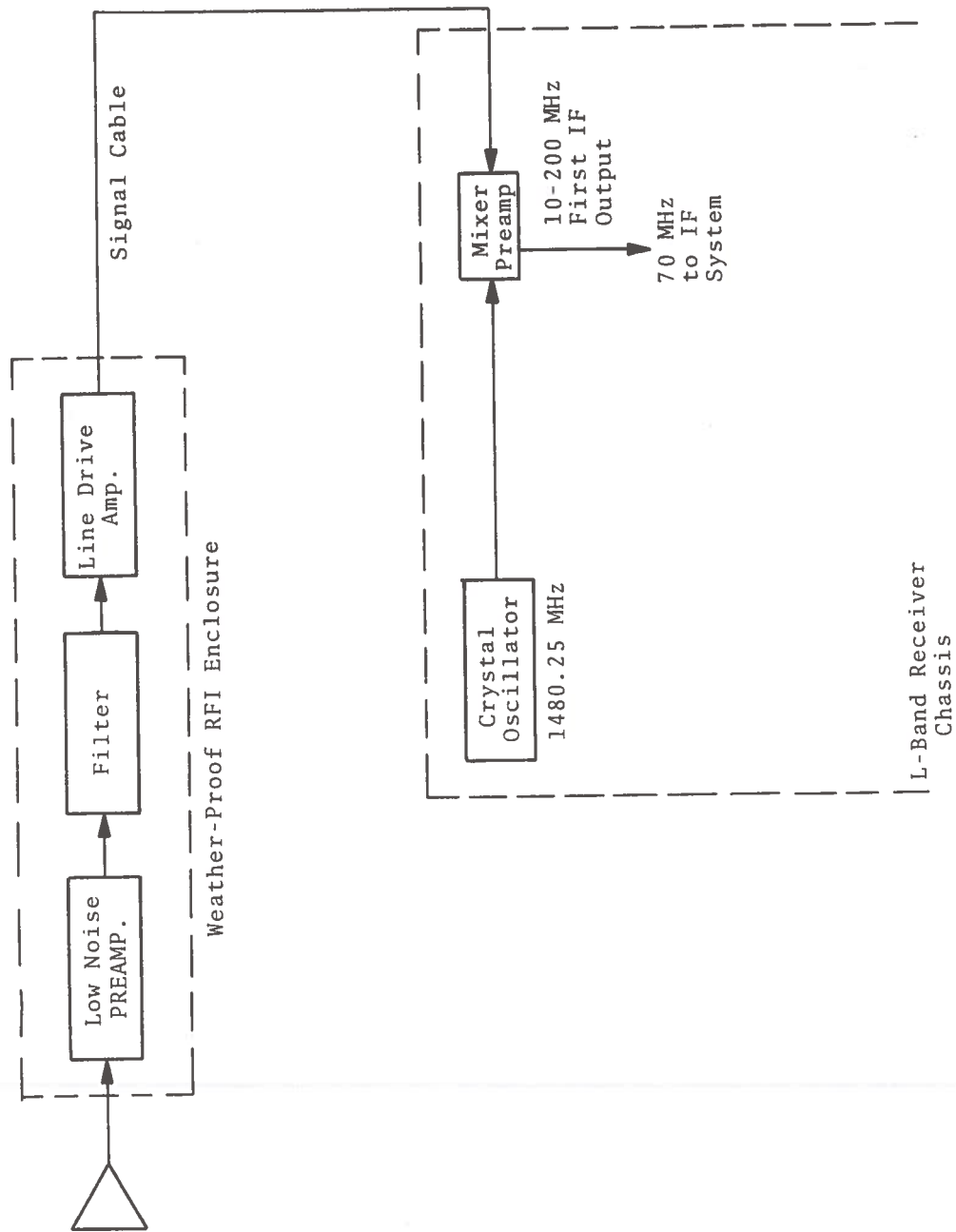


Figure 3-5. L-Band Section of ADCP's Receiver

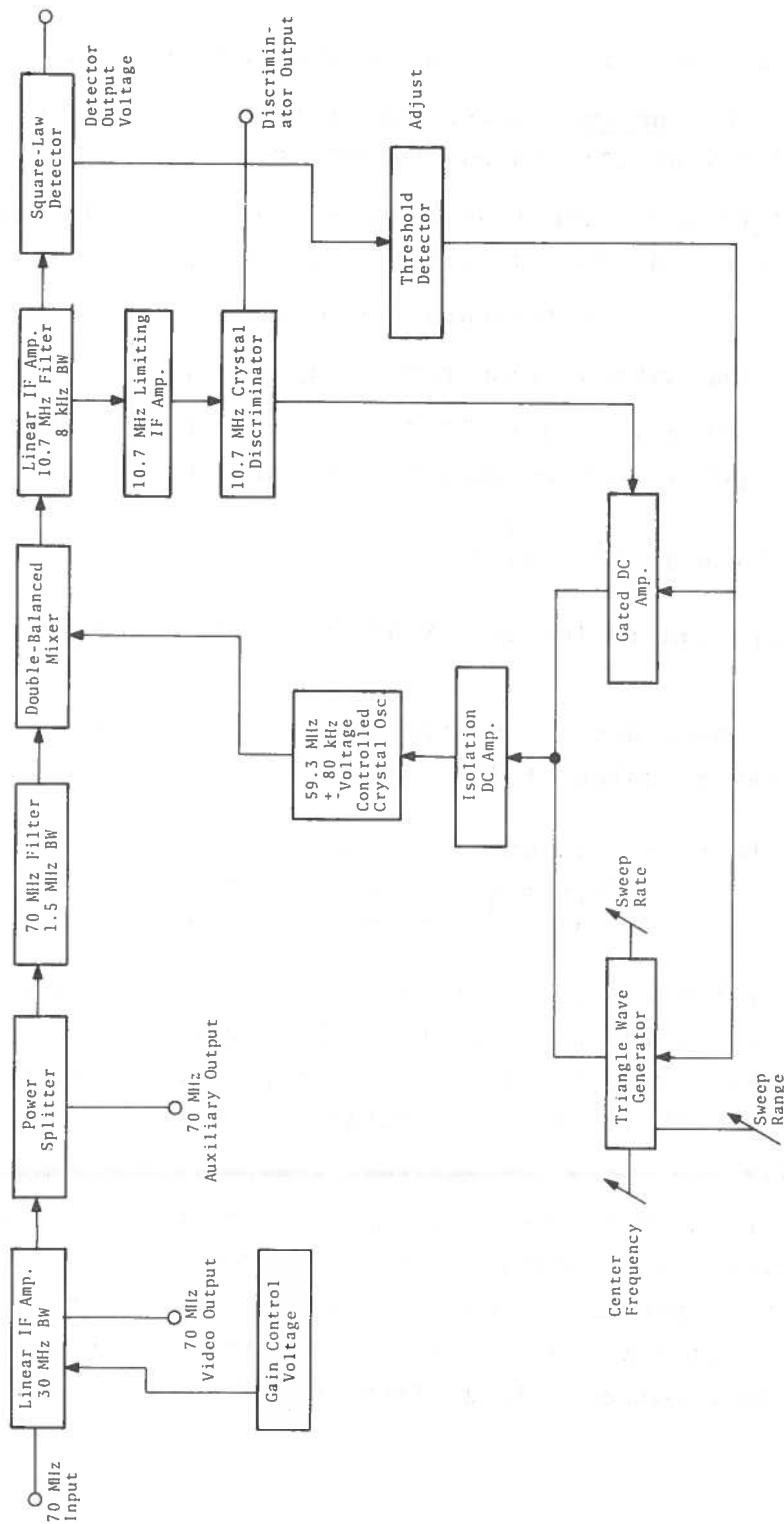


Figure 3-6. Intermediate Frequency Portion of the ADCP Receiver

where:

- T_S : is the overall system noise temperature, (K),
 T_R : is the receiver noise temperature, (K), for a noise figure of 2.7 dB this is equivalent to 250 K.
 L : is transmission line loss estimated at 0.1 dB and expressed as an efficiency factor 0.98
 T_A : is the sky temperature estimated at 20 K;
 T_O : is the ambient temperature at 290 K.

Thus $T_S = 250 + 19.6 + 5.80 = 275.4$ K for the above values. The receiver noise power density then becomes from equation (2-7):

$$N_O = (1.38 \times 10^{-23})(275.4) = 3.81 \times 10^{-21} \text{ w/Hz} \quad (3-2)$$

which when expressed in dBw is $5.8 \text{ dBw/Hz} - 210 \text{ dBw/Hz} = -204.2 \text{ dBw/Hz}$.

The noise power density at the input to the 70 MHz section of the receiver may be calculated as follows:

$$\begin{aligned} -204.2 \text{ dBw/Hz} + 45 \text{ dB} - 1 \text{ dB} + 25 \text{ dB} = -135.2 \text{ dBw/Hz} \\ \text{(NPD)} \quad \quad \quad \left(\begin{array}{c} \text{Preamp} \\ \text{Gain} \end{array} \right) \quad \left(\begin{array}{c} \text{Cable} \\ \text{Loss} \end{array} \right) \quad \left(\begin{array}{c} \text{Mixer} \\ \text{IF Gain} \end{array} \right) \end{aligned} \quad (3-3)$$

This may now be expressed in more applicable and convenient units. The receiver bandwidth is 8 kHz or 39 dB greater than 1 Hz and the power may be expressed in dBm. Therefore the actual noise floor of the receiver with its 8 kHz bandwidth is -66.2 dBm.

The second and third intermediate frequency portions of the receiver are shown in Figure 3-4. The 70 MHz intermediate frequency amplifier has a bandwidth of 30 MHz centered at 70 MHz. A detected video output of the bandpass is provided. The intermediate frequency gain is 60 dB and is adjustable. The gain is set by applying the required voltage from an adjustable precision power supply.

The 70 MHz is converted down to 10.7 MHz (the second intermediate frequency) and square-law detected. The bandpass at 10.7 MHz is determined by a 8 kHz crystal filter. Figure 3-7 is a family of curves of the detector's output DC voltage for the corresponding 70 MHz signal strength as a function of the gain control voltage. Figure 3-8 is a plot of the response for just the 10.7 MHz amplifier, filter and square-law detector.*

3.3 ADCP L-BAND CALIBRATION

Since the receiving system does not have a calibration signal that may be injected into the radio frequency input port only relative signal strengths may be measured. Thus, using initial calibrations such as Figure 3-7 and the assumption that the gain and system noise are relatively stable allow the received signal strength to be approximated.

The detector voltage which corresponds to the system noise as a check to establish that the overall system noise or system gain have not greatly deteriorated. Starting with the fact that the system noise is -66.4 dBm from Figure 3-8 the detector output voltage may be determined for the appropriate gain control voltage being employed. The output signal-to-noise ratio is thus:

$$(S/N)_{dB} = 20 \log \frac{V_{Det.Sig.}}{V_{Det.Noise}} \quad (3-4)$$

where $V_{Det.Sig.}$ is the detector voltage with the signal present (Nominally 8-10 volts) and $V_{Det.Noise}$ is the detector voltage due to just the system noise (nominally 50 to 100 mV.).

The detector voltage is digitized by an 8-bit analog-to-digital converter which has a full scale voltage of 10 volts. Consequently, the least significant bit of the analog-to-digital converter is 38.6 mV.

*That response departs from the straight line for the square-law detector voltage because of the negative 50 mV. offset in the DC amplifier following the detector.

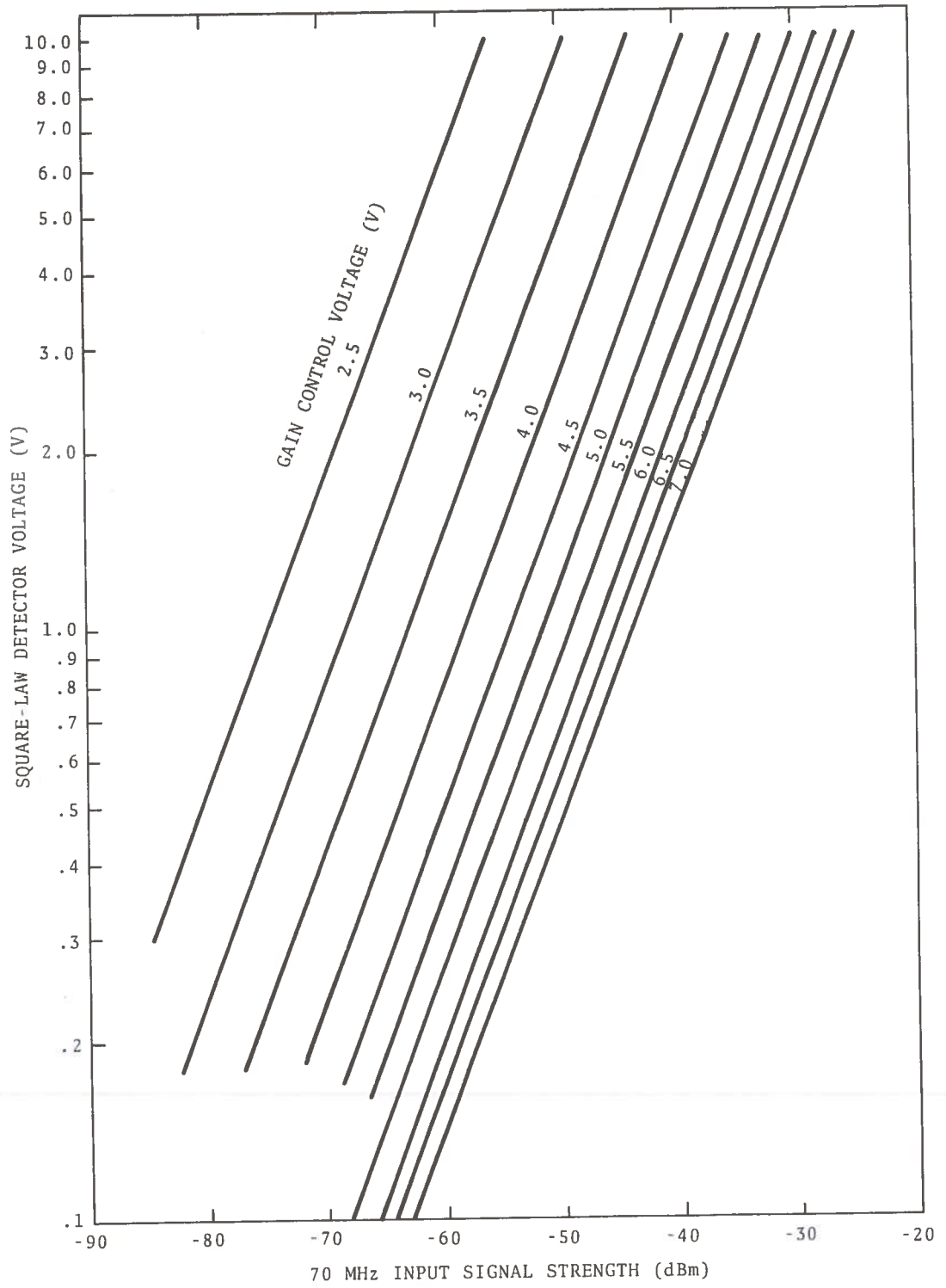


Figure 3-7. ADCP's L-Band Receiver Detector Voltage Versus the 70 MHz Input Signal Strength

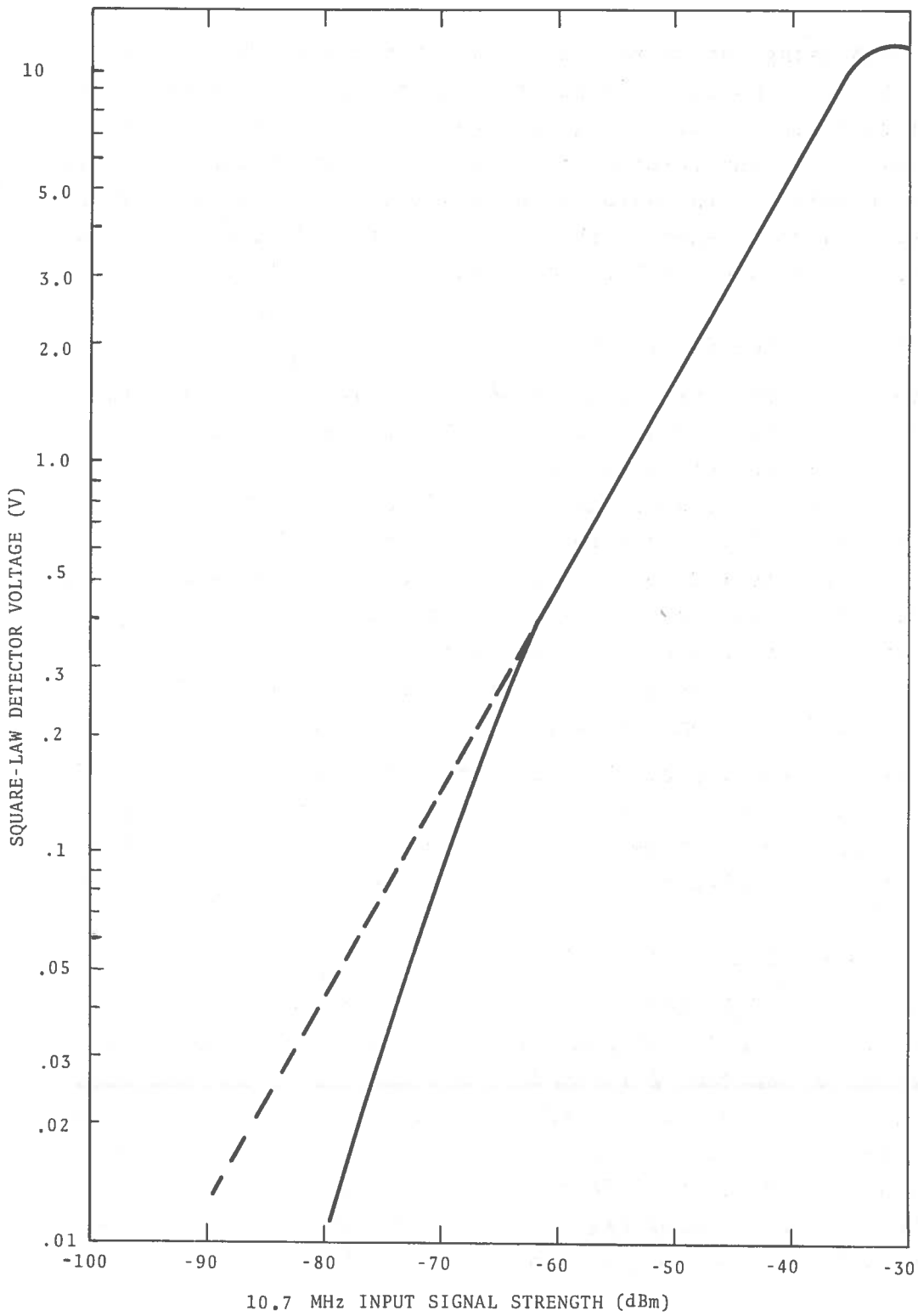


Figure 3-8. ADCP's L-Band Receiver Response for the 10.7 MHz Amplifier, Filter and Square-Law Detector

Though using the system noise is not the best way of monitoring system performance, it does, through the use of the analog-to-digital converter, provide a gross check on system performance. The stability of the receiver is more accurately checked by noting the stationarity of the data during a six-minute data run. This, in fact, is accomplished by the data analysis and data reduction programs in the computer located at the Westford station.

3.4 AUTOMATIC RECEIVER TUNING

Figure 3-6 depicts the second intermediate frequency circuits at 10.7 MHz and the second local oscillator control circuits. With no signal present the second local oscillator slowly sweeps back and forth 80 kHz about its center frequency. When a signal falls within the 10.7 MHz intermediate frequency filter and is detected, the detected voltage is compared with a pre-set threshold voltage. If the detector voltage is above the pre-set voltage, the sweep is stopped and the value of the sweep voltage is held on the oscillator. The pre-set voltage is adjustable and is normally set for a signal-to-noise ratio of 10 dB.

Once the sweeping of the oscillator is stopped the automatic frequency control developed by the crystal discriminator is added to the fixed sweep voltage, thus the received signal is continuously tuned or tracked by the automatic frequency control action.

3.5 L-BAND RADIO LINK CALCULATIONS

Section 2.3 illustrates the procedure for the link calculations employing the ATS-5 spacecraft. The ATS-6 effective radiated power ($P_T G_T$ of Equation 2-1) is 43.3 dBw (at the -3 dB beam edge field of view). The power sharing of the four Position Location and Aircraft Communications Experiment carriers puts the 1550.250 carrier down 8 dB so that effective radiated power at 1550.250 is 35.3 dBw. Table 3-1 summarizes the L-band downlinks to the ADCP from the ATS-5 and ATS-6 spacecraft.

TABLE 3-1. L-BAND LINK POWER BUDGET

Factor	Satellite	
	ATS-5	ATS-6
S/C ERP at 1550.250 (dBw)	22	35.3 ¹
Nominal Path Loss (dB)	-188.7	-188.5 ²
Platform Antenna Gain (dB)	+ 27	+ 27
Platform Feedline Loss (dB)	- 0.1	- 0.1
Ground Pointing Error (dB)	- 0.5	- 0.5
S/C Pointing Error (dB)	- 1.6	- 3.2
Polarization Loss (dB)	- 0.2	- 0.2
Tropospheric Attenuation Loss (dB)	- 0.2	- 0.2
Received Carrier Power (dB)	-144.3	-130.2 ²
Platform System Noise Temp. (K)	275.4	275.4
Platform Receiver Noise Power Density (dB/Hz)	-204.2	-204.2
Carrier to NPD Ratio (dB/Hz)	59.9	74.0
Platform Rec. (BW = 8 kHz)	- 39	- 39
Platform Signal-to-Noise Ratio (dB)	+ 20.9	+ 35.0

1. PLACE power sharing

2. Approximate value

3.6 ADCP VHF SYSTEM

The VHF equipment used in the remote platform configuration is depicted in Figure 3-9. The antenna is a crossed log-periodic array connected for circulator polarization. The final VHF power amplifier operates at 300 watts. The VHF receiver has a noise figure of 3.5 dB and a bandwidth of 15 kHz. The VHF exciter which drives the power amplifier operates at 40 watts. The modulation employed is narrow-band FM with a deviation of 5 kHz.

The demodulated tone from the receiver's frequency discriminator is fed to the digital correlator. Likewise, the digital tone to be transmitted is fed from the tone generator to the VHF exciter. The tone is 2.441 kHz in frequency and the modulation for the tone is phase shift keying (PSK).

The digital correlator/generator is the interface between the VHF transmit and receiver equipment and the remote platform's computer. The correlator decodes the received digital commands and routes them to the computer. Also, when the computer wishes to make a transmission, the digital information is sent to the interface which in turn activates the transmitter and supplies the proper modulation signals to the transmitter.

The VHF link budgets for the remote platform are given in Table 3-2A,B.

3.7 ADCP COMPUTER PROGRAMS

The platform uses a Digital Equipment Corporation PDP 11/05 minicomputer for control of the L-band data acquisition and storage. The principal use of the computer, however, is for VHF communication control. The control commands to the remote computer are relayed via VHF radio through either the ATS-1 or -3 spacecraft. The command and control functions originate from the main base station in Westford and are relayed to the remote platform.

The operation of the programs in the platform and the computer programs in the base station at Westford is most easily explained by discussing the commands and their operation. Table 3-3 lists the commands available. (See also General Electric, 1975).

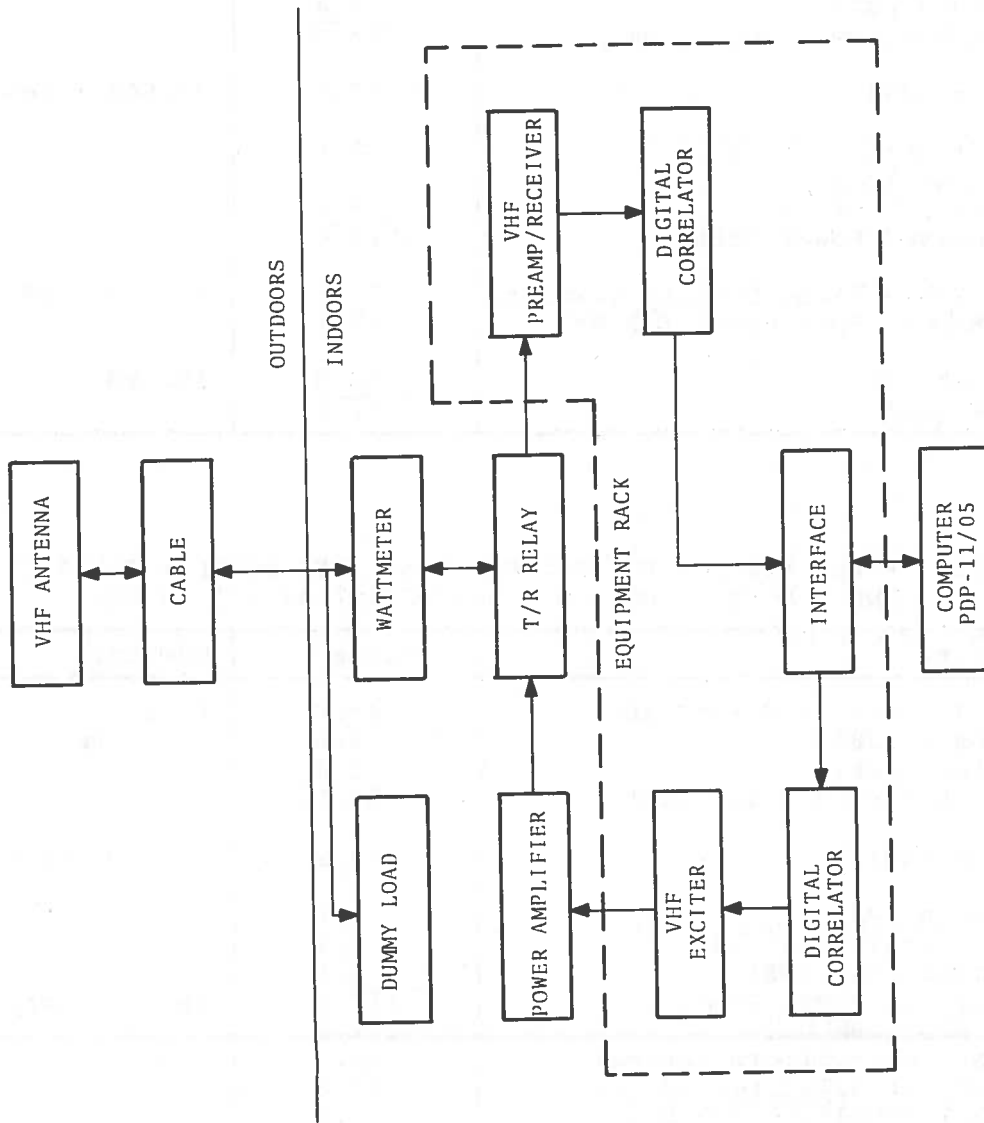


Figure 3-9. Detailed Functional Block Diagram of the VHF Portion of the Remote Facility

TABLE 3-2A. POWER BUDGETS FOR THE VHF UPLINKS BETWEEN THE ADCP AND THE ATS-1 OR ATS-3 SPACECRAFT AT 149.22 MHz

Quantity	Value	Comments
Transmit Power (dBm)	55.0	300 w
Platform Antenna Gain (dB)	7.0	
Circuit Loss (dB)	- 1.4	
Effective Radiated Power (dBm)	<u>60.6</u>	
Space Loss (dB)	-167.5	22,500 miles
Spacecraft Antenna Gain (dB)	8.0	
Circuit Loss (dB)	- 1.5	
Polarization Loss (dB)	- 3.0	
Total Received Power (dBm)	<u>-103.4</u>	
Receiver Noise Power Density (dBm/Hz)	-170.5	NF = 3.5 dB
Carrier/NPD in Spacecraft (dB-Hz)	67.1	
Receiver		
IF Noise BW (dB)	50.0	100 kHz
S/N in IF (dB)	<u>17.1</u>	

TABLE 3-2B. POWER BUDGETS FOR THE VHF DOWNLINKS BETWEEN THE ADCP AND THE ATS-1 OR ATS-3 SPACECRAFT AT 135.60 MHz

Quantity	Value	Comments
Spacecraft Transmit Power (dBm)	46.0	40 w
Antenna Gain (dB)	8.0	
Circuit Loss (dB)	- 1.8	
Effective Radiated Power (dBm)	<u>52.2</u>	
Space Loss (dB)	-166.9	22,500 miles
Antenna Gain (dB)	7.0	
Platform Circuit Loss (dB)	- 1.3	
Polarization Loss (dB)	- 3.0	
Total Received Power (dBm)	<u>-112.0</u>	NF = 2.5 dB
Receiver NPD (dBm/Hz)	-171.5	
Carrier/NPD at Platform (dB-Hz)	52.5	
Carrier/NPD at Satellite (dB-Hz)	67.1	
Carrier/NPD Resultant (dB-Hz)	59.0	
IF Noise BW (dB)	42.0	
S/N in IF (dB)	<u>17.0</u>	

TABLE 3-3. ADCP COMPUTER COMMANDS

Command Name	Command Sent	Status Returned
Hello	TH	HR HI HO
Open	TO	OR OI
Date	TD	DR DI DO
Next	TN	NH NO NM
End	TE	EH EO EM
List	TL	LM
Finish	TF	FF
Information	TI	IH IO IV
Summary	TS	SH SO SV SS SM SR
Kill	TK	KV KH KO KS KI
Period	TC	CR
Modify	TM	MH MO ME MT MV
Check	TM	MM

TABLE 3-3. (Continued)

Command Name	Command Sent	Status Returned
Reboot	TR	RH RO RE RV
Block	TB	BH BO BV BE
Verify	TV	BM BW BR IM IR IK KK SM SR SK VR VD VE RR MR
Abort	TA	AN
Print a Message	TP	PH
Query Received Message	TQ	QR QK QM PR PM PK

The Hello command is normally the first command sent. If the platform is taking data, the acknowledgement for the Hello will say data acquisition is in progress. If it is desired to stop taking data, then an Open command should be sent. If it is not desired to stop taking data, then another Hello command should be sent. If an Open command were sent first, then it would stop the data acquisition if it were in progress. In any case either a Hello or Open command must be sent first. Without the proper command sequency the platform will not perform any control function that has been sent to it.

The platform computer contains a software clock. If for some reason it is necessary to set or reset the clock, the date command is used.

A data acquisition schedule may be put into the computer. This schedule has provisions for four individual data acquisition periods.

The Next command is used to set the start time and date for the desired period. The End command is used to set the stop time and date for the desired period. The List command is used to call back to Westford and list the operating schedule for the platform's four data acquisition periods. This command is used to check that the dates have in fact been set in properly. The special date of January 1, 1971, when placed in the start time of the first data acquisition period will instantly initiate data acquisition and continue until the end time of the first period. This is regardless of the start times of the other data acquisition periods.

The Finish command terminates the VHF operation and a Hello or Open command must be given to restart the VHF operations. If a Finish command is not given the platform will automatically execute the Finish command if no commands have been sent during the previous 15 minutes.

The platform contains two buffers that are used for saving information that is of interest to the base station. The entries are made into these buffers by the platform program for relay back to the base station at a later time. One buffer contains a

list of program errors that has occurred. There are about 50 different error messages that may be logged. The time at which the error occurred is logged as well as the coded message which describes the error.

The second buffer contains a summary of the data that has been taken. It contains the time of the data period, which spacecraft has been used (ATS-5 or -6), and where the information is stored on the DECTape.®

The buffer with information about computer errors is recalled by using the Information command. The buffer with data summary is recalled via the Summary command.

The two buffers may be cleared upon command from the base station. By sending a Kill command and then an Information command, the information buffer is set to be cleared. Likewise, the summary buffer is set to be cleared by sending a Kill command followed by a Summary command. The buffers are actually cleared when a third command is sent, the Verify command.

The Kill command by itself will clear both the information and summary buffers and will also reset the data tape recording index back so the data recording will be at the beginning of the DECTape.®

The data acquisition rate may be changed upon command. When the data acquisition concerns the ATS-5 L-band signal, the data acquisition program de-spins the satellite signal and saves the measurements only from the peak of the spin period. The data acquisition rate of the continuous wave signal from the ATS-6, however, may be taken at any rate from once every 300 milliseconds to once every 3.0 seconds.

The Period command allows the main station to determine the current acquisition rate for the ATS-5 and what the current acquisition rate is for the ATS-6. It is also used to change the ATS-6 acquisition rate if desired.

The Modify command allows the actual instructions and constants in the platform's computer memory to be modified, the

command is intended for modifying the many constants that are in the platform's program.

The Check command allows a ten-word section of the core memory of the platform to be read back to the base station. The Check command is generally used to check some of the constants and variables of the platform program.

If for some unforeseen reason errors occur after a certain set of instructions in the platform's computer core are executed, or for some reason the same error continuously occurs, provisions have been incorporated to remedy such a problem. The Reboot command will reload the entire program into core again. One of the two DECTape[®] units connected with the PDP 11/05 computer contains a copy of the program. When the Reboot command is sent from Westford to the platform, the copy of the program on the DECTape[®] is read into the computer core from the magnetic tape. Obviously if some catastrophic computer "crash" occurred, the program would have to be reloaded by using the load switch on the PDP 11/05. However, if the small portion of the program that is involved in reloading the program is not destroyed, then the program may be reloaded by the remote Reboot command.

The data measurements are recorded on the data DECTape[®] in sections or blocks. Each block contains about six minutes of data and the entire tape will hold about 60 hours of data. Each data block is numbered so that they may be individually accessed. The first four words of the block contain in code form a summary of what is recorded in that particular block.

The Block command is used to request blocks of data be relayed from the platform to the Westford station. It takes approximately six-seconds to relay back one block of data or one hour of data can be relayed back in one minute.

Commands which if executed by mistake might be disastrous or commands which involve transmitting back large amounts of data (i.e., long transmissions) are actually affected by a sequence of commands. This feature is incorporated such that if it is realized that a mistake has been made or a command has been misinterpreted

that condition may be aborted before a disaster occurs. The control command which does the verification in the command sequence is the Verify command.

The various commands which have this feature are the Kill command and the Kill commands which selectively clear the summary or information buffer. The Reboot command also requires a verification command. The block data command requires two Verify commands. The Summary command and the Inform command which relay back their respective buffers also require the Verify command to actually execute their operation, as does the Modify command.

Moreover, if during a command sequence including a Verify it is desired to abort the sequence, an Abort command may be given. This will clear all the commands of the sequence, such that the sequence may be restarted with some other request parameter or just be terminated completely.

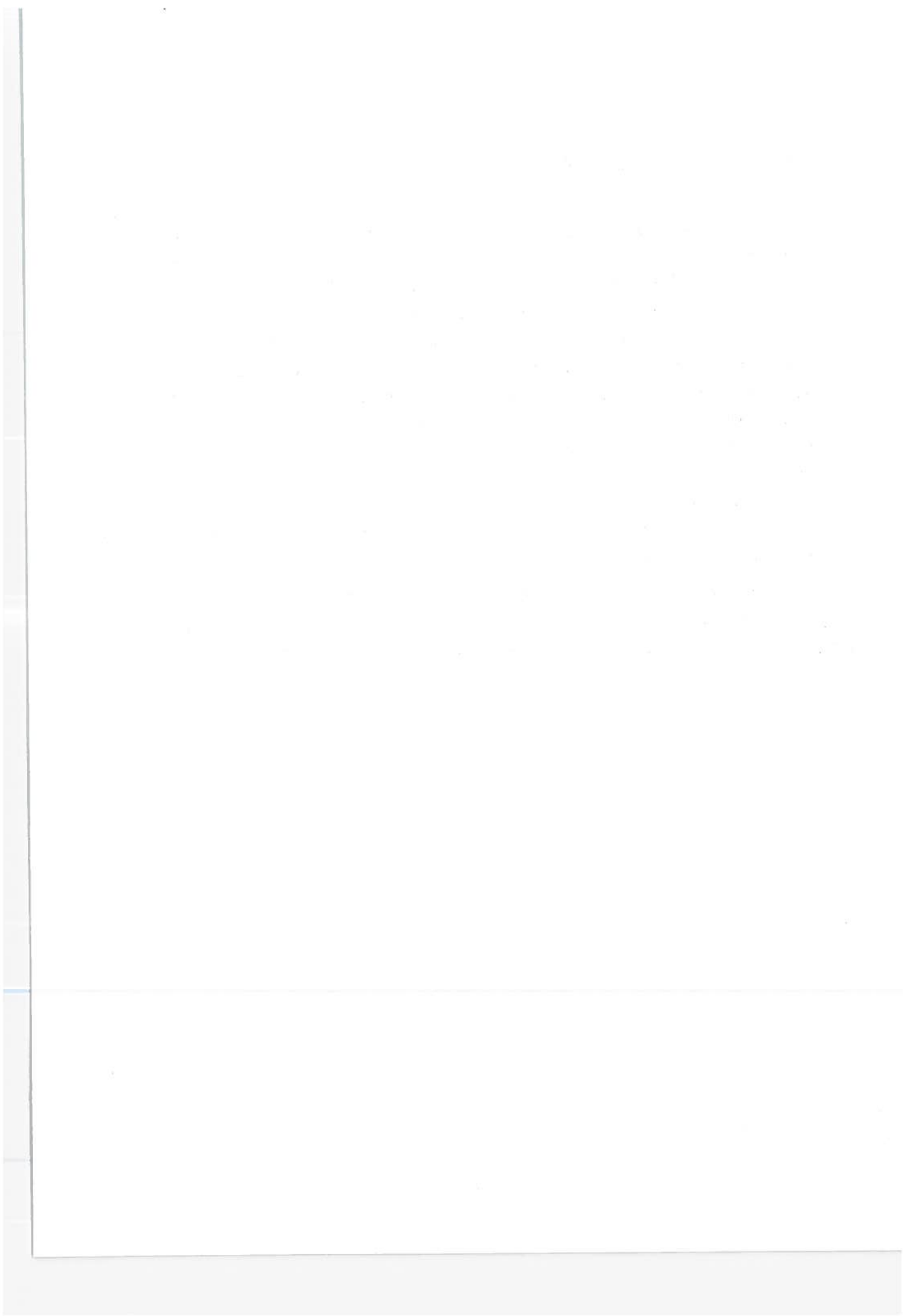
A set of commands are also available for sending teletype messages between the Westford facility and the platform. The set of commands allows a teletype conversation to be carried on between the operator at Westford and personnel at the remote platform. The commands were intended, however, for leaving messages in a buffer in the platform.

A message may be sent from Westford to the platform and will reside in a buffer there. At some later time an operator may come to the platform and request the message be typed on the teletype unit. The message which is stored in the platform computer is then typed out for the operator to read. The operator may also enter a message into a buffer in the platform's computer via the teletype. This message may in turn be relayed back to Westford during the next VHF period. It is not necessary for an operator to be present at the platform when a message is sent to the platform or when a message is returned back to Westford from the platform. If, however, an operator is present at the platform during a VHF period it is possible to communicate via teletype.

3.8 WESTFORD COMPUTER PROGRAMS FOR OPERATION OF THE REMOTE PLATFORM

The computer control program in the Westford station allows the remote platform to be operated using the commands just discussed. As the data blocks are relayed back to Westford they are reformatted at Westford and stored on the computer's disc. The format in which the platform data measurements are stored in the same format as the data measurements made at Westford. Consequently, the data reduction and processing program used to process the Westford data also is used to process the platform data. In addition, a routine of the Westford computer program takes the digital data that was relayed back and stored on a disc and converts it to an analog voltage which is written out on a chart recorder. Sets of calibration marks are written onto the strip-chart also. An example of such is given in Figure 4-7.

Consequently, the platform data is analyzed in the same manner as the Westford data and an analog strip-chart recording of the digital data is also constructed from the digital data.



4. ATS-5 L-BAND DATA

4.1 DISCUSSION

The data to be presented in this chapter comprises 625 hours of observations which are listed in Table B-1. The observation period consists of 12-minute intervals taken every quarter hour. The measurements from each data measurement interval are computer analyzed. The computer reads the magnetic tape containing the measurement values and computes the probability density function and probability distribution function. These reduced data are then labeled as the the time of observation with respect to sunset at the ionospheric penetration point at the 350 kilometer altitude and stored on the computer's disk.

The data plots to be presented are a combination of the data for a week as explained in Section 2.4. The individual weeks are combined to form the plots representative of the month and the months are combined to form the seasonal plots. The plots for the individual weeks are contained in Appendix C.

The large amount of data contained herein makes it impossible to present the density and distribution plot for each measurement interval. In order to make the amount of reduced data manageable, a single number is used to represent each measurement interval. These numbers are the root-mean-square for the calculated density and the 90th percentile of the distribution. These values are computer calculated each time the density and distribution are calculated.

The root-mean-square of the density may be thought of as follows. Consider the density to be composed of two impulses each of amplitude equal to one half. Thus the pulses would be located symmetrically about the median. The spacing of the pulses above and below the median is the root-mean-square.

The 90th percentile is that signal level below the median, above which the signal strength stays 90 percent of the time.

The difficulty in presenting the data focuses about determining the need to represent the width of the density plots. The width of the density, but more particularly the variation in width of the density is an indication of the fluctuation of the signal. The root-mean-square is used as the measure of the width of the density. The 90th percentile was picked as a means of indicating the relative number of occurrences of the larger fluctuations. The 90th percentile was picked because the confidence of that interval is quite good considering the amount of data in a 12-minute sample.

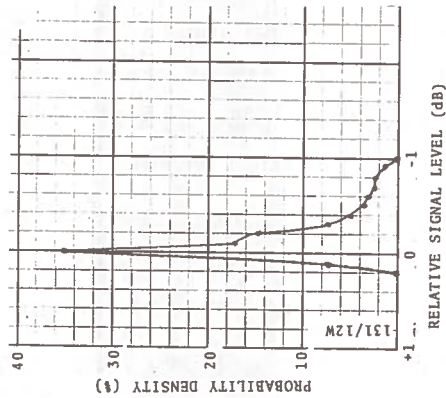
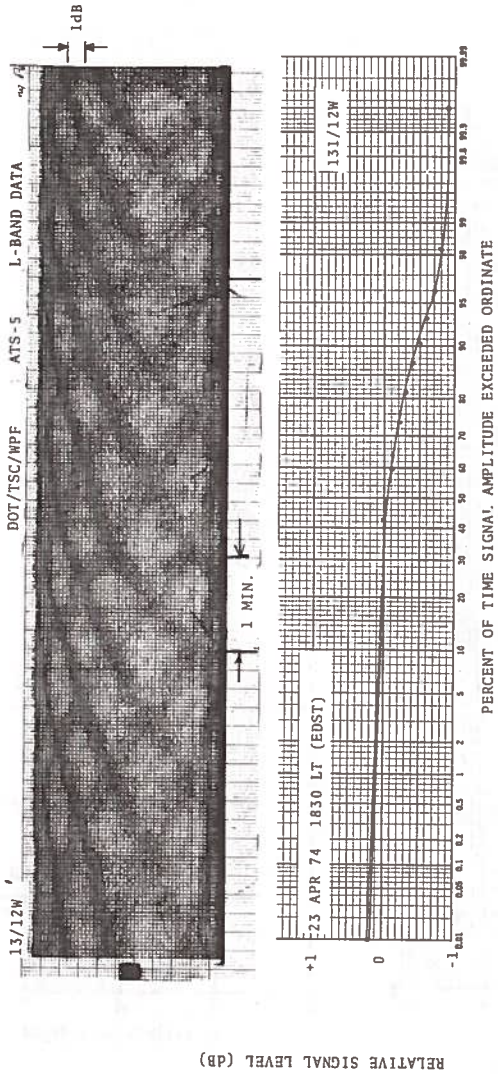
In addition to the data plots the maximum values of the root-mean-square and 90th percentile values are tabulated for each hour of the week. These tabulations and summary tables appear in Appendix D. Summary plots of these tabulations are included in this chapter.

Also in this chapter are plots of scintillation level for the levels of Planetary Magnetic Index, Kp, that occurred during the observations. The diurnal variations in the scintillation level for the different values of Kp are also shown.

Figures 4-1 through 4-5 are selected typical examples of the measured data that illustrate the analog recordings and the calculated results from these same data samples.

Figure 4-6 presents the strip-chart of the ATS-5 signal for 11 July 1974 from 0000 EDST to approximately 0011 EDST. Note the scintillation on all three channels. The variations occur on the East channel even though the East receiver is having some gain problems. The peak-to-peak variation is greater than 1 dB in this example.

Figure 4-7 is a sample of a computer prepared strip-chart recording taken on 22 July 1974 with the automatic data collection platform while located at the Westford Propagation Facility. Figure 4-8 and 4-9 show the computer prepared statistics for the three particular data blocks.



DOE/TSC/WESTFORD PROPAGATION FACILITY
 NASA/ATS-5 Spacecraft in MBFT Mode
 WPF Uplink at 1651.270 MHz
 Downlink at 1550.250 MHz @ S/N = 30 dB
 BW = 1 kHz; Median Signal Level = -116.0 dBm
 23 April 1974; Start Time = 1830 EDST
 File Duration = 12 minutes

Figure 4-1. Example of Analog Data and Computer Calculated Statistics (23 April 1974)

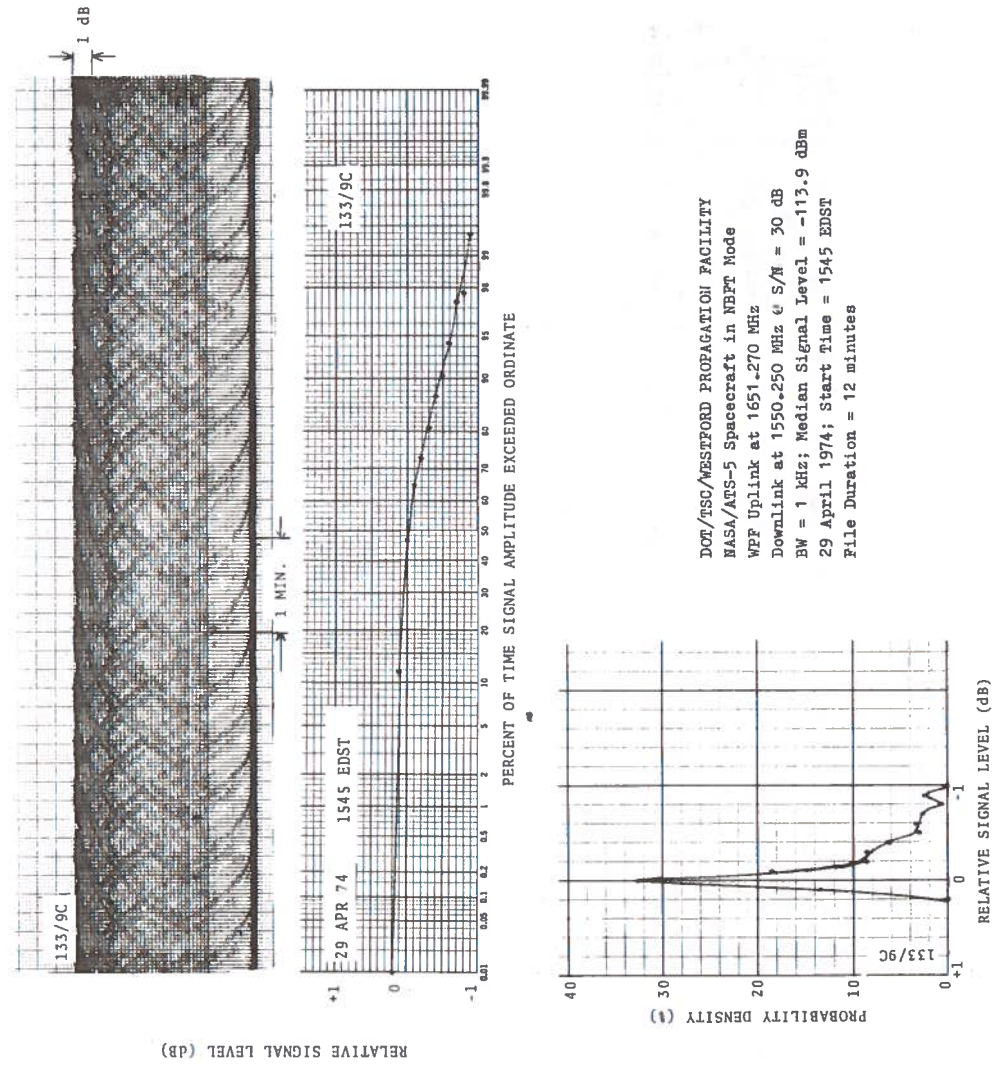
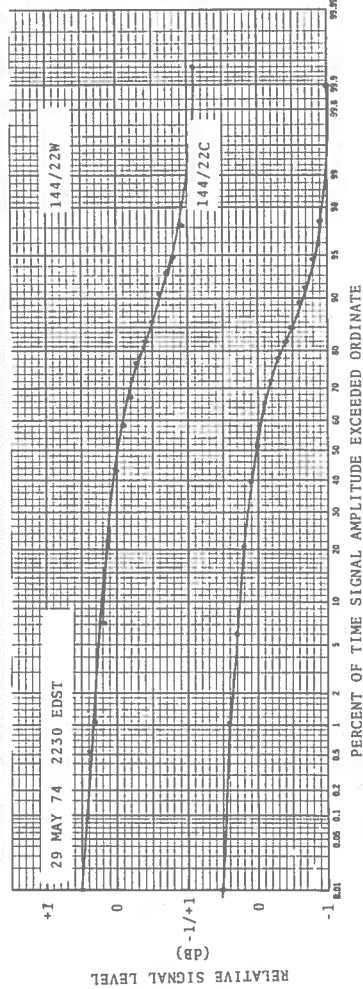
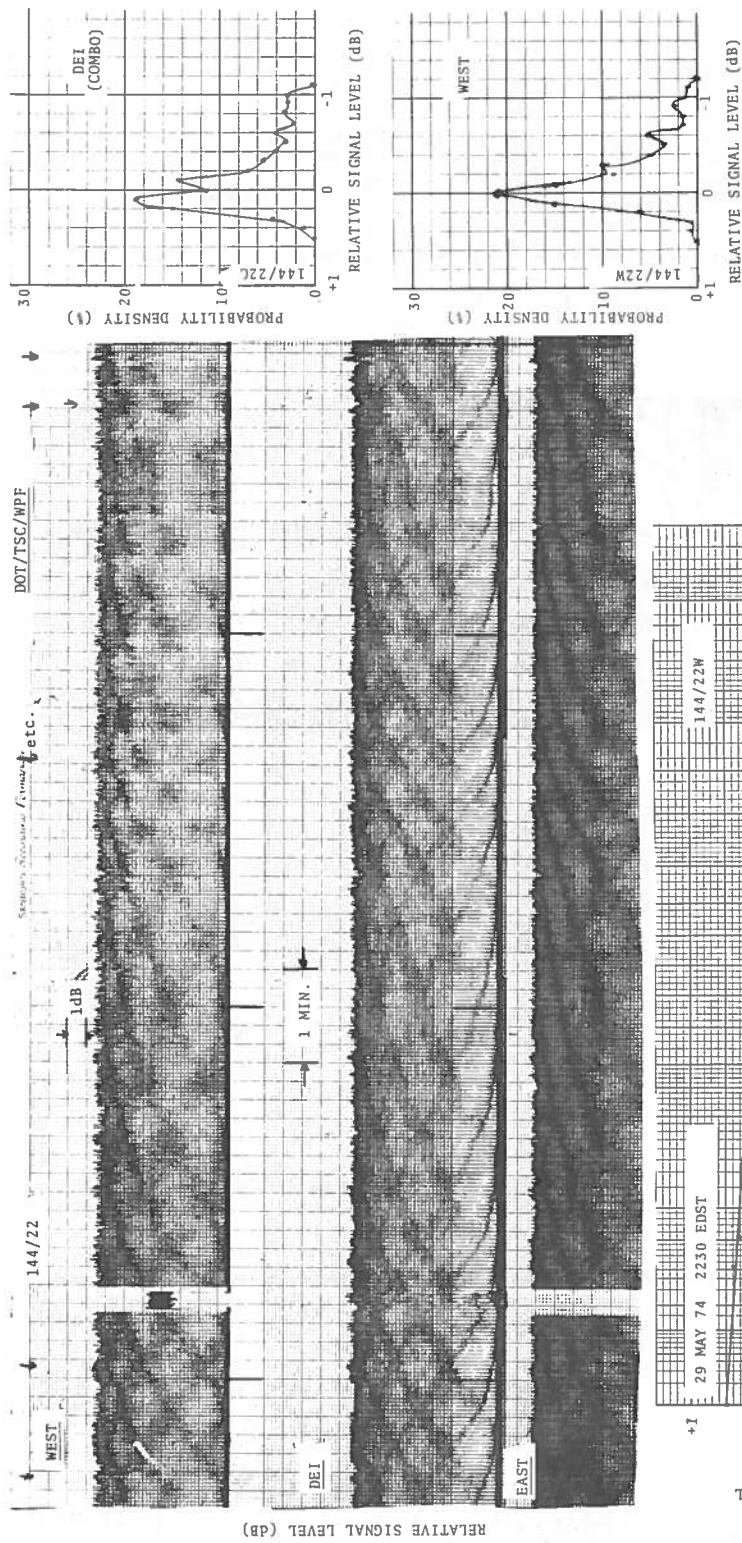


Figure 4-2. Example of Analog Data and Computer Calculated Statistics (29 April 1974)



DOT/MSC/WESTFORD PROPAGATION FACILITY
 NASA/ATS-5 Spacecraft in NBFT Mode
 WPP Uplink at 1651.270 MHz
 Downlink at 1550.250 MHz @ S/N = 30 dB
 BW = 1 kHz; Median Signal Level = -120.6 dBm (West)
 Median Signal Level = -121.5 dBm (Combo)
 29 May 1974; Start time = 2230 EDST
 File Duration = 12 minutes

Figure 4-3. Example of Analog Data and Computer Calculated Statistics (29 May 1974, 2230 EDST)

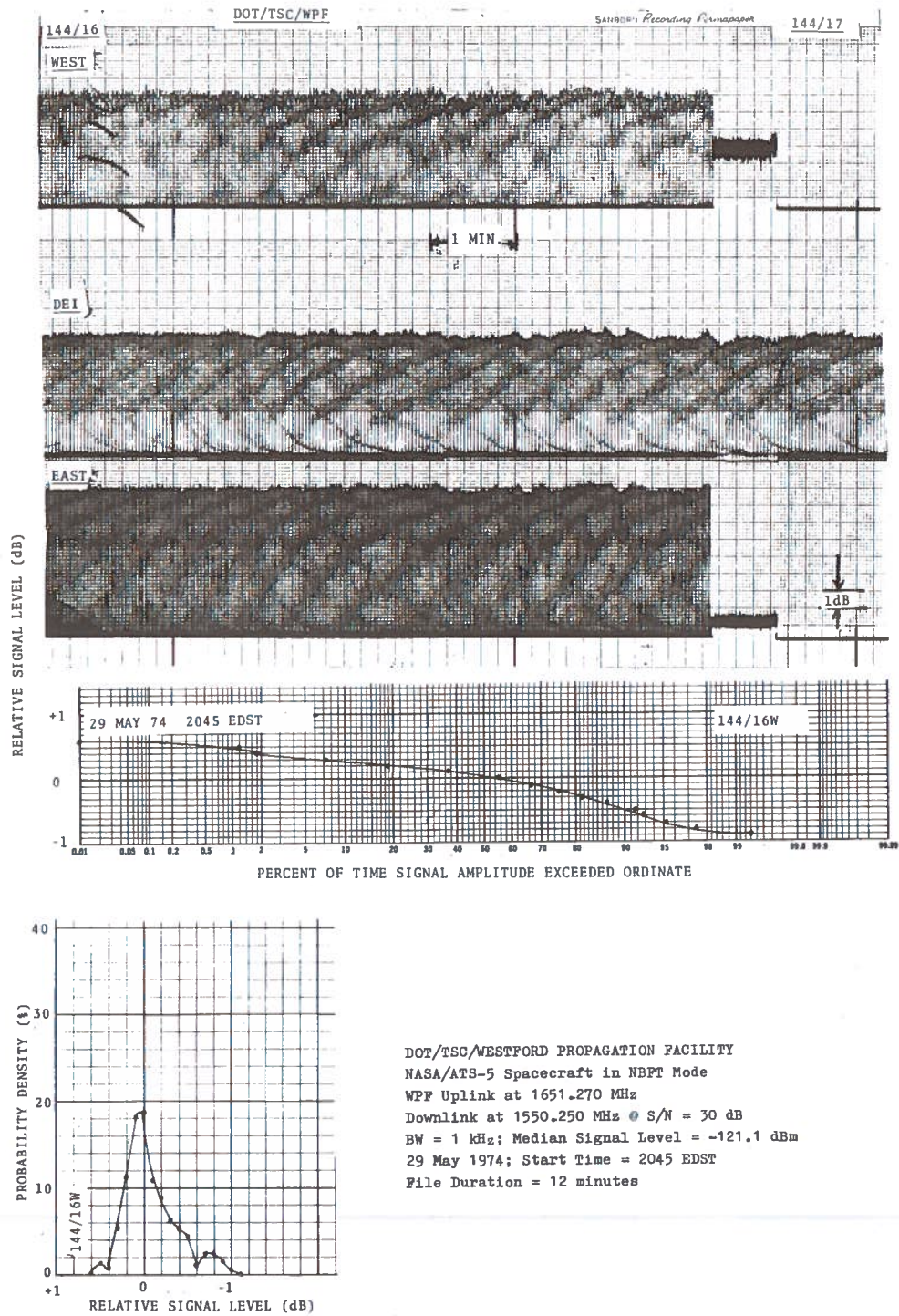
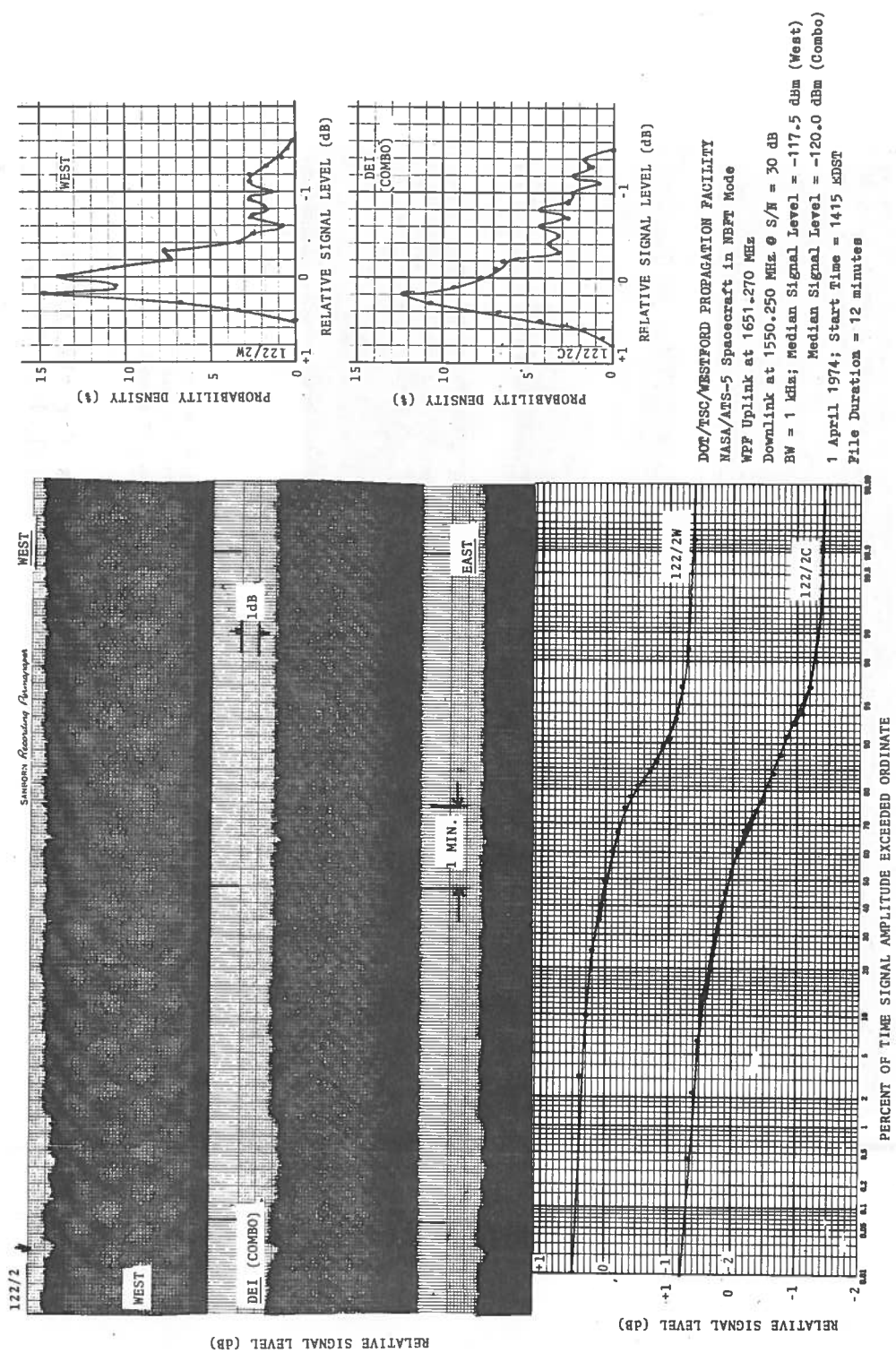
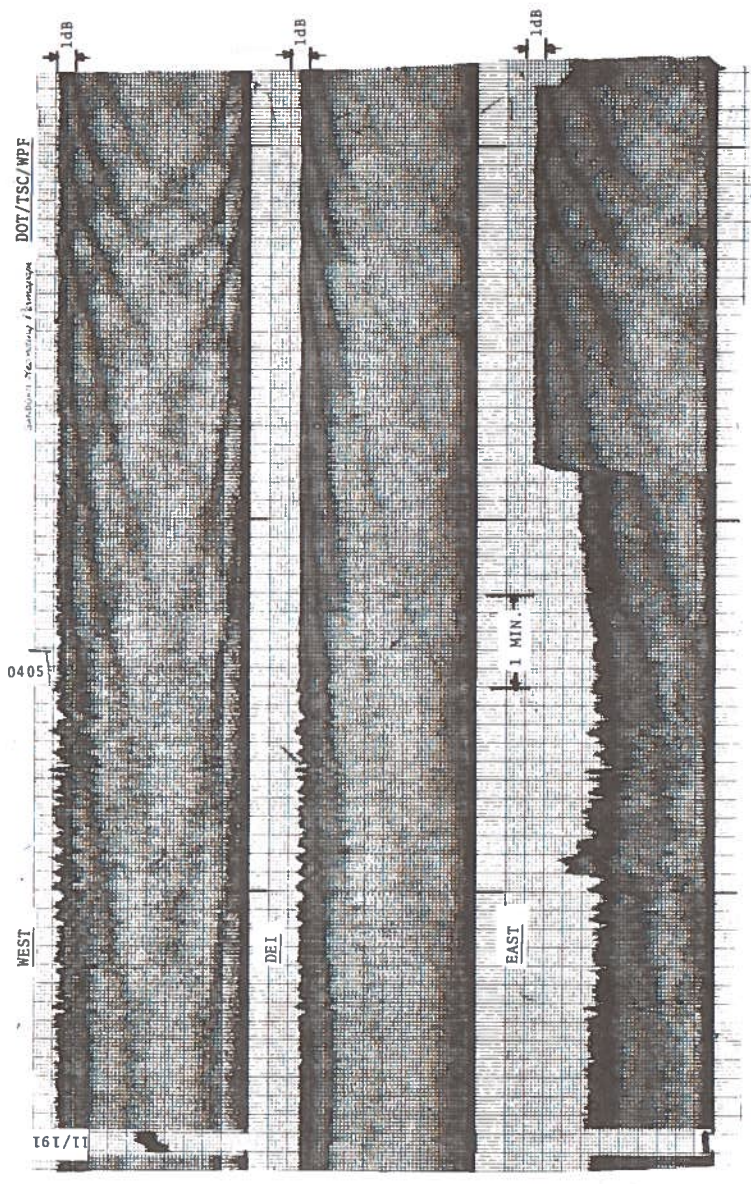


Figure 4-4. Example of Analog Data and Computer Calculated Statistics (29 May 1974, 2045 EDST)



DOT/TSC/WESTFORD PROPAGATION FACILITY
 NASA/ATS-5 Spacecraft in NBFT Mode
 WPF Uplink at 1651.270 MHz
 Downlink at 1550.250 MHz. θ S/N = 30 dB
 BW = 1 MHz; Median Signal Level = -117.5 dBm (West)
 Median Signal Level = -120.0 dBm (Combo)
 1 April 1974; Start Time = 1415 KDST
 File Duration = 12 minutes

Figure 4-5. Example of Analog Data and Computer Calculated Statistics (1 April 1974)



DOT/TSC/WESTFORD PROPAGATION FACILITY
 NASA/ATS-5 Spacecraft in NBFT Mode
 WPF Uplink at 1651.270 MHz; Downlink at 1550.250 MHz @ S/N = 30 dB
 BW = 1 KHz; Median Signal Level = -117.6 on DEI; -117.7 on West
 11 July 1974; Start File at 0000 EDST; File Duration = 12 minutes

Figure 4-6. Analog Strip-chart Recordings for the ATS-5 L-Band Signal on 3 Channels (11 July 1974)

ATS-5 L-BAND DATA 22 JULY 1974 DOT/TSC/WPF

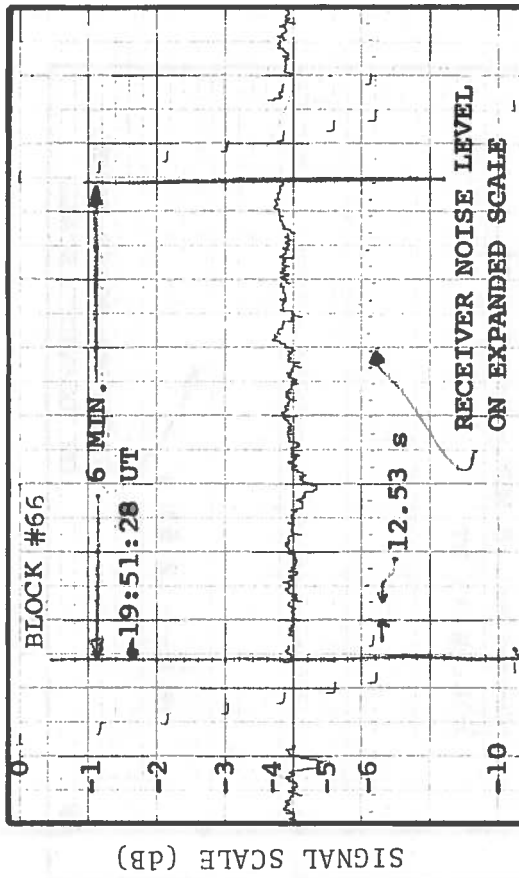


Figure 4-7a. Example of a Computer Generated Strip-Chart Record from Automatic Data Collection Platform Data (22 July 1974).

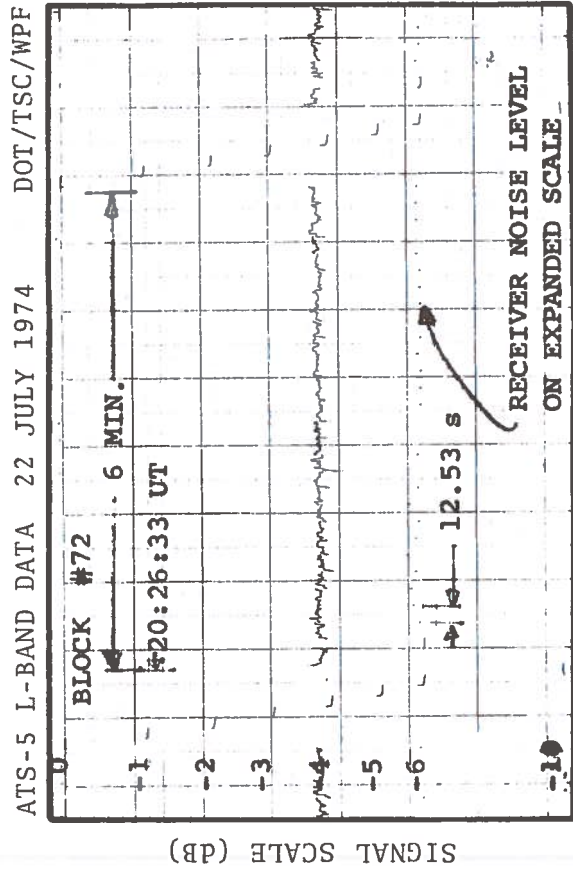


Figure 4-7b. Example of a Computer Generated Strip-Chart Record from Automatic Data Collection Platform Data (22 July 1974).

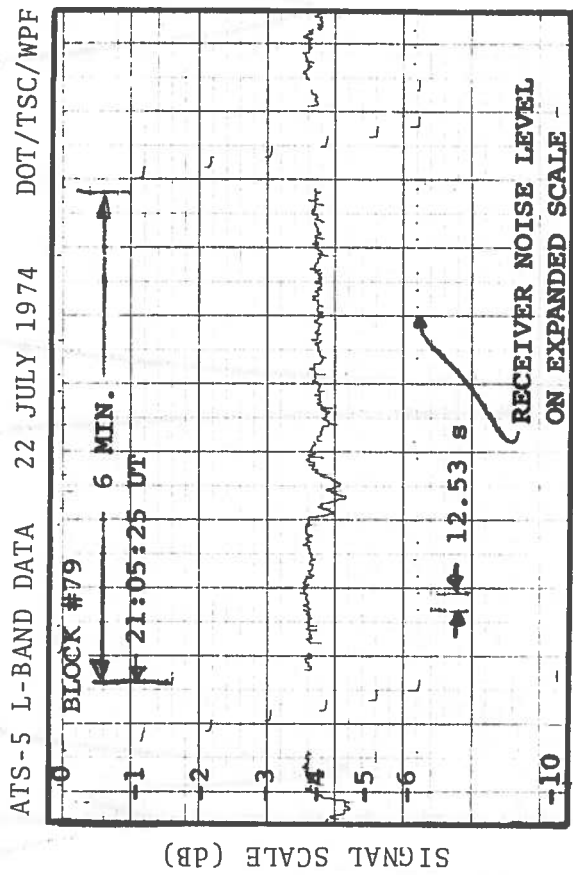


Figure 4-7c. Example of a Computer Generated Strip-Chart Record from Automatic Data Collection Platform Data (22 July 1974).

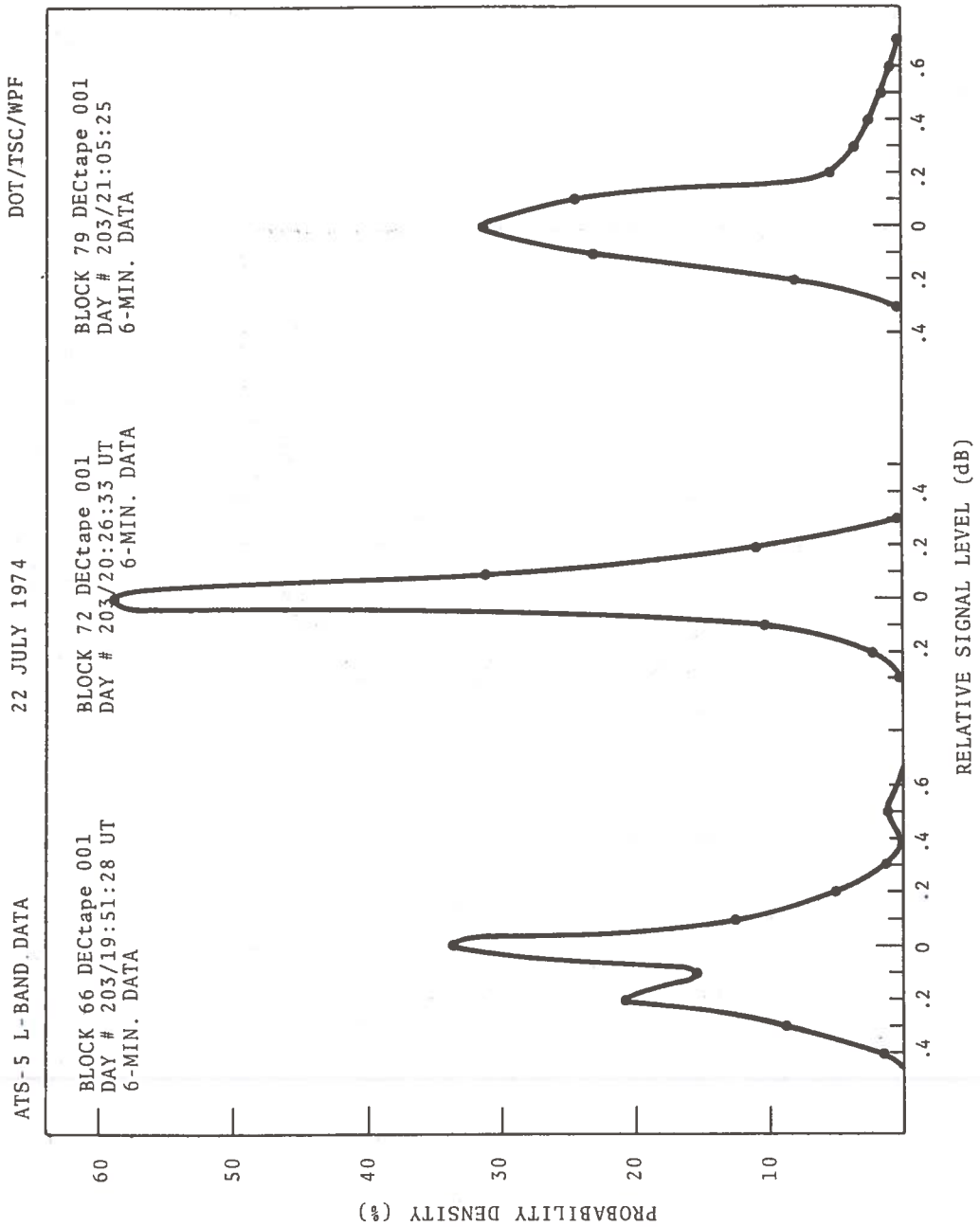


Figure 4-8. Probability Density Plots for Automatic Data Collection Platform Data (22 July 1974)

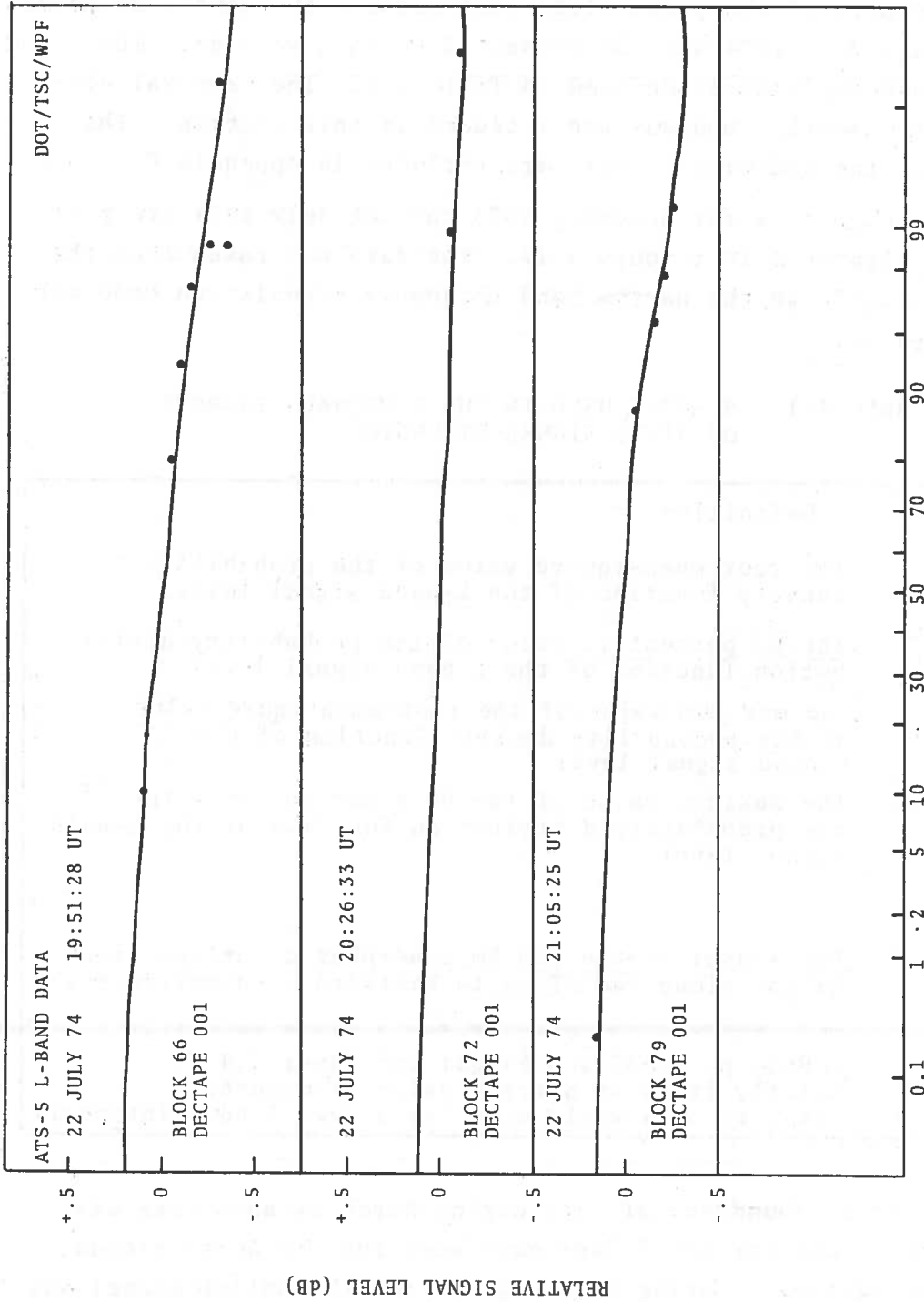


Figure 4-9. Probability Distribution Plots for Automatic Data Collection Platform Data (22 July 1974)

4.2 TEMPORAL ANALYSIS

The results of the probability analysis for the months December 1973 through July 1974 will be presented in this section. The diagrams use the symbols defined in Table 4-1. The temporal diagram for the monthly medians are included in this section. The diagrams of the individual weeks are included in Appendix C.

The monthly data for December 1973 through July 1974 are presented in Figures 4-10 through 4-17. The data was taken from the ATS-5 spacecraft in the narrow-band frequency translation mode with the DOT uplink.

TABLE 4-1. SYMBOLS USED IN THE TEMPORAL DIAGRAMS OF ATS-5 SIGNAL STRENGTH

Symbol	Definition
.	The root-mean-square value of the probability density function of the L-band signal level.
O	The 90 percentile value of the probability distribution function of the L-band signal level.
Δ	The maximum value of the root-mean-square value of the probability density function of the L-Band signal level.
□	The maximum value of the 90th percentile value of the probability distribution function of the L-band signal level.
350 SS	The sunset at the 350 km ionospheric intersection height along the ATS-5 to Westford propagation path.
Kp	The planetary magnetic index defined in Valley (1965) p. 11-32 and Piggot and Rawer (1972). Briefly it is an average value of magnetic activity on a world wide basis over 3 hour intervals

There is an abundance of data during March because data was taken 8 hours per day for 5 days each week for the weeks around the vernal equinox. During this time period the uplink signal was supplied in most cases by the General Electric Radio-Optical Obser-

DOT/TSC/WPF

DECEMBER 1973

ATS-5 L-BAND DATA

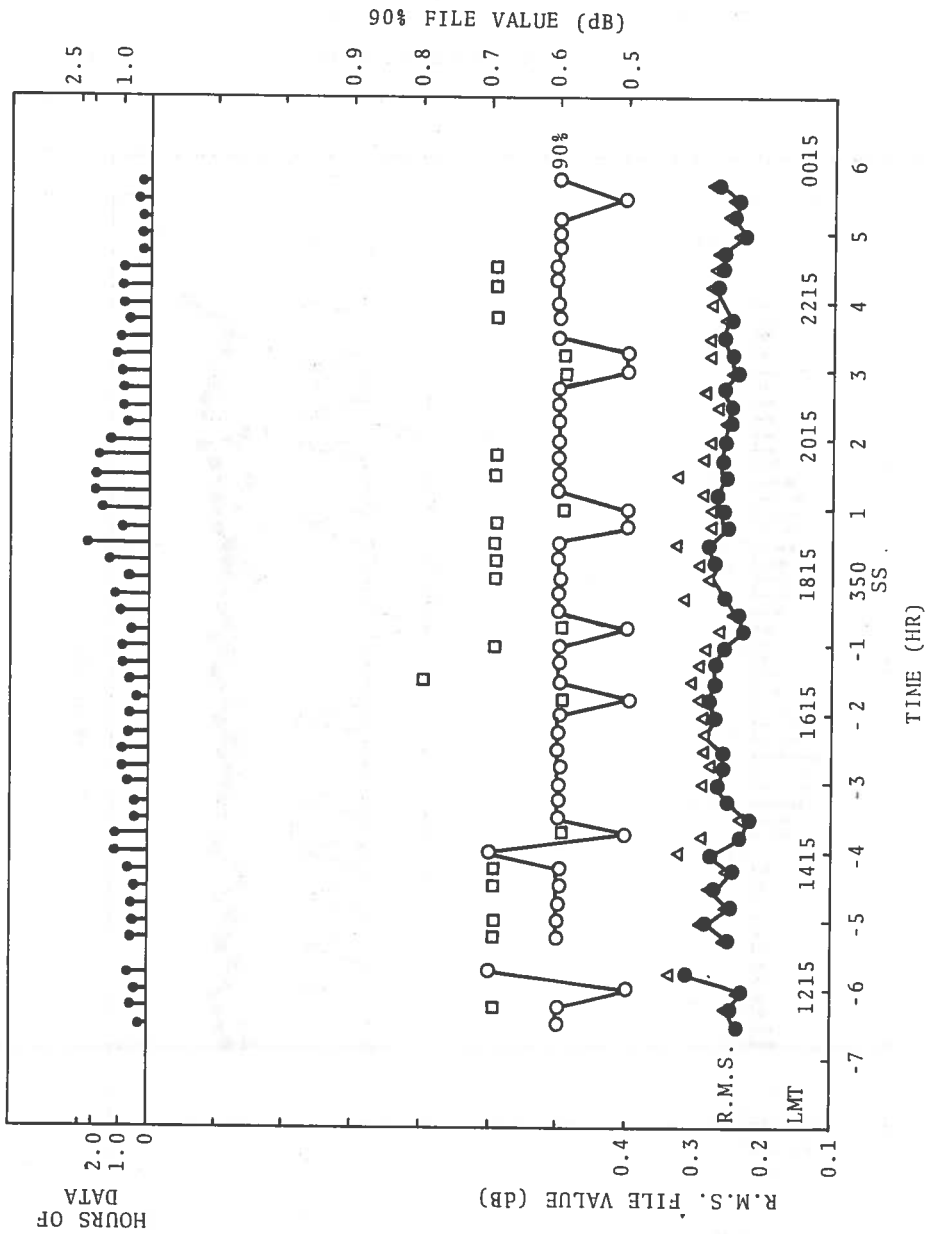


Figure 4-10. Temporal Diagram for December 1973

DOT/TSC/WPF

ATS-5 L-BAND DATA JANUARY 1974

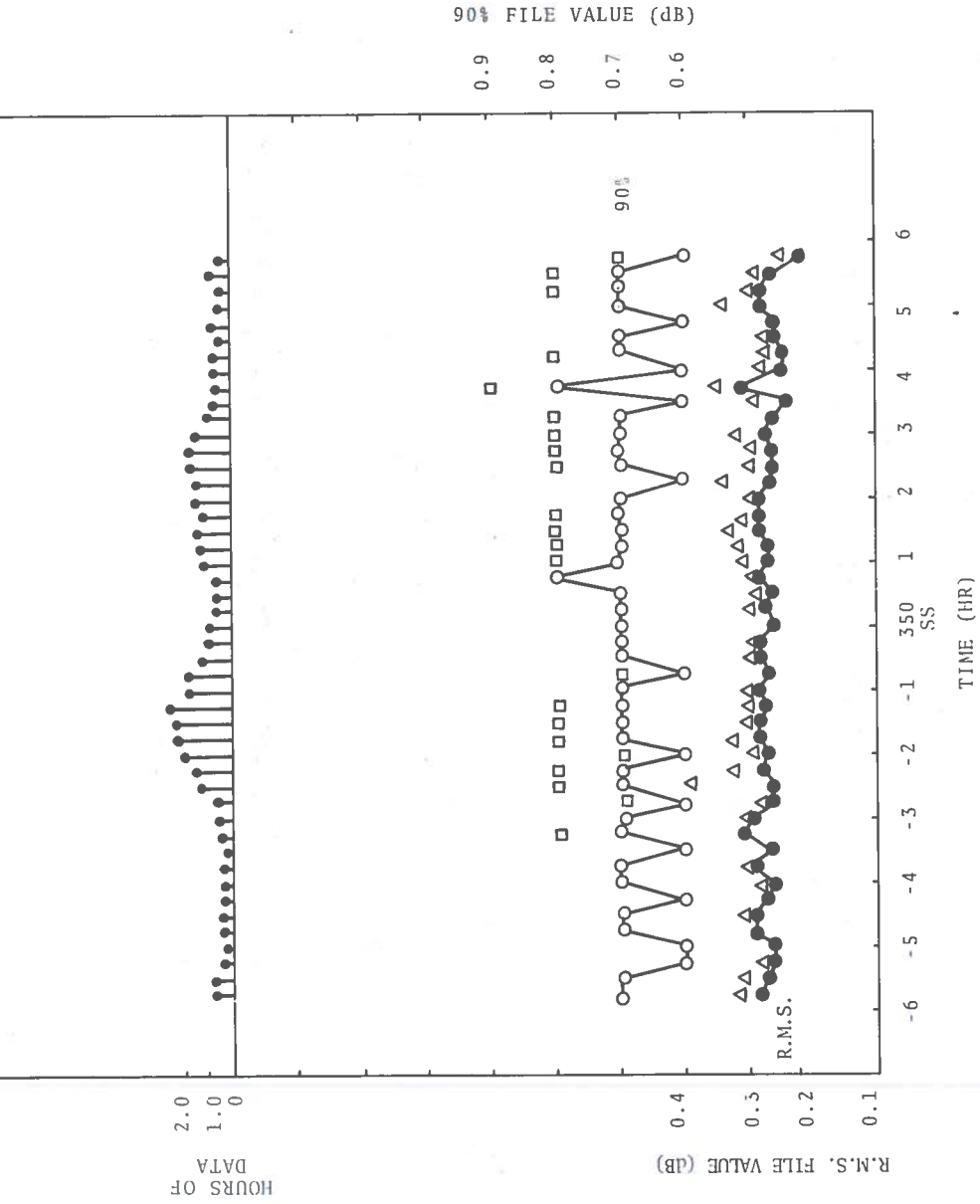


Figure 4-11. Temporal Diagram for January 1974

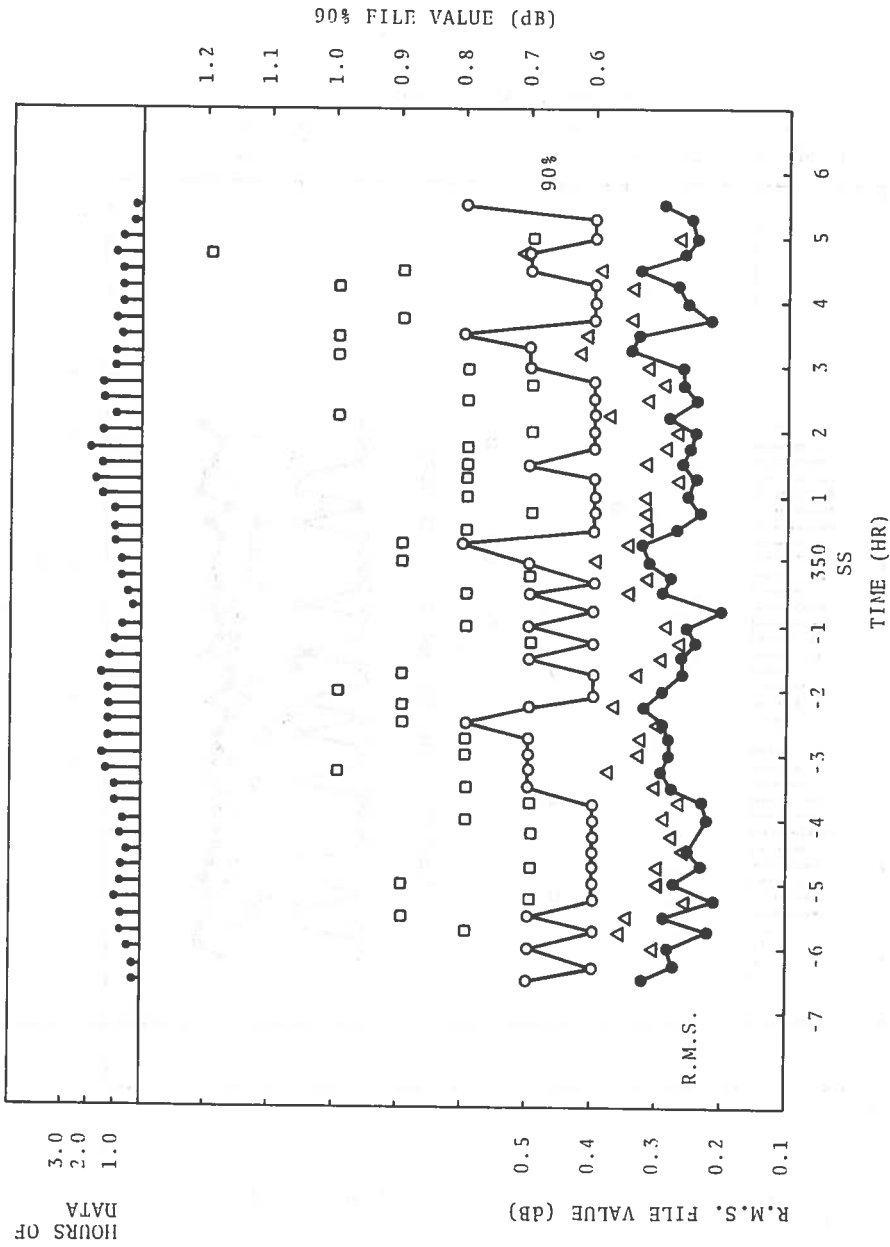


Figure 4-12. Temporal Diagram for February 1974

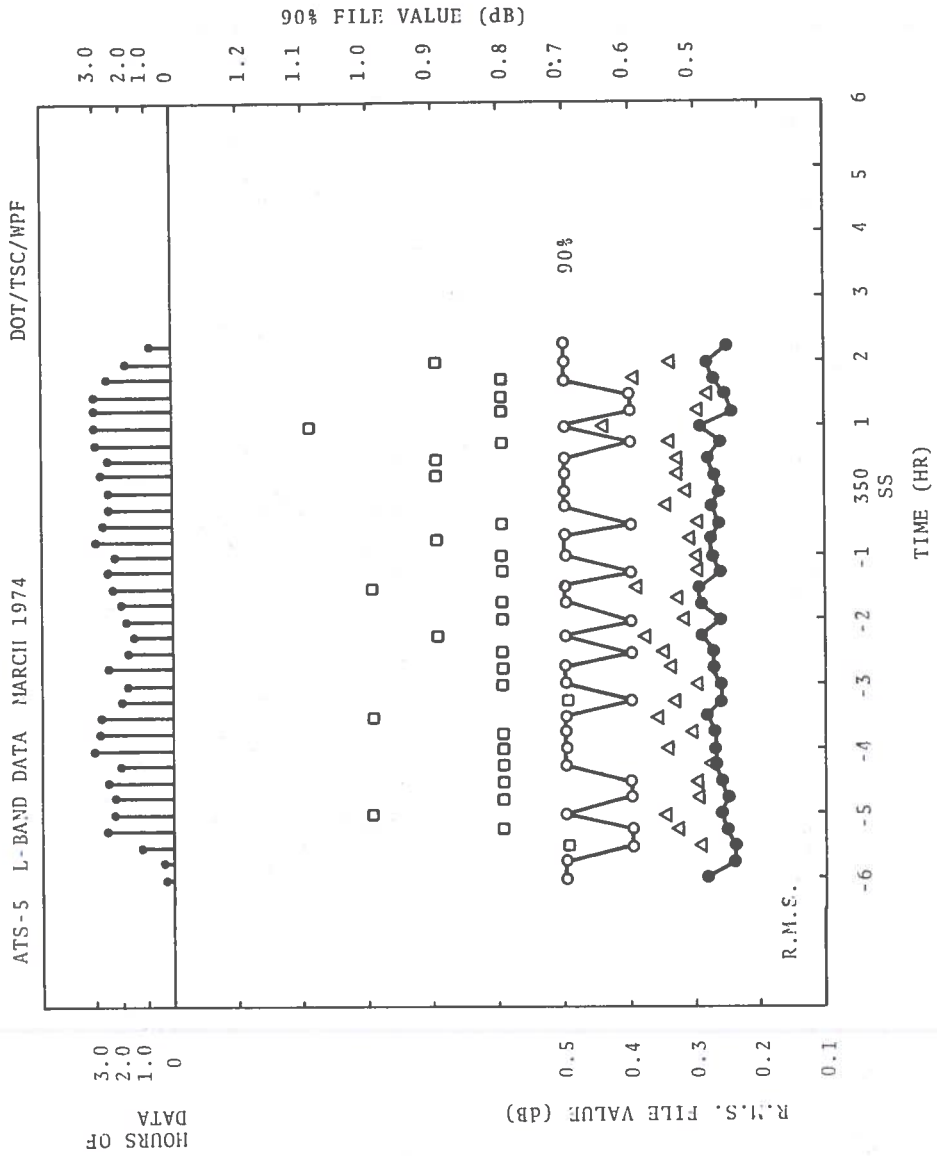


Figure 4-13. Temporal Diagram for March 1974

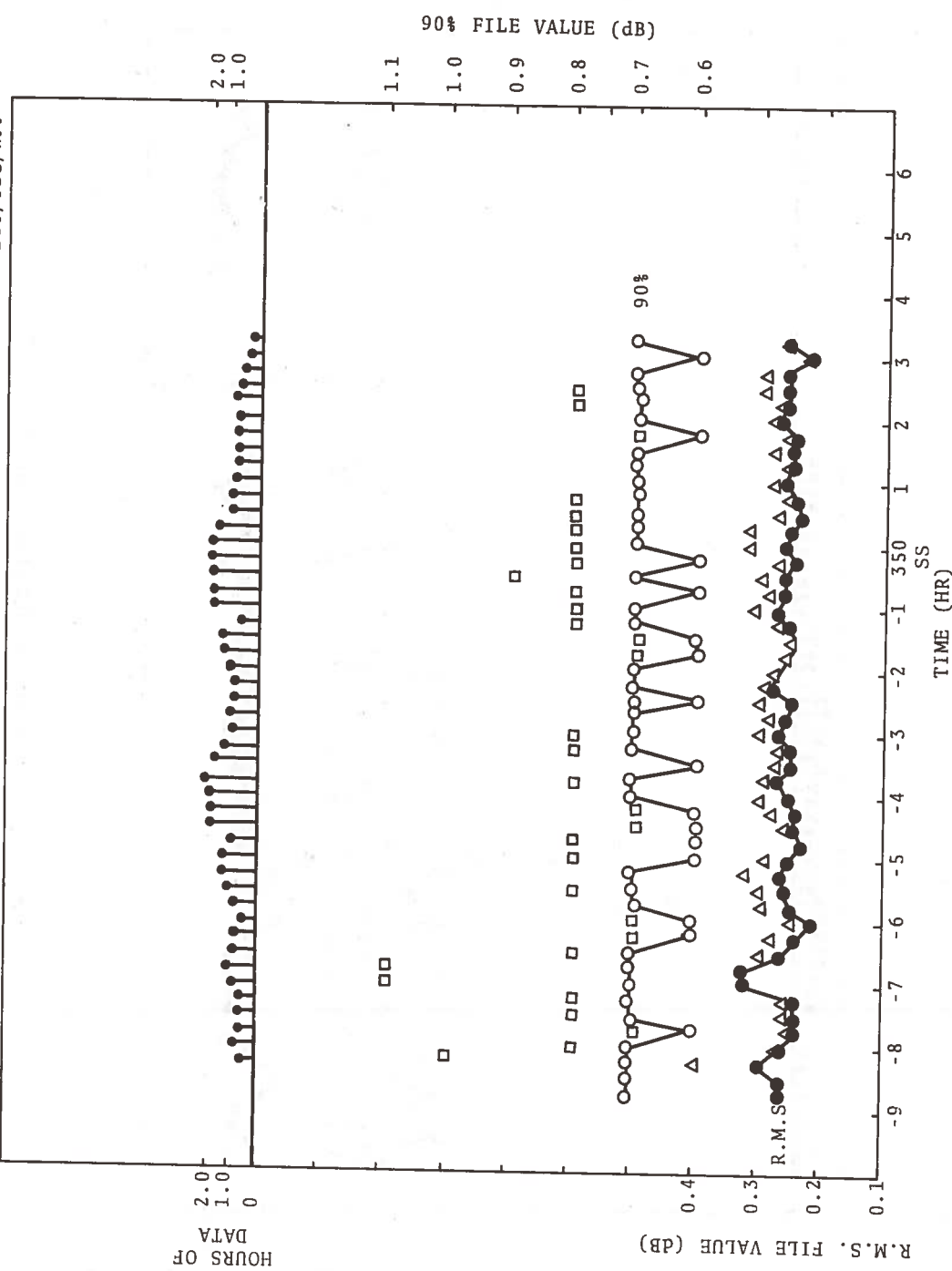


Figure 4-14. Temporal Diagram for April 1974

DOT/TSC/WPF

ATS-5 L-BAND DATA MAY 1974

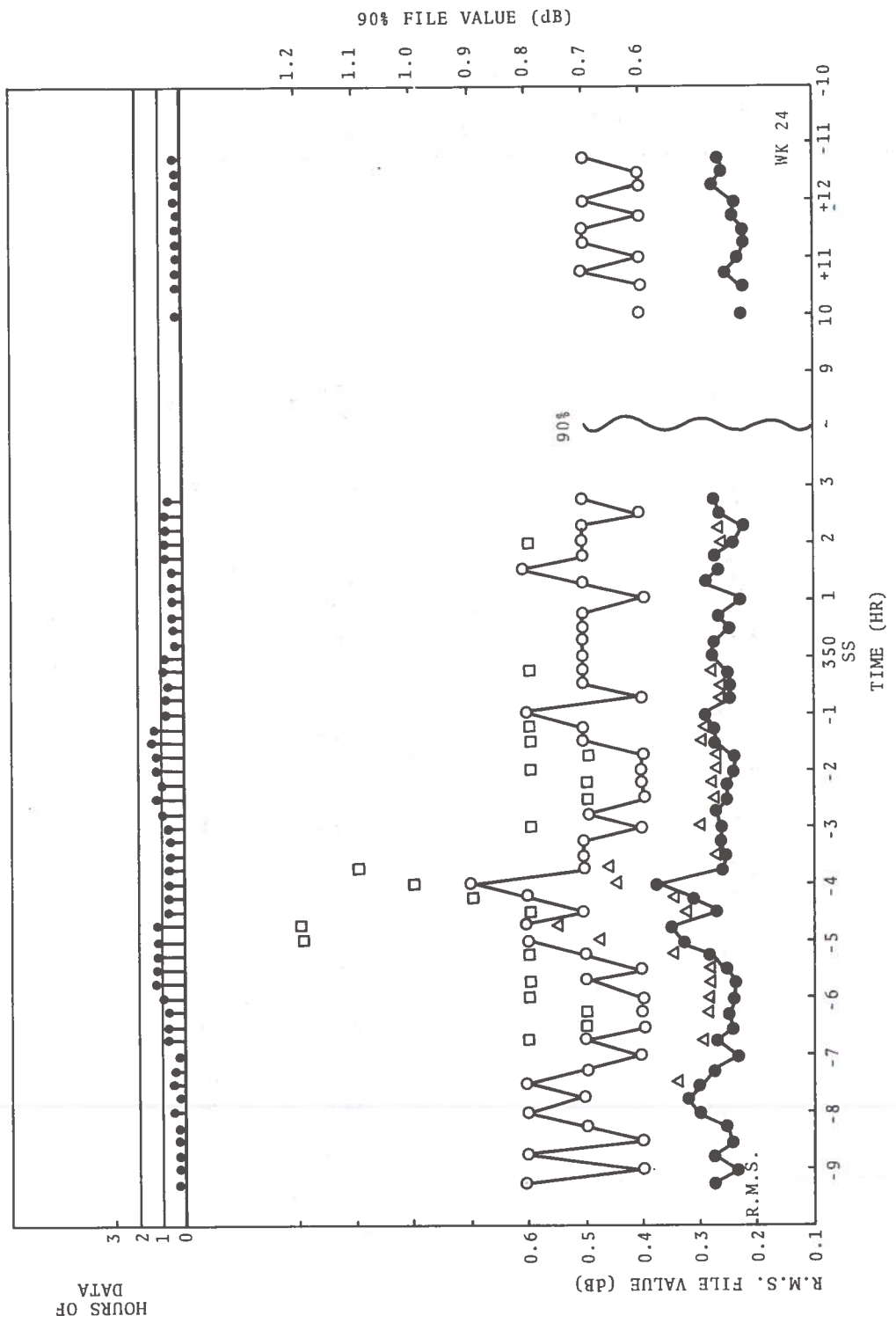


Figure 4-15. Temporal Diagram for May 1974

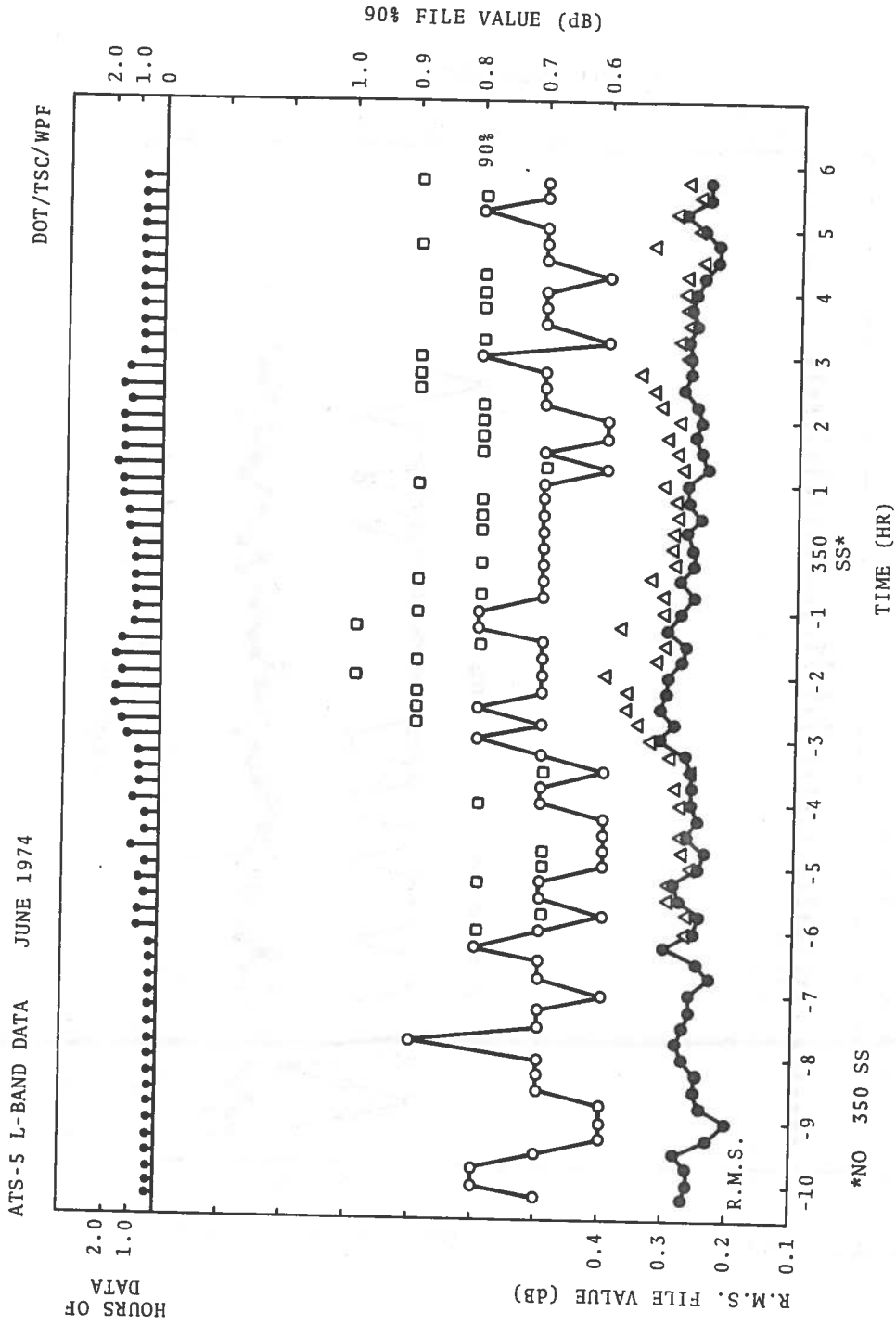


Figure 4-16. Temporal Diagram for June 1974

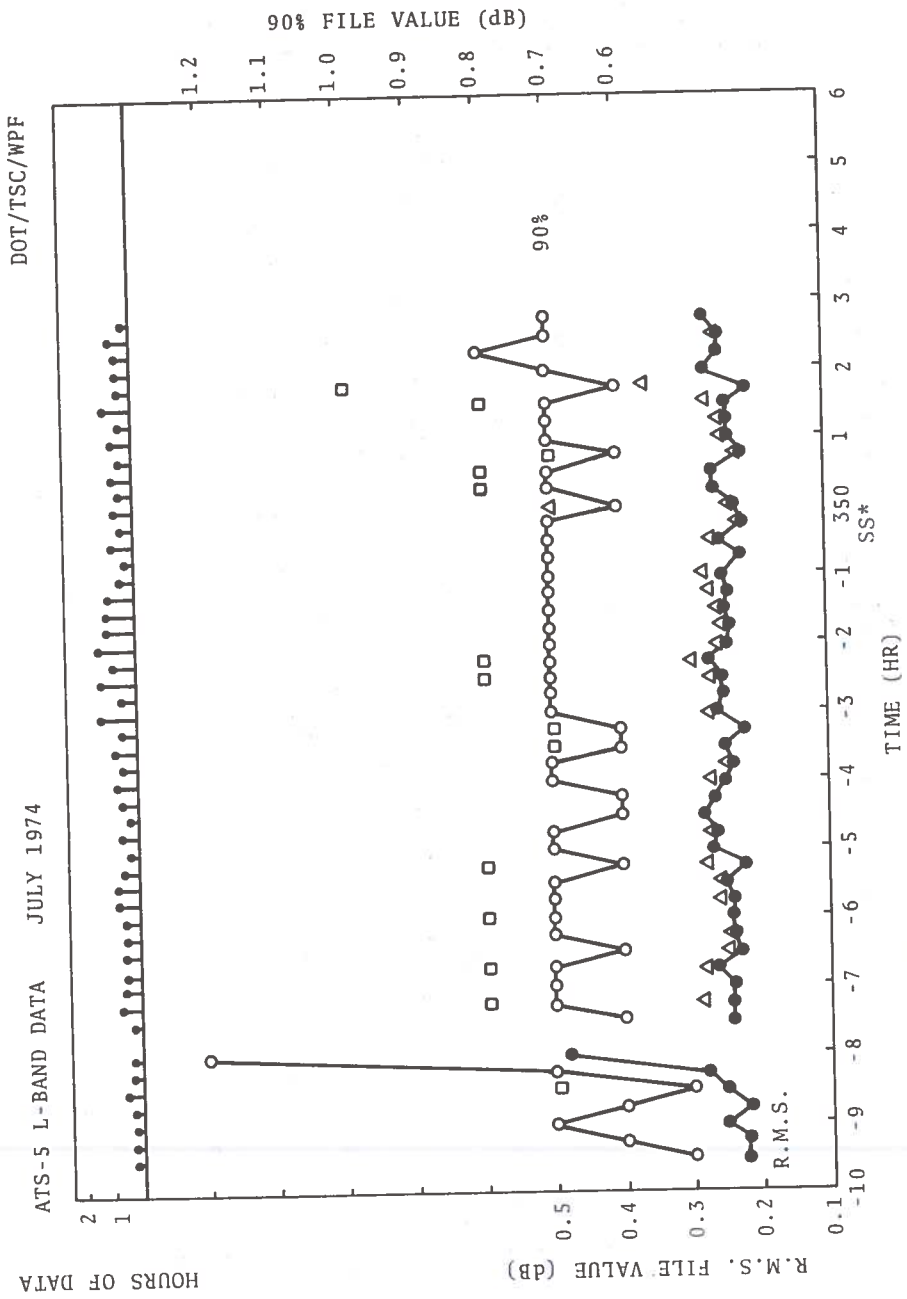


Figure 4-17. Temporal Diagram for July 1974

vatory near Schnectady, New York as there were equipment problems at the Westford facility.

April is made to compose of 5 weeks the last week including 1 May 1974.

During May there were four "normal" weeks and one special test, shown in the time blocks +10.00 and -11.25. One week consists of one day, i.e. 29 May 1974.

The data for June consist of three weeks which have no sunset at the 350 km penetration point along the Westford-to-ATS-5 propagation path. The 350 km sunset for the week of 6 June 1974 is 0015 EDST. The 350 km sunset for the last three weeks of June 1974 was chosen to be 2000 EDST.

July has one week (1 - 2 July) which has no 350 km sunset and the other two weeks had actual 350 km sunsets of 0015. The 350 SS for the first week of July 1974 was chosen to be 2000 EDST.

4.3 SEASONAL ANALYSIS

The data for the individual months were combined statistically to arrive at seasonal temporal diagrams. They are presented in the following sections.

4.3.1 Winter

Figure 4-18 presents the temporal diagrams for December 1973, January 1974 and February 1974 and the combination of the three into a "winter" seasonal temporal diagram. The plots for December 1973, January 1974 and February 1974 come from Figures 4-10 through 4-12, respectively.

Figure 4-19 presents the temporal diagram for "winter" months along with the maximum file values of both the root-mean-square and 90th percentile values.

4.3.2 Spring

Figure 4-20 presents the temporal diagrams for March, April and May 1974 and the combination of the three into a "spring"



Figure 4-18. Temporal Diagrams for December 1973, January 1974 and February 1974 and the Combination into a "Winter" Curve

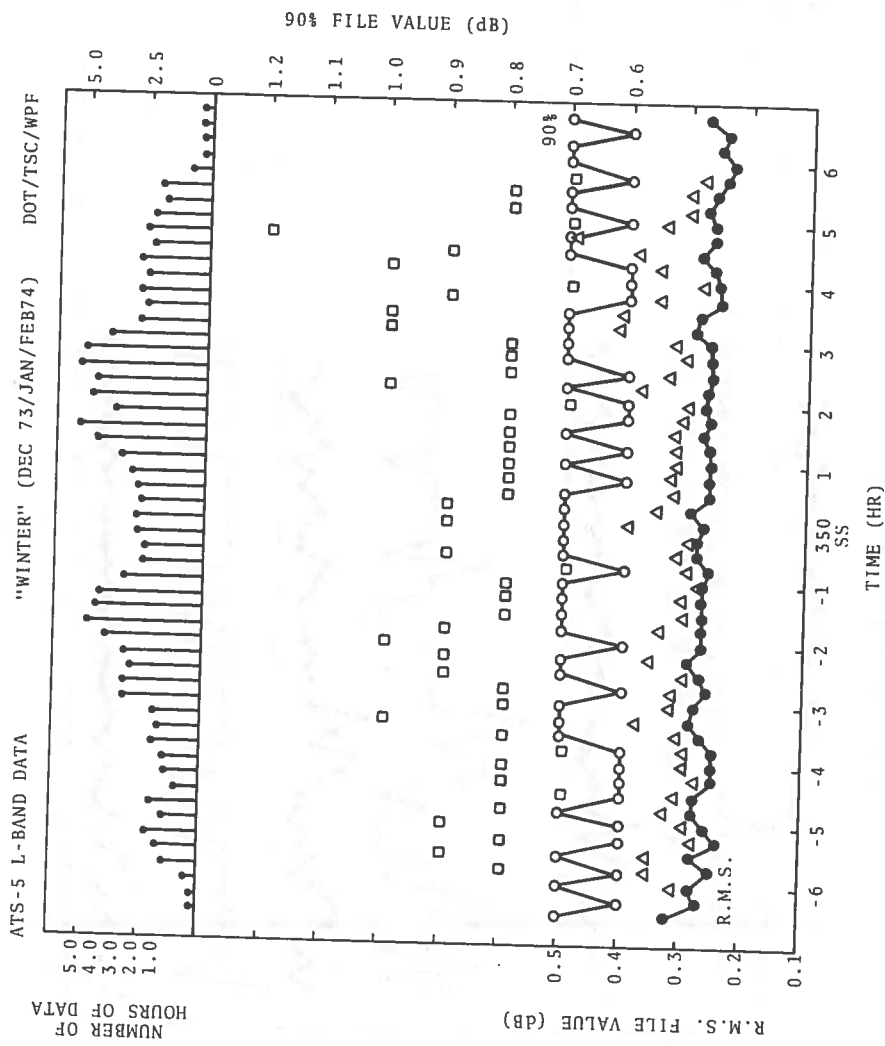


Figure 4-19. Temporal Diagram for "Winter"

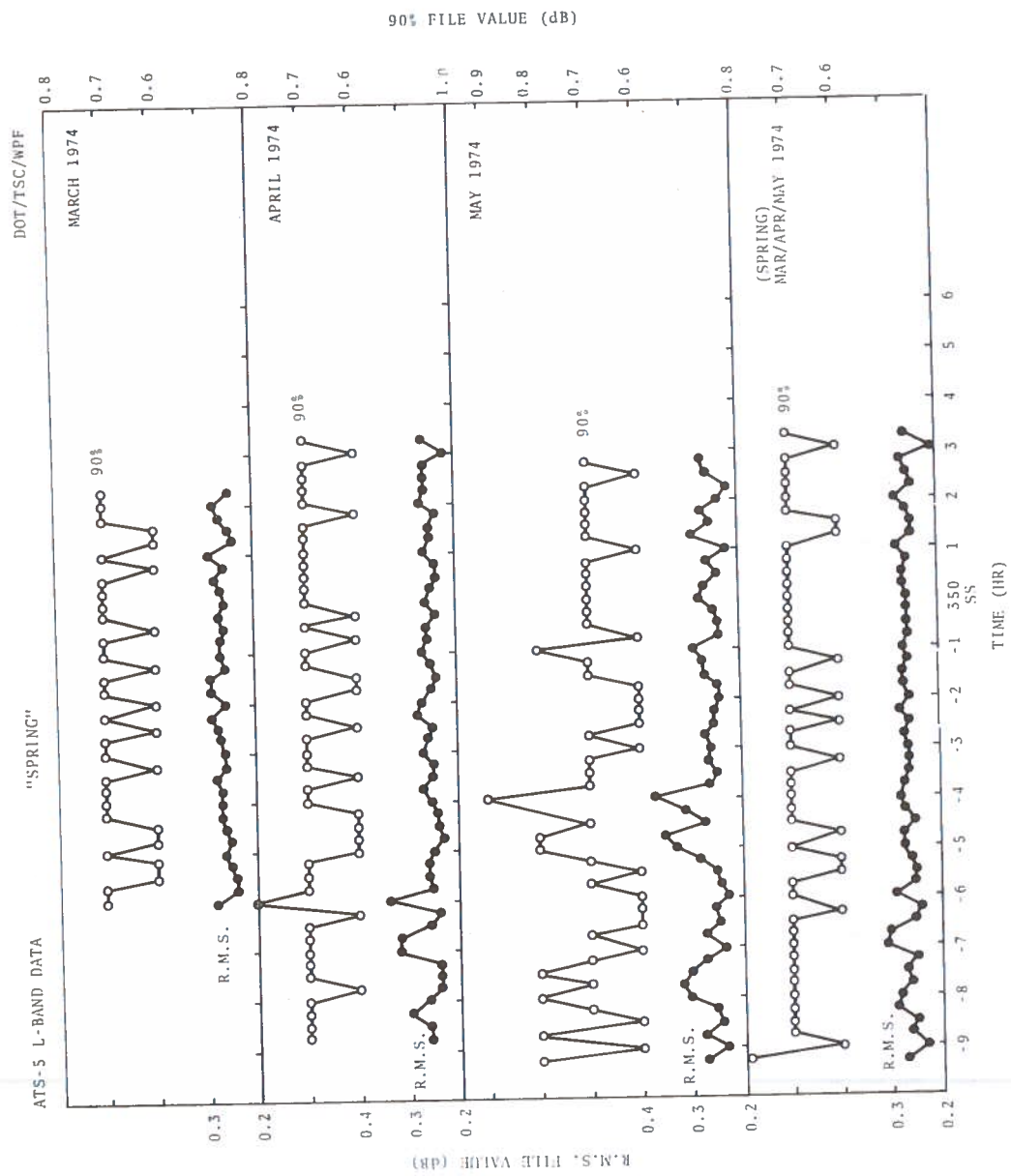


Figure 4-20. Temporal Diagrams for March 1974, April 1974 and May 1974 Along with the Combination into a "Spring" Curve

seasonal temporal diagram. The plots for March, April and May 1974 came from Figures 4-13 through 4-15, respectively.

Figure 4-21 presents the temporal diagram for "spring" months along with the maximum file values of both the root-mean-square and the 90th percentile values.

4.3.3 Summer

Figure 4-22 presents the temporal diagrams for June and July 1974 and the combination of the two into a "summer" seasonal temporal diagram. The plots for June and July 1974 come from Figures 4-16 and 4-17, respectively.

Figure 4-23 presents the temporal diagram for "summer" months along with the maximum file values of both the root-mean-square and the 90th percentile values.

4.3.4 Seasonal Summary

Figure 4-24 presents the temporal diagrams for "winter", "spring" and "summer" from Figures 4-18, 4-20 and 4-22, respectively. The error bar signs indicate the limits where there is five hours worth of data between the signs. This mode of presentation was considered useful for comparison purposes. About the only feature common to all three seasonal curves is the maximum in root-mean-square file values at -2.25 hours.

4.4 DISTRIBUTION OF THE MAXIMUM VALUES

The monthly and seasonal plots presented in the previous section have the maximum values of root-mean-square and 90th percentile plotted on them along with the statistically averaged data. However, the maximum values of the individual time intervals of the individual weeks have also been tabulated. The tabulations are given in Appendix D and the results of these tabulations are presented in Table 4-2. The results for the root-mean-square values is presented graphically in Figure 4-25.

Several pieces of information can be drawn from these data.

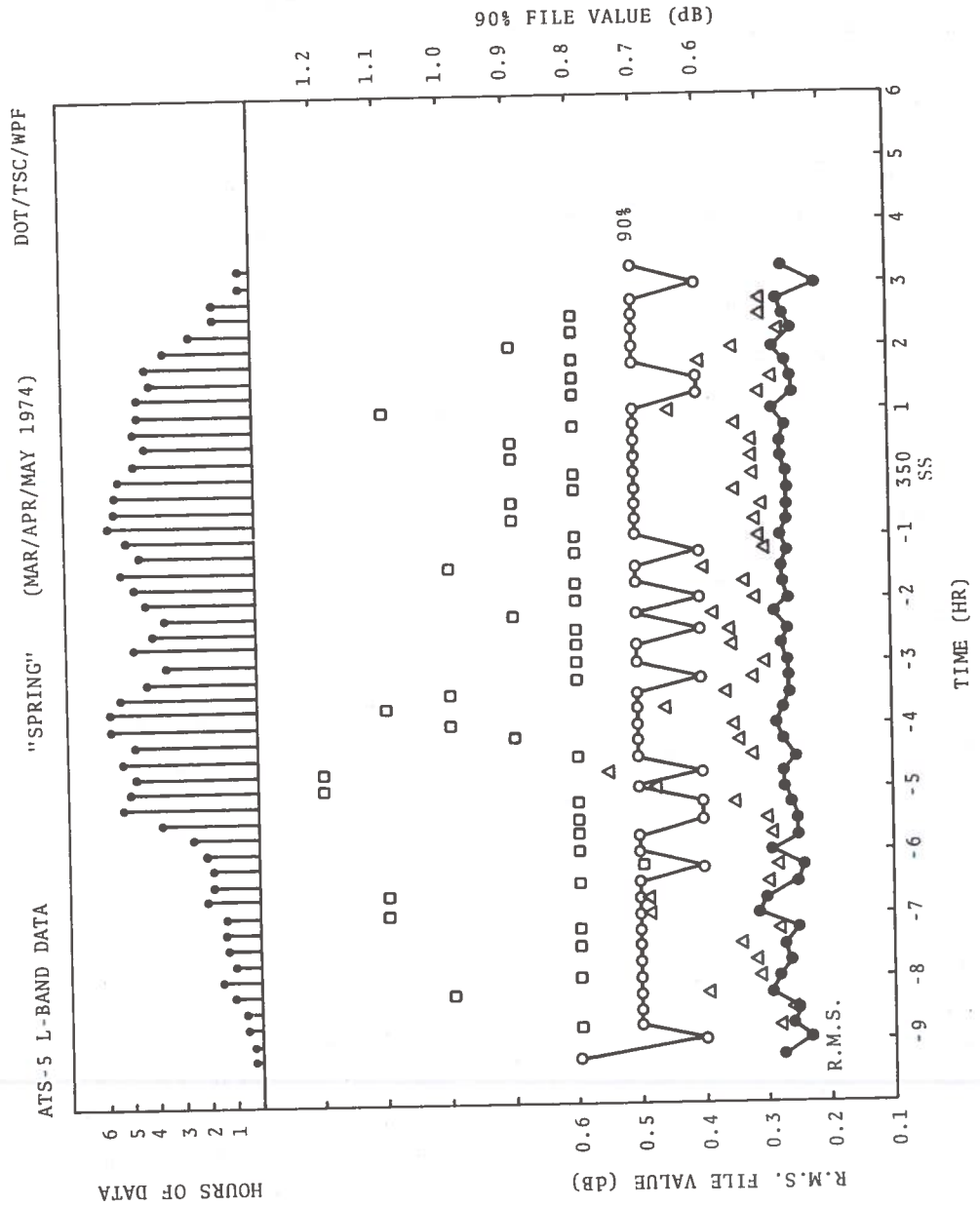
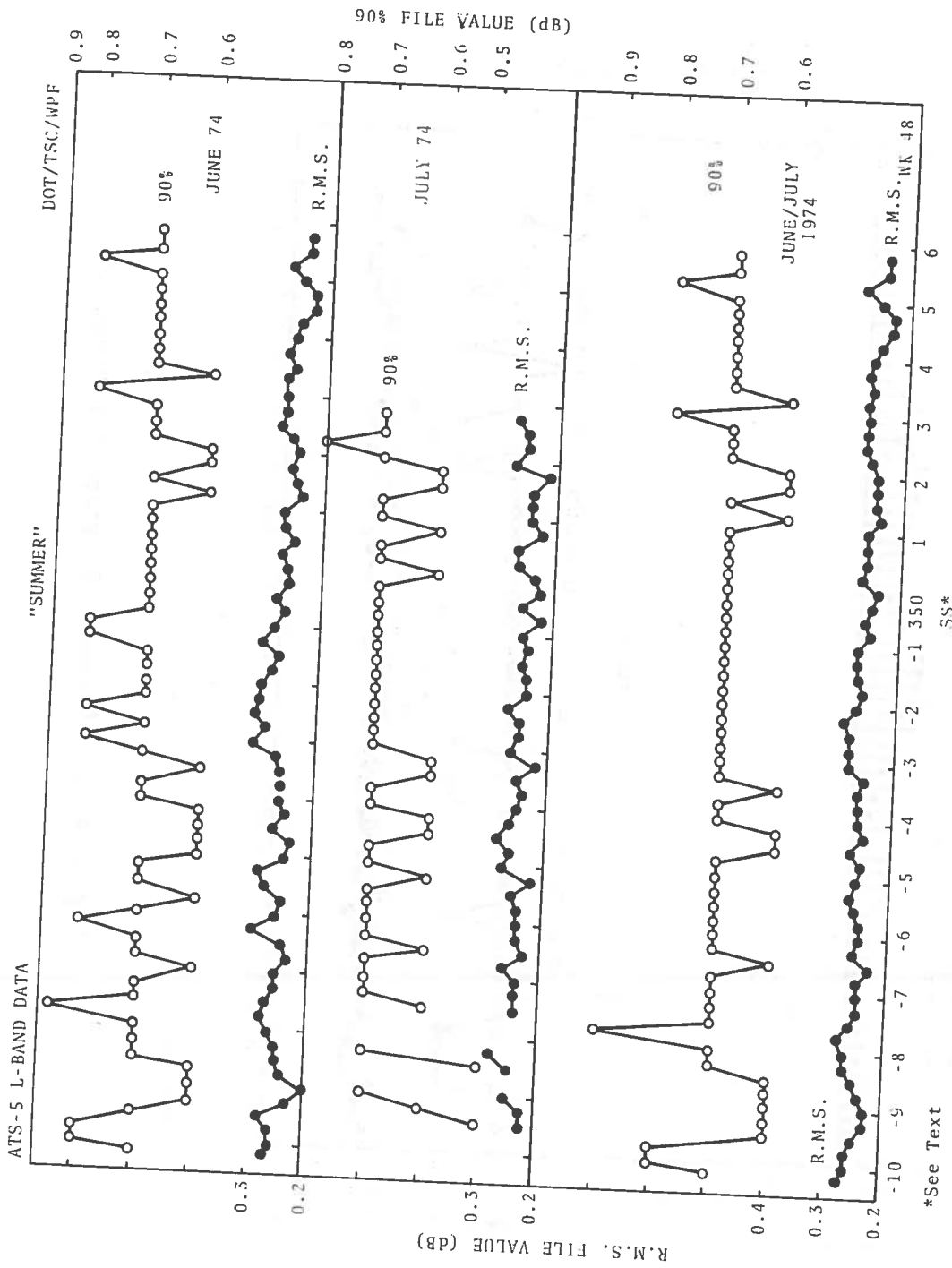
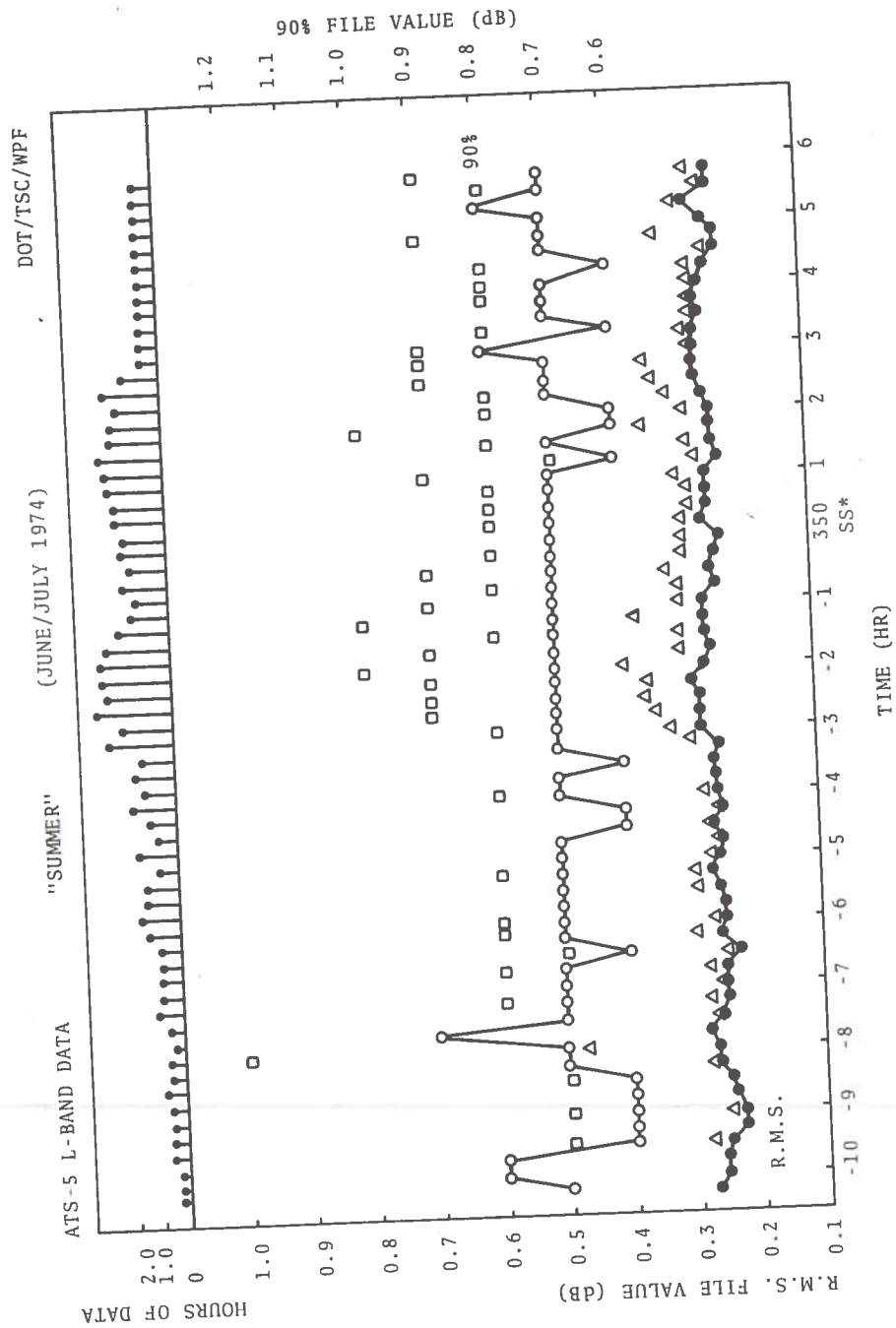


Figure 4-21. Temporal Diagram for "Spring"



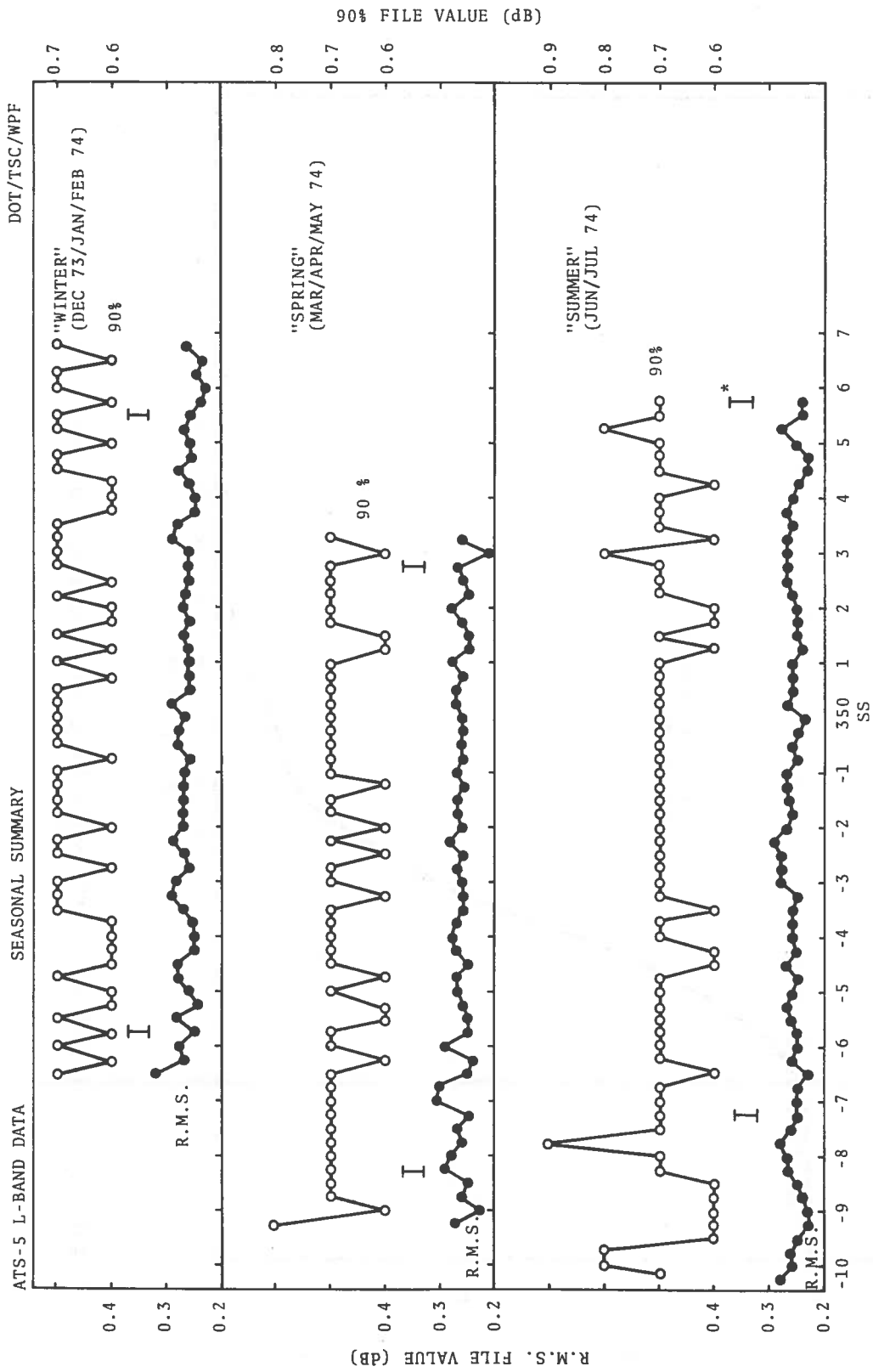
*See Text

Figure 4-22. Temporal Diagram for June 1974 and July 1974 Along with the Combination into a "Summer" Curve



*See Text

Figure 4-23. Temporal Diagrams for "Summer"



*Greater than 5 hours of data.

Figure 4-24. Temporal Diagrams for "Winter", "Spring" and "Summer"

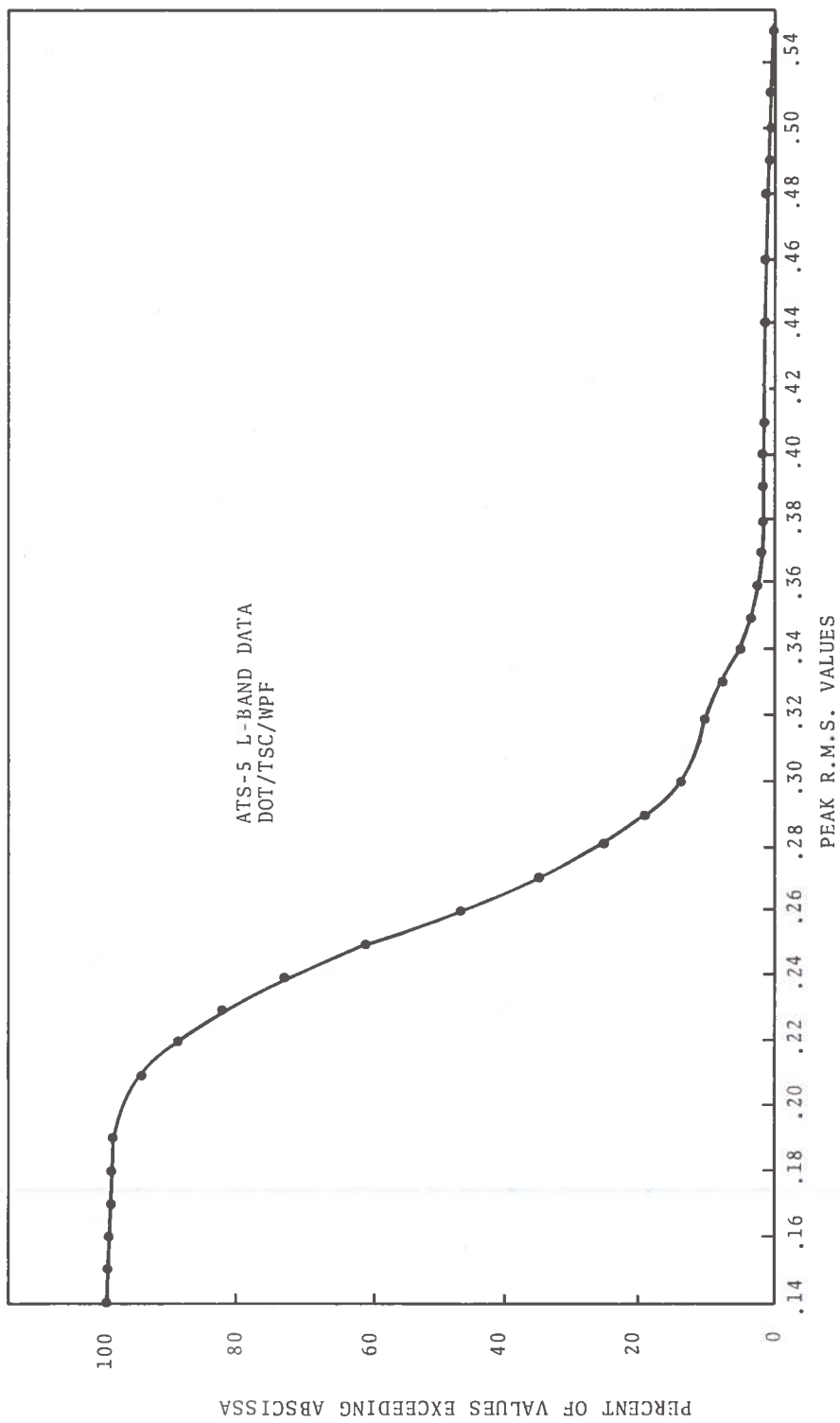


Figure 4-25. Cumulative Frequency Distribution Plotted From Data of Table 4-2

TABLE 4-2. FREQUENCY DISTRIBUTION FOR DATA OF TABLE D-9

DISTRIBUTION OF MAXIMUM VALUES			DOT/TSC/WPF		
ATS-5 L-BAND DATA					
R.M.S. Value (dB)	#	%	Cumulative % D	100-D %	
0.14	0	0	0	100.0	} 10.2%
0.15	1	0.2	0.2	99.8	
0.16	3	0.3	0.5	99.5	
0.17	2	0.3	0.8	99.2	
0.18	1	0.2	1.0	99.0	
0.19	4	0.4	1.4	98.6	
0.20	15	1.5	2.9	97.1	
0.21	24	2.3	5.2	94.8	
0.22	52	5.0	10.2	89.8	
0.23	62	6.0	16.2	83.8	
0.24	102	10.0	26.2	73.8	} 70.1%
0.25	129	12.6	38.8	61.2	
0.26	138	13.5	52.3	47.7	
0.27	135	13.0	65.3	34.7	
0.28	97	9.0	74.3	25.7	
0.29	62	6.0	80.3	19.7	
0.30	70	7.0	87.3	12.7	
0.31	26	2.5	89.8	10.2	
0.32	29	3.0	92.8	7.2	
0.33	22	2.0	94.8	5.2	
0.34	13	1.3	96.1	3.9	} 19.7%
0.35	11	1.0	97.1	2.9	
0.36	4	0.4	97.5	2.5	
0.37	3	0.3	97.8	2.2	
0.38	5	0.5	98.3	1.7	
0.39	3	0.3	98.6	1.4	
0.40	1	0.2	98.8	1.2	
0.41	1	0.2	99.0	1.0	
0.44	2	0.2	99.2	0.8	
0.46	1	0.1	99.3	0.7	
0.48	2	0.2	99.5	0.5	
0.49	1	0.1	99.6	0.4	
0.50	1	0.1	99.7	0.3	
0.51	1	0.1	99.8	0.2	
0.55	2	0.2	100.0	0.0	
TOTALS	1026	100.0	-	-	

For example, 79.6 percent of the maximum amplitude values lie between 0.23 and 0.30 dB. The median value is 0.26 dB. It is seen that approximately 70 percent of the amplitude values centered at 0.26 dB cover the amplitude range 0.23 through 0.29 dB. Thus, 10.2 percent of the values lie between 0.14 and 0.22 dB and 19.7 percent of the maximum values lie between 0.30 and 0.55 dB. Thus, of the 1026 maximum values recorded approximately twice as many are in the scintillating range (greater than 0.30 dB) than are in the exceedingly calm range (less than 0.22 dB).

4.5 GEOMAGNETIC VARIATIONS

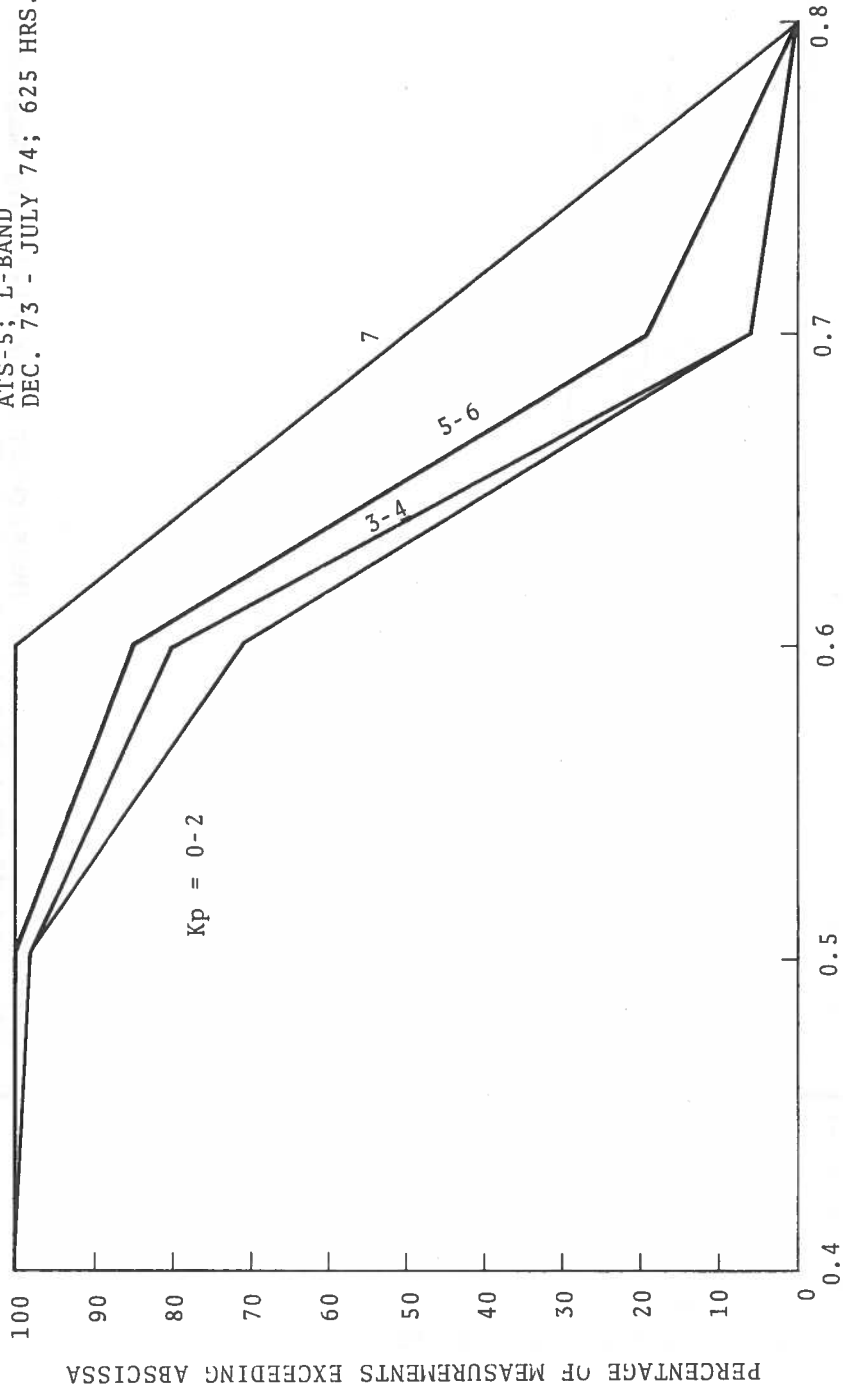
To check for correlation between the time periods of our observed scintillation and time periods of the variations of the geomagnetic field the following was done. First, the value of the geomagnetic field was approximated by use of the widely used planetary magnetic index, Kp. This index is indicated on each of the weekly temporal diagrams found in Appendix C. Secondly, the 90th percentile values were averaged into a 3-hour period corresponding to the appropriate time period for the measurement of the planetary magnetic index. This "3-HR. scintillation index" is abbreviated as "3-HR. SI". Figure 4-26 presents the results of the 625 hours of data.

As can be seen from this figure, high values of "3-HR. SI" correspond to high values of planetary magnetic index. This is illustrated in another way by the presentation given in Figure 4-27. Here the frequency distribution, or histogram, of scintillation measurements is plotted versus the value of the planetary magnetic index. The histogram is very narrow for the "3-HR. SI" of 0.5 dB indicating no times of high magnetic disturbance. As the "3-HR. SI" increases so does the width of the histogram which allows values of magnetic index up to 7.

4.6 OBSERVED SEMI-DIURNAL VARIATIONS

The diurnal variations of the scintillation were examined for two classes of magnetic activity. The first class included Kp

WESTFORD, MASS., USA
 ATS-5; L-BAND
 DEC. 73 - JULY 74; 625 HRS.



"3-HR. SCINTILLATION INDEX" (dB)
 (90% LEVEL OF THE PROBABILITY DISTRIBUTION)

Figure 4-26. Comparison of "3-HR Scintillation Index" with Planetary Magnetic Index Kp (Dec. 1973 - July 1974)

DEC. 73 - JULY 74 625 HRS.
Westford, Mass. USA

DOT/TSC/WPF

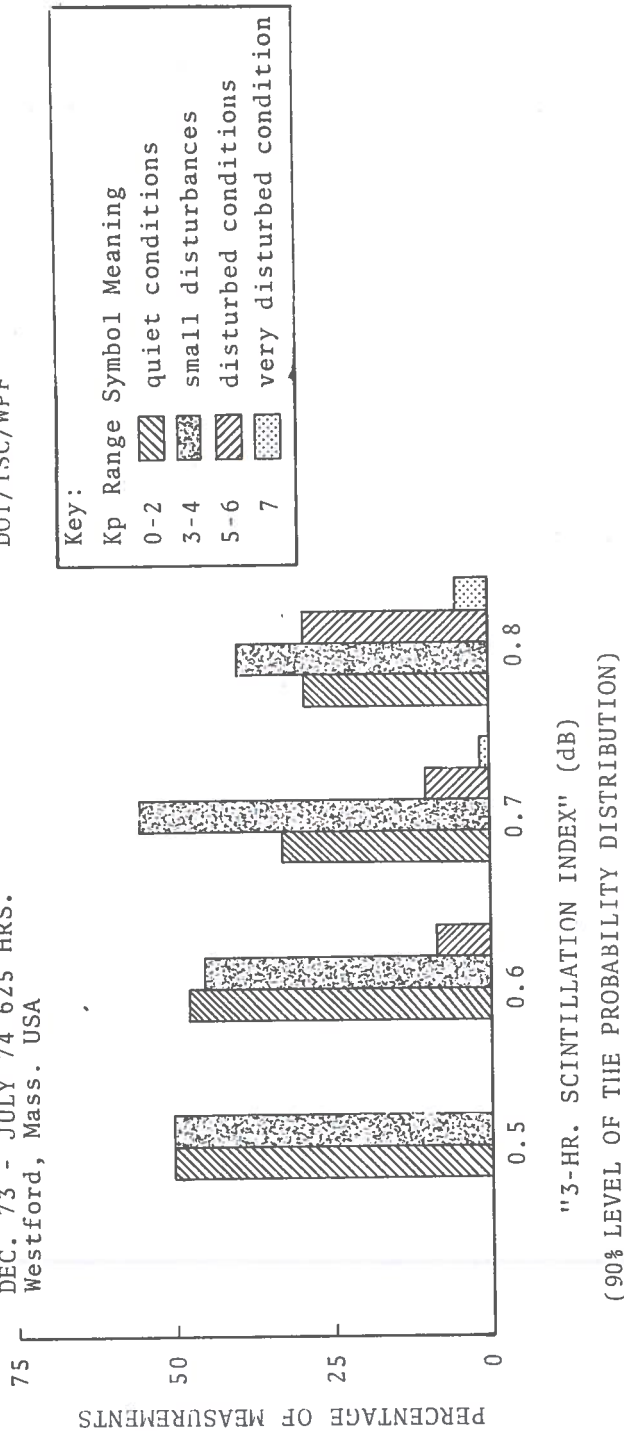


Figure 4-27. Histogram of Scintillation Measurements by Planetary Magnetic Index and "3-HR Scintillation Index"

values of 0 to 1 and the other class was for Kp values of approximately 5 (i.e. 4,5,6). The hourly averages of the 90th percentile values of the probability distributions function were formed and are denoted as "1-HR. SI".

Figure 4-28 presents a plot of the results of the present scintillation measurements. The scintillation index values represent over 24 hours worth of data in some places. In general, there appears to be a peak in scintillation at about 1800 LMT and a minimum at 2300 and 0000 LMT.

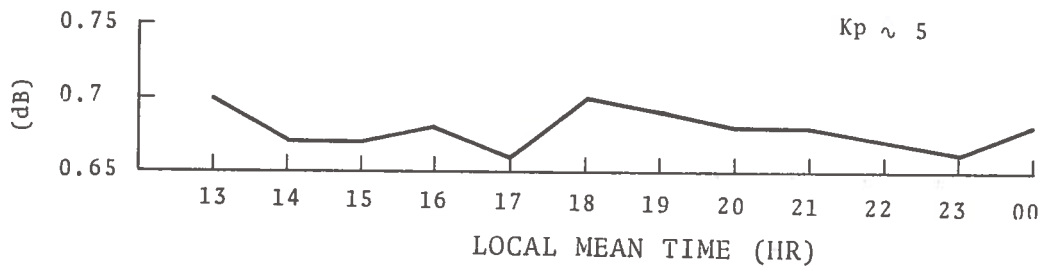
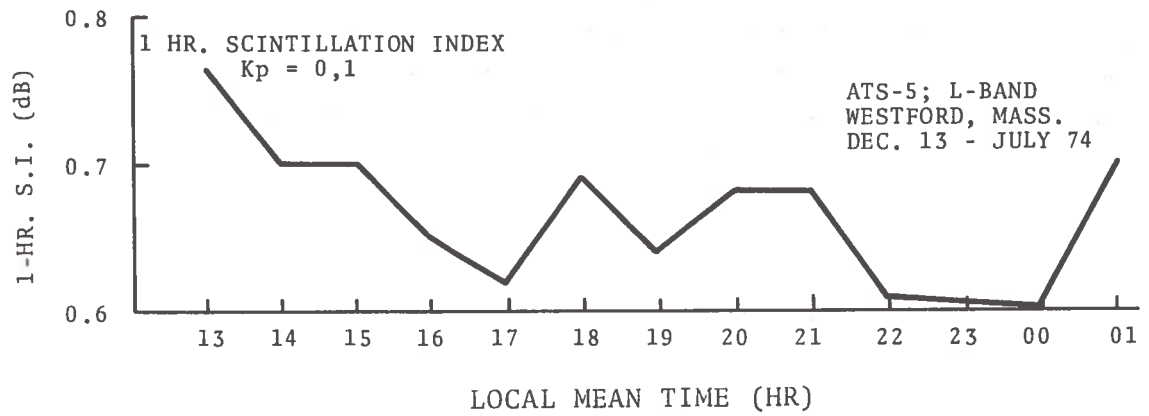


Figure 4-28. Diurnal Variation of 1-Hour Scintillation Index for the 625 Hours of Observations

5. CONCLUSIONS & RECOMMENDATIONS

5.1 CONCLUSIONS

The measurements presented herein represent a significant amount of L-band data that has been collected and analyzed as part of a carefully controlled experiment. The measurements are representative of winter and spring in the midlatitudes during solar sunspot minimum. The observing times were selected to sample the propagation path during hopefully and most stable times as well as during unstable time of the diurnal cycle.

From these data several conclusions may be drawn. Scintillation of L-band signals does exist in midlatitudes. Of the 2500 15-minute observing periods covered by this report 10.2 percent were found to be undisturbed with a root-mean-square fluctuation level of 0.22 dB or less. At the same time 0.84 percent of the observing periods were found to have disturbed propagation conditions with the 90th-percentile level for the period exceeding 1.0 dB. The 1 dB 90th-percentile level corresponds to approximately a 2 db peak-to-peak fluctuation level.

A careful study of Figures 4-10, 4-11, 4-12, 4-13, 4-14, 4-15, 4-16 and 4-17 shows that root-mean-square fluctuation levels of 0.27 dB to 0.33 dB are typical, however, 0.4 and 0.5 dB are not uncommon. The root-mean-square of the fluctuations is a very sensitive indicator of the fluctuation level.

The figures also reveal that the 90th-percentile levels are typically 0.4 and 0.5 dB; however, 90th-percentile levels in excess of 1 dB are not uncommon. The peak-to-peak fluctuations are about twice the 90th-percentile level for 90th-percentile levels in the 1 dB range.

Since the root-mean-square and the 90th-percentile levels are the result of 12-minute measurement intervals the extreme fluctuations during an observing period are smoothed. The largest peak-to-peak fluctuation that was observed on the strip-chart

recording was 3 dB. Likewise the smallest root-mean-square fluctuation level for a 12-minute observing period was found to be 0.15 dB.

The occurrence of the scintillation appears to be most prevalent during the hours of sunset though moderate scintillations have been observed well before and well after sunset. The spring months, however, appear to have scintillation more often and they are more severe and they do not appear to be related to ionospheric sunset.

An attempt was made to find some correlation between the observed periods of scintillation, planetary magnetic index (Kp) and data from ionospheric soundings. There appears to be some relation between Kp and the observed periods of scintillation, though it is inconclusive and needs a great deal of more careful study and experimentation. The observed scintillation periods were also correlated with ionospheric soundings made at Wallops Island, Virginia. There appears to be no correlation between foF2 nor spread-F and our measured scintillation data.

Figures 4-2 and 4-3, though a little rougher than normal, are typical of the signal. There are, however, occasions when the signal is very steady as in Figure 4-1. There appears to be a small amount of "residual" scintillation present most of the time. Earlier measurements had also indicated this. At present we have no explanation except to postulate that there may be small-scale turbulence or winds are always present in the F-region of the ionosphere.

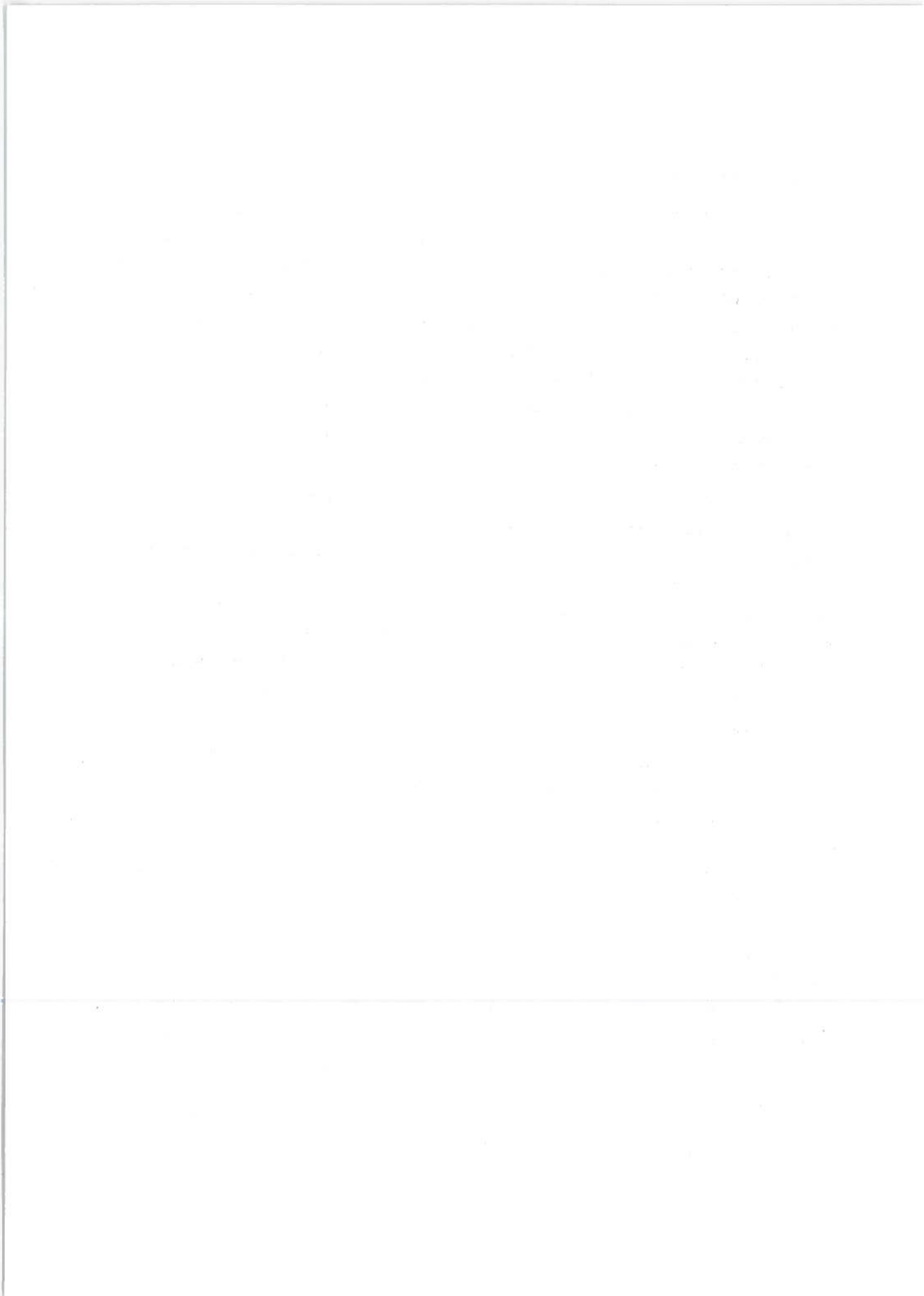
It is felt that one of the important points that is illustrated by this report is that a large sample of data of a fundamental physical phenomenon may be obtained by relatively simple apparatus. Now that the hardware and software have been developed and are operational they may be used to perform additional measurements particular to a communication system. For example, knowing only the amplitude signal statistics typical of the month of May, the actual statistical reliability of a communication system may be inferred from these amplitude measurements. Obviously, the estimate will be greatly improved since at least amplitude statistics typical of May are known.

5.2 RECOMMENDATIONS

The first recommendation is that the present L-band data be carefully analyzed in order to find some strong correlation with known geophysical effects and data such as the magnetic index and ionospheric soundings. This is important because when some observable geophysical effect can be shown to be related to microwave scintillations then a workable theory may be developed to explain and calculate the expected scintillation. As soon as a workable explanation has been developed then channel characterization and prediction of scintillation may be made and easily verified experimentally.

The second recommendation is that a measurement program be continued to complete the present amplitude data base for a complete year at a midlatitude station and at the same time concurrently measure the phase statistics of an L-band signal. Such a program will extend the amplitude data base and complement the present data base of SHF measurements. Most important is the initiation of a program which is meant to provide the essential phase statistics which are necessary in characterizing an L-band communications channel.

It is recommended that the DOT/TSC Automatic Data Collection Platform (ADCP) be deployed to a high geomagnetic latitude geographical location. This equipment could be straightforwardly modified, as described in Appendix E, to make L-band phase scintillation measurements applicable to wide-band and narrow-band scintillation characterization. The existing computer software in the remote ADCP may be used, as is, to provide the phase or amplitude measurements every third to one-half second. As described in Section 3, the amplitude/phase measurements will be relayed back to the Westford site by VHF. Thus, the amplitude/phase data would be available from the Westford locations and the site chosen for the ADCP. By selecting the remote location properly, the path geometry of the remote site and the Westford site may be arranged to give some additional geophysical and geometric details of the observed scintillations.



6. REFERENCES

- Brown, W.E., III, G.G. Haroules and W.I. Thompson, III, (1974A), Description of a ground facility for conducting ionospheric scintillation measurements with the ATS-5 spacecraft, Report No. DOT-TSC-OST-73-2, DOT/Transportation Systems Center, Cambridge, Mass.
- Brown, W.E., III, G.G. Haroules and W.I. Thompson, III, (1974B), Description of a remote ionospheric scintillation data collection facility, Report No. DOT-TSC-OST-73-17, DOT/Transportation Systems Center, Cambridge, Mass.
- Campbell, W.H. and S. Matsushita, (1967), World maps of conjugate coordinates and L contours, *J. Geophysical Res.* 72, 3518-3521.
- Christiansen, R.M., (1971), Preliminary report of S-band propagation disturbance during ALSEP mission support, Nov. 19, 1969 - June 30, 1970, Report No. X-861-71-239, NASA/Goddard Space Flight Center, Greenbelt, Maryland.
- Craft, H.D., Jr. and L.H. Westerlund, (1972), Scintillation at 4 and 6 GHz caused by the ionosphere, AIAA Paper No. 72-179 at the AIAA 10th Aerospace Science Mts., San Diego, Calif., American Institute of Aeronautics and Astronautics, New York.
- Evans, J.E., L.L. Newkirk, and B.M. McCormac, (1969) North polar, south polar, world maps and tables of invariant magnetic coordinates for six altitudes: 0, 100, 300, 600, 1000 and 3000 km, Report No. DASA 2347, Lockheed Palo Alto Research Lab., Palo Alto, CA, AD-861004.
- Evans, J.V. and J.M. Holt, (1973), The combined use of satellite differential Doppler and ground-based measurements of ionospheric studies, *IEEE Trans. Antennas & Propagation*, AP-21, (5), 685-692.
- General Electric Co., (1975), Specification and description - ground responder control computer program, Report on Contract No. DOT-TSC-485, General Electric Co., Schenectady, New York.

REFERENCES (CONTINUED)

- Golden, T.S., (1970), Amplitude effects on the auroal ionosphere on satellite telemetry at 136 and 1700 MHz, Report No. X-520-70-397, NASA/Goddard Space Flight Center, Greenbelt, Maryland.
- Golden, T.S., (1971), A brief review of ionospheric scintillation fading effects as observed in NASA Satellite Tracking and Data Acquisition Network, Report No. X-810-71-402, NASA/Goddard Space Flight Center, Greenbelt, Maryland.
- Golden, T.S. and W.B. Sessions, (1972), Simultaneous L-band and VHF ionospheric fading effects at the geomagnetic equator, Report No. X-810-72-227, NASA/Goddard Space Flight Center, Greenbelt, Maryland
- Kraus, J.D., (1966), Radio Astronomy, McGraw-Hill, New York, p. 102.
- Lincoln, J.V., (1974), Editor Geomagnetic and solar data, December 1973, J. Geophysical Research, 79, (10), 1586; 79, (13), 2006 for January 1974; 79, (16), 2555, for February 1974; 79, (19), 2936, for March 1974; 79, (22), 3244 for April 1974; 79, (25), 3886, for May 1974; 79, (28), 4350, for June 1974; 79, (31), 4828; for July 1974.
- NASA, (1974), ATS-5 Predictions for 1973-1974, NASA/Goddard Space Flight Center, Greenbelt, Maryland.
- Piggott, W.R. and K. Rawer, Editors, (1972), U.R.S.I. Handbook of Ionogram Interpretation and Reduction, 2nd. Edition Report No. UAG-23, World Data Center A for Solar-Terrestrial Physics, NOAA, Boulder, Colorado.
- Ponnappa, P.C., (1973), L-band (1550 MHz) power spectrum of ionospheric fading signals, Private communication.
- Rufenach, C.L., (1974), Wavelength dependence of radio scintillation: Ionosphere and interplanetary irregularities, J. Geophysical Res. 79. (10, 1562-1566.
- Skinner, N.J., R.F. Kelleher, J.B. Hacking and C.W. Benson, (1971), Scintillation fading of signals in the SHF band, Nature (Physical Science), 232, July 5, 19-21.

REFERENCES (CONTINUED)

- Taur, R.R., (1973), Ionospheric scintillation at 4 to 6 GHz, COMSAT Tech. Rev. 3, 145-163.
- Taur, R.R., (1974), Ionospheric scintillation at frequencies above 1 GHz, COMSAT Tech. Rev., 4, (2), 461-476.
- Valley, S.L., Editor, (1965), Handbook of Geophysics & Space Environments, McGraw-Hill, New York.
- Wernick, A.W., C.H. Liu, (1974), Ionospheric irregularities causing scintillation of GHz frequency radio signals, J. Atmospheric & Terr. Phys. 36, (5), 871-879.
- Wernick, A.W., C.H. Liu, M.Y. Youakim and K.C. Yeh, (1973), A Theoretical study of scintillation of transionospheric radio signals, Final Report No. UILU-ENG-73-2559 on Contract No. NGR-14-005-189, Ionosphere Radio Lab., Univ. Illinois, Urbana.

1. The first part of the document discusses the importance of maintaining accurate records of all transactions. It emphasizes that proper record-keeping is essential for the success of any business and for the protection of the interests of all parties involved. The document outlines the various methods and systems that can be used to ensure the accuracy and reliability of the records.

2. The second part of the document focuses on the role of the accounting department in the overall management of the organization. It highlights the need for the accounting department to provide timely and accurate financial information to the management and to the external stakeholders. The document also discusses the various responsibilities and functions of the accounting department, including the preparation of financial statements, the management of the company's assets, and the monitoring of the company's financial performance.

3. The third part of the document discusses the importance of maintaining accurate records of all transactions. It emphasizes that proper record-keeping is essential for the success of any business and for the protection of the interests of all parties involved. The document outlines the various methods and systems that can be used to ensure the accuracy and reliability of the records.

4. The fourth part of the document discusses the importance of maintaining accurate records of all transactions. It emphasizes that proper record-keeping is essential for the success of any business and for the protection of the interests of all parties involved. The document outlines the various methods and systems that can be used to ensure the accuracy and reliability of the records.

APPENDIX A

SITING REQUIREMENTS FOR THE AUTOMATIC DATA COLLECTION PLATFORM

A.1 SIZE AND WEIGHT

The Automatic Data Collection Platform (ADCP) is described in Brown, Haroules and Thompson (1974A) in great detail. Section 3 of the present report also describes the platform and the software involved in its operation. The electronic equipment that makes up the platform except for the power amplifier and the ASR-33 teletype unit is all mounted in two individual 4-foot high cabinets. The cabinets are fitted with locking doors both in front and rear, cooling blowers are mounted on the rear of the cabinets, and casters on the heavy duty bases. The power amplifier may be placed on top of one of the cabinets if desired and the teletype unit may be removed from its stand and placed atop the other cabinet. The power amplifier is mounted in a ruggedized box at present.

Figure A-1 is a physical layout of the platform's equipment and Figure A-2 is a physical layout of the antenna structure.

The overall equipment weight is 600 pounds and the antennas and tower weigh 350 pounds. Specific shipping weights are given in Table A-1.

The L-band and VHF antennas are mounted on a single 20-foot high tower. The six-foot L-band reflector antenna is mounted aside the tower on an adjustable mount and the VHF antenna is mounted on a pole extending out from the top of the tower.

A.2 POWER REQUIREMENTS

The AC power consumption is tabulated in Table A-2.

A.3 ELEVATION ANGLES FROM VARIOUS GEOGRAPHICAL SITES TO THE ATS SERIES OF SPACECRAFT

Table A-3 shows the elevation angles for suggested remote platform sites. St. Johns Newfoundland is the optimum choice for a high latitude site and San Juan, Puerto Rico is an optimum

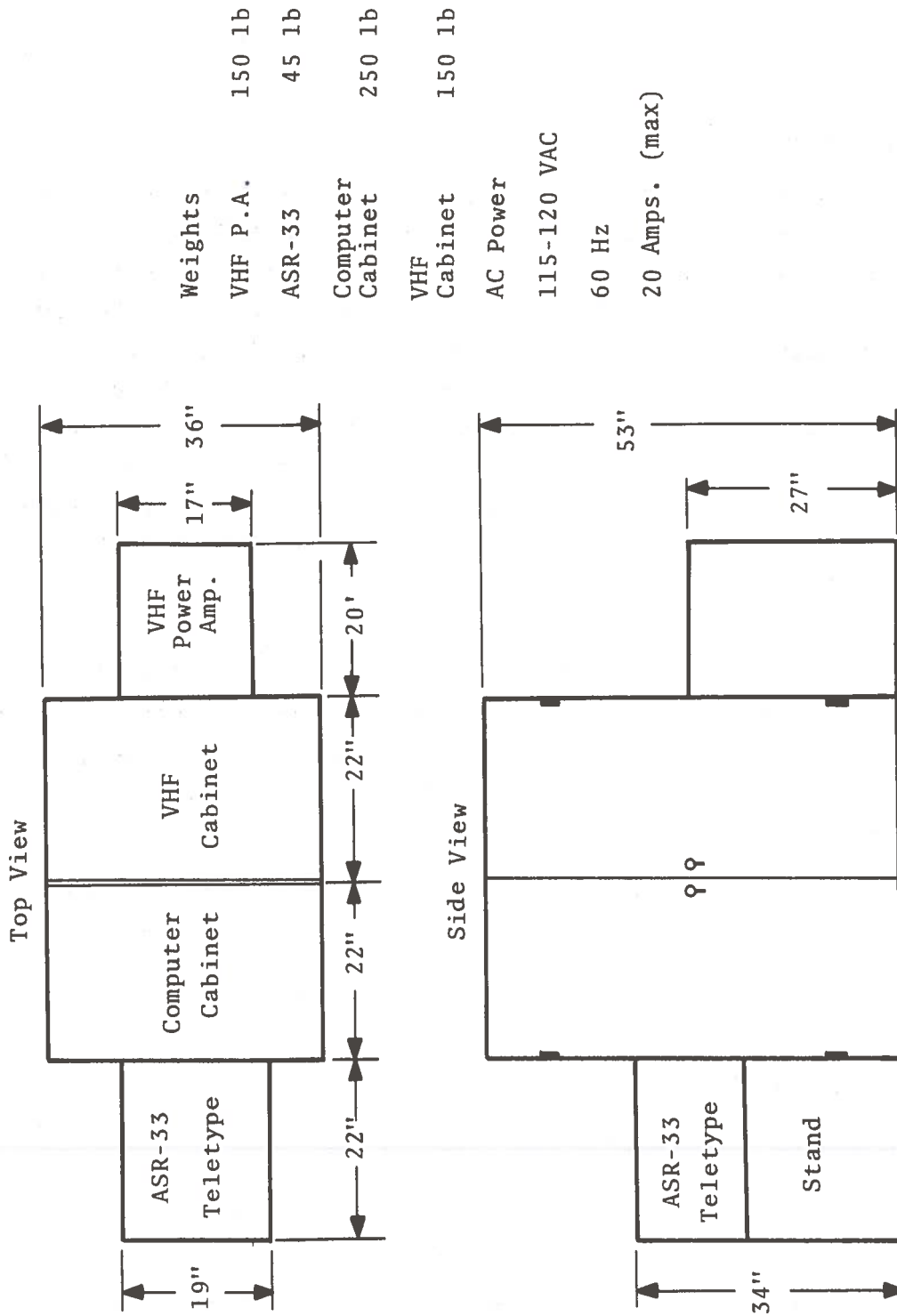


Figure A-1. Physical Layout of Automatic Data Collection Platform

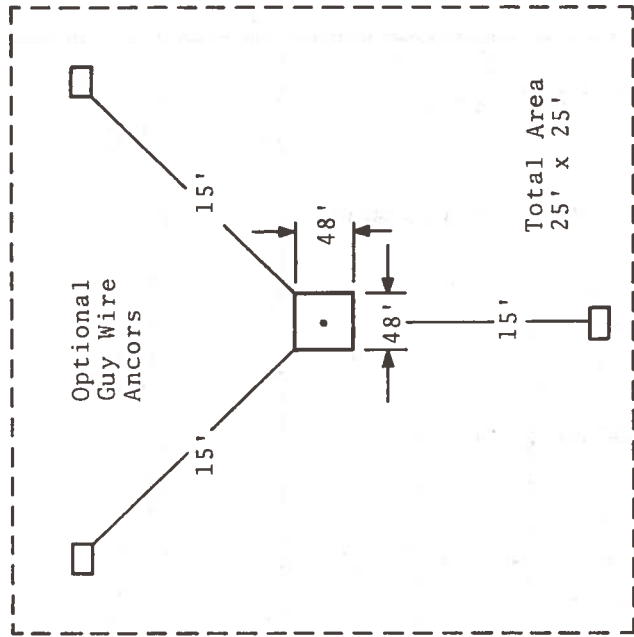
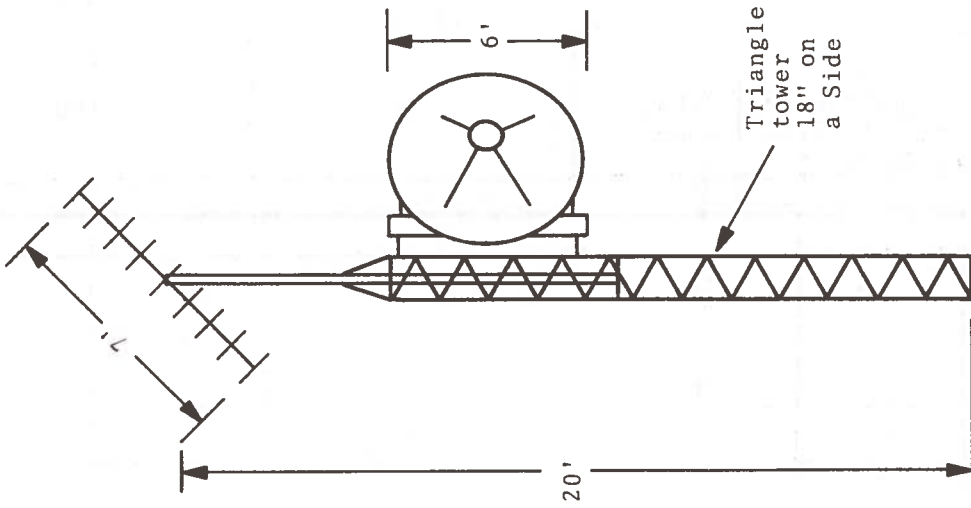


Figure A-2. Platform Antenna System Layout

TABLE A-1. TABLE OF SHIPPING WEIGHTS AND SIZES OF EQUIPMENT IN THE AUTOMATIC DATA COLLECTION PLATFORM

Item	Dimensions (inches)	Shipping Weight (pounds)
Cabinet with Computer	42 H 30 L 21 W	250
Cabinet with Radio Equipment	42 H 30 L 21 W	250
VHF Power Amplifier	27 H 16 L 20 W	250
ASR-33 Teletype Unit	30 H 19 L 24 W	80
2 ten-foot Sections of Tower	10 L 10 W 120 H	160
Parabolic Reflector Support	48 L	120
Parabolic Reflector	72 Diameter	30
VHF Antenna	96 H 48 L 48 W	150
Power Cable, Coaxial Cable, Guy Wire, Guy Wire Clamps, Guy Wire Anchors		300
	Total Shipping Weight	1600

TABLE A-2. POWER REQUIREMENTS OF THE AUTOMATIC DATA COLLECTION PLATFORM

Voltage (VAC)	Frequency (Hz)	Current (amperes)	Notes
115-120	60	8	nominal no transmitting
		13	nominal with VHF transmitting
		20	peak with VHF transmitting and DECTape [®] unit in operation

TABLE A-3. ELEVATION ANGLES FROM VARIOUS SITES TO THE ATS-5, AND 6 SPACECRAFTS

Site	Elevation Angle (degrees)		
	ATS-3 (69°W)	ATS-5 (105°W)	ATS-6 (94°W)
Westford (42N 72W)	40°	30°	36°
Bermuda (32N 64W)	52°	33°	40°
St. Johns, Newfoundland (64N 52W)	32°	16°	21°
Reykjavik Iceland (64N 20W)	7°	--	--
Azores (38N 28W)	27°	--	12°
San Juan, Puerto Rico (17N 67W)	67°	42°	52°
Narssarssuaq, Greenland (Denmark) (61N 45W)	20°	--	10°

choice for an equatorial site. Both sites are located on the Atlantic Ocean coverage of the ATS-5 spacecraft.

A.4 SETUP TIME ESTIMATES

The installation, setup and checkout time for the remote platform is three to five days. The pacing item is the installation of the antenna. The power cable from the equipment to the main power source is 200-feet long and the radio frequency cable length may be up to 200 feet in total length.

A.5 SPECIFICATION SUMMARY OF THE AUTOMATIC DATA COLLECTION PLATFORM

Table A-4 presents a complete specification summary of the automatic data collection platform.

TABLE A-4. SPECIFICATION SUMMARY OF THE AUTOMATIC DATA COLLECTION PLATFORM

L-Band
a) Antenna: 6-ft. Diameter; 27 dB gain; RHCP 7° beamwidth
b) Receiver RF Bandpass: 1540-1560 MHz (Determined by a filter following the preamplifier)
c) System NF = 3 dB (SSB including all losses)
d) Second IF Predetection BW = 8 kHz (Determined by replaceable crystal filter)
e) Linear Dynamic Range of Second IF Square-law Detector: 30 dB ± 0.5 dB
f) Second IF Crystal Discriminator Output: 8 kHz BW
g) First IF Output Linear, 70 MHz 30 MHz BW, 0 dBm

TABLE A-4. (Continued)

<p>h) System G/T + 2 dB/°K (Assuming a total path loss of -190 dB and a S/C EIRP of +2 dBw the C/N is 60.6 dB/Hz or 21.6 dB in 8 kHz filter)</p>
<p>VHF</p> <p>a) Antenna Crossed-log Periodic with 7 dB gain</p> <p>b) Rec. Freq. 135.575 or 135.600 or 135.625 MHz (135.625 used with Westford)</p> <p>c) Xmit freq 149.195 or 149.220 or 149.245 MHz (149.245 used with Westford)</p> <p>d) Rec. Demodulation 14 kHz IF BW Special Discriminator</p> <p>e) Xmit Modulation NBFM with 5 kHz Deviation</p> <p>f) Rec. NF: 2 dB</p> <p>g) Xmit Power: 250 watts</p> <p>h) Type of Modulation: Voice or 2.44 kHz Digital PSK</p> <p>i) S/N Ratio operating through ATS-1 or 3 at full power is 20 dB.</p>
<p>Computer Data Acquisition/Storage and Control</p> <p>a) Type PDP 11/05: 8 kbit core memory</p> <p>b) Interface - 8 bit A/D converter for Digitizing L-band Square-law Detector (0-10.0 V Range)</p> <p>c) Data Acquisition</p> <p>1) De spin ATS-5</p> <p>2) CW with remotely controllable data acquisition rate of 0.3 to 3.0 s.</p>

TABLE A-4. (Continued)

- d) Data storage capacity: 60 hours on single DEC-tape[®].
- e) Data return rate via VHF to Westford
1 hour of data in 1 min.
- f) Simplex teletype using the computer over the VHF link with Westford computer.
- g) Complete computer control via VHF from Westford using the Westford computer and VHF transmit/receive station.
- h) Control functions: automatic (platform computer control) and remote control possible. They are multiplexed onto the ASR-33 control. These are intended for operating switches or relays on ancillary equipment.

APPENDIX B

TABLE OF OBSERVATION TIMES

Table B-1 presents a complete summary of the observing times for the ATS-5 scintillation measurements described in this report.

TABLE B-1. SUMMARY OF ATS-5 L-BAND SCINTILLATION OBSERVATIONS

Begin	Local Time (EDST)		Data Hours	Type of Signal	Uplink	Comments & Notes
	Begin	End				
1973						1
03 December	1215*	03 December 1715*	5.00	NBFT	DOT	
04 December	1215*	04 December 2100*	8.75	Beacon	-	
05 December	1515*	05 December 1900*	3.75	Beacon	-	
06 December	1900*	06 December 2300*	4.00	Beacon	-	
07 December	1630*	08 December 0100*	8.50	Beacon	-	
10 December	1300*	10 December 2245*	9.75	NBFT	DOT	
11 December	1545*	11 December 2100*	5.25	NBFT	DOT	
12 December	1900*	13 December 0000*	5.00	NBFT	DOT	
18 December	1534*	18 December 2130*	6.00	NBFT	DOT	
19 December	1900*	20 December 0000*	5.00	NBFT	DOT	
26 December	1300*	26 December 1730*	4.50	NBFT	DOT	
27 December	1530*	27 December 2130*	6.00	NBFT	DOT	
28 December	1900*	29 December 0000*	5.00	NBFT	DOT	
1974						
02 January	1233*	02 January 1730*	5.00	NBFT	DOT	
03 January	1533*	03 January 2130*	6.00	NBFT	DOT	
04 January	1900*	05 January 0000*	5.00	NBFT	DOT	
07 January	1336	07 January 1830	5.00	NBFT	DOT	
08 January	1633	08 January 2200	5.50	NBFT	DOT	
09 January	2046	10 January 0100	4.25	NBFT	DOT	
14 January	1336	14 January 1830	5.00	NBFT	DOT	
15 January	1639	15 January 2230	6.00	NBFT	DOT	
16 January	2011	17 January 0100	5.00	NBFT	DOT	
21 January	1332	21 January 1830	5.00	NBFT	DOT	
22 January	1635	22 January 2230	6.00	NBFT	DOT	

* Eastern Standard Time

TABLE B-1. (CONTINUED)

Begin	Local Time (EDST)		Data Hours	Type of Signal	Uplink	Comments & Notes
	End					
1974						
23 January	2015	24 January	4.75	NBFT	DOT	
28 January	1334	28 January	5.00	NBFT	DOT	
29 January	1638	29 January	5.00	NBFT	DOT	
04 February	1830	04 February	5.00	NBFT	DOT	
05 February	1907	05 February	3.25	NBFT	DOT	
06 February	2005	07 February	5.00	NBFT	DOT	
11 February	1330	11 February	5.00	NBFT	DOT	
13 February	1647	13 February	5.45	NBFT	DOT	
14 February	2030	15 February	4.50	NBFT	DOT	
18 February	1355	18 February	4.50	NBFT	DOT	
19 February	1630	19 February	6.00	NBFT	DOT	
20 February	2005	21 February	5.00	NBFT	DOT	
25 February	1331	25 February	5.00	NBFT	DOT	
26 February	1635	26 February	6.00	NBFT	DOT	
27 February	2006	28 February	5.00	NBFT	DOT	
05 March	1632	05 March	6.00	NBFT	DOT	
08 March	1216	08 March	4.75	NBFT	GE	Beacon too.
11 March	1500	11 March	7.75	NBFT	GE	Beacon too.
12 March	1500	12 March	8.00	NBFT	GE	
13 March	1603	13 March	7.00	NBFT	GE	
14 March	1900	15 March	8.00	NBFT	GE	
15 March	1900	15 March	4.00	NBFT	GE	
18 March	1500	18 March	8.00	NBFT	GE	
19 March	1505	20 March	9.00	NBFT	GE	
20 March	1516	20 March	7.75	NBFT	DOT+	Beacon too.
21 March	1500	21 March	8.00	NBFT	DOT	GE too.
25 March	1531	25 March	7.50	NBFT	GE	
26 March	1503	26 March	8.00	NBFT	GE	

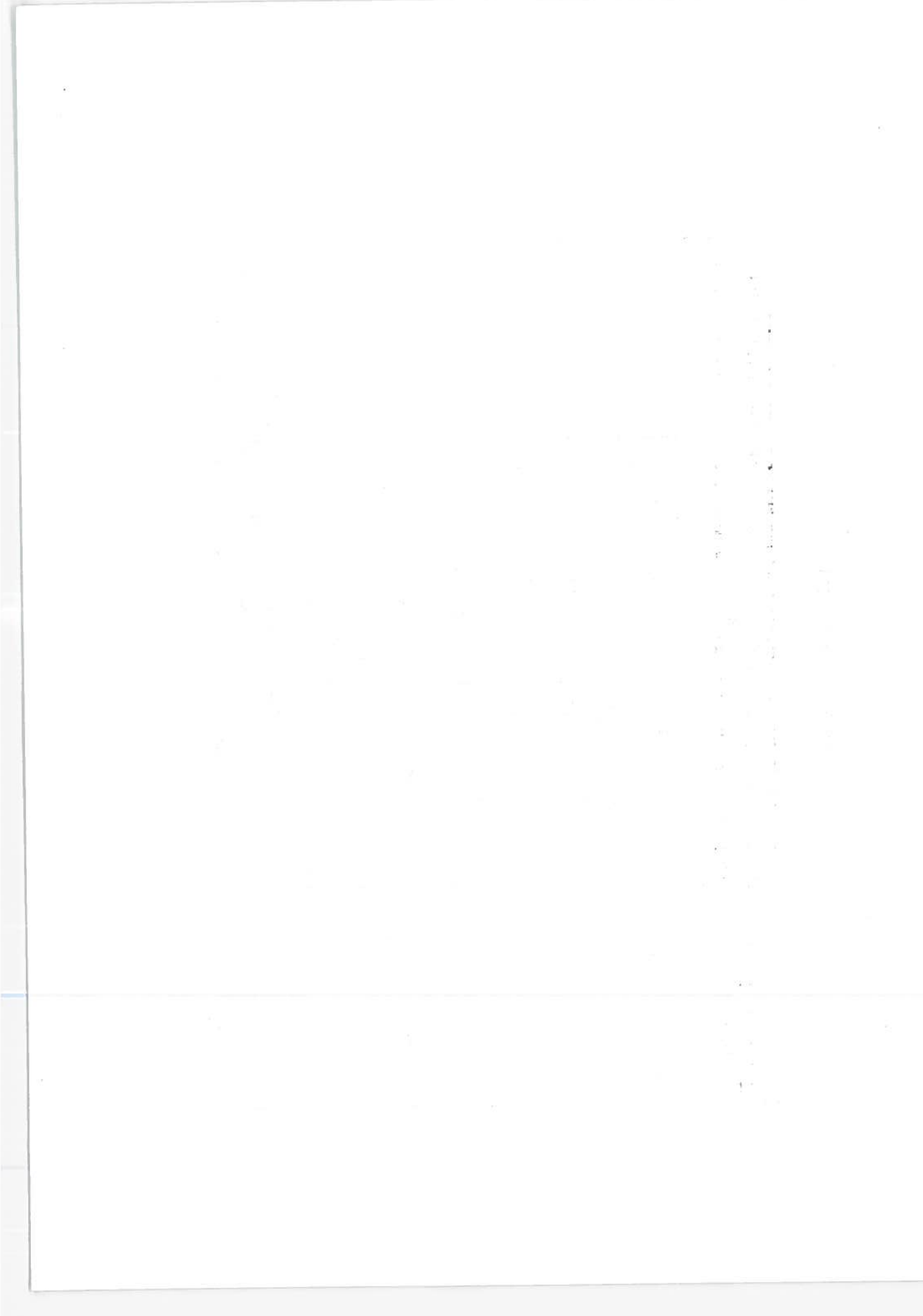
TABLE B-1. (CONTINUED)

Begin	Local Time (EDST)		Data Hours	Type of Signal	Uplink	Comments & Notes
	Begin	End				
1974						
27 March	1530	27 March	7.50	NBFT	GE	Beacon too.
28 March	1506	28 March	8.00	NBFT	GE	Beacon too.
29 March	1546	29 March	7.25	NBFT	GE	Beacon too.
01 April	1400	01 April	3.75	NBFT	DOT	
02 April	1630	02 April	6.00	NBFT	DOT	
03 April	2021	04 April	4.25	NBFT	DOT	
08 April	1334	08 April	5.00	NBFT	DOT	
09 April	1637	09 April	6.00	NBFT	DOT	
10 April	2005	11 April	5.00	Beacon	-	
15 April	1337	15 April	5.00	NBFT	DOT	
16 April	1637	16 April	5.50	NBFT	DOT	
17 April	2115	18 April	3.75	NBFT	DOT	
22 April	1341	22 April	4.75	NBFT	DOT	
23 April	1637	23 April	6.00	NBFT	DOT	
24 April	2020	25 April	4.75	NBFT	DOT	
29 April	1348	29 April	4.75	NBFT	DOT	
30 April	1631	30 April	6.00	NBFT	DOT	
01 May	2000	02 May	6.00	NBFT	DOT	
07 May	1705	07 May	6.00	NBFT	DOT	
08 May	2015	09 May	5.75	NBFT	DOT/GE	
13 May	1430	13 May	4.50	NBFT	DOT/GE	
14 May	1700	14 May	6.00	NBFT	DOT	
15 May	2019	16 May	5.75	NBFT	DOT	
16 May	0900	16 May	3.00	NBFT	DOT	ADCP on
20 May	1419	20 May	4.75	NBFT	DOT	
22 May	1847	22 May	1.75	NBFT	DOT	
29 May	1704	29 May	6.00	NBFT	DOT	

TABLE B-1. (CONTINUED)

Begin	Local Time (EDST)		Data Hours	Type of Signal	Uplink	Comments & Notes
		End				
1974						
03 June	1400	03 June	1900	NBFT	DOT	
04 June	1715	04 June	2300	NBFT	DOT	
05 June	2006	06 June	0200	NBFT	DOT	
10 June	1403	10 June	1900	NBFT	DOT	
11 June	1715	11 June	2300	NBFT	DOT	
12 June	2102	13 June	0200	NBFT	DOT	
17 June	1404	17 June	1845	NBFT	DOT	
18 June	1700	18 June	2300	NBFT	DOT	
19 June	2031	20 June	0200	NBFT	DOT	
24 June	1438	24 June	1900	NBFT	DOT	
25 June	1705	25 June	2247	NBFT	DOT	
26 June	2005	27 June	0200	NBFT	DOT	
01 July	1405	01 July	1900	NBFT	DOT	
02 July	1706	02 July	2300	NBFT	DOT	
08 July	1402	08 July	1900	NBFT	DOT	
09 July	1709	09 July	2300	NBFT	DOT	
10 July	2134	11 July	0145	NBFT	DOT	
15 July	1407	15 July	1900	NBFT	DOT	
16 July	1704	16 July	2248	NBFT	DOT	
17 July	2006	18 July	0200	NBFT	DOT	
22 July	1418	22 July	1900	NBFT	DOT	ADCP on too.

Note 1. Symbols used in this table are defined in the list of symbols.



APPENDIX C
WEEKLY TEMPORAL DIAGRAMS

The weekly data for December 1973 are presented in Figure C-1 through C-4. The weekly data for January 1974 is presented in Figure C-5 through C-9. February 1974 weekly temporal diagrams are contained in Figures C-10 through C-13. March 1974 weekly temporal diagrams are presented in Figures C-14 through C-17. The weekly diagrams for April 1974 are given in Figures C-18 through C-22. Figures C-23 through C-26 are for May 1974. The weekly temporal diagrams for June 1974 are contained in Figures C-27 through C-30. Finally, the weekly temporal diagrams for the July 1974 data is presented in Figures C-31 through C-34.

The Kp values come from Lincoln (1974).

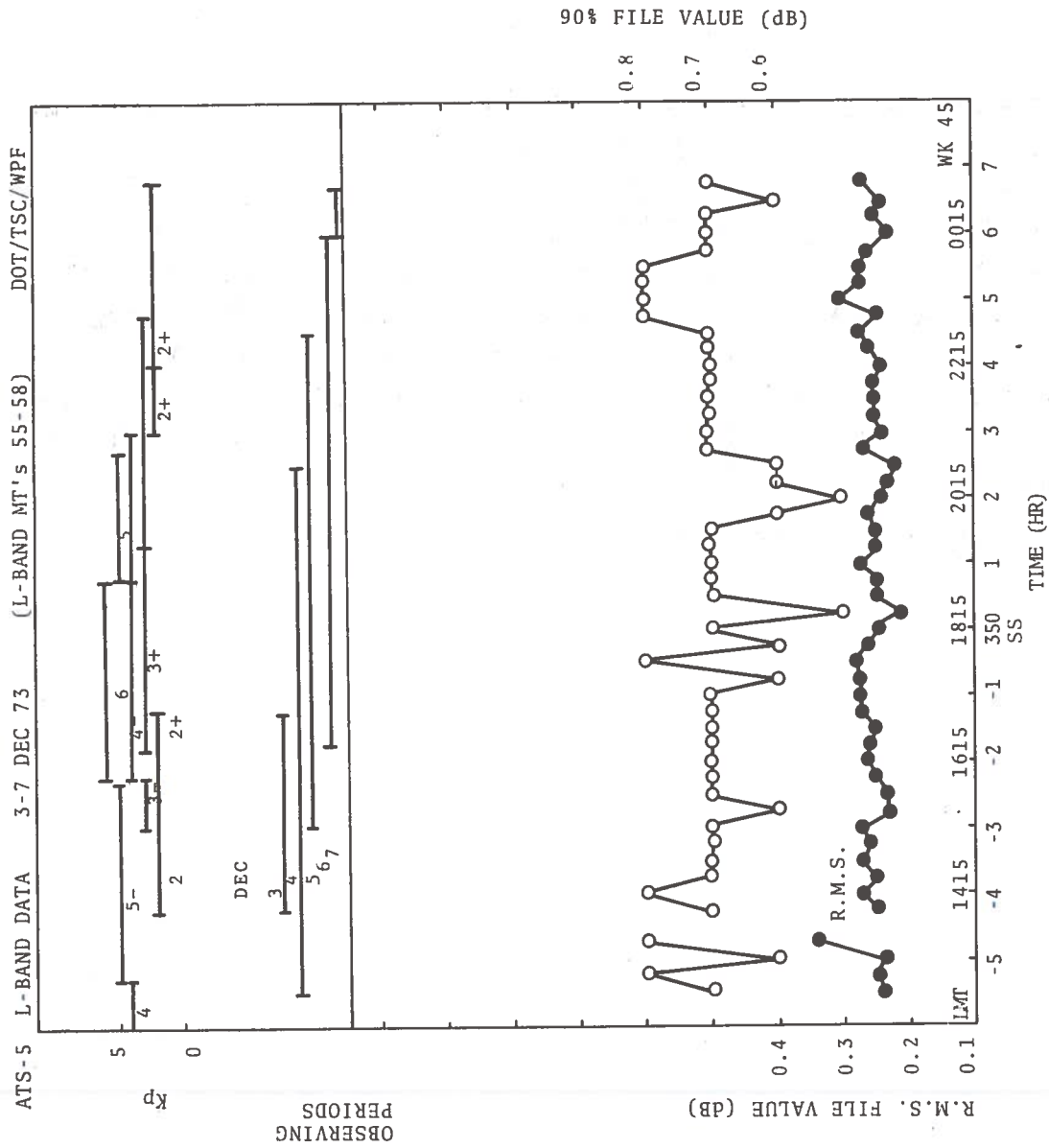


Figure C-1. Temporal Diagram for 3-7 December 1973

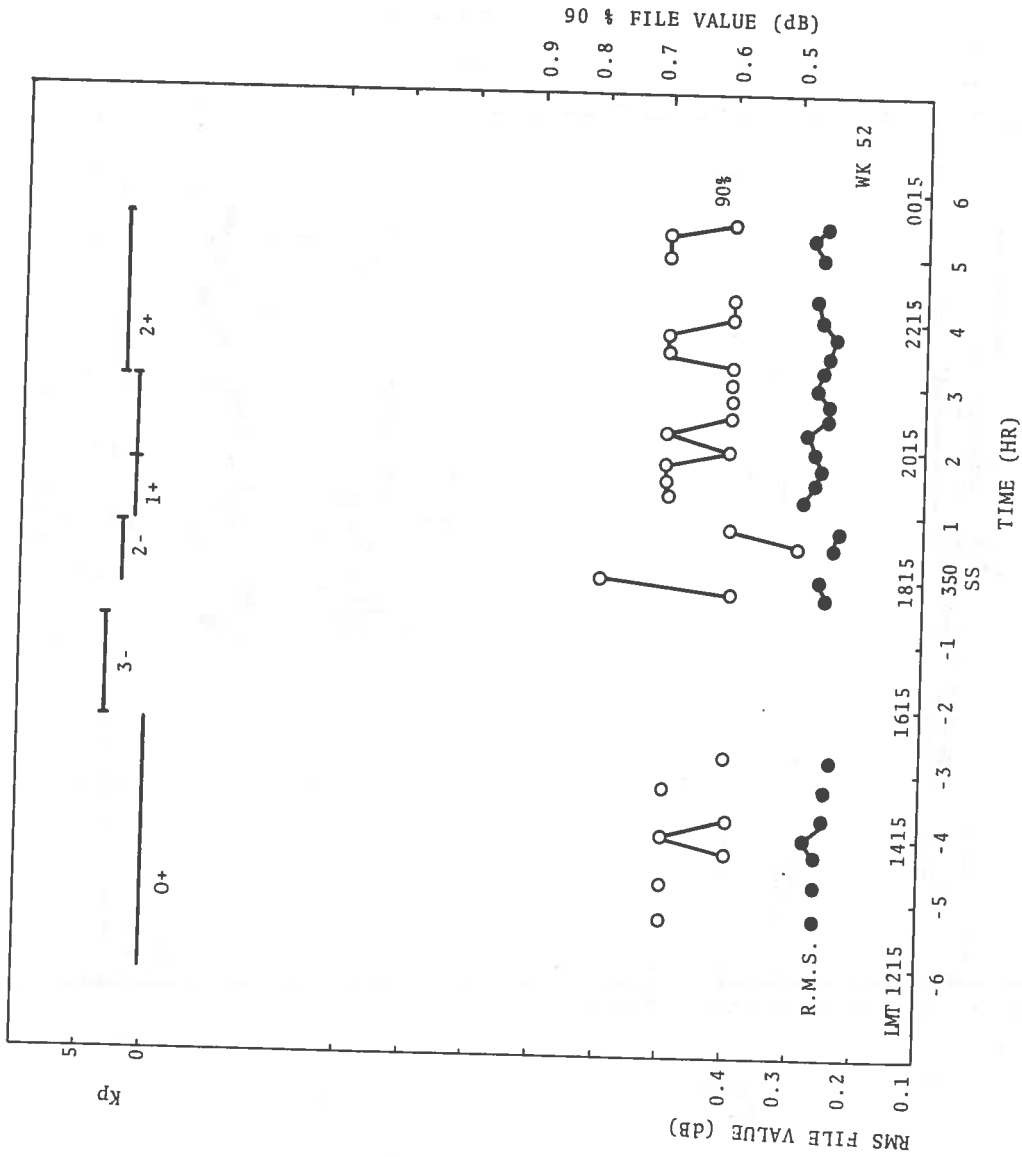


Figure C-2. Temporal Diagram for 10-13 December 1973

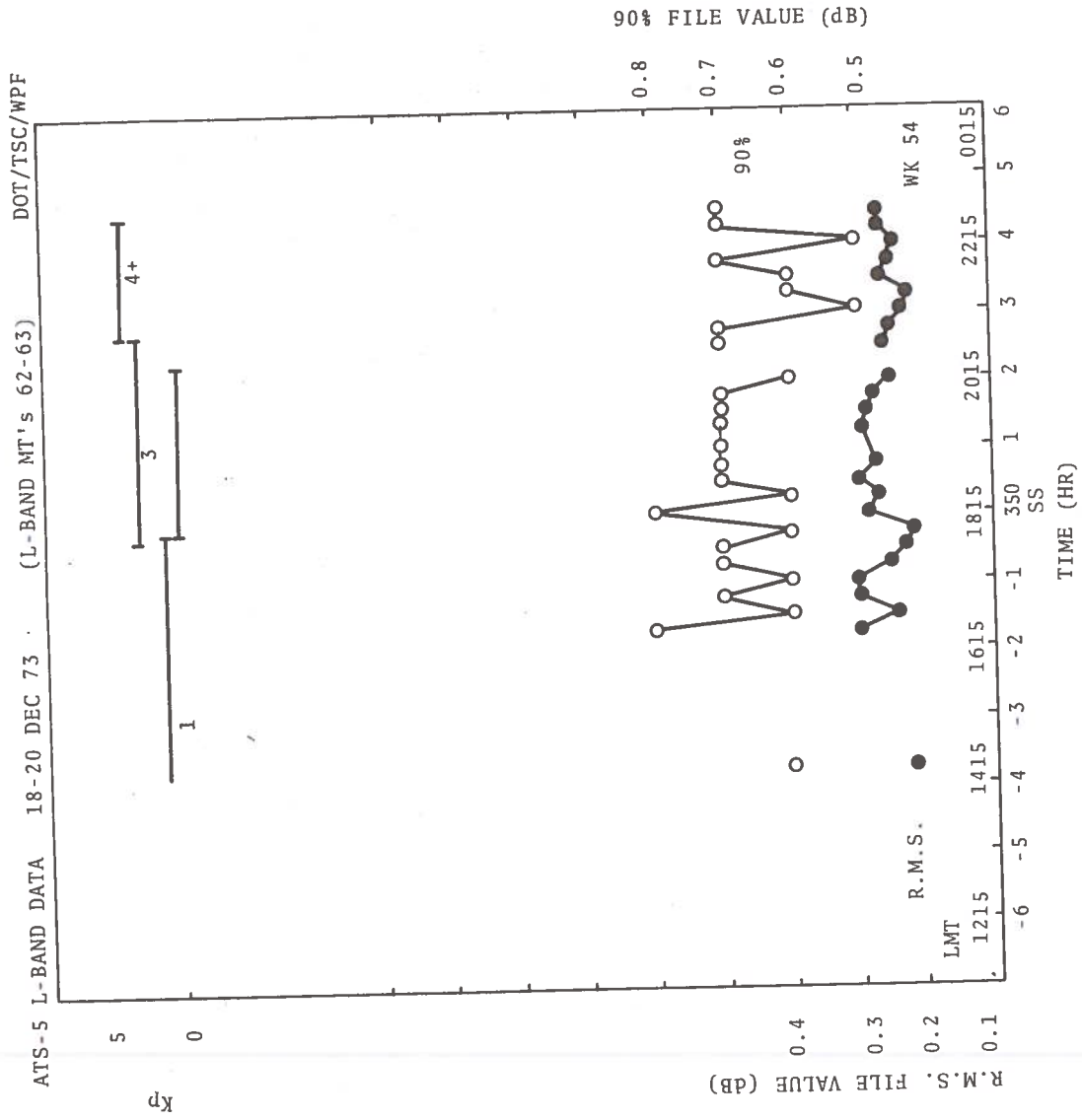


Figure C-3. Temporal Diagram for 18-20 December 1973

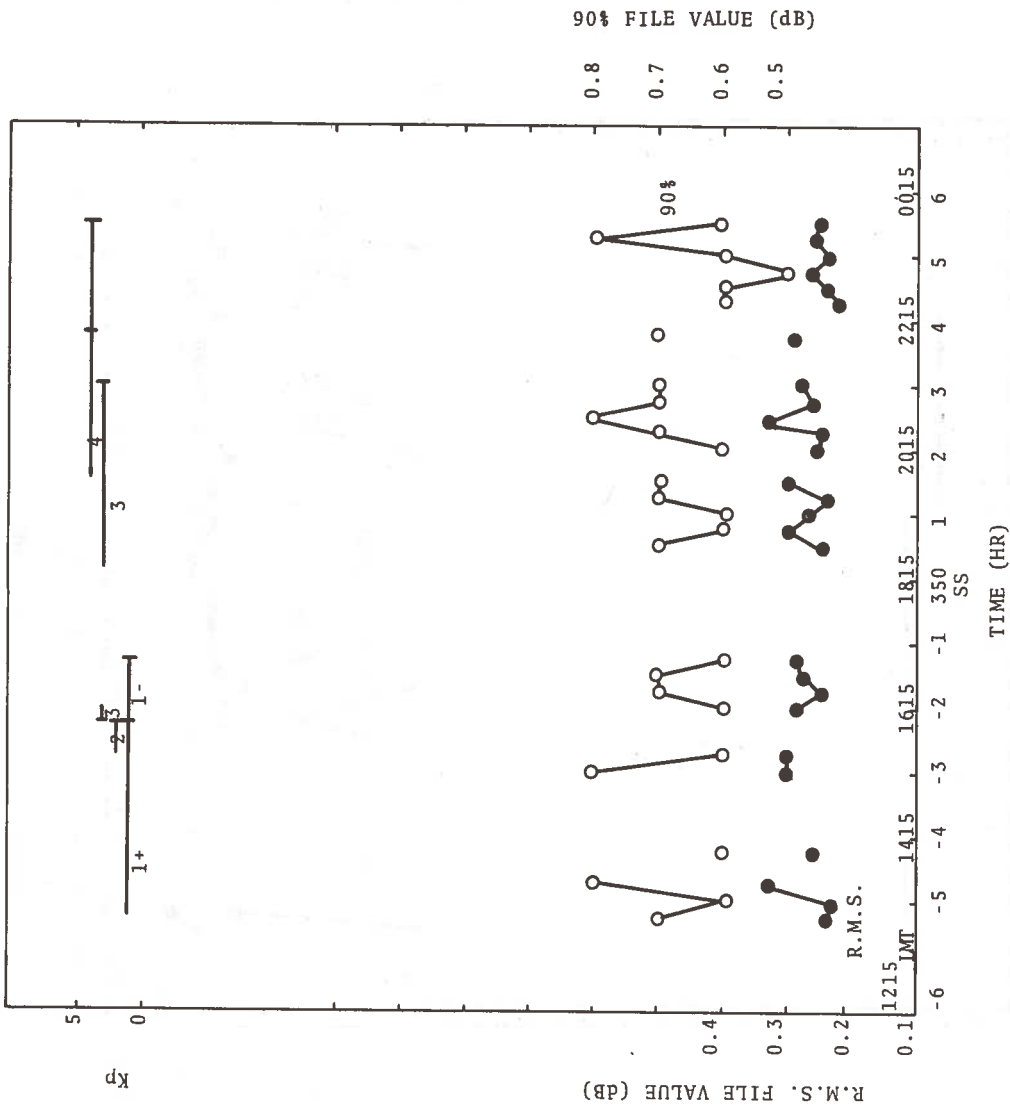


Figure C-4. Temporal Diagram for 26-29 December 1973

ATS-5 L-BAND DATA 2-5 JAN 74 (L-BAND MT's 67-69) DOT/TSC/WPF

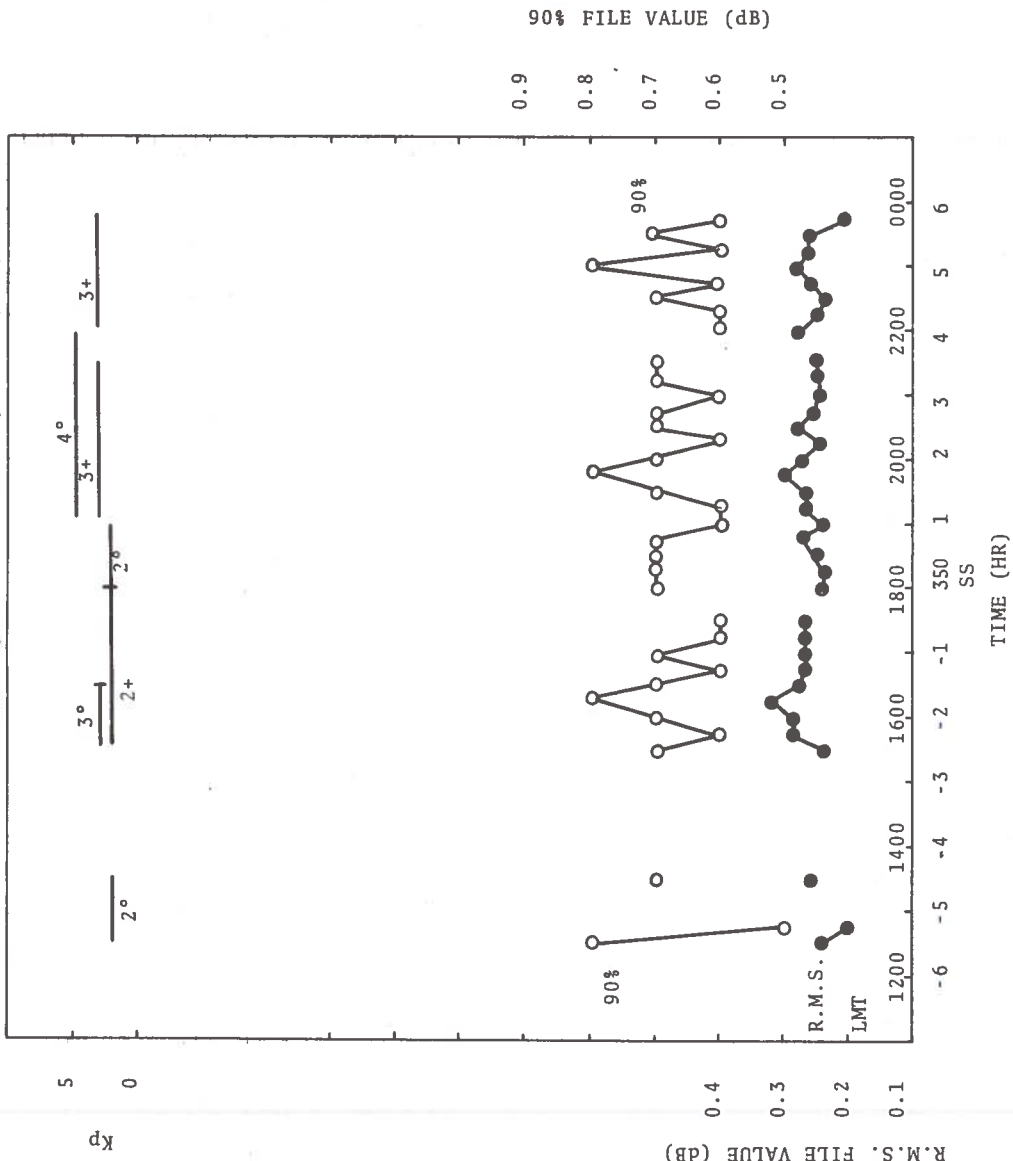


Figure C-5. Temporal Diagram for 2-5 January 1974

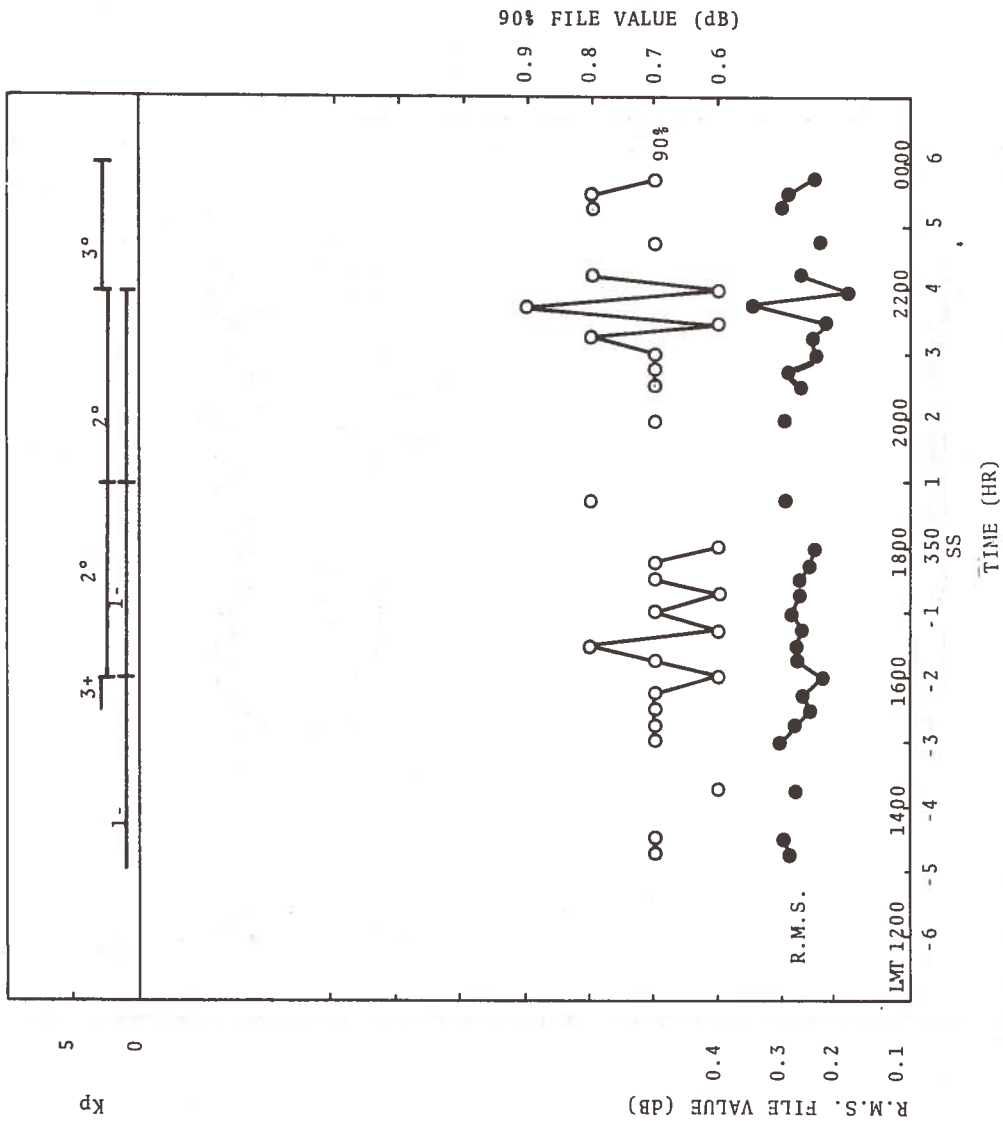


Figure C-6. Temporal Diagram for 7-10 January 1974

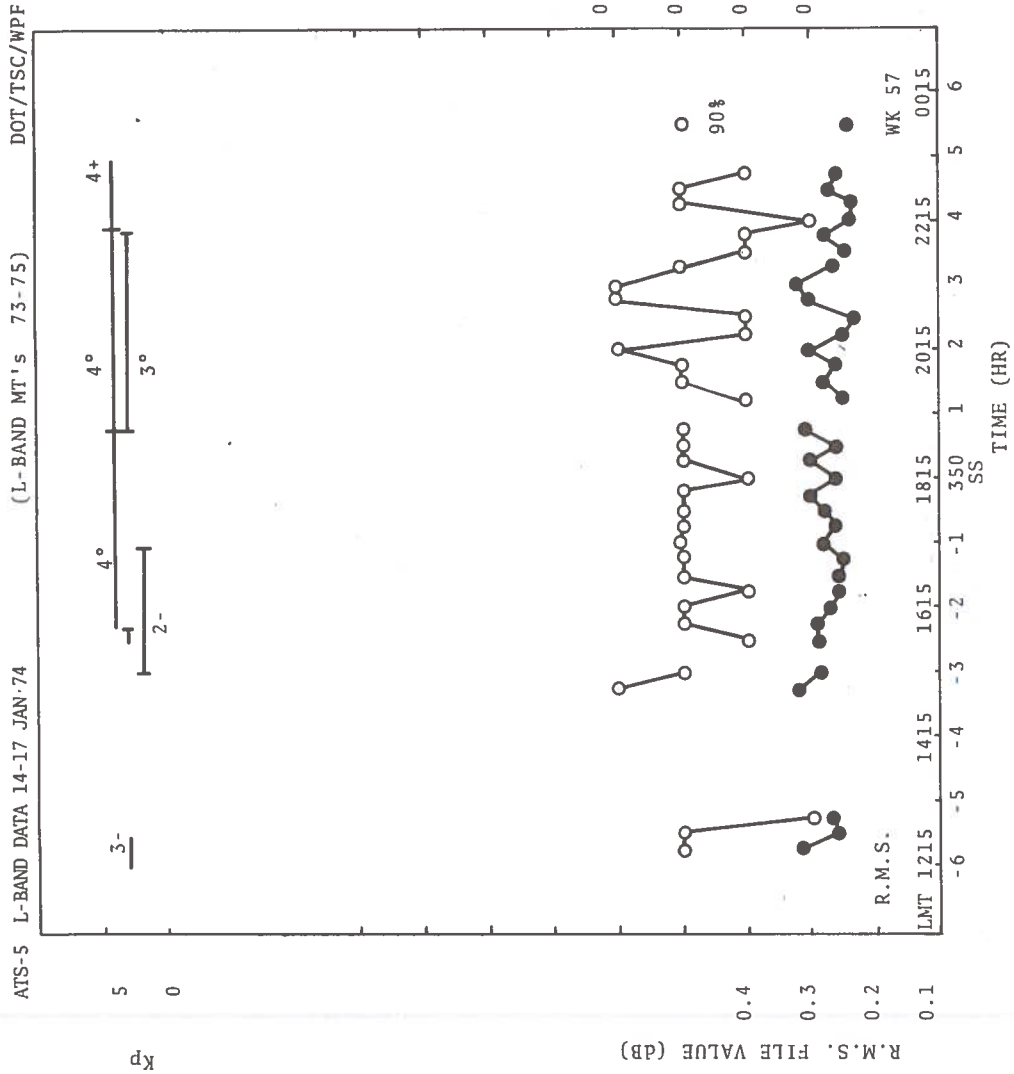


Figure C-7. Temporal Diagram for 14-17 January 1974

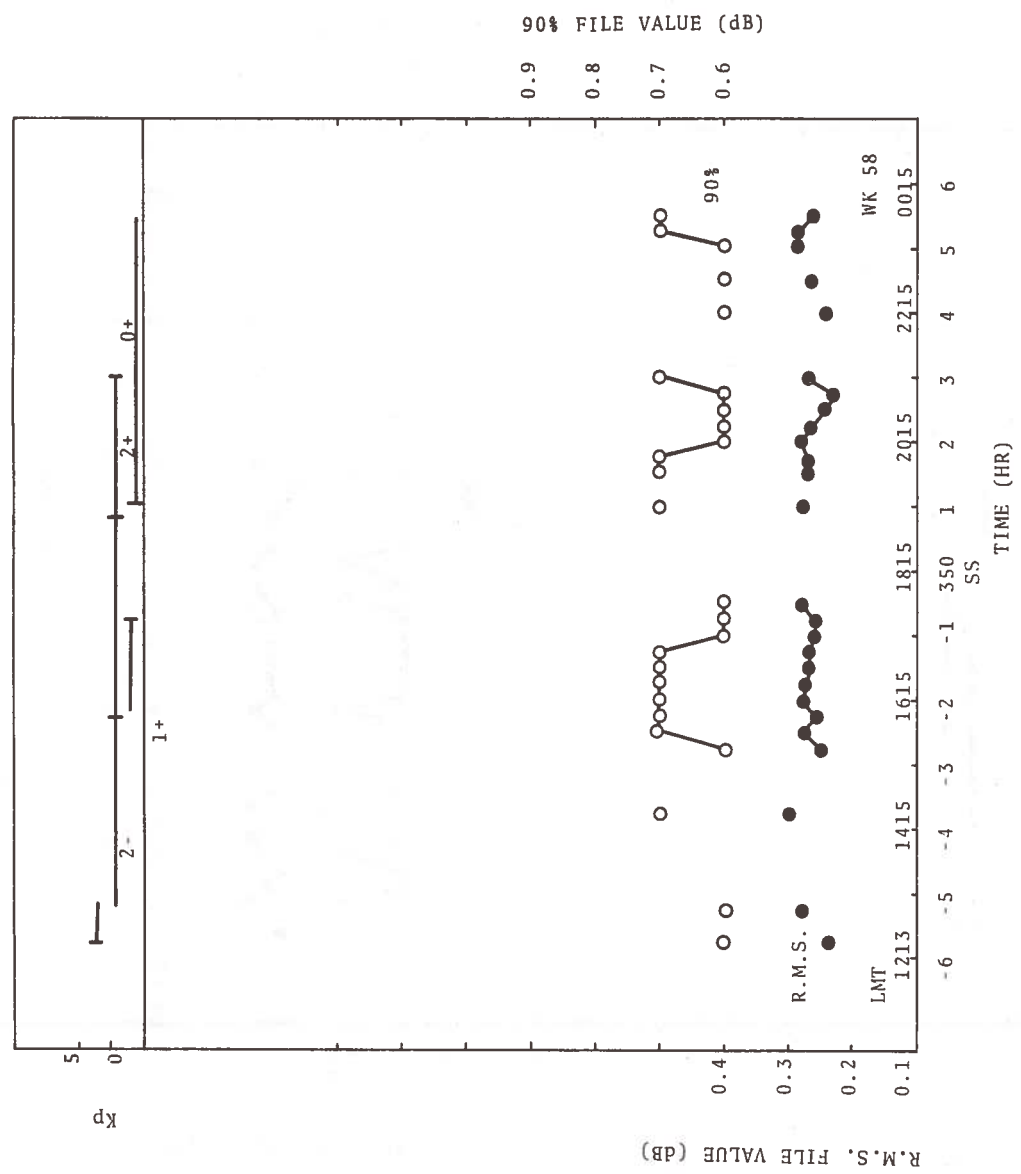


Figure C-8. Temporal Diagram for 21-24 January 1974

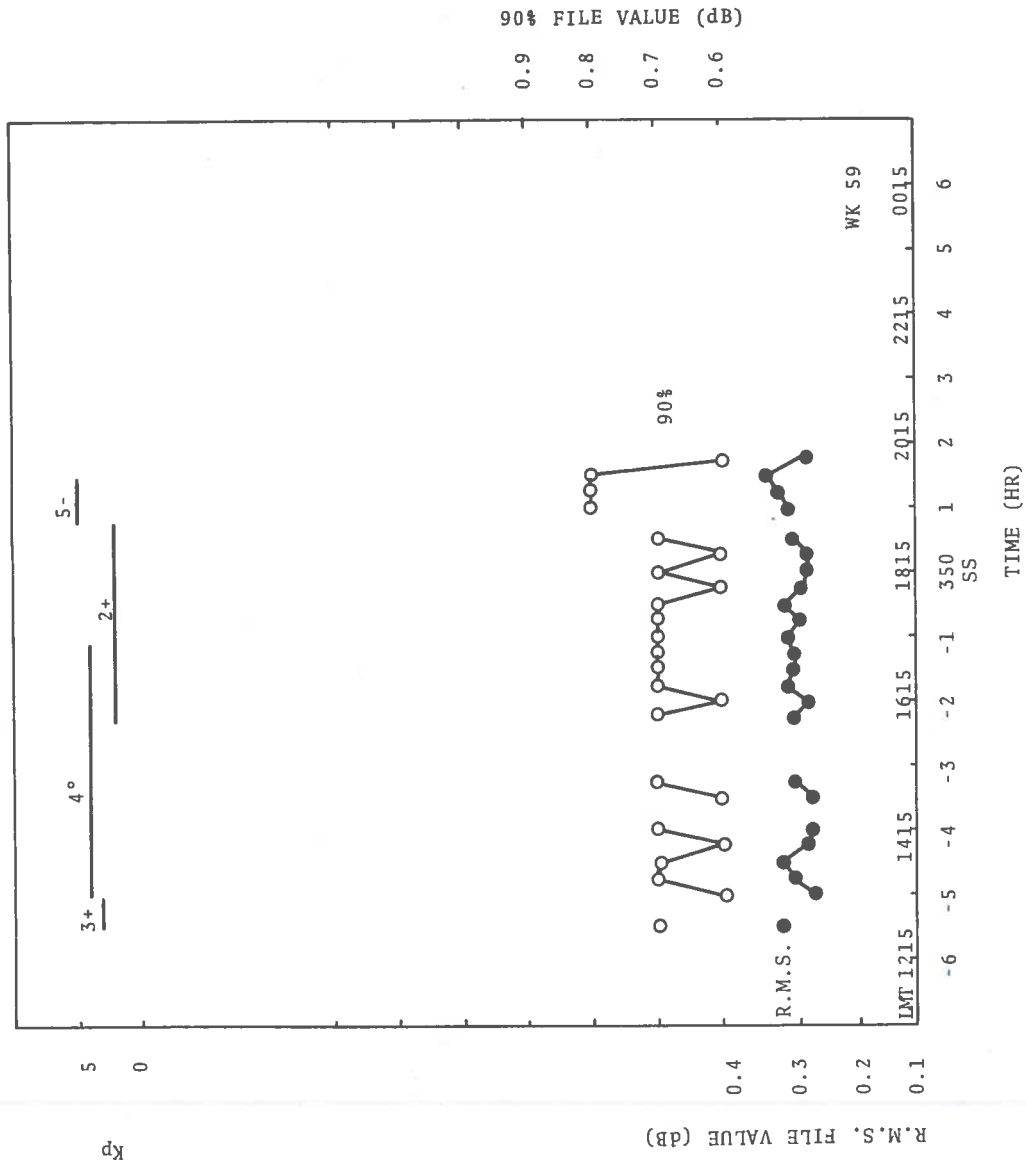


Figure C-9. Temporal Diagram for 28-30 January 1974

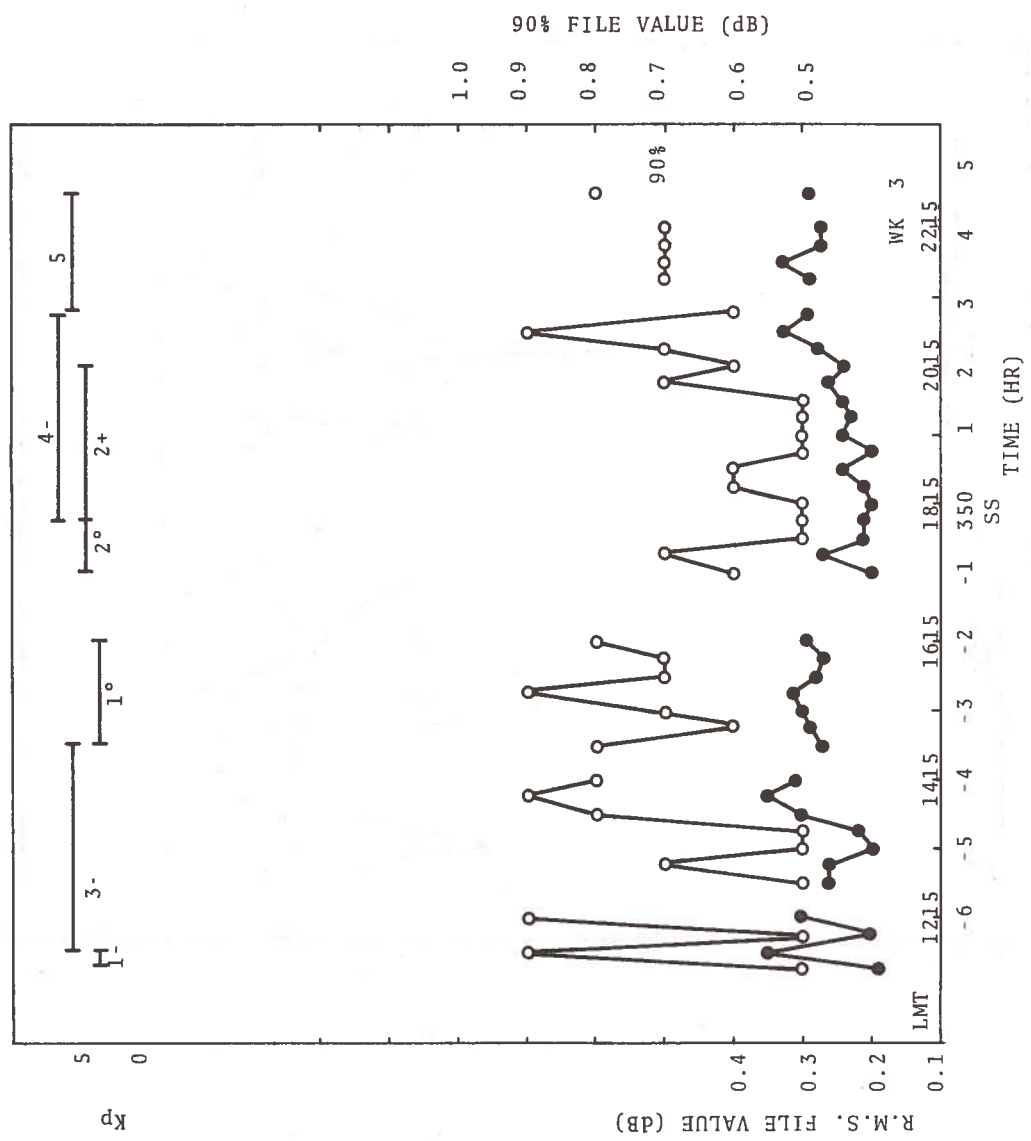


Figure C-10. Temporal Diagram for 4-7 February 1974

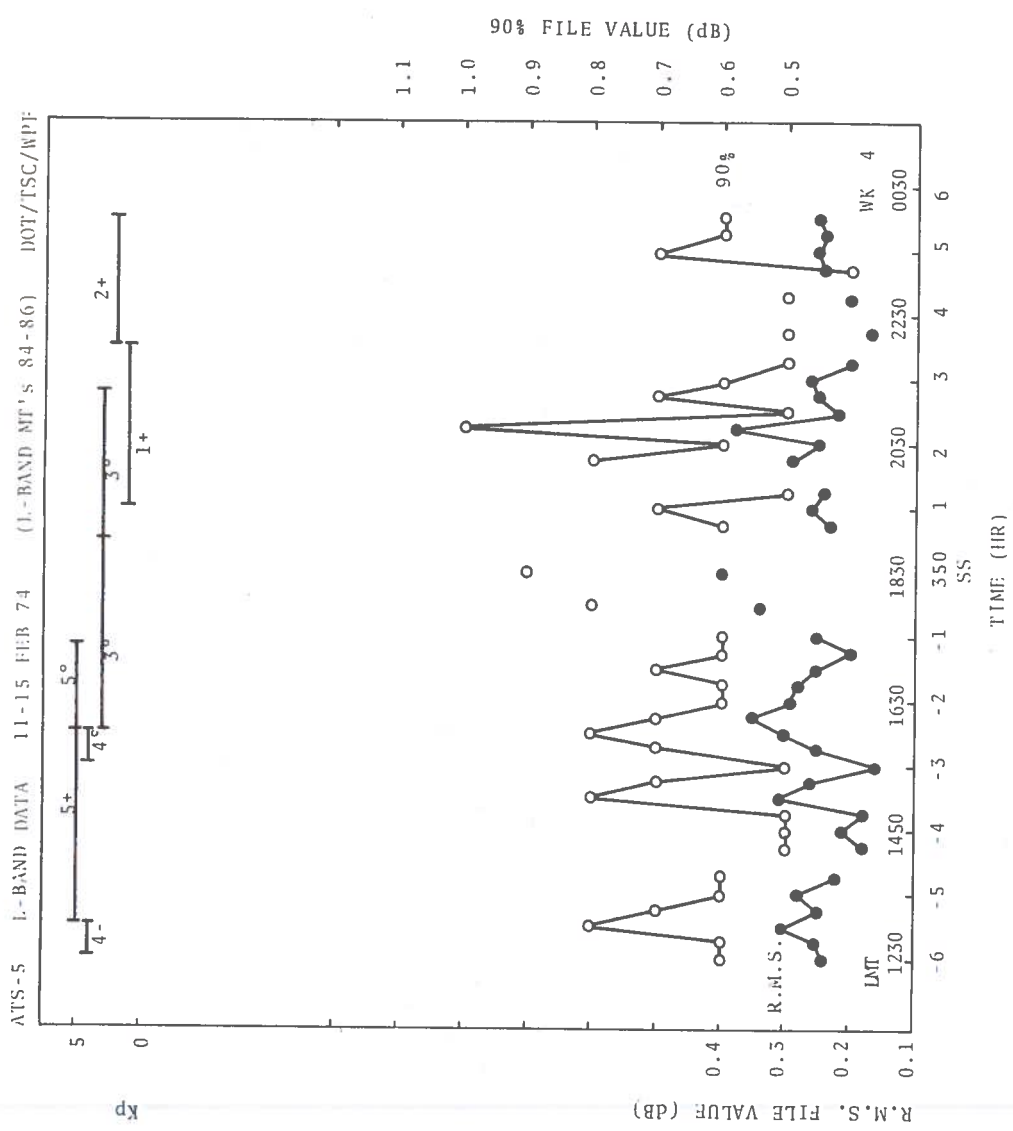


Figure C-11 Temporal Diagram for 11-15 February 1974

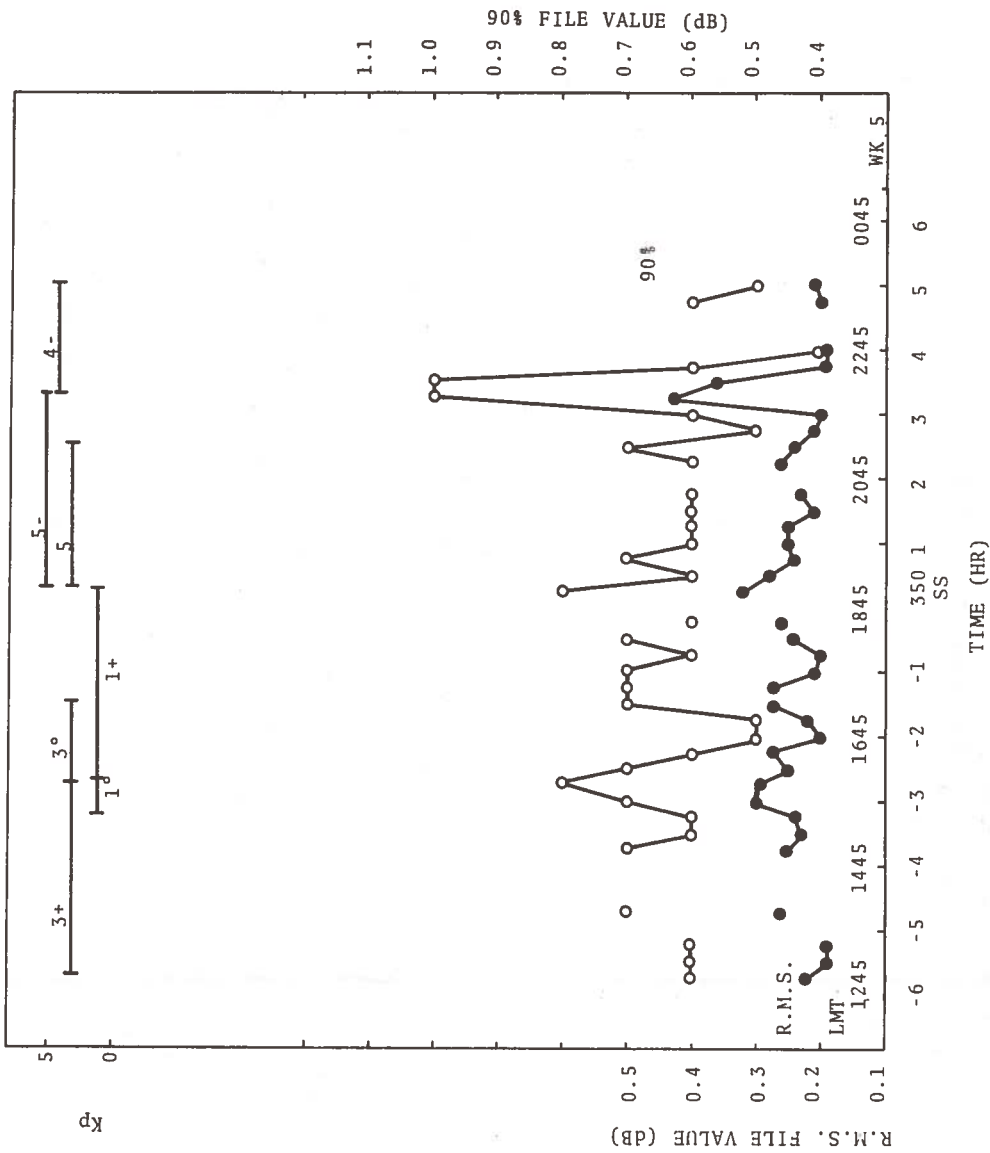


Figure C-12. Temporal Diagram for 18-21 February 1974

ATS-5 L-BAND DATA 25-28 FEB 74 (L-BAND MT's 90-92) DOT/TSC/WPF

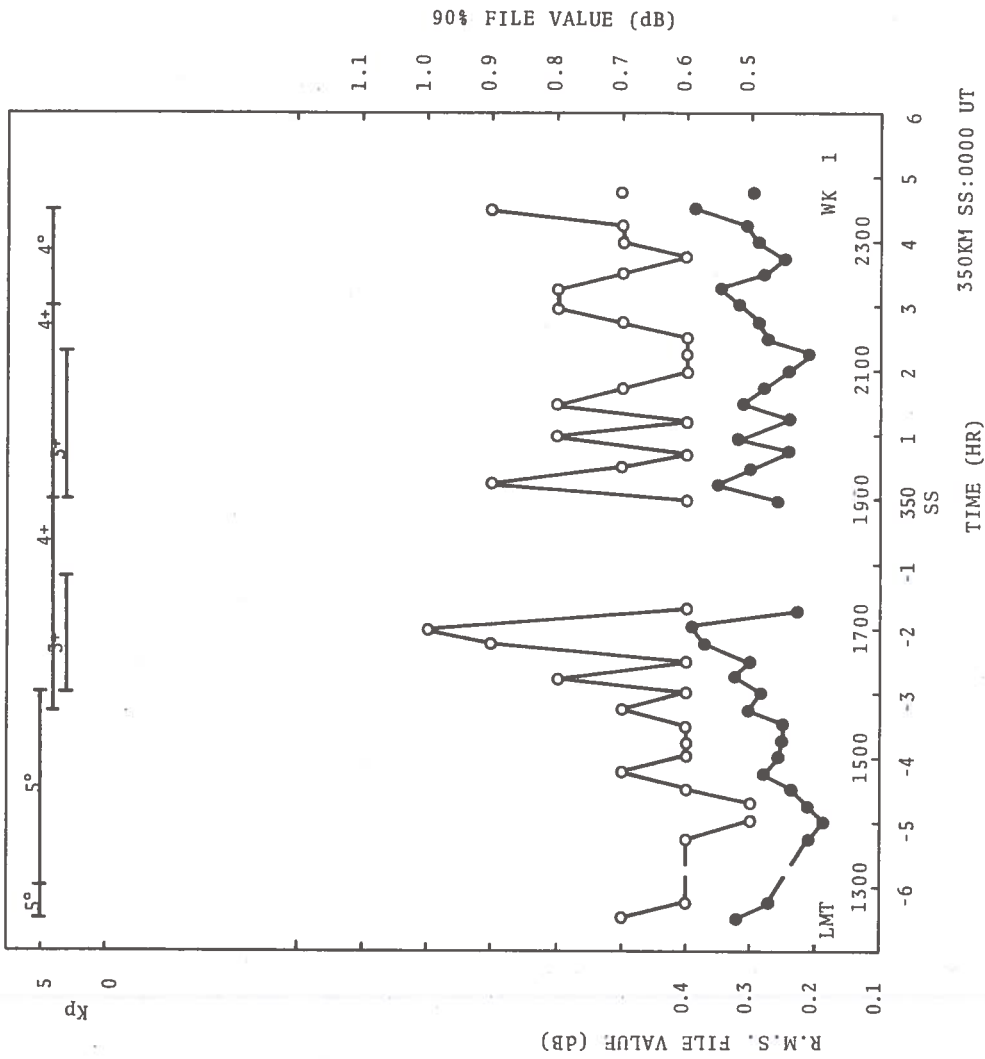


Figure C-13. Temporal Diagram for 25-28 February 1974

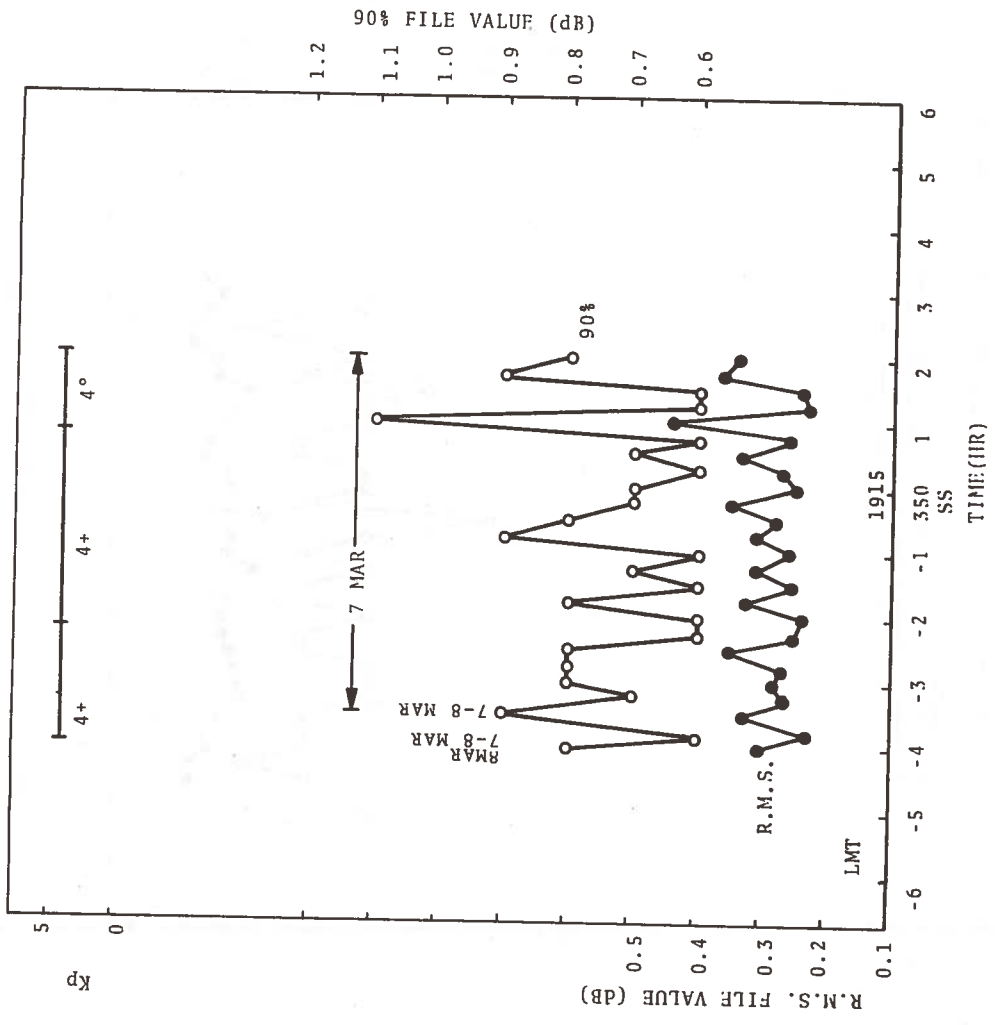


Figure C-14. Temporal Diagram for 5-8 March 1974

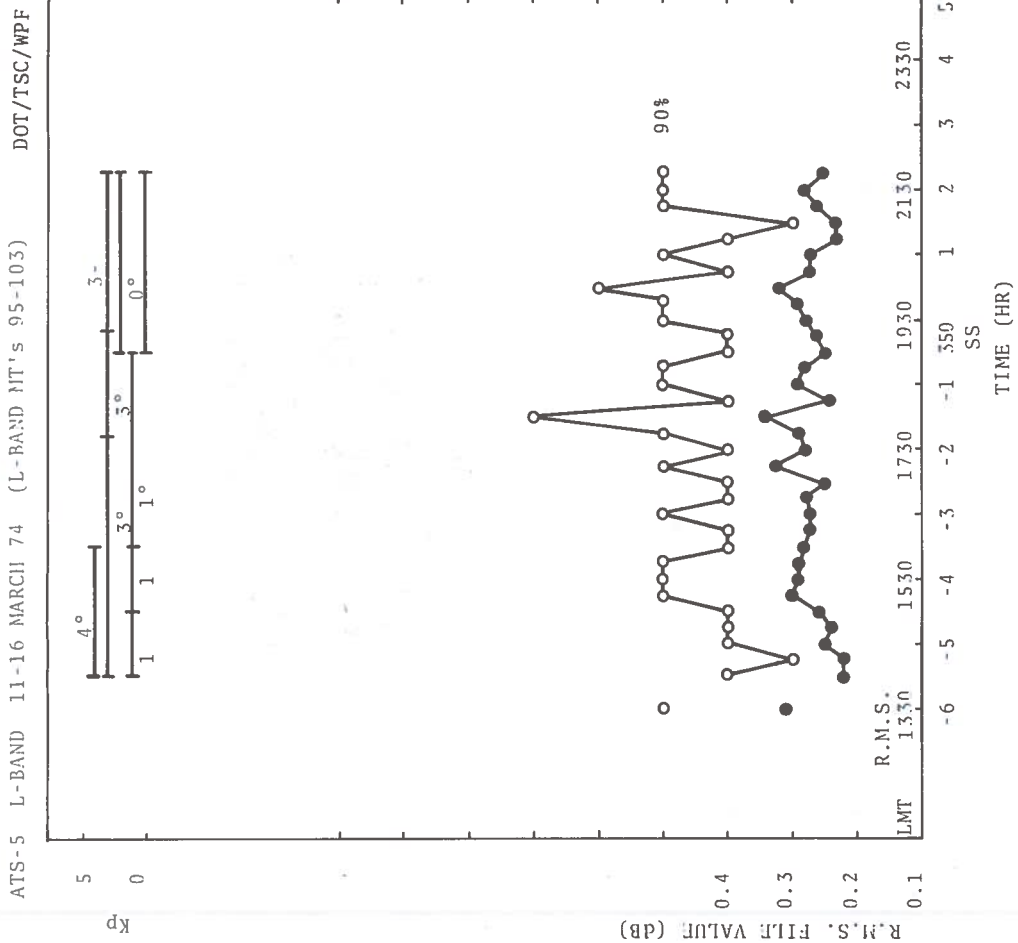


Figure C-15. Temporal Diagram for 11-16 March 1974

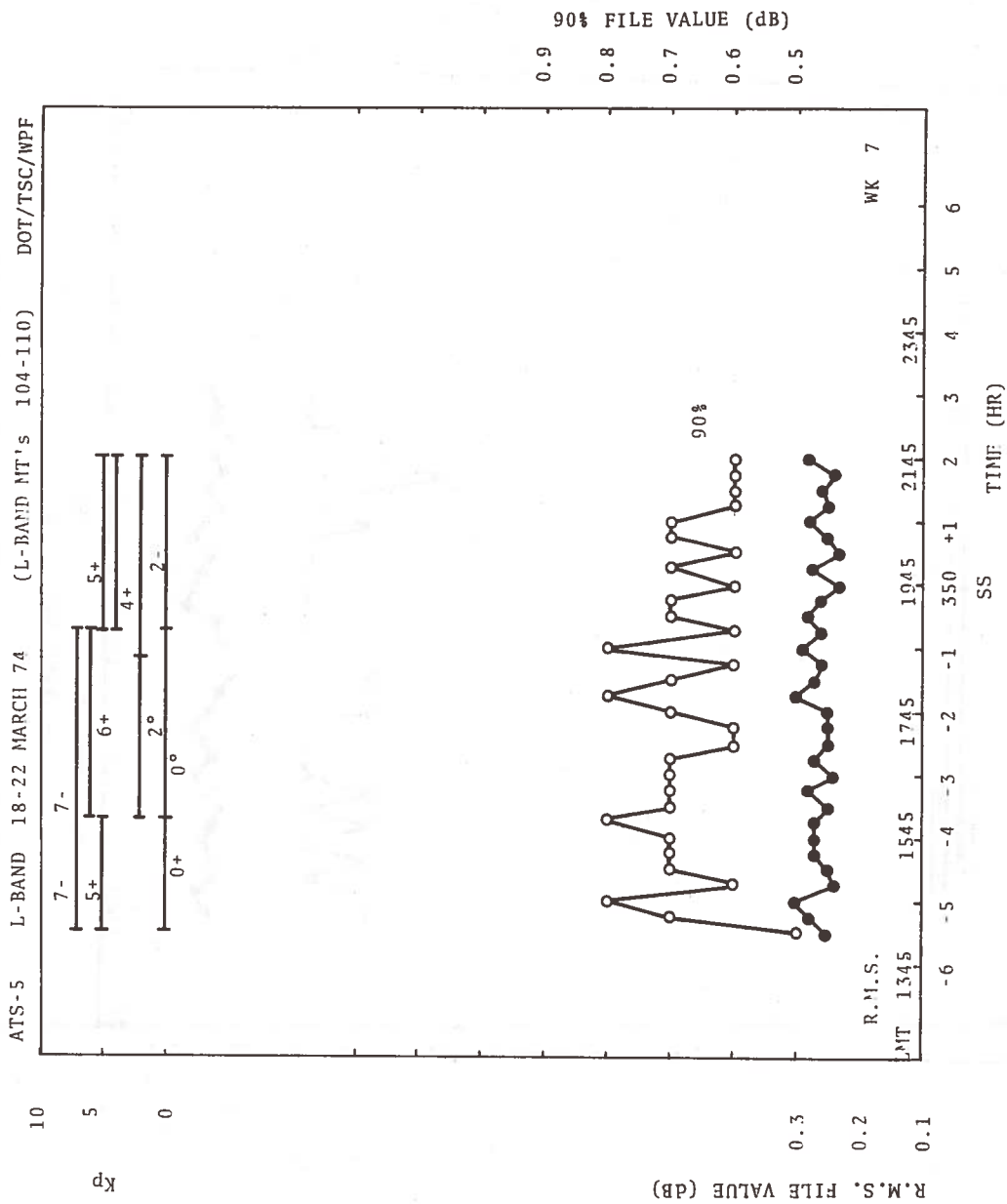


Figure C-16. Temporal Diagram for 18-22 March 1974

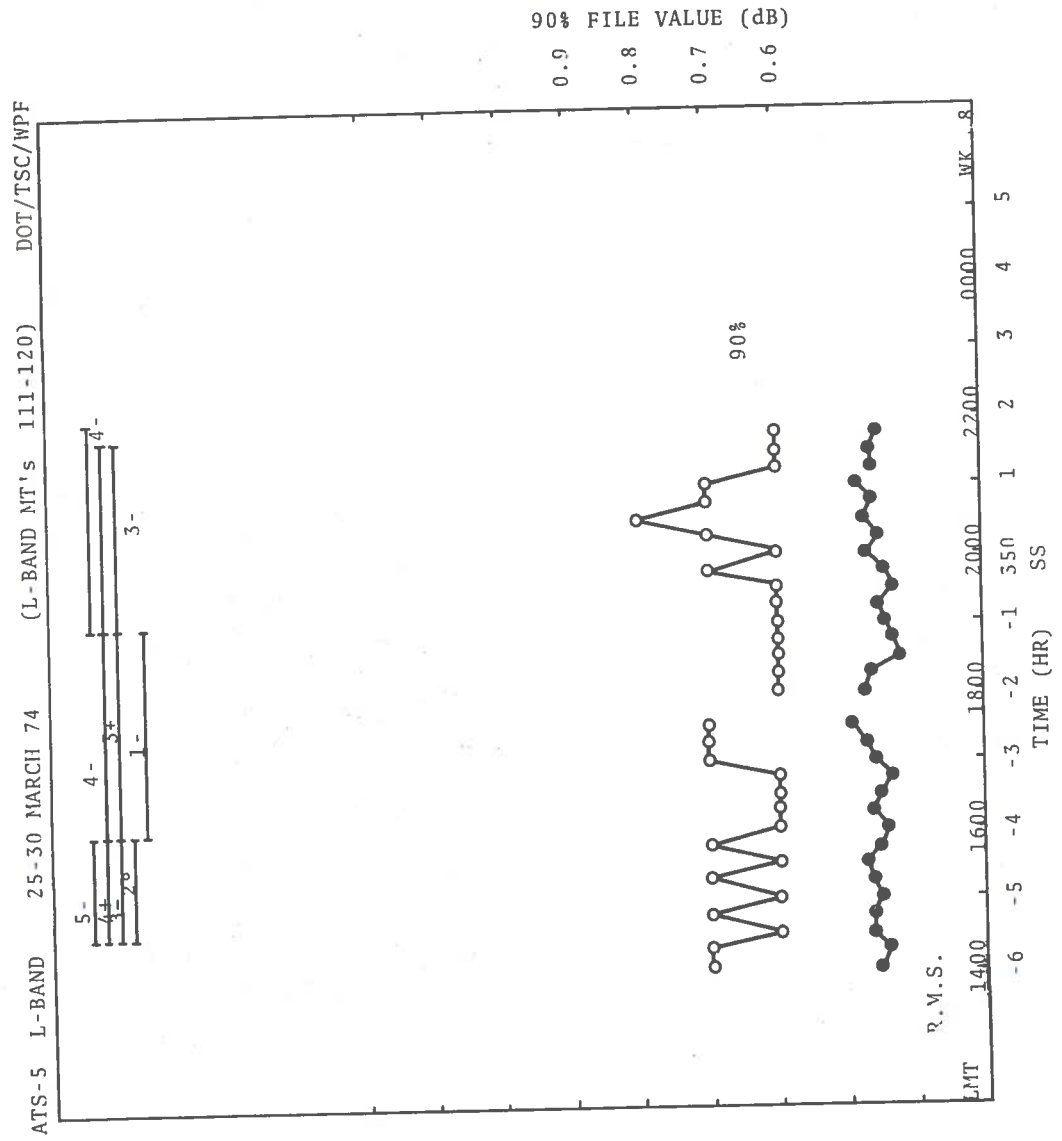


Figure C-17. Temporal Diagram for 25-30 March 1974

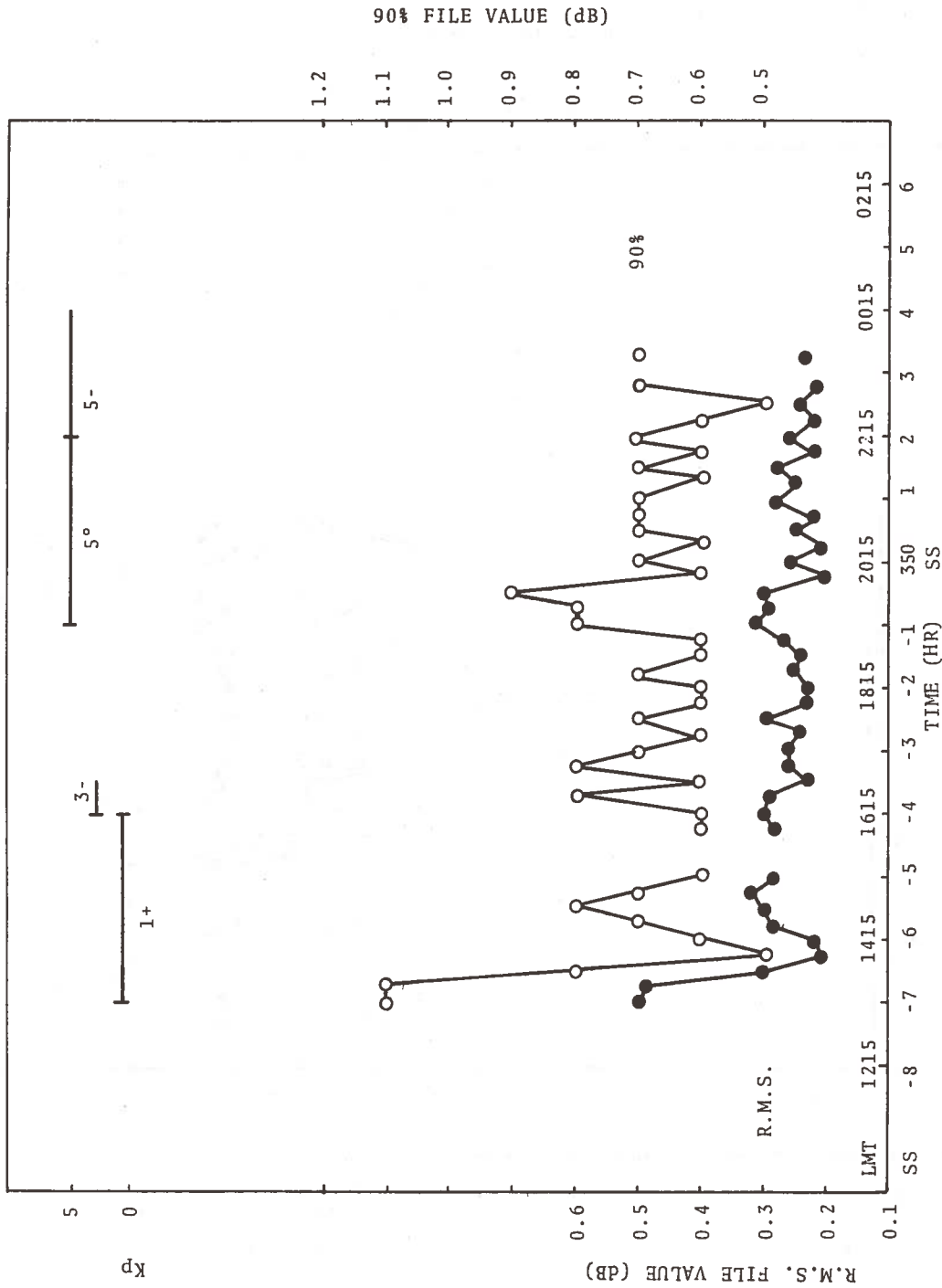


Figure C-18. Temporal Diagram for 1-4 April 1974

ATS-5 L-BAND DATA 8-10 APR 74 (L-BAND MT's 124-125) DOT/TSC/WPF

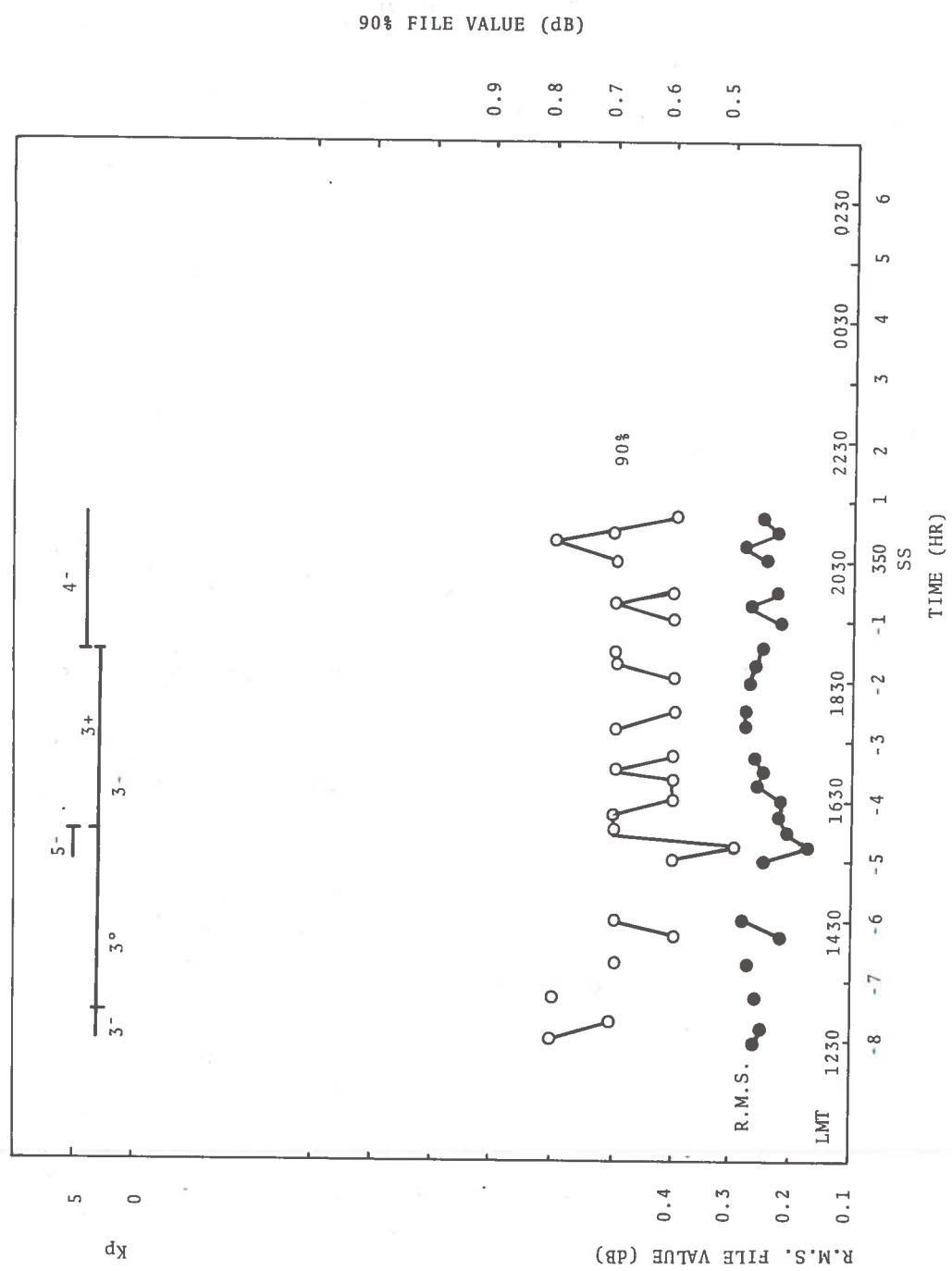


Figure C-19. Temporal Diagram for 8-10 April 1974

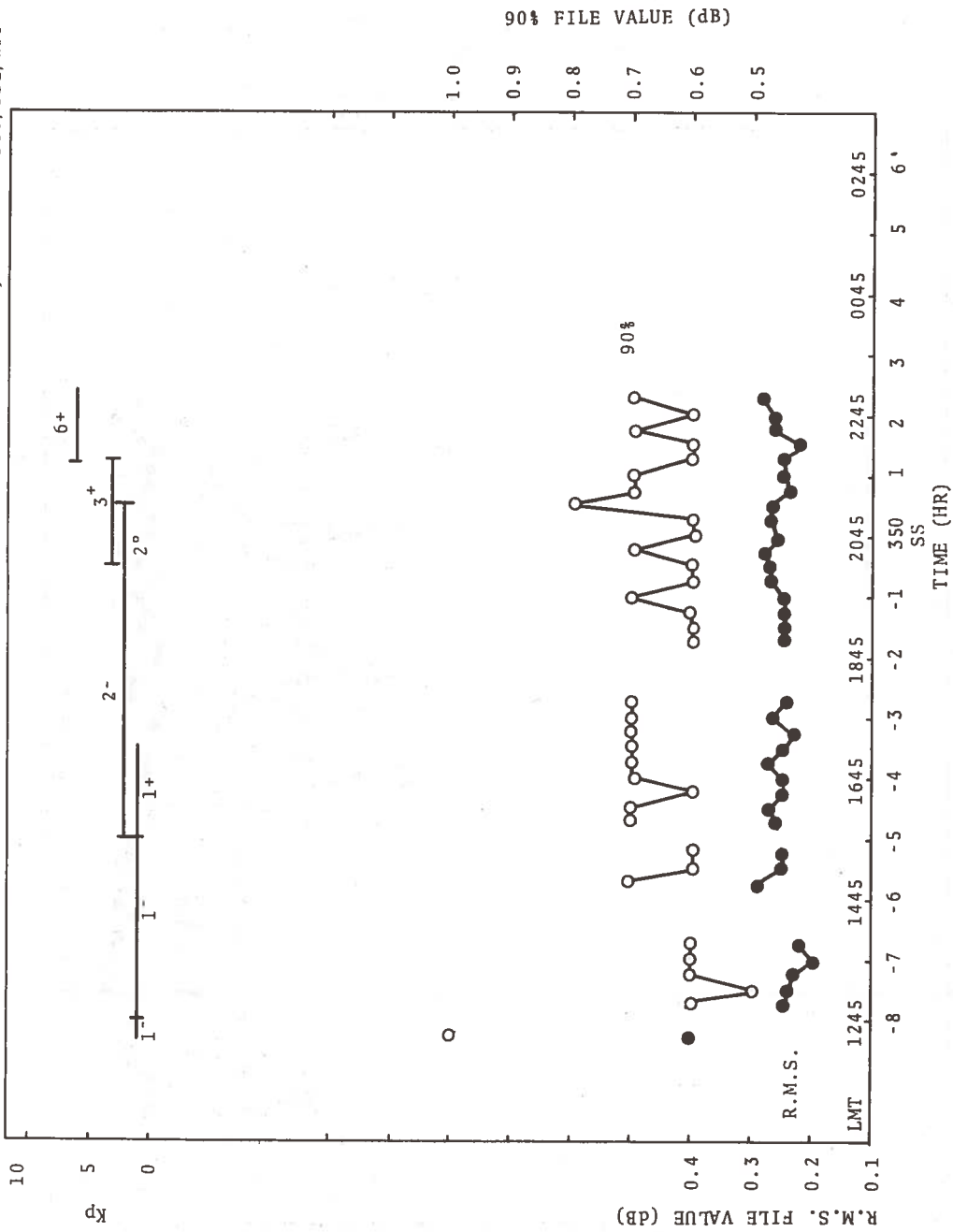


Figure C-20. Temporal Diagram for 15-18 April 1974

ATS-5 L-BAND DATA 22-25 APR 74 (L-BAND MT's 130-132) DOT/TSC/WPF

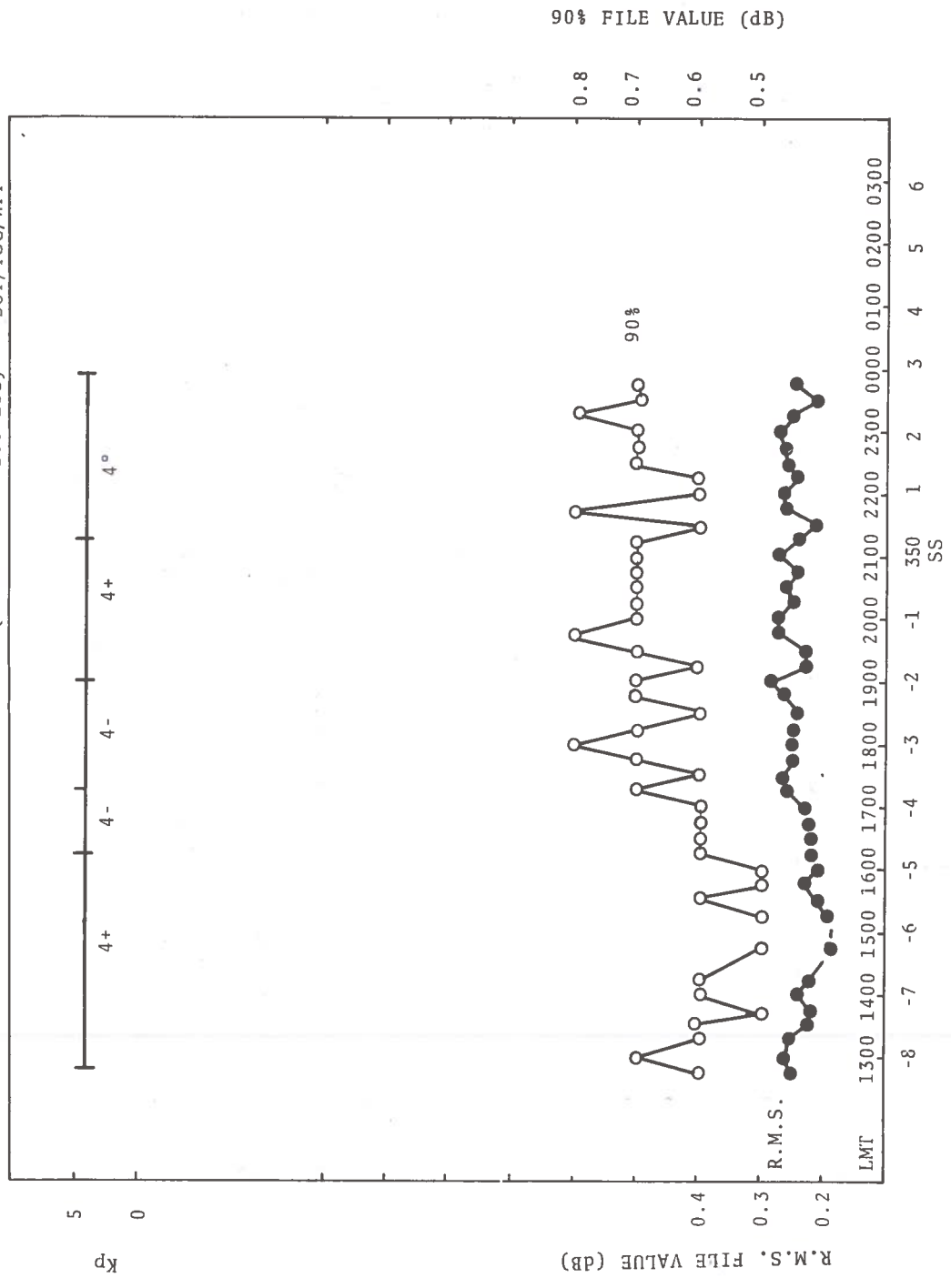


Figure C-21. Temporal Diagram for 22-25 April 1974

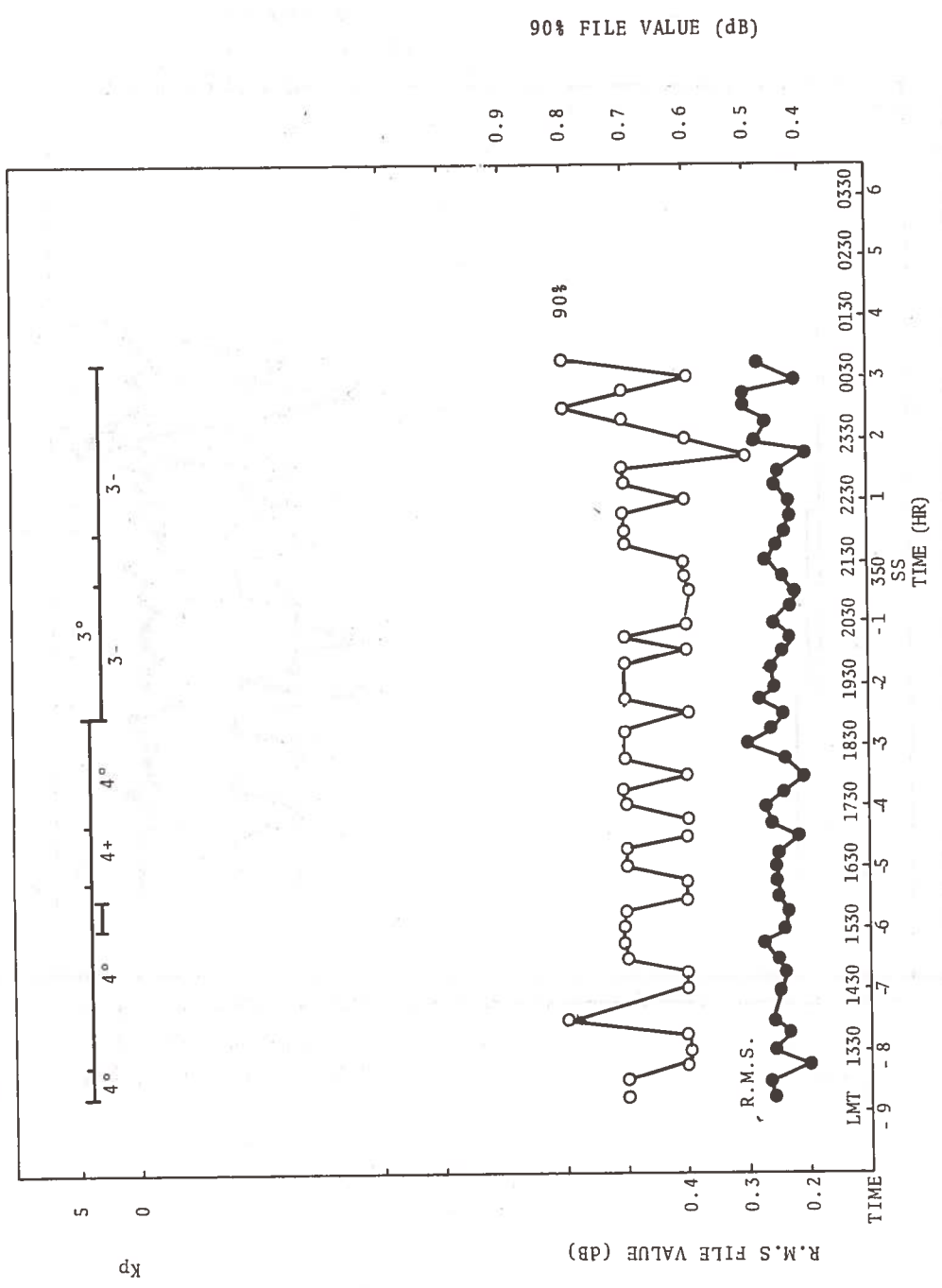


Figure C-22. Temporal Diagram for 29 April - 2 May 1974

ATS-5 L-BAND DATA 7-9 MAY 74 (L-BAND MT's 136-137) DOT/TSC/WPF

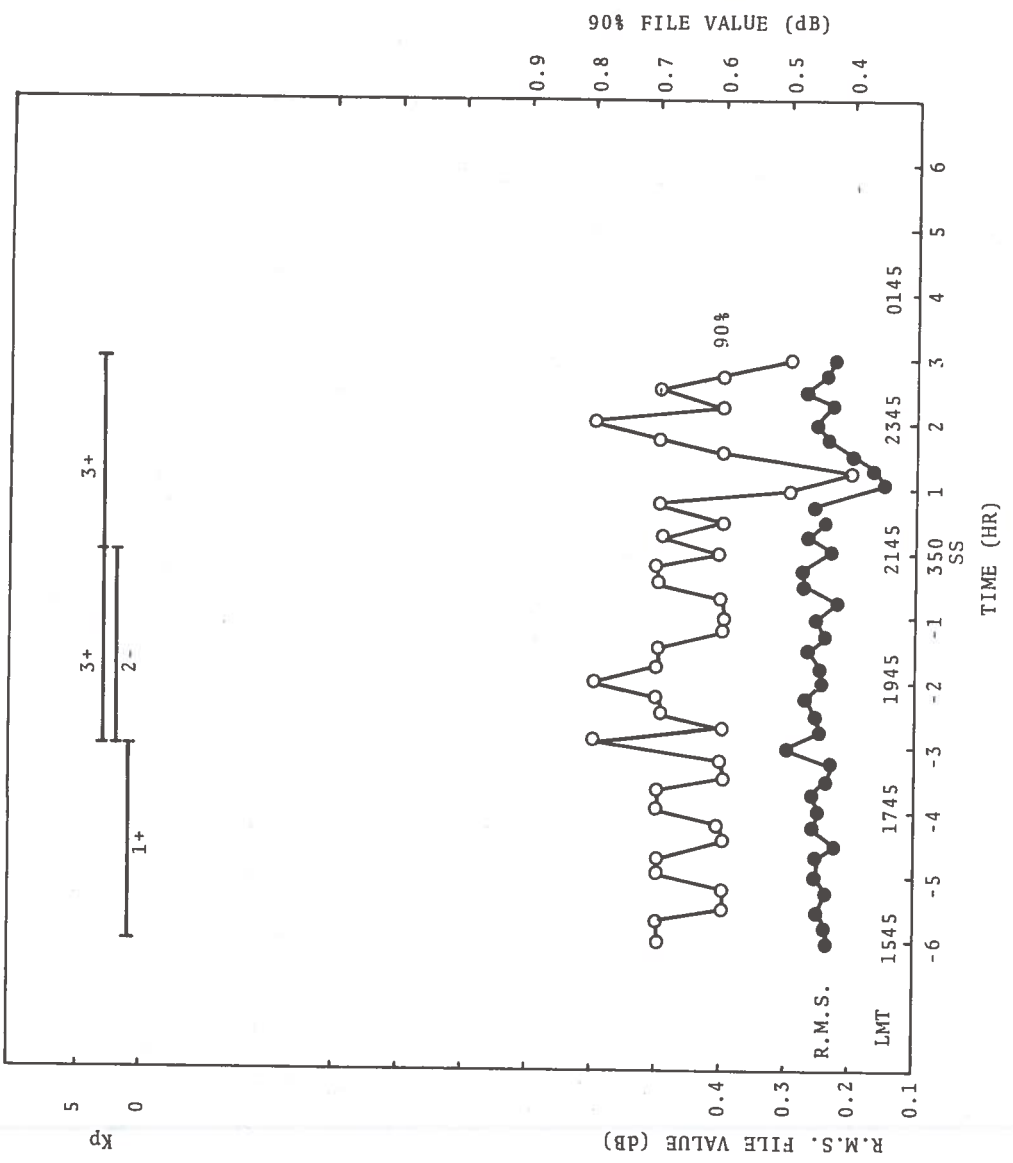


Figure C-23. Temporal Diagram for 7-9 May 1974

ATS-5 L-BAND DATA (L-BAND MT'S 138-140) 13-16 MAY 74 DOT/TSC/WPF

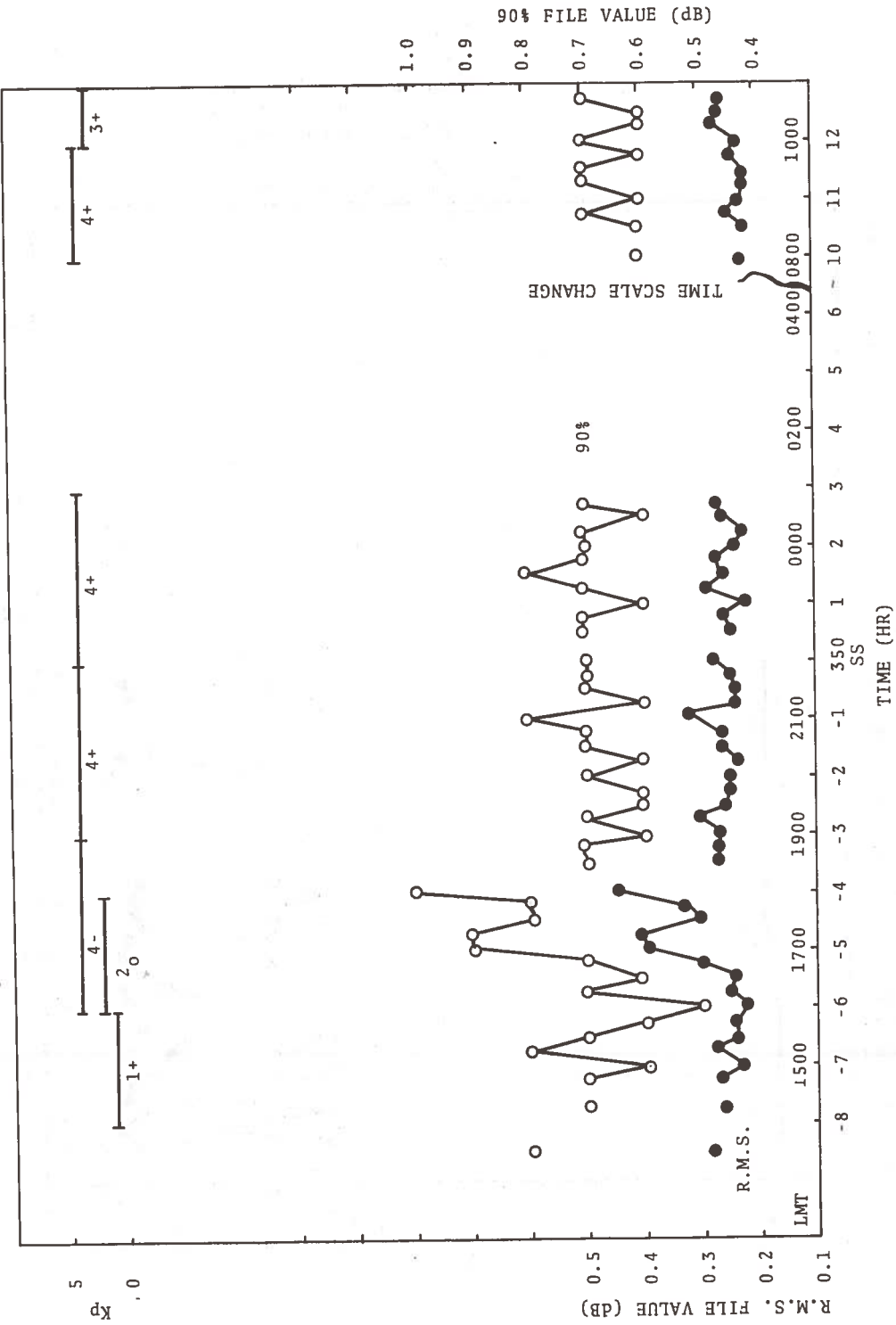


Figure C-24. Temporal Diagram for 13-16 May 1974

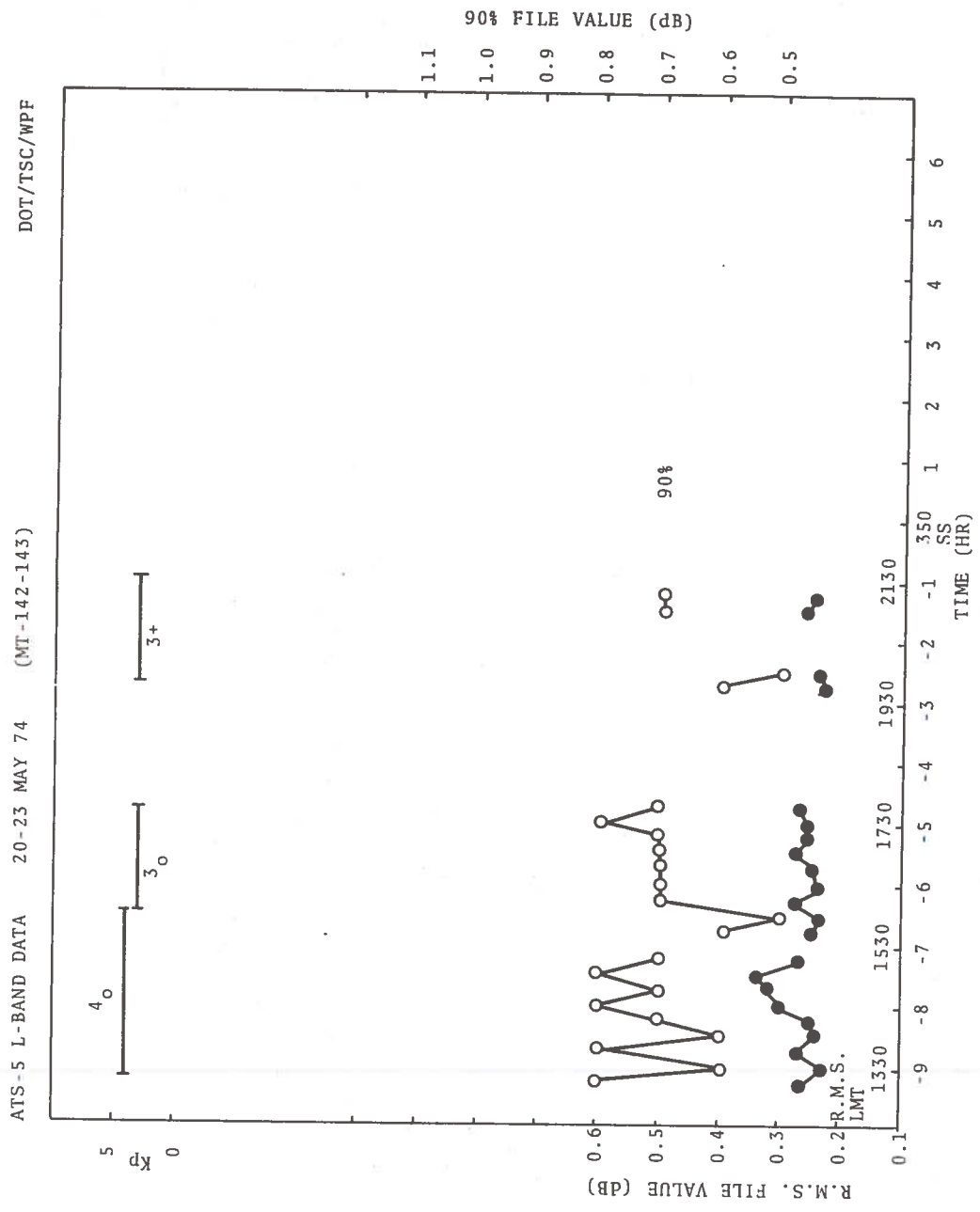


Figure C-25. Temporal Diagram for 20-23 May 1974

ATS-5 L-BAND DATA 28 MAY 74 (MT-144) DOT/TSC-WPF

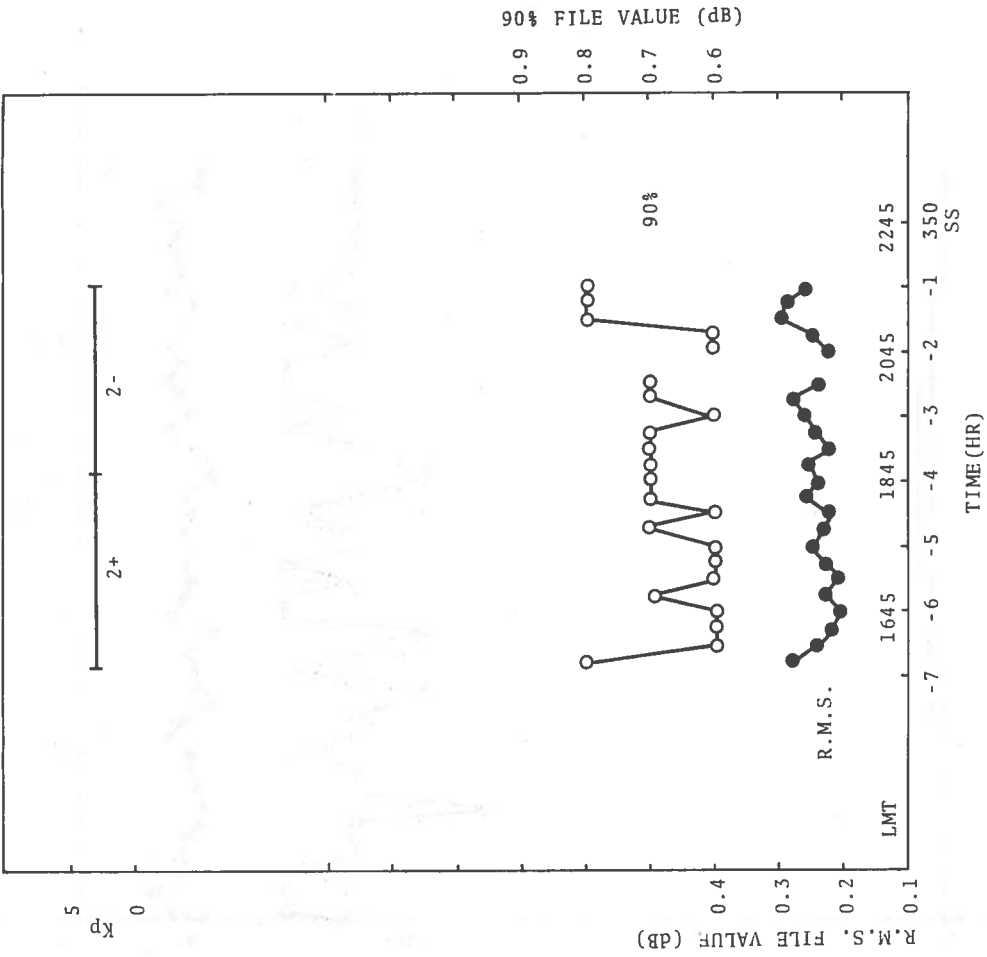


Figure C-26. Temporal Diagram for 28 May 1974

ATS-5 L-BAND DATA 3-6 JUN 74 (L-BAND MT's 145-147) DOT/TSC/WPF

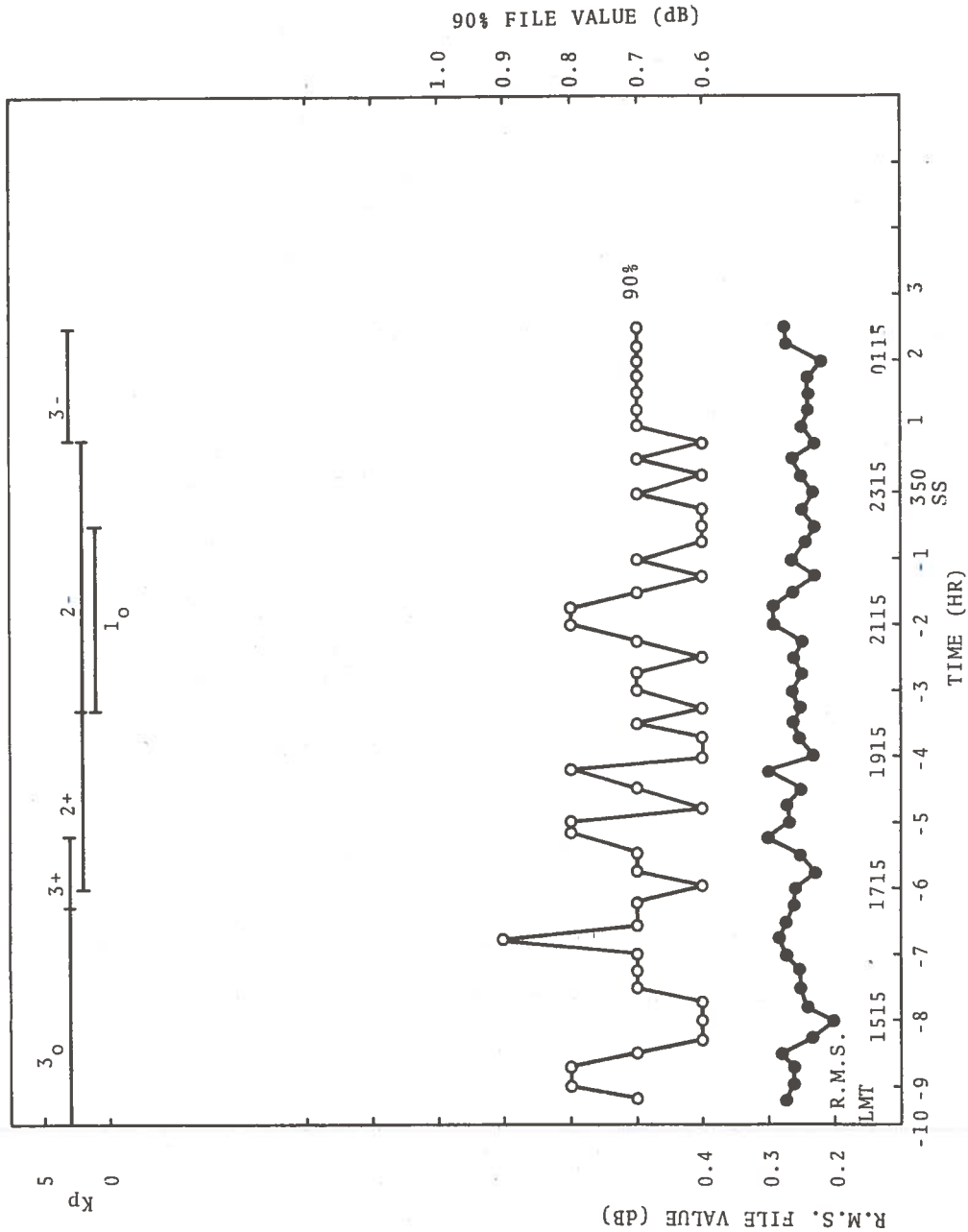


Figure C-27. Temporal Diagram for 3-6 June 1974

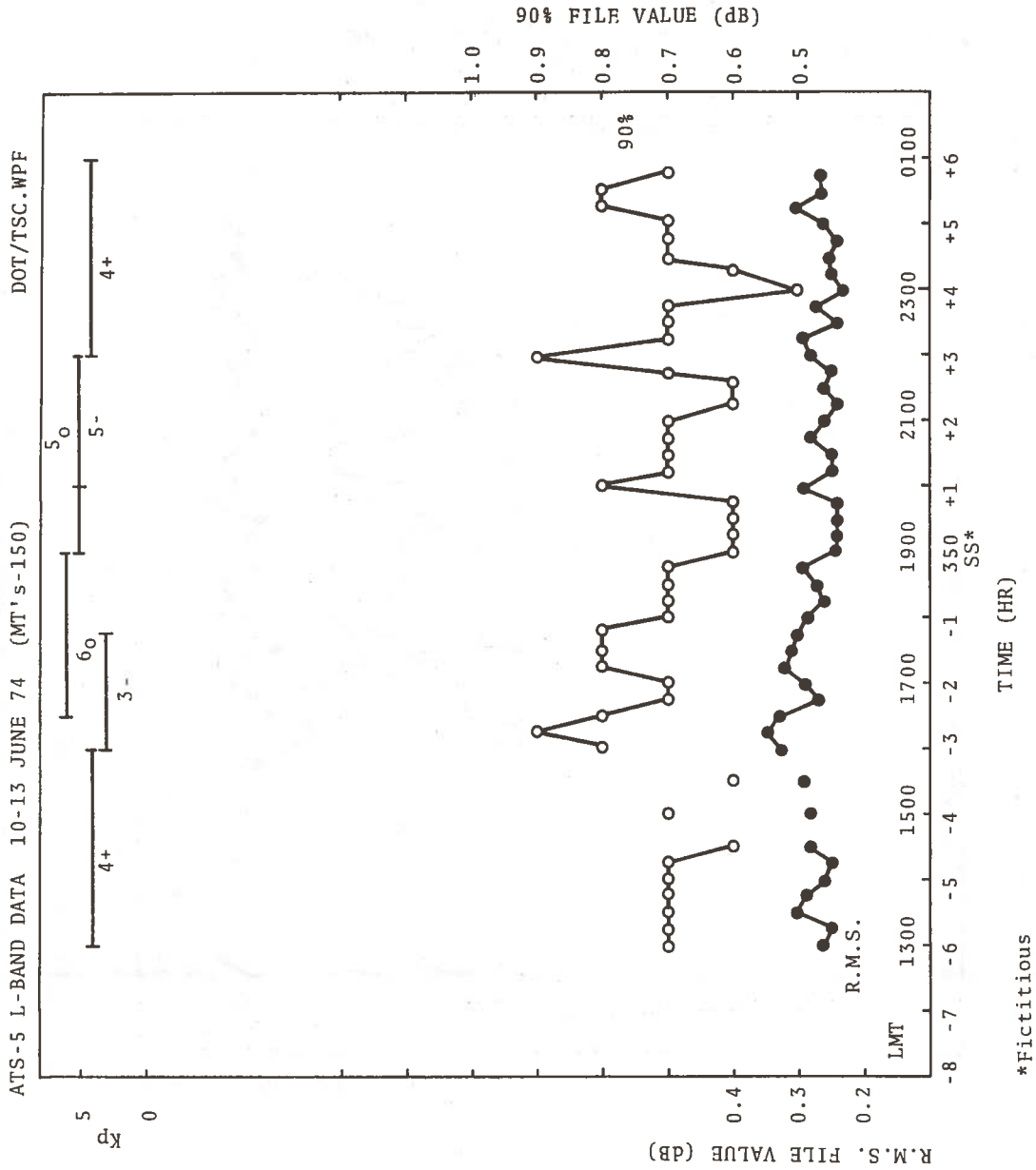


Figure C-28. Temporal Diagram for 10-13 June 1974

ATS-5 L-BAND DATA 17-20 JUNE 74 (L-BAND MT's 151-153) DOT/TSC/WPF

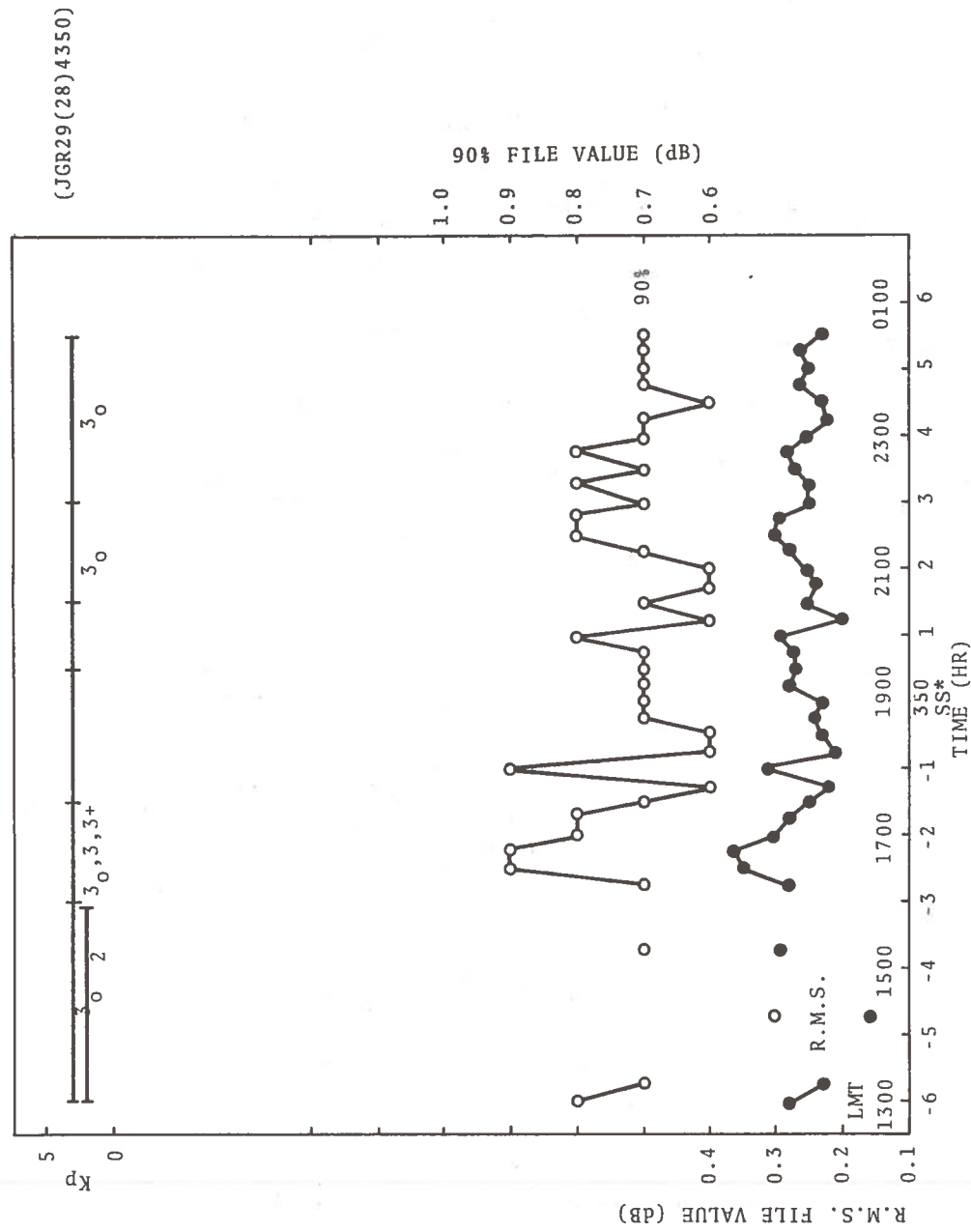


Figure C-29. Temporal Diagram for 17-20 June 1974

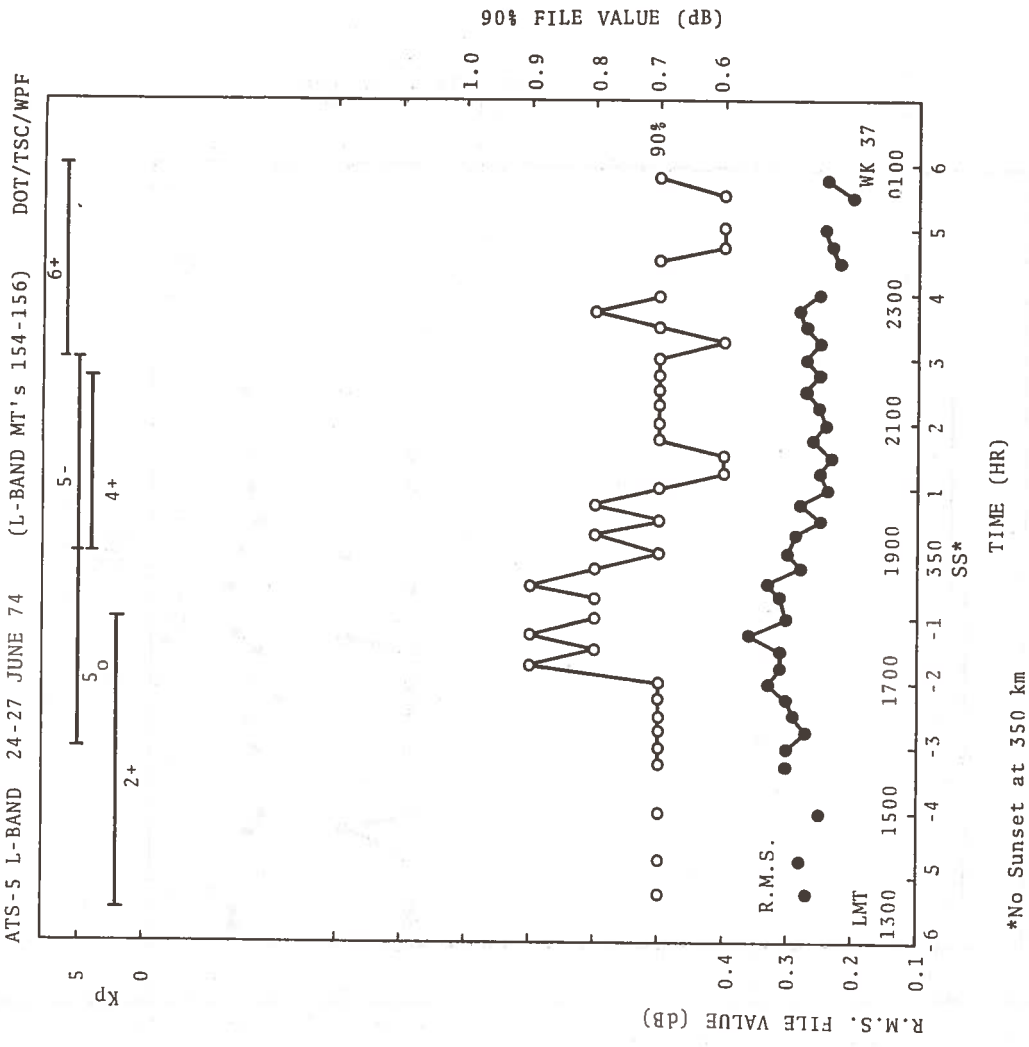


Figure C-30. Temporal Diagram for 24-27 June 1974

ATS-5 L-BAND DATA 1-2 JULY 74 (L-BAND MT's 157-158) DOT/TSC/WPF

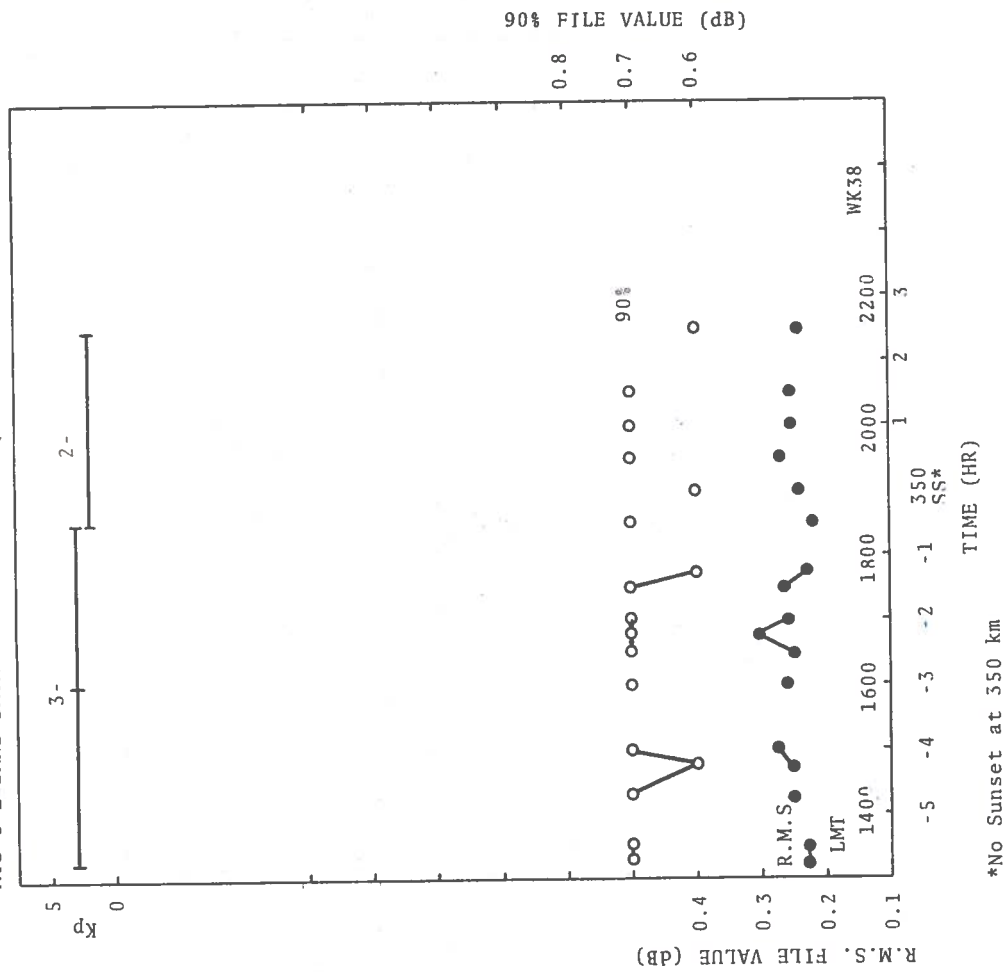


Figure C-31. Temporal Diagram for 1-2 July 1974

ATS-5 L-BAND DATA 8/9 JULY 74 (L-BAND MT's 159-161) DOT/TSC/WPF

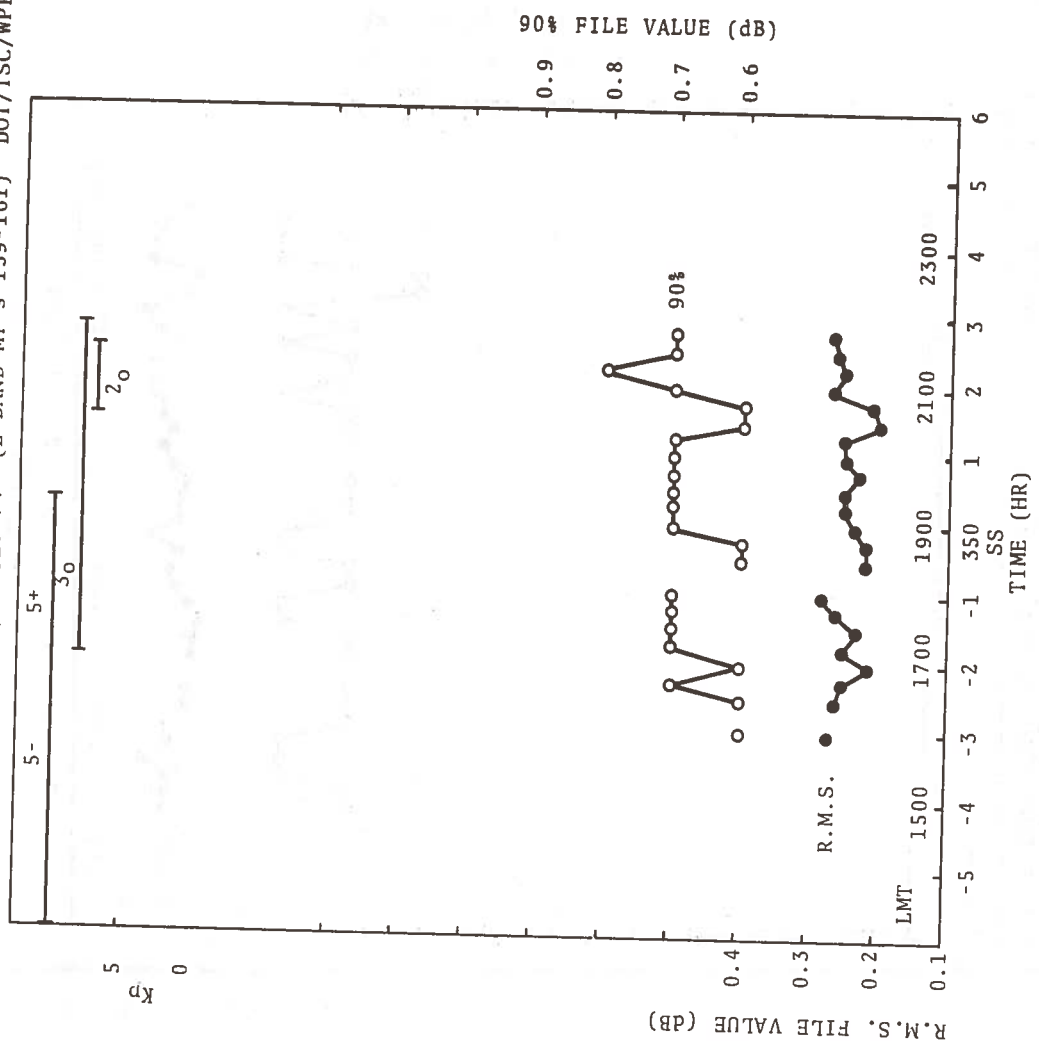


Figure C-32. Temporal Diagram for 8-9 July 1974

ATS-5 L-BAND DATA 15 JULY 74-18 JULY 74 (L-BAND MT's 162-164) DOT/TSC/WPF

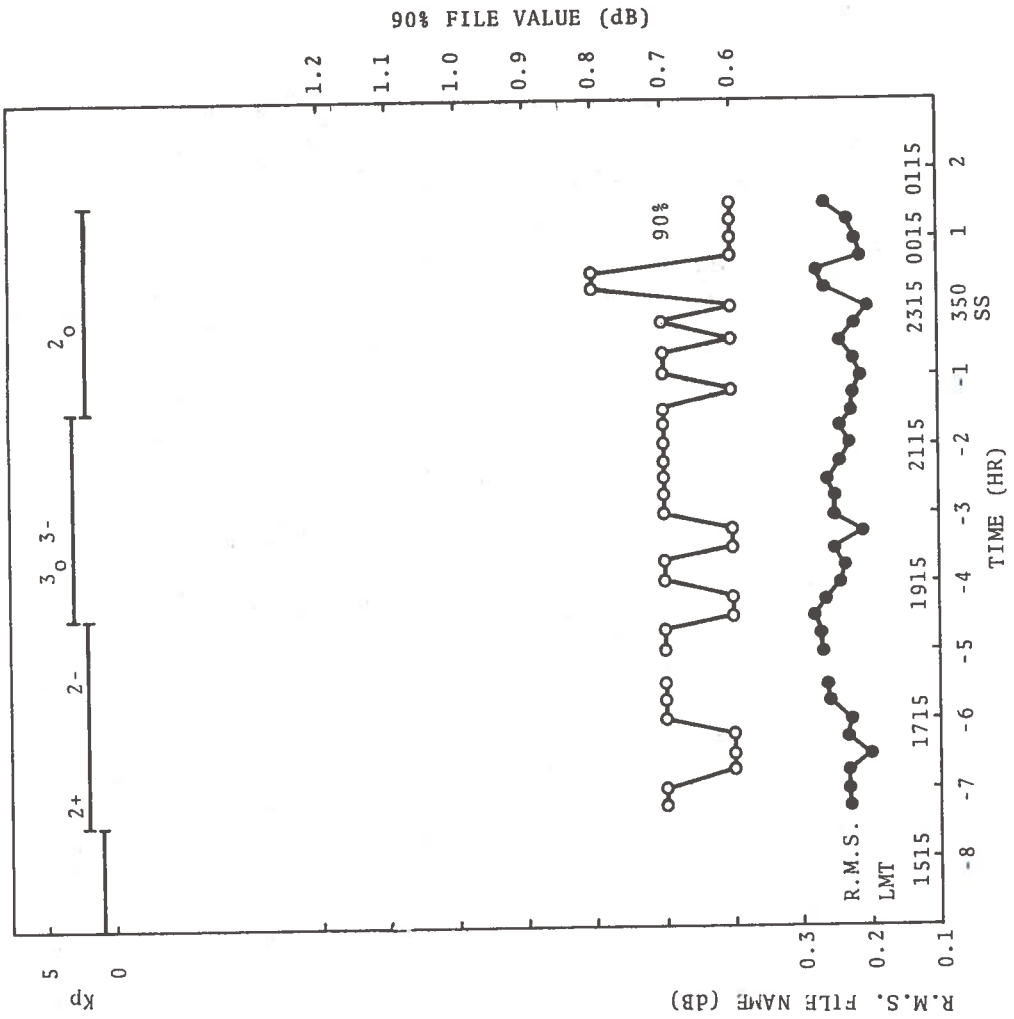


Figure C-33. Temporal Diagram for 15-18 July 1974

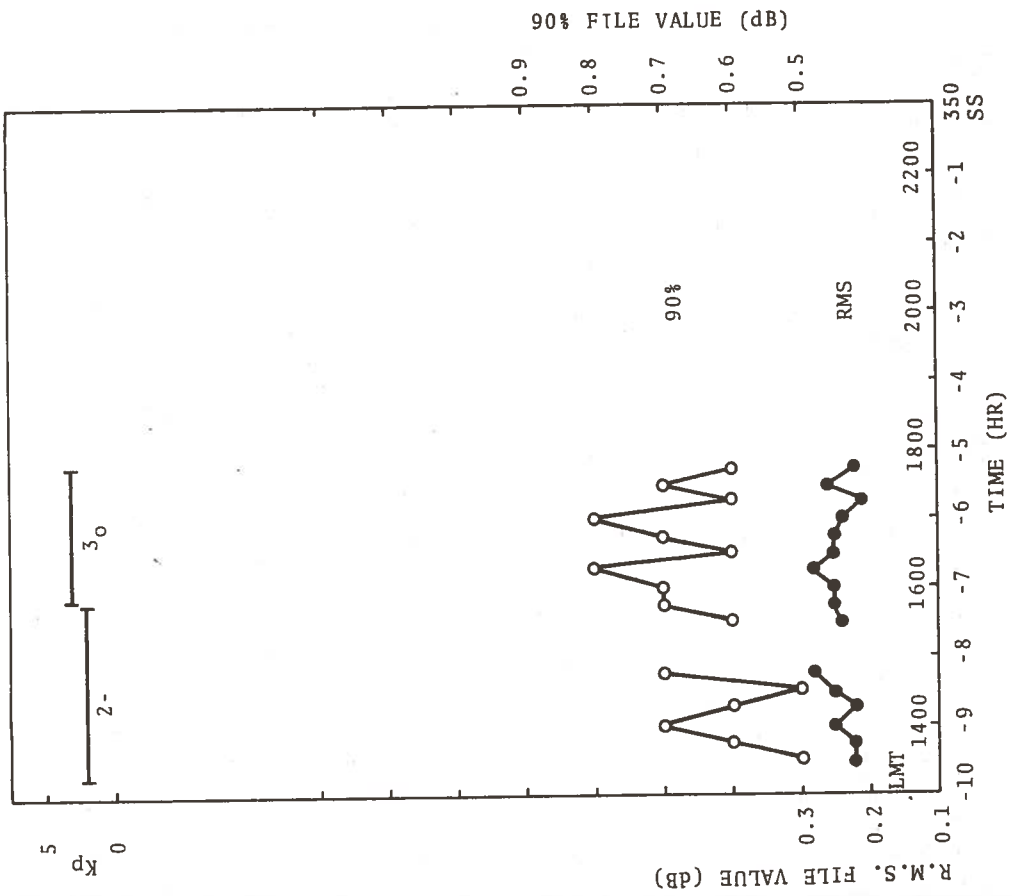
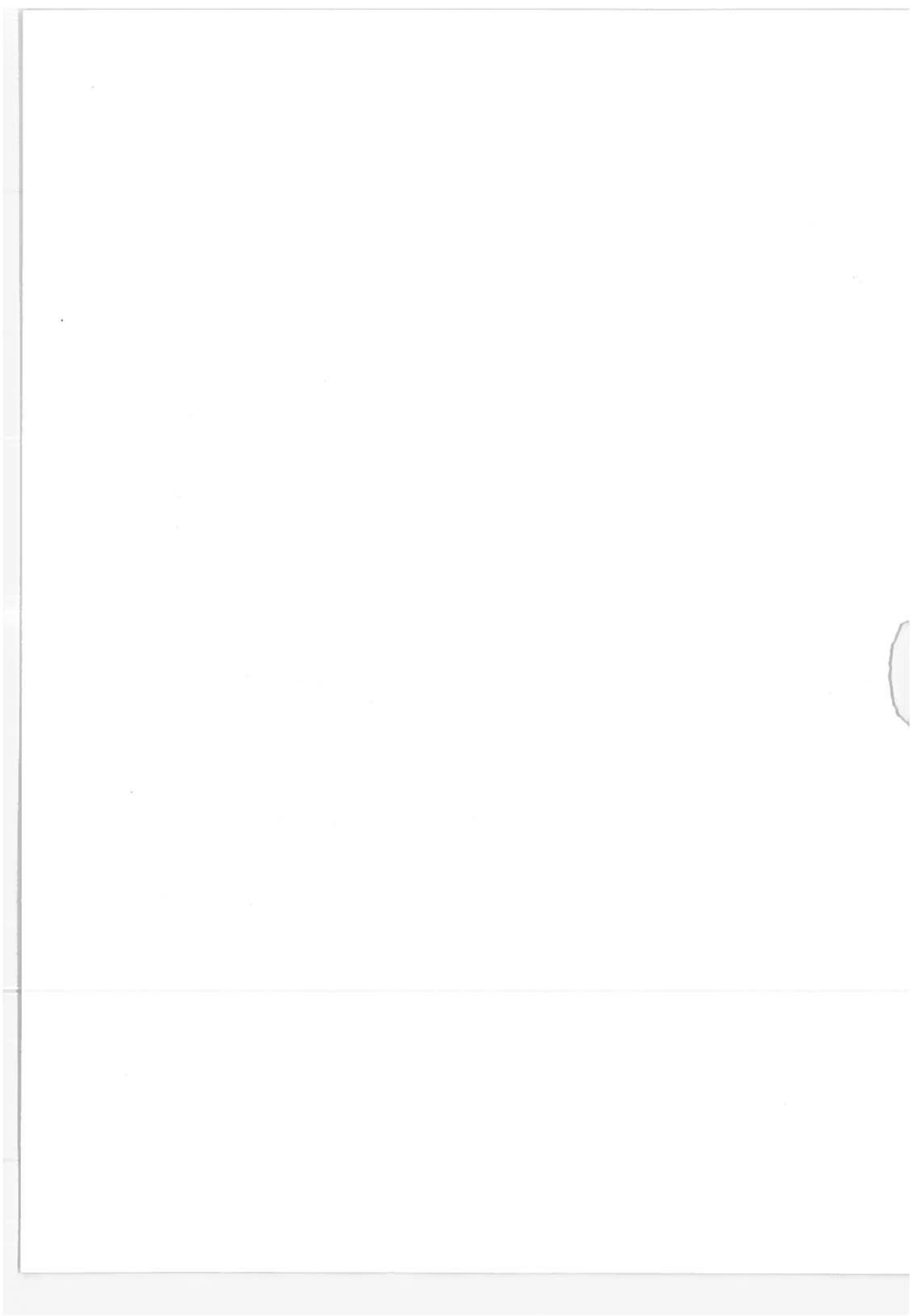


Figure C-34. Temporal Diagram for 22 July 1974



APPENDIX D

ANALYSIS OF MAXIMUM VALUES

Table D-1 through D-8 present the distribution of the maximum 15-minute amplitude data by month. Each of the entries in the tables consists of the following information:

- (a) The number of points, (No number means one).
- (b) The maximum root-mean-square value of a 15-minute measurement in decibels.
- (c) The maximum 90th-percentile value (15-minute scintillation index) in decibels.

Thus the entry 2-.23/.7 means there were two data points, a maximum root-mean-square value of 0.23 dB and a maximum 90th percentile value of 0.7 dB. The totals columns are plotted in the appropriate monthly plots in Section 4.

Table D-9 presents a tally sheet and frequency distributions of the data of Tables D-1 through D-8.

Table 4-3 presents the frequency distribution for the data of Table D-9 and Figure 4-25 presents the cumulative frequency distribution for the data of Table 4-3. The median value is 0.26 dB. It is seen that approximately 70 percent of the amplitude values centered at 0.26 dB cover the amplitude range 0.23 through 0.99 dB. Thus 10.2 percent of the values lie between 0.14 and 0.22 dB and 19.7 percent of the maximum values lie between 0.30 and 0.55 dB. Thus, of the 1026 maximum values recorded approximately twice as many are in the scintillating range (greater than 0.3 dB) than are in the exceedingly calm range (less than 0.22 dB).

D.1 ANALYSIS OF SEASONAL TRENDS

Table D-10 is derived from Table D-9 and presents the tally sheet and frequency distribution (expressed in percent) of the R.M.S. maximum values. Figure D-1 presents the results in graphical form.

TABLE D-1. DISTRIBUTION OF THE ROOT-MEAN-SQUARE AND 90TH-PERCENTILE MAXIMUM 15-MINUTE VALUES FOR DECEMBER 1973

ATS-5 L-BAND DATA; DEC 73					TOTAL; 125	DOT/TSC/WPF
NUMBER OF DATA POINTS; MAXIMUM VALUES						
TIME INTERVAL	DEC 73 3-7	DEC 73 10-13	DEC 73 18-20	DEC 73 26-29	TOTALS	
BF 5.50	.24/.7				1-	.24/.7
5.25	.25/.8	.26/.7	.24/.7		3-	.26/.8
BF 5.00	.24/.6	-	.23/.6		2-	.24/.6
4.75	.34/.8	.26/.7	.33/.8		3-	.34/.8
4.50	-	-	-		-	-
4.25	2-.27/.8	.26/.6	-		3-	.27/.8
BF 4.00	.27/.8	.28/.7	-		2-	.28/.8
3.75	.25/.7	.25/.6	-		2-	.25/.7
3.50	2-.27/.8	-	-		2-	.27/.8
3.25	2-.26/.8	.25/.7	-		3-	.26/.8
BF 3.00	4-.33/.8	-	.30/.8		5-	.33/.8
2.75	3-.24/.7	.24/.6	.30/.6		5-	.30/.7
2.50	2-.24/.7	-	-		2-	.24/.7
2.25	2-.26/.7	-	-		2-	.26/.7
BF 2.00	2-.26/.7	-	-	.29/.6	3-	.29/.7
1.75	3-.28/.7	-	-	.25/.7	4-	.28/.7
1.50	3-.28/.7	-	-	.29/.7	4-	.29/.7
1.25	3-.29/.8	-	-	-	3-	.29/.8
BF 1.00	3-.29/.7	-	-	-	3-	.29/.7
0.75	.27/.6	-	.30/.7	-	2-	.30/.7
0.50	2-.31/.9	-	.24/.6	-	3-	.31/.9
0.25	2-.28/.7	.25/.6	.30/.7	-	4-	.30/.7
SS 0.00	2-.27/.7	.26/.8	.29/.6	-	4-	.29/.8
0.25	.21/.5	-	.25/.7	.27/.7	3-	.27/.7
0.50	.25/.7	.24/.5	.23/.7	.25/.7	4-	.25/.7
0.75	2-.28/.7	.23/.6	.22/.6	.32/.6	5-	.32/.7
AF 1.00	2-.27/.7	-	.28/.8	.27/.6	4-	.28/.8
1.25	3-.28/.7	2-.29/.8	(.27/.6)	.24/.7	6-	.29/.8
1.50	3-.27/.7	2-.29/.7	2-.31/.7	2-.33/.8	9-	.33/.8
1.75	.26/.6	2-.28/.7	.27/.7	-	4-	.28/.7
AF 2.00	.24/.5	2-.28/.7	2-.24/.7	2-.28/.6	7-	.28/.7
2.25	2-.24/.7	2-.28/.7	2-.29/.7	2-.25/.7	8-	.29/.7
2.50	3-.24/.7	.25/.6	2-.28/.7	2-.33/.8	8-	.33/.8
2.75	2-.27/.8	.25/.6	2-.28/.7	2-.28/.7	7-	.28/.8
AF 3.00	2-.25/.7	.27/.6	.25/.6	2-.29/.7	6-	.28/.7
3.25	2-.26/.7	.26/.6	-	-	3-	.26/.7
3.50	2-.27/.7	.25/.7	.26/.7	-	4-	.27/.7
3.75	.22/.7	.24/.7	.25/.7	.29/.7	4-	.29/.7
AF 4.00	2-.25/.7	.26/.6	.23/.7	-	4-	.26/.7
4.25	2-.28/.7	.27/.6	.22/.6	.22/.6	5-	.28/.7
4.50	2-.28/.7	-	.26/.6	.24/.6	4-	.28/.7
4.75	.25/.8	-	.25/.7	.26/.5	3-	.26/.7
AF 5.00	.24/.8	.26/.7	.24/.5	.24/.6	4-	.26/.8
5.25	.27/.8	.28/.7	.26/.7	.26/.8	4-	.28/.8
5.50	.27/.8	.26/.6	.26/.7	.25/.6	4-	.27/.8
5.75	.26/.7	-	-	-	1-	.26/.7
AF 6.00	.23/.7	-	-	-	1-	.23/.7
6.25	.25/.7	-	-	-	1-	.25/.7
6.50	.24/.6	-	-	-	1-	.24/.6
6.75	.27/.7	-	-	-	1-	.27/.7

TABLE D-2. DISTRIBUTION OF THE ROOT-MEAN-SQUARE AND 90TH-PERCENTILE MAXIMUM 15-MINUTE VALUES FOR JANUARY 1974.

ATS-5 L-BAND DATA JAN 74 NUMBER OF DATA POINTS; MAXIMUM VALUES						DOT/TSC/WPF
						TOTAL: 129
TIME INTERVAL	JAN 74 2-5	JAN 74 7-10	JAN 74 14-17	JAN 74 21-24	JAN 74 28-30	TOTALS & MAX VALUE
BF 5.75	.25/.7		.32/.7	.24/.6		3-.32/.7
5.50	.25/.7		.26/.7		.31/.7	3-.31/.7
5.25			.27/.5	.28/.6		2-.28/.6
BF 5.00					.26/.6	1-.26/.6
4.75		.27/.7			.29/.7	2-.29/.7
4.50		.30/.7			.31/.7	2-.31/.7
4.25					.27/.6	1-.27/.6
BF 4.00				1-.28/.7		1-.28/.7
3.75		.28/.6		.30/.7		2-.30/.7
3.50					.26/.6	1-.26/.6
3.25			.32/.8		.30/.7	2-.32/.8
BF 3.00		.30/.7	.29/.7			2-.29/.7
2.75		.28/.7		2-.26/.6		3-.28/.7
2.50		2-.26/.7	2-.29/.8	.28/.7	.38/.8	5-.38/.8
2.25	.29/.6	.27/.7	.29/.8	2-.27/.7	.32/.7	6-.32/.8
BF 2.00	.29/.7	.24/.6	2-.27/.7	2-.29/.6	2-.28/.7	8-.29/.7
1.75	2-.32/.8	.28/.7	2-.27/.6	2-.28/.7	2-.32/.7	9-.32/.8
1.50	2-.29/.7	.28/.8	2-.27/.7	2-.28/.7	2-.30/.7	9-.30/.8
1.25	2-.30/.7	2-.28/.7	2-.26/.7	2-.28/.8	2-.30/.7	10-.30/.8
BF 1.00	2-.30/.8	.24/.7	.25/.7	2-.26/.6	.30/.7	7-.30/.7
0.75	2-.28/.7	2-.27/.6	.26/.7	.26/.6	.28/.7	7-.28/.7
0.50		.27/.7	.28/.7	.28/.6	.30/.7	5-.30/.7
0.25		.26/.7	.30/.7		.28/.6	4-.30/.7
SS 0.00		.25/.6	.26/.7		.27/.7	4-.27/.7
0.25			.30/.7		.27/.6	3-.30/.7
0.50			.26/.7		.29/.7	3-.29/.7
0.75	.27/.7	.30/.8	.27/.7			3-.30/.8
AF 1.00	2-		.31/.7	.28/.7	.30/.8	5-.31/.8
1.25	2-		2-.32/.7		.31/.8	5-.32/.8
1.50	2-		2-.32/.7	.28/.7	.33/.8	6-.33/.8
1.75	2-.31/.8		.28/.7	.27/.6		5-.31/.8
AF 2.00	2-	.30/.7	2-.30/.7	.28/.7	.27/.6	6-.30/.7
2.25	2		2-	.27/.6	-	5-.27/.6
2.50	2-.29/.7	2-.19/.5	2-.30/.8	.26/.7	-	7-.30/.8
2.75	2-	2-.30/.7	2-.30/.8	.25/.7	-	7-.30/.8
AF 3.00	2-	.25/.7	2-.32/.8	.27/.6	-	6-.32/.8
3.25	2-.27/.7	.25/.8	.26/.7	-	-	4-.27/.8
3.50		.23/.6	.24/.6	-	-	3-.24/.6
3.75	.29/.7	.35/.9	.28/.6	-	-	3-.35/.9
AF 4.00	.28/.6	.20/.6	.24/.5	-	-	3-.28/.6
4.25	.25/.6	.27/.8	.24/.7			3-.27/.8
4.50			.27/.7			2-.27/.7
4.75		.24/.7	.26/.6			3-.26/.7
AF 5.00			.34/.7			2-.34/.7
5.25		.30/.8				2-.30/.6
5.50		.29/.8	.24/.7			3-.29/.8
5.75	.21/.6	.25/.7				2-.25/.7

TABLE D-3. DISTRIBUTION OF THE ROOT-MEAN-SQUARE AND 90TH-PERCENTILE MAXIMUM 15-MINUTE VALUES FOR FEBRUARY 1974

ATS-5 L-BAND DATA; FEB 74		TOTAL: 149			DOT/TSC/WPF
NUMBER OF DATA POINTS; MAXIMUM VALUES					
TIME INTERVAL	FEB 74 4-7	FEB 74 11-15	FEB 74 18-21	FEB 74 25-28	TOTALS
BF 6:50				.32/.7	1-.32/.7
6:25				.27/.6	1-.27/.6
BF 6:00	-	.24/.6		.31/.7	1-.31/.7
5:75		.36/.8	.22/.6	-	3-.36/.8
5:50	.35/.9	.30/.8	.19/.6	-	3-.35/.9
5:25		.26/.7	.19/.6	.21/.6	4-.26/.7
BF 5:00	.30/.9	.30/.7	-	.19/.5	3-.30/.9
4:75	-	.24/.7	.26/.7	.21/.5	3-.34/.7
4:50	.26/.5	-	-	.24/.6	2-.26/.6
4:25		.18/.5	-	.28/.7	3-.28/.7
BF 4:00		.29/.8	-	.26/.6	3-.29/.8
3:75		.27/.7	.25/.7	.25/.6	4-.27/.7
3:50	.3/.8	.31/.8	.23/.6	.25/.6	4-.31/.8
3:25	.35/.9	.38/1.0	.24/.6	2-.32/.8	5-.38/1.0
BF 3:00	.31/.8	.16/.5	2-.31/.8	2-.30/.7	6-.33/.8
2:75	.27/.8	2-.29/.8	.29/.8	.33/.8	5-.33/.8
2:50	.27/.8	2-.30/.9	.25/.7	.30/.6	5-.30/.9
2:25	.29/.6	.43/1.0	2-.33/.8	.37/.7	5-.43/1.0
BF 2:00	.30/.7	.29/.6	2-.26/.5	.39/1.0	5-.39/1.0
1:75	.31/.9	2-.33/.9	2-.25/.6	.23/.6	6-.33/.9
1:50	.28/.7	2-.25/.7	2-.30/.7	-	5-.30/.7
1:25	.27/.7	2-.21/.6	.27/.7	-	4-.27/.7
BF 1:00	.29/.8	.25/.6	.21/.7	-	3-.29/.8
0:75	-	-	.20/.6	-	1-.20/.6
0:50	-	.34/.8	.24/.7	-	2-.34/.8
0:25	.27/.7	.32/.6	.26/.6	-	3-.32/.7
SS 0:00		.40/.9	-	.26/.6	3-.40/.9
0:25	.27/.7	-	2-.33/.9	.35/.9	4-.35/.9
0:50	.21/.5	-	2-.32/.8	.30/.7	4-.32/.8
0:75	.21/.5	.23/.6	.32/.7	.24/.6	4-.32/.7
AF 1:00	2-.20/.6	.26/.7	2-.26/.6	.32/.8	6-.32/.8
1:25	2-.24/.7	.24/.5	2-.27/.7	2-.26/.8	7-.27/.8
1:50	2-.25/.6	-	2-.24/.7	2-.32/.8	6-.32/.8
1:75	2-.21/.5	2-.29/.8	2-.25/.6	2-.29/.7	8-.29/.8
AF 2:00	2-.25/.5	2-.27/.7	-	2-.24/.6	6-.27/.7
2:25	.23/.5	.38/1.0	.26/.6	.21/.6	4-.38/1.0
2:50	.24/.5	2-.23/.5	2-.32/.8	.28/.6	6-.32/.8
2:75	2-.28/.7	2-.25/.7	.21/.5	.29/.7	6-.29/.7
AF 3:00	.24/.6	.26/.6	.20/.6	.32/.8	4-.32/.8
3:25	.28/.7	.20/.5	.43/1.0	.35/.8	4-.32/1.0
3:50	.33/.9	-	.41/1.0	.28/.7	3-.41/1.0
3:75	.24/.6	.16/.5	.34/.9	.25/.6	4-.34/.9
AF 4:00	.26/.6	-	.25/.6	.29/.7	3-.29/.7
4:25	.29/.7	.34/1.0	-	.31/.7	3-.24/1.0
4:50	.33/.7	.24/.4	-	.39/.9	3-.39/.9
4:75	.27/.7	.25/.7	.51/1.2	.30/.7	4-.51/1.2
AF 5:00	.27/.7	.20/.5	.21/.5	-	3-.27/.7
5:25	-	.25/.6			1-.25/.6
5:50	.29/.8				1-.29/.8

TABLE D-4. DISTRIBUTION OF THE ROOT-MEAN-SQUARE AND 90TH-PERCENTILE MAXIMUM 15-MINUTE VALUES FOR MARCH 1974

ATS-5 L-BAND DATA; MAR 74 NUMBER OF DATA POINTS; MAXIMUM VALUES				TOTAL: 119	DOT/TSC/WPF
TIME INTERVAL	MAR 74 5-8	MAR 74 11-16	MAR 74 18-22	MAR 74 25-30	TOTALS
BF 6.00				.25/.7	.25/.7
5.75				.25/.7	.24/.7
5.50		2-.23/.6	2-.29/.7	2-.27/.7	5-.29/.7
5.25		3-.22/.5	3-.33/.8	4-.26/.7	10-.33/.8
BF 5.00		3-.25/.6	.35/1.0	5-.29/.8	9-.35/1.0
4.75		2-.24/.6	3-.3/.8	4-.29/.8	9-.30/.8
4.50		2-.30/.8	4-.30/.8	4-.29/.7	10-.30/.8
4.25		2-.33/.8	3-.27/.8	3-.26/.7	8-.33/.8
BF 4.00	.31/.8	3-.34/.8	4-.28/.8	4-.26/.7	12-.34/.8
3.75	2-.24/.7	3-.31/.8	3-.30/.8	3-.28/.7	11-.31/.8
3.50	2-.36/1.0	3-.30/.7	4-.27/.7	2-.25/.6	11-.36/1.0
3.25	.27/.7	3-.28/.7	2-.33/.7	2-.23/.6	8-.33/.7
BF 3.00	.28/.8	3-.30/.7	2-.23/.7	.26/.7	7-.30/.8
2.75	.27/.8	4-.34/.8	3-.24/.8	2-.23/.5	10-.34/.8
2.50	.35/.8	3-.27/.6	2-.28/.8	.29/.7	7-.35/.8
2.25	.25/.6	3-.38/.9	2-.26/.6		6-.38/.9
BF 2.00	.24/.6	3-.32/.8	.26/.7	2-.31/.7	7-.32/.8
1.75	.33/.8	3-.31/.7	2-.29/.8	2-.27/.6	8-.33/.8
1.50	.33/.6	3-.39/1.0	4-.31/.9	.22/.6	9-.39/1.0
1.25	.30/.7	3-.30/.8	4-.27/.7	2-.23/.6	10-.30/.8
BF 1.00	.26/.6	4-.30/.8	2-.30/.8	2-.25/.6	9-.30/.8
0.75	.31/.9	5-.30/.8	4-.27/.7	2-.25/.6	12-.31/.9
0.50	.28/.8	5-.29/.8	3-.30/.8	2-.25/.7	11-.30/.8
0.25	.35/.7	4-.27/.7	3-.28/.7	2-.25/.7	10-.35/.7
SS 0.00	.25/.7	4-.32/.7	3-.25/.7	2-.27/.6	10-.32/.7
0.25	.27/.6	4-.33/.9	4-.27/.8	2-.29/.7	11-.33/.9
0.50	.33/.7	4-.36/.9	4-.25/.6	1-.27/.8	10-.36/.9
0.75	.26/.6	5-.34/.8	4-.27/.8	2-.27/.7	12-.34/.8
AF 1.00	.44/1.1	5-.30/.8	4-.34/.8	2-.27/.7	12-.24/1.1
1.25	.24/.6	5-.29/.7	4-.30/.8	2-.6/.7	12-.30/.8
1.50	.24/.6	5-.22/.5	4-.28/.8	2-.28/.7	12-.28/.8
1.75	.40/.9	5-.32/.8	3-.26/.6	.25/.6	10-.40/.9
AF 2.00	.34/.8	4-.33/.9	2-.29/.8		7-.34/.9
2.25		2-.25/.7			2-.25/.7

TABLE D-5. DISTRIBUTION OF THE ROOT-MEAN-SQUARE AND 90TH-PERCENTILE MAXIMUM 15-MINUTE VALUES FOR APRIL 1974

ATS-5 L-BAND DATA; APR74		TOTAL: 193				DOT/TSC/WPF
NUMBER OF DATA POINTS:		MAXIMUM VALUES				
INTERVAL	APR 74 1-4	APR 74 8-10	APR 74 15-18	APR 74 22-25	APR 74 29APR-2MAY	TOTALS
BF 8.75					.26/.7	1-.26/.7
8.50					.26/.7	1-.26/.7
8.25			.4/1.0	.25/.6	.20/.6	3-.4/1.0
BF 8.00		.26/.8	.27/.7	.26/.7	.26/.6	4-.27/.7
7.75		.25/.7	-	.25/.6	.23/.6	3-.25/.7
7.50		-	.24/.5	.23/.6	.26/.8	3-.26/.8
7.25		.26/.8	.23/.6	.22/.5	-	3-.26/.8
BF 7.00	.5/1.1	-	.20/.6	.26/.6	.25/.6	4-.5/1.1
6.75	.49/1.1	.28/.7	.22/.6	.22/.6	.24/.6	5-.49/1.1
6.50	.3/.8	.22/.6	-	.22/.6	.25/.7	4-.3/.8
6.25	.21/.5	.28/.7	-	.20/.5	.28/.7	4-.28/.7
BF 6.00	.22/.6	-	-	-	2-.35/.7	3-.25/.7
5.75	.29/.7	-	.28/.7	.20/.5	.24/.7	4-.29/.7
5.50	.3/.8	-	.27/.7	.21/.6	2-.27/.7	5-.30/.8
5.25	.32/.7	-	2-.27/.7	.23/.5	2-.25/.6	6-.32/.7
BF 5.00	.29/.6	.24/.6	.26/.7	.21/.5	2-.26/.8	6-.29/.8
4.75	-	.17/.5	-	2-.23/.6	2-.24/.8	5-.24/.8
4.50	.28/.6	.21/.7	2-.31/.7	2-.23/.6	2-.23/.6	8-.31/.7
4.25	.24/.6	.22/.7	2-.25/.7	2-.25/.6	2-.28/.7	8-.28/.7
BF 4.00	2-.3/.7	.22/.6	2-.25/.7	2-.23/.6	.27/.7	8-.30/.7
3.75	2-.29/.8	2-.28/.7	2-.24/.7	2-.27/.7	.24/.7	8-.29/.8
3.50	.23/.6	2-.27/.7	2-.25/.7	.26/.6	.21/.6	7-.27/.7
3.25	.26/.8	2-.27/.7	.24/.7	.25/.7	.24/.7	6-.27/.8
BF 3.00	.26/.7	-	.27/.7	.25/.8	.30/.8	4-.30/.8
2.75	.24/.6	.28/.7	.25/.7	.25/.7	.26/.7	5-.28/.7
2.50	.30/.7	.28/.6	-	.24/.6	.24/.6	4-.30/.7
2.25	.23/.6	-	-	.26/.7	2-.29/.7	4-.29/.7
BF 2.00	.23/.6	.27/.6	-	.28/.7	2-.27/.7	5-.28/.7
1.75	.25/.7	.26/.7	.25/.6	.23/.6	2-.26/.7	6-.26/.7
1.50	.24/.6	.25/.7	.25/.6	2-.24/.7	.24/.6	6-.25/.7
1.25	.27/.6	-	.27/.7	(.27/.8)	.27/.6	3-.27/.8
BF 1.00	2-.31/.8	.22/.6	.25/.7	2-.28/.7	2-.27/.6	8-.31/.8
0.75	2-.29/.8	.27/.7	.27/.6	2-.28/.7	2-.23/.6	8-.29/.8
0.50	2.30/.9	-	2-.28/.7	2-.26/.7	2-.22/.6	8-.30/.9
0.25	2-.26/.6	.22/.6	.27/.7	2-.26/.8	2-.23/.6	8-.27/.8
SS 0.00	2-.32/.7	.24/.8	2-.27/.6	2-.28/.7	.27/.6	8-.32/.8
0.25	2-.32/.8	.28/.8	.27/.7	2-.23/.6	.25/.7	7-.32/.8
0.50	.25/.7	.22/.7	.27/.8	.21/.6	.24/.7	5-.27/.8
0.75	.20/.6	.25/.6	.24/.7	.26/.8	.23/.7	5-.26/.8
AF 1.00	.28/.7	-	.25/.7	.26/.6	.23/.6	4-.28/.7
1.25	.25/.6		.25/.6	.24/.6	.22/.7	4-.25/.7
1.50	.28/.7		.22/.6	.26/.7	.25/.7	4-.28/.7
1.75	.22/.6		.26/.7	.26/.7	.20/.5	4-.26/.7
AF 2.00	.26/.7		.26/.6	.27/.7	.28/.6	4-.28/.7
2.25	.22/.6		.26/.7	.25/.8	.27/.7	4-.27/.7
2.50	.24/.5			.32/.7	.30/.8	3-.20/.8
2.75	.22/.7			.25/.5	.30/.7	3-.30/.7
AF 3.00	-			-	.22/.6	1-.22/.6
3.25	.23/.7				.25/.7	2-.25/.7

TABLE D-6. DISTRIBUTION OF THE ROOT-MEAN-SQUARE AND 90TH-PERCENTILE MAXIMUM 15-MINUTE VALUES FOR MAY 1974

ATS-5 L-BAND DATA; MAY 74					TOTAL: 119	DOT/TSC/WPF
NUMBER OF DATA POINTS; MAXIMUM VALUES						
TIME INTERVAL	MAY 74 7-9	MAY 74 13-16	MAY 74 20-23	MAY 74 29	TOTAL	
9.25			.26/.8		1-.26/.8	
BF 9.00			.23/.6		1-.23/.6	
8.75			.27/.8		1-.27/.8	
8.50			.24/.6		1-.24/.6	
8.25			.25/.7		1-.25/.7	
BF 8.00		.30/.8	.31/.8		2-.31/.8	
7.75			.32/.7		1-.32/.7	
7.50		.26/.7	.34/.8		2-.34/.8	
7.25		.27/.7	.27/.7		2-.27/.7	
BF 7.00			.23/.6		1-.23/.6	
6.75		.29/.8	.27/.7	.28/.8	3-.29/.8	
6.50		.24/.7	.24/.5	.24/.6	3-.24/.7	
6.25		.24/.6	.28/.7	.22/.6	3-.28/.7	
BF 6.00		2-.23/.7	.28/.8	.21/.6	4-.28/.8	
5.75	.27/.7	2-.28/.8	.26/.7	.23/.7	5-.28/.8	
5.50	.23/.6	2-.26/.7	.28/.7	.21/.6	5-.28/.7	
5.25	.22/.6	2-.35/.8	.26/.7	.23/.6	5-.35/.8	
BF 5.00	.22/.6	2-.48/1.2	.26/.8	.25/.6	5-.48/1.2	
4.75	.28/.7	2-.55/1.2	.24/.6	.23/.7	5-.55/1.2	
4.50		2-.32/.8		.22/.6	3-.32/.8	
4.25		2-.34/.9		.26/.7	3-.34/.9	
BF 4.00	.22/.6	.44/1.0		.24/.7	3-.44/1.0	
3.75	.27/.7	.46/1.1		.26/.7	3-.46/1.1	
3.50	.26/.6	.27/.7		.22/.7	3-.27/.7	
3.25	.24/.6	.27/.7		.24/.7	3-.27/.7	
BF 3.00	.30/.8	.26/.6		.26/.6	3-.30/.8	
2.75	.25/.6	.23/.7	.23/.6	.28/.7	4-.28/.7	
2.50	.25/.7	2-.27/.6	.22/.5	.24/.7	5-.27/.7	
2.25	2-.28/.7	2-.27/.7			4-.28/.7	
BF 2.00	2-.27/.8	2-.26/.7		.22/.6	5-.27/.8	
1.75	2-.27/.7	2-.25/.7		.24/.6	5-.27/.7	
1.50	2-.28/.7	2-.28/.7	.26/.7	.30/.8	6-.30/.8	
1.25	2-.25/.7	2-.26/.7		.29/.8	5-.29/.8	
BF 1.00	.26/.6	.32/.8		.26/.8	3-.32/.8	
0.75	.22/.6	2-.26/.6			3-.26/.6	
0.50	.26/.6	2-.6/.7			3-.26/.7	
0.25	2-.28/.8	2-.26/.7			4-.28/.8	
SS 0.00	2-.22/.6	.28/.7			3-.28/.7	
0.25	.27/.7				1-.27/.7	
0.50	.24/.6	.24/.7			2-.24/.7	
0.75	.26/.7	.25/.6			2-.26/.7	
AF 1.00	.15/.5	.22/.6			2-.22/.6	
1.25	.17/.4	.29/.7			2-.29/.7	
1.50	.22/.7	.26/.8			2-.26/.8	
1.75	.24/.7	.27/.7			3-.27/.7	
AF 2.00	.26/.8	.24/.7			3-.26/.8	
2.25	.25/.7	.27/.7			3-.27/.7	
2.50	.28/.7	.26/.6			3-.28/.7	
2.75	.24/.6	.27/.7			3-.27/.7	
AF 3.00						

TABLE D-7. DISTRIBUTION OF THE ROOT-MEAN-SQUARE AND 90TH-PERCENTILE MAXIMUM 15-MINUTE VALUES FOR JUNE 1974

ATS-5 L-BAND DATA; JUNE 74					TOTAL: 101	DOT/TSC/WPF
NUMBER OF DATA POINTS; MAXIMUM VALUES						
TIME INTERVAL	JUN 74 3-6	JUN 74 10-13	JUN 74 17-20	JUN 74 24-27	TOTAL	
BF 10.25	.27/.7				1-.27/.7	
10.00	.26/.8				1-.26/.8	
9.75	.26/.8				1-.26/.8	
9.50	.28/.7				1-.28/.7	
9.25	.23/.6				1-.23/.6	
BF 9.00	.20/.6				1-.20/.6	
8.75	.24/.6				1-.24/.6	
8.50	.25/.7				1-.25/.7	
8.25	.25/.7				1-.25/.7	
BF 8.00	.27/.7				1-.27/.7	
7.75	.26/.9				1-.26/.9	
7.50	.27/.7				1-.27/.7	
7.25	.26/.7				1-.26/.7	
BF 7.00	.26/.6				1-.26/.6	
6.75	.23/.7				1-.23/.7	
6.50	.25/.7				1-.25/.7	
6.25	.30/.8				1-.30/.8	
BF 6.00	.27/.8	.26/.7	.27/.8		3-.27/.8	
5.75	.27/.6	.25/.7	.23/.7		3-.27/.7	
5.50	.25/.7	.30/.7			2-.30/.7	
5.25	.30/.8	.24/.7		.27/.7	3-.30/.8	
BF 5.00	.23/.6	.26/.7			2-.26/.7	
4.75	.28/.6	.25/.7	.16/.5	.28/.7	4-.28/.7	
4.50	.26/.6	.28/.6			2-.28/.6	
4.25	2-.25/.6				2-.25/.6	
BF 4.00	2-.28/.8	.28/.7		.25/.7	4-.28/.8	
3.75	2-.25/.7		.29/.7		3-.29/.7	
3.50	2-.26/.7	.24/.6			3-.26/.7	
3.25	2-.26/.7			.30/.7	3-.30/.7	
BF 3.00	2-.29/.8	.33/.8		2-.30/.7	5-.33/.8	
2.75	2-.32/.9	.35/.9	2-.26/.7	.27/.7	6-.35/.9	
2.50	2-.27/.8	2-.35/.8	2-.37/.9	.29/.7	7-.37/.9	
2.25	2-.24/.7	2-.24/.8	2-.37/.9	.27/.7	7-.37/.9	
BF 2.00	2-.27/.8	2-.29/.7	.30/.8	.40/1.0	6-.40/1.0	
1.75	2-.26/.7	2-.32/.8	2-.28/.8	.31/.9	7-.32/.9	
1.50	2-.23/.6	2-.31/.8	.26/.7	.29/.8	6-.31/.8	
1.25	.25/.6	.30/.8	.22/.6	.38/1.0	4-.38/1.0	
BF 1.00	.23/.7	.28/.7	.31/.9	.39/.8	4-.31/.9	
0.75	.25/.6	.26/.7	.21/.6	.31/.8	4-.31/.8	
0.50	.26/.7	.27/.7	.23/.6	.33/.9	4-.33/.9	
0.25	.23/.6	.29/.7	.26/.7	.29/.8	4-.29/.8	
SS 0.00	.25/.7	.24/.6	.23/.7	.30/.7	4-.30/.7	
0.25	.24/.7	.24/.6	.28/.7	2-.30/.8	5-.30/.8	

TABLE D-7. (CONTINUED)

ATS-5 L-BAND DATA; JUNE 74 NUMBER OF DATA POINTS; MAXIMUM VALUES					DOT/TSC/WPF
TIME INTERVAL	JUN 74 3-6	JUN 74 10-13	JUN 74 17-20	JUN 74 24-27	TOTAL
0.50	.28/.8	.24/.6	.27/.7	2-.24/.8	5-.28/.8
0.75	.24/.7	.24/.6	2-.27/.8	2-.29/.8	6-.29/.8
AF 1.00	.22/.7	2-.29/.8	2-.31/.9	.24/.7	6-.31/.9
1.25	.27/.7	2-.26/.7	2-.23/.6	2-.28/.6	7-.28/.7
1.50	.27/.7	2-.26/.8	2-.29/.8	.23/.6	6-.29/.8
1.75		.28/.7	2-.29/.8	2-.31/.8	6-.31/.8
AF 2.00		2-.29/.7	2-.29/.8	2-.28/.7	6-.29/.8
2.25		2-.25/.7	2-.32/.8	.25/.7	5-.32/.8
2.50		2-.27/.6	2-.33/.9	2-.24/.8	6-.33/.9
2.75		2-.28/.7	2-.35/.9	.25/.7	5-.35/.9
AF 3.00		.28/.9	.25/.7	.27/.7	3-.28/.9
3.25		.29/.7	.25/.8	.25/.6	3-.29/.8
3.50		.24/.7	.27/.7	.27/.7	3-.27/.7
3.75		.27/.7	.26/.7	.28/.8	3-.28/.8
AF 4.00		.23/.5	.26/.8	.22/.6	3-.28/.8
4.25		.24/.6	.25/.7	.28/.8	3-.28/.8
4.50		.25/.7	.20/.6	.22/.7	3-.25/.7
4.75		.24/.7	.23/.6	.33/.9	3-.33/.9
AF 5.00		.26/.7	.26/.7	.22/.6	3-.26/.7
5.25		.30/.8	.25/.7	.25/.7	3-.30/.8
5.50		.26/.8	.26/.7	.20/.6	3-.26/.8
5.75		.26/.5	.28/.9	.24/.7	3-.28/.9

TABLE D-8. DISTRIBUTION OF THE ROOT-MEAN-SQUARE AND 90TH-PERCENTILE MAXIMUM 15-MINUTE VALUES FOR JULY 1974

ATS-5 L-BAND DATA; JULY 74 TOTAL: 92					DOT/TSC/WPF
TIME INTERVAL	JULY 74 1-3	JULY 74 8-9	JULY 74 16-18	JULY 74 22-23	TOTALS
BF 10.00					
09.75					
09.50				.22/.5	1-.22/.5
09.25				.22/.6	1-.22/.6
BF 09.00				.25/.7	1-.25/.7
08.75				-	-
08.50			.3/.7	.25/.5	2-.3/.7
08.25				.28/.7	1-.28/.7
BF 08.00			.48/1.0	-	1-.48/1.0
07.75			-	-	-
07.50			-	.24/.6	1-.24/.6
07.25			2-.29/.8	.25/.7	3-.29/.8
BF 07.00			2-.29/.7	.25/.7	3-.29/.7
06.75			.23/.6	.28/.8	2-.28/.8
06.50			.2/.6	.25/.6	2-.25/.6
06.25			.23/.6	.25/.7	2-.25/.7
BF 06.00			.23/.7	.24/.8	2-.24/.8
05.75	.23/.7		.26/.7	.21/.6	3-.26/.7
05.50	.23/.7		.26/.7	.26/.7	3-.26/.7
05.25	-		.28/.8	.22/.6	2-.28/.8
BF 05.00	-		.27/.7		1-.27/.7
04.75	.25/.7		.27/.7		2-.27/.7
04.50	-		.28/.6		1-.28/.6
04.25	.25/.6		(.26/.6)		1-.26/.6
BF 04.00	.27/.7		2-.24/.7		3-.27/.7
03.75	-		2-.25/.7		2-.25/.7
03.50	.25/.6		2-.25/.7		3-.25/.7
03.25	-		2-.22/.7		2-.22/.7
BF 03.00	2-.27/.7	.27/.6	2-.27/.7		5-.27/.7
02.75	-		2-.25/.7		2-.25/.7
02.50	.25/.7	2-.27/.7	2-.27/.8		5-.27/.8
02.25	.3/.7	-	2-.26/.8		3-.3/.8
BF 02.00	.26/.7	2-.24/.7	2-.23/.7		5-.26/.7
01.75	-	2-.25/.7	2-.25/.7		4-.25/.7
1.50	2-.26/.7	.25/.7	.23/.7		4-.26/.7
1.25	.23/.6	2-.27/.7	.22/.6		+-.27/.7
BF 1.00	-	.28/.7	.21/.7		2-.28/.7
0.75	-	-	.22/.7		1-.22/.7
0.50	.27/.7	.22/.6	.24/.6		3-.27/.7
0.25	-	.22/.6	.22/.7		2-.22/.7
SS 0.00	.24/.6	.24/.7	.20/.6		3-.24/.7
0.25	-	.25/.7	.26/.8		2-.26/.8
0.50	.27/.7	.25/.7	.27/.8		3-.27/.8
0.75	-	.23/.7	.21/.6		2-.23/.7
AF 1.00	.25/.7	.25/.7	.22/.6		3-.25/.7
1.25	-	.25/.7	.23/.6		2-.25/.7
1.50	.25/.7	2-.27/.8	.26/.6		4-.27/.8
1.75	-	2-.36/1.0			2-.36/1.0
AF 2.00	-	2-.27/.7			2-.27/.7
2.25	-	2-.25/.8			2-.25/.8
2.50	.24/.7	2-.26/.7			3-.26/.7
2.75		.27/.7			1-.27/.7

TABLE D-9. TALLY SHEET AND FREQUENCY DISTRIBUTION FOR DATA OF TABLES D-1 THROUGH D-8

ATS-5 L-BAND DATA - DISTRIBUTION OF SCINTILLATION													
R.M.S./90% (dB)	DEC 73	JAN 74	FEB 74	MAR 74	APR 74	MAY 74	JUN 74	JUL 74	TOTALS	#	%	%	
.15/.5						1	100					1	100
TOTALS						1	100					1	100
.16/.5			2	100									
TOTALS			2	100								1	100
.17/.4						1	100						
TOTALS					1	100						1	100
.18/.5			1	100									
TOTALS			1	100								1	100
.19/.4													
.19/.5		1	100										
.19/.6			2	67									
TOTALS		1	100	3	100							2	50
.20/.4													
.20/.5		1	100	2	40								
.20/.6			1	100	3	60							
TOTALS		1	100	5	100							1	100
.21/.5	1	100	7	64									
.21/.6		1	100	3	27								
.21/.7			1	9									
TOTALS	1	100	11	100	6	100	2	67	1	5	8	1	11
.22/.5													
.22/.6	3	75	1	100	1	33	13	65	9	69	2	100	5
.22/.7	1	25			6	30	3	23	3	23	3	33	13
TOTALS	4	100	1	100	3	100	20	100	13	100	2	100	9
.23/.4													
.23/.5			2	40	1	20							
.23/.6	2	40	1	100	3	60	1	20	2	12	4	44	36
.23/.7	3	60			1	20	2	100	9	100	9	100	62
TOTALS	5	100	1	100	5	100	5	100	17	100	9	100	62
.24/.4													
.24/.5	3	16	1	12	2	15							
.24/.6	6	32	3	38	7	54	4	57	10	43	3	43	33
.24/.7	9	48	4	50	3	23	2	29	8	35	7	44	44
.24/.8	1	4			1	14	3	13	1	14	2	23	23
TOTALS	19	100	8	100	13	100	7	100	23	100	16	100	9
.25/.5													
.25/.6	6	29	2	22	9	60	6	50	10	33	3	37	4
.25/.7	13	62	6	67	5	33	6	50	15	50	5	63	7
.25/.8	2	9	1	11			4	13	4	13	1	100	1
TOTALS	21	100	9	100	15	100	12	100	30	100	8	100	23
SUBTOTAL	50	-	21	-	56	-	27	-	103	-	50	-	57
													395

TABLE D-9. (CONTINUED)

	DOT/TSC/WPF																
	DEC 73	JAN 74	FEB 74	MAR 74	APR 74	MAY 74	JUN 74	JUL 74	TOTALS								
	#	#	#	#	#	#	#	#	#	#	#	#	#	#	#	#	#
.26/.5	1	5	1	8	6	21	32	2	11	7	2	2	20	2	1		
.26/.6	6	30	7	59	15	51	45	13	72	10	13	6	60	41	30		
.26/.7	10	50	3	25	8	28	23	2	11	5	2	2	20	73	53		
.26/.8	3	15	1	8	8	28	23	1	11	5	1	1	20	21	15		
.26/.9	20	100	12	100	29	100	100	18	100	22	100	10	100	138	100		
TOTALS																	
.27/.5	4	22	1	8	6	25	6	1	8	1	6	1	7	25	18		
.27/.6	9	50	9	75	16	65	14	7	59	14	82	7	73	86	64		
.27/.7	5	28	2	17	2	8	2	4	33	2	12	4	20	23	17		
.27/.8	18	100	12	100	24	100	17	12	100	17	100	15	100	155	100		
.27/.9																	
TOTALS																	
.28/.6	1	7	1	17	3	17	3	1	11	10	77	1	25	13	13		
.28/.7	13	86	5	83	14	78	44	14	44	10	77	5	56	68	70		
.28/.8	1	2	1	9	5	5	56	1	5	3	23	3	25	16	17		
.28/.9	15	100	6	100	18	100	9	18	100	13	100	9	100	97	100		
TOTALS																	
.29/.6	2	20	2	17	3	50	5	3	50	5	33	4	67	6	10		
.29/.7	6	60	4	33	3	50	5	3	50	2	67	2	33	30	48		
.29/.8	2	20	6	50	6	100	10	6	100	3	100	6	75	26	42		
.29/.9	10	100	12	100	24	100	17	12	100	17	100	15	100	62	100		
TOTALS																	
.30/.6	1	25	1	10	3	38	3	3	40	4	100	4	100	2	3		
.30/.7	2	50	5	50	3	50	21	3	38	3	100	4	40	32	46		
.30/.8	1	25	2	20	11	79	4	4	60	3	100	6	60	33	47		
.30/.9	4	100	2	20	1	12	14	1	100	3	100	10	100	3	4		
TOTALS																	
.31/.7	1	50	2	40	2	34	2	1	50	1	100	1	100	10	39		
.31/.8	1	40	2	40	2	33	2	1	50	1	100	2	50	10	39		
.31/.9	1	50	1	20	2	33	2	2	50	1	100	2	50	6	22		
TOTALS																	
.32/.6	1	100	1	10	1	67	1	33	67	1	33	1	50	2	7		
.32/.7			2	20	2	67	2	2	33	2	67	1	50	11	38		
.32/.8			7	70	1	33	2	2	67	2	67	1	50	15	52		
.32/.9			10	100	3	100	3	3	100	3	100	2	100	1	5		
TOTALS																	
SUBTOTAL	70	102	67	70	90	62	61	35	557								

TABLE D-9. (CONTINUED)

ATS-5 L-BAND DATA TALLY SHEET										DOT/TSC/WPF									
	DEC 73		JAN 74		FEB 74		MAR 74		APR 74		MAY 74		JUN 74		JUL 74		TOTALS		
	#	%	#	%	#	%	#	%	#	%	#	%	#	%	#	%	#	%	
.33/.6							1	13									1	5	
.33/.7					1	14	2	25									3	13	
.33/.8	4	100	1	100	3	43	3	38					1	50			12	55	
.33/.9					3	43	2	25					1	50			6	27	
TOTALS	4	100	1	100	7	100	8	100					2	100			22	100	
.34/.7			1	100	1	25											2	15	
.34/.8	1	100			1	25	5	100			1	50					8	62	
.34/.9					1	25					1	50					2	15	
.34/1.0					1	25											1	8	
TOTALS	1	100	1	100	4	100	5	100			2	100					13	100	
.35/.7							1	34									1	9	
.35/.8					1	25	1	33			1	100	1	50			4	36	
.35/.9			1	100	3	75							1	50			5	46	
.35/1.0							1	33									1	9	
TOTALS			1	100	4	100	3	100			1	100	2	100			11	100	
.36/.8					1	100											1	25	
.36/.9							1	50								1	100	2	50
.36/1.0							1	50								1	100	2	50
TOTALS					1	100	2	100								1	100	4	100
.37/.7					1	100											1	33	
.37/.9					1	100							2	100			2	67	
TOTALS					1	100							2	100			3	100	
.38/.8			1	100			1	100									1	20	
.38/.9					2	100											1	20	
.38/1.0					2	100	1	100					1	100			3	60	
TOTALS			1	100	2	100	1	100					1	100			5	100	
.39/.9					1	50											1	33	
.39/1.0					1	50	1	100									2	67	
TOTALS					2	100	1	100									3	100	
.40/.9					1	100	1	100									2	50	
.40/1.0									1	100			1	100			2	50	
TOTALS					1	100	1	100	1	100			1	100			4	100	
.41/1.0					1	100											1	100	
TOTALS					1	100											1	100	
.44/1.0							1	100			1	100					1	50	
.44/1.1							1	100			1	100					1	50	
TOTALS							1	100			1	100					1	100	
.46/1.1											1	100					1	100	
TOTALS											1	100					1	100	
.48/1.0														1	100		1	50	
.48/1.2														1	100		1	50	
TOTALS														1	100	1	100	2	100
.49/1.1									1	100							1	100	
TOTALS									1	100							1	100	
.50/1.1									1	100							1	100	
TOTALS									1	100							1	100	
.51/1.2					1	100											1	100	
TOTALS					1	100											1	100	
.55/1.2											1	100					1	100	
TOTALS											1	100					1	100	
SUBTOTALS	5		4	-	24	-	22	-	3	-	7	-	8	-	2	-	75		
GRAND TOTAL	125		127		147		119		196		119		101		92		1026		

TABLE D-10. TALLY SHEET AND FREQUENCY DISTRIBUTION OF DATA IN
TABLE D-9 BY MONTHS

MONTH	DISTRIBUTION OF 15-MINUTE SCINTILLATION INDEX VALUES ATS-5 L-BAND DATA						DOT/TSC/WPF					
	R.M.S. 0.1-0.2 (dB) #	%	R.M.S. 0.2-0.3 (dB) #	%	R.M.S. 0.3-0.4 (dB) #	%	R.M.S. 0.4-0.5 (dB) #	%	R.M.S. 0.5-0.6 (dB) #	%	TOTAL #	TOTAL %
DEC 73	0	0	14	90	6	12	10	0	0	0	125	100
JAN 74	9	1	11	71	19	36	28	0	0	0	127	100
FEB 74	55	6	11	63	26	46	31	20	2	1	147	100
MAR 74	0	0	9	62	23	43	36	20	2	2	119	100
APR 74	9	1	22	91	7	13	7	20	2	1	196	100
MAY 74	18	2	13	86	5	10	8	30	3	3	119	100
JUN 74	9	1	9	75	12	23	23	10	1	1	101	100
JUL 74	0	0	11	97	2	3	3	0	0	0	92	100
TOTAL	100	11	100	816	100	186	-	100	10	-	1026	-

NOTE: Equinox is on March 21
Solstices are on about December 22 and June 22
*Percentage of the 8-month period.

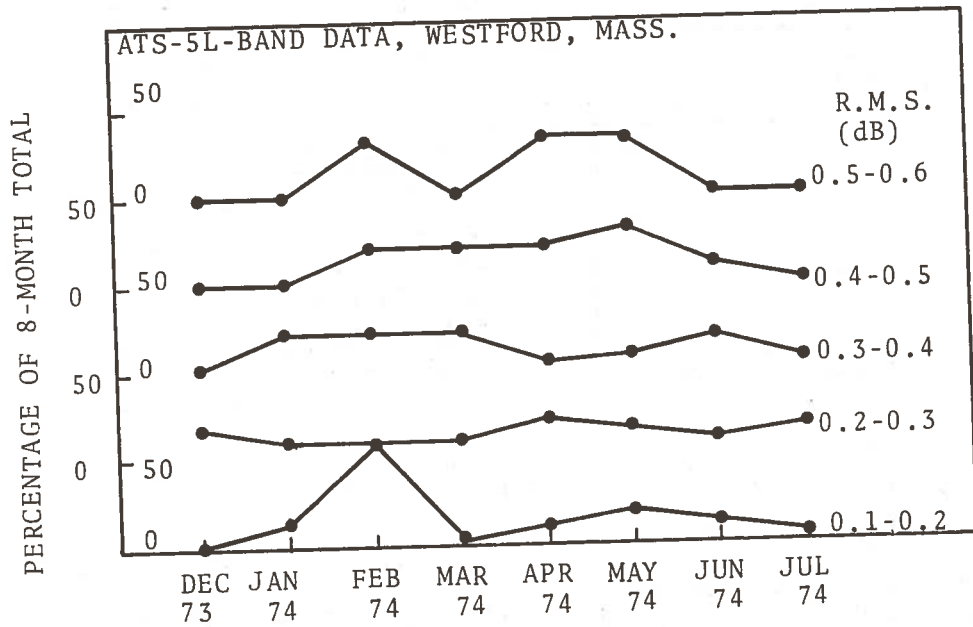


Figure D-1. Plot of Maximum R.M.S. File Values versus Time of Year for the ATS-5 L-Band Amplitude Measurements (From Table D-10)

Figure D-1 shows the relative strengths of the width of the probability density function for the 15-minute measurement periods. Only the maximum values for each hour relative to sunset have been included in the data here. It composes values corresponding to approximately 256 hours of observation. The strongest amplitude variations (R.M.S. values of 0.5 - 0.6 dB) fall in the months around the spring equinox (March 21).

TABLE D-11 APPROXIMATE VALUES OF SCINTILLATION RELATIVE TO R.M.S. FILE VALUES

R.M.S. File Value Interval (dB)	Relative Signal Fluctuation
0.1 - 0.2	Exceedingly calm
0.2 - 0.3	'normal' signal level variations
0.3 - 0.4	moderate scintillation
0.4 - 0.5	scintillation
0.5 - 0.6	heavy scintillation

In February 1974 there was quite a bit of calm and disturbed signal levels.

During the solstices (December 21 and June 21) the data looks relatively calm with essentially no R.M.S. signal level variations greater than 0.4 dB during December, January or June and July. However, during the spring equinox the signal level did have values in the 0.4 - 0.6 dB range during the months of February, through May with a slight amount scintillation in June. Thus, this limited sample of data seems to show slight seasonal variations as would be expected from scintillation theory.

APPENDIX E

ADAPTATION OF PHASE MEASUREMENT CAPABILITY TO THE WESTFORD SITE AND THE AUTOMATIC DATA COLLECTION PLATFORM

The procedure to implement phase measurements using the Westford receivers is straightforward. The high-speed analog-to-digital converters would sample the 20 kHz intermediate frequency of the vector voltmeters. Figure 2-7 would be modified as shown in Figure E-1. The 10 MHz second intermediate frequency signal is divided in two. One portion is fed directly to a vector voltmeter as previously done. The other portion is shifted in phase by 90 degrees and fed to a second vector voltmeter. The two vector voltmeters are phase-controlled by the station's 10 MHz standard as was done previously in the amplitude measurement program. Consequently, the two 20 kHz intermediate frequencies from the voltmeters are in phase quadrature with each other. These two intermediate frequency signals are digitized with the two high-speed analog-to-digital converters.

Since the analog-to-digital converters are commanded by the same computer pulse, the measurement is made by the two converters at the same instant. The two 8-bit outputs of the converters are routed to the high and low byte of a computer word. This one computer word contains both analog-to-digital measurements.

All of the local oscillators in the Westford facility are derived from the main station standard which has good short-term and long-term frequency stability. The 1 kHz bandwidth of the vector voltmeters is more than sufficient to allow for any uplink transmitter, spacecraft or receiver oscillator frequency change as well as any spacecraft doppler frequency changes and at the same time provides a good signal-to-noise ratio.

A more formal description of a phase measurement is given below. When a pure sinusoidal signal undergoes scintillation effects, the received signal may be represented in terms of quadrature components as:

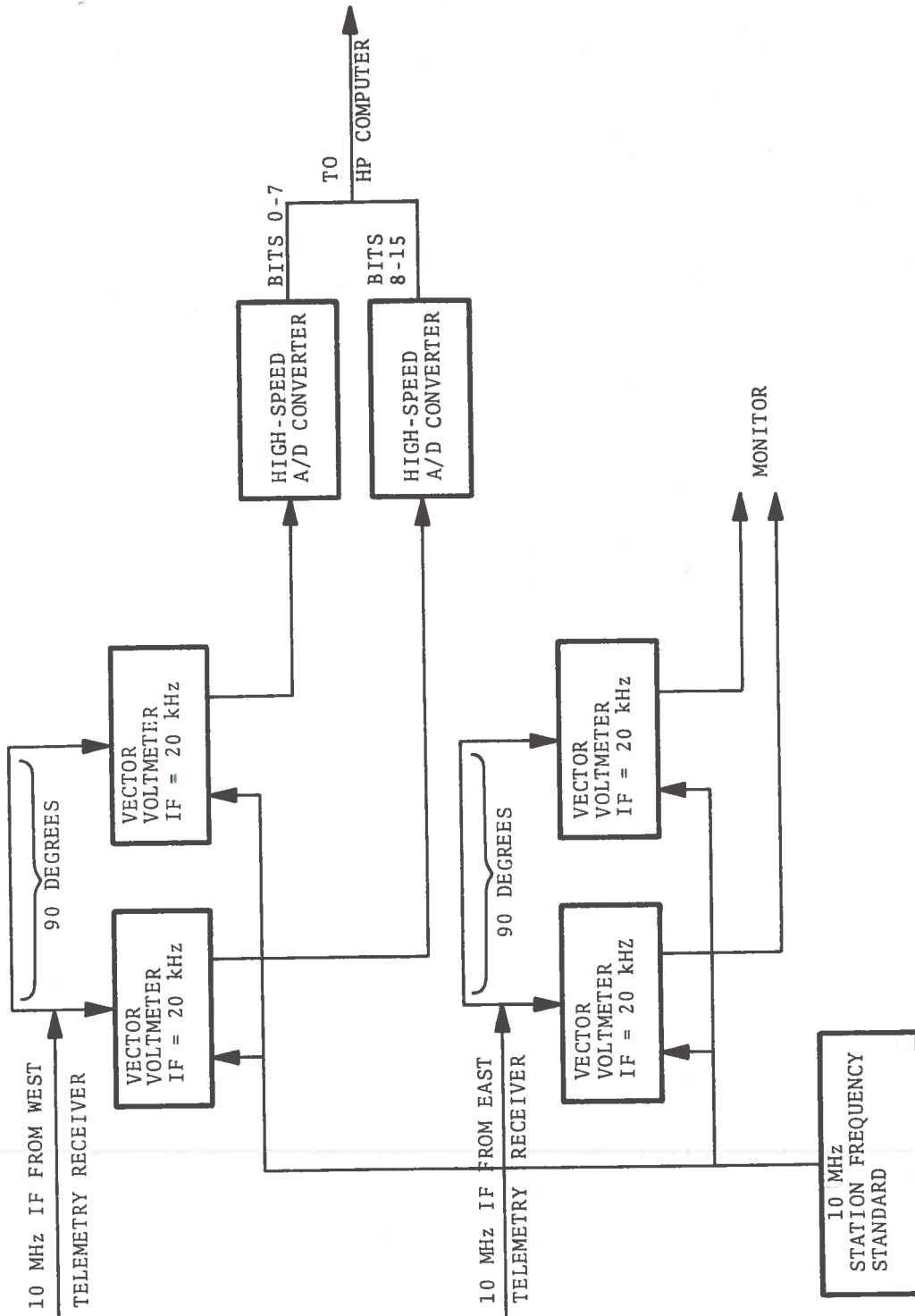


Figure E-1. Block Diagram of a Phase Measurement System for L-Band

$$R(t) = A_c(t) \cos \omega_o(t) + A_s(t) \sin \omega_o(t) + n(t) \quad (E-1)$$

where $f_o = \omega_o/2\pi$ is the received frequency and $n(t)$ is the additive noise. Likewise, $R(t)$ may be represented in terms of amplitude and phase as:

$$R(t) = A(t) \cos(\omega_o(t) - \theta(t)) + n(t) \quad (E-2)$$

and from trigonometry:

$$A_c(t) = A(t) \cos(\theta(t)) \quad (E-3)$$

$$A_s(t) = A(t) \sin(\theta(t)) \quad (E-4)$$

from which it follows:

$$A(t) = \left(A_c^2(t) + A_s^2(t) \right)^{1/2} \quad (E-5)$$

$$\theta(t) = \tan^{-1} \left[A_s(t)/A_c(t) \right] \quad (E-6)$$

The signals from the two vector voltmeters are thus $A_c(t)$ and $A_s(t)$ and are after the data processing by the computer $A(t)$ and $\theta(t)$ will be calculated. Both the amplitude and phase calculation will be presented in a probability density or histogram presentation. Likewise, since the raw intermediate frequency signals are available in digital form the complex power spectrum may be easily identified.

Since the digital sampling is greater than twice the radio frequency bandwidth of the signal and the magnitude and sign of each component has been preserved it is possible to continuously determine the phase even through complete revolutions of 2π .

The description of the remote platform in Section 3 illustrated how it operates when making amplitude measurements. It is possible to easily incorporate a vector voltmeter into the receiver's intermediate frequency system for making both amplitude or phase measurements.

In this case, however, the phase measuring features of the vector voltmeter are used. The frequency reference for the vector voltmeter is the 10.7 MHz crystal oscillator which is part of the

discriminator. The discriminator controls the second local oscillator and has a long time constant (several seconds) so that it will not adversely effect the short-term phase measurements.

The implementation of the phase measuring capability into the ADCP would involve incorporation of one of the vector voltmeters presently used in the Westford facility. Through the actual connection of the vector voltmeter is straightforward the phase stability of the 1500 MHz first local oscillator must be established as must the phase stability of the 10.7 MHz oscillator used in the discriminator.

Consequently, the addition of the phase measurement hardware to the present ADCP receiver may be easily accomplished, however, since the inherent integrity of the platform's receiver's oscillation is not as good as those used in the Westford facility they must be very carefully calibrated.

The present detector or the vector voltmeter detector may be used for making amplitude measurements. The vector voltmeter because of its narrow bandwidth would provide a 9 dB signal-to-noise level improvement.

The present computer program in the platform may be used as it and would provide phase or amplitude measurements every third to a half seconds.

The amplitude phase measurements will be relayed back to the Westford site by VHF as previously discussed in Section 3. Thus the amplitude phase data would be available from two locations.

By selecting the remote location properly the path geometry of the remote site and the Westford site may be arranged to give some additional geophysical and geometric details of the observed scintillations.